



**HAL**  
open science

# Hydro-mechanical behaviour of bentonite-based materials used for high-level radioactive waste disposal

Qiong Wang

► **To cite this version:**

Qiong Wang. Hydro-mechanical behaviour of bentonite-based materials used for high-level radioactive waste disposal. Other. Université Paris-Est; Tongji university (Shanghai, Chine), 2012. English. NNT : 2012PEST1170 . pastel-00806392

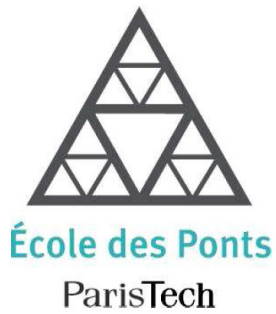
**HAL Id: pastel-00806392**

**<https://pastel.hal.science/pastel-00806392>**

Submitted on 30 Mar 2013

**HAL** is a multi-disciplinary open access archive for the deposit and dissemination of scientific research documents, whether they are published or not. The documents may come from teaching and research institutions in France or abroad, or from public or private research centers.

L'archive ouverte pluridisciplinaire **HAL**, est destinée au dépôt et à la diffusion de documents scientifiques de niveau recherche, publiés ou non, émanant des établissements d'enseignement et de recherche français ou étrangers, des laboratoires publics ou privés.



UNIVERSITÉ —  
— PARIS-EST

THESE

Pour obtenir le grade de

**Docteur de l'Université Paris-Est**

**Discipline : Géotechnique**

Présentée par

**Qiong WANG**

**Hydro-mechanical behaviour of bentonite-based materials used  
for high-level radioactive waste disposal**

Soutenue le lundi 10 Decembre 2012 devant le jury composé de :

Prof. Tom SCHANZ	Rapporteur	Ruhr-Universität Bochum
Prof. Cristina JOMMI	Rapporteur	Politecnico di Milano
Prof. Wei-Min YE	Examineur	Tongji University
Dr. Xiang-Ling LI	Examineur	Euridice Group, SCK/CEN
Dr. Gilles ARMAND	Examineur	Agence Nationale pour la Gestion des Déchets Radioactifs
Dr. Jean-Dominique BARNICHON	Examineur	Institut de Radioprotection et de Sécurité Nucléaire
Dr. Anh Minh TANG	Examineur	Ecole des Ponts ParisTech
Prof. Yu-Jun CUI	Directeur de thèse	Ecole des Ponts ParisTech



*To my parents and my husband Ma Yongtao*



## Résumé

La présente étude concerne le comportement hydromécanique des matériaux compactés à base de bentonite pour le stockage des déchets radioactifs en grande profondeur. Trois matériaux candidats ont été étudiés : la bentonite pure (MX80), le mélange bentonite/argilite broyée et le mélange bentonite/sable. Une étude expérimentale sur la pression de gonflement du mélange bentonite/argilite a été premièrement réalisée. Cette étude a mis en évidence l'effet de la salinité de l'eau, de la procédure et la durée d'hydratation, du vide technologique et des méthodes expérimentales. Une bonne relation entre la pression de gonflement et la densité sèche finale de la bentonite a été élaborée. Ensuite, des essais de rétention d'eau, des essais d'hydratation et des essais oedométriques à succion contrôlée ont été réalisés sur des échantillons à différentes porosités tout en considérant la présence du vide technologique. En introduisant les paramètres comme indice des vides de la bentonite et le ratio volume d'eau, une analyse globale des effets des vides sur la réponse hydromécanique de la barrière ouvragée a été effectuée. Pour avoir un meilleur aperçu de l'évolution de l'étanchéité dans le cas de vide technologique, l'effet de la densité sèche finale (densité après fermeture de vide technologique) et du temps d'hydratation sur la microstructure a été, de même, étudié. La perméabilité de ce matériau à l'état non saturé a été ensuite étudiée en réalisant des essais de rétention d'eau et d'infiltration ainsi que par des observations de la microstructure. Les résultats obtenus ont permis de relier la variation de la perméabilité à l'état non saturé aux changements de la microstructure. Une expérimentation en modèle réduit reproduisant à une échelle 1/10<sup>ème</sup> les essais in-situ (SEALEX) a été effectuée ; ceci pour étudier la reprise des vides à long terme d'un mélange compacté bentonite/sable, tout en considérant la présence du vide technologique. Les résultats ont été utilisés pour interpréter les observations de l'essai in situ. A une échelle de temps réduite, cette étude fournit des informations utiles pour estimer la durée et l'efficacité de la conception en place. Finalement, les données expérimentales obtenues au laboratoire sur le mélange bentonite/sable ont été interprétées dans le cadre du modèle de Barcelone (BExM). Après comparaison des résultats expérimentaux avec le modèle, les performances et les limitations du modèle ont été analysées.

**Mots clés:** comportement hydromécanique, bentonite MX80, microstructure, vide technologique, comportement à long terme, modélisation.



## **Abstract**

This study deals with the hydro-mechanical behaviour of compacted bentonite-based materials used as sealing materials in high-level radioactive waste repositories. The pure MX80 bentonite, mixtures of MX80/crushed claystone and MX80/sand were used in the investigation. An experimental study on the swelling pressure of the bentonite-based materials was first performed. The results evidenced the effects of water chemistry, hydration procedure and duration, technological void and experimental methods. Emphasis was put on the relationship between the swelling pressure and the final dry density of bentonite. Afterwards, the water retention test, hydration test and suction controlled oedometer test were conducted on samples with different voids including the technological void and the void inside the soil. By introducing the parameters as bentonite void ratio and water volume ratio, an overall analysis of the effects of voids on the hydro-mechanical response of the compacted material was performed. To get a better insight into the seal evolution in case of technological void, the effects of final dry density and hydration time on the microstructure features were also characterized. Then, the hydraulic properties under unsaturated state were investigated by carrying out water retention test and infiltration test as well as the microstructure observation. The results obtained allowed relating the variation of hydraulic conductivity to the microstructure changes. A small scale (1/10) mock up test of the SEALEX in situ experiment was also performed to study the recovery capacity of bentonite-based material with consideration of technological void. The results were used for interpreting the in-situ observations. With a reduced time scale, it provides useful information for estimating the saturation duration and sealing effectiveness of the field design. Finally, the experimental data obtained in the laboratory on bentonite/sand mixture were interpreted in the framework of the Barcelona Expansive Model (BExM). By comparing the model with the experimental results, the performance and limitation of the model were analyzed.

**Key words:** Hydro-mechanical, MX80 bentonite, microstructure, technological void, long term behaviour, modeling.



## **Acknowledgements**

The work presented in this thesis would not have been possible without the help of many people who were always there when I needed them the most. I take this opportunity to acknowledge them and extend my sincere gratitude.

First of all, I would like to express my deep and sincere gratitude to my supervisor, Prof. Yu-jun Cui, for his consistent patience and encouragement throughout my period of candidature. I thank him for the systematic guidance and great effort he put into training me in the scientific field. His immense knowledge and his logical way of thinking have been of great value for me.

I would also wish to express my gratitude to Dr. Anh Minh Tang for extended discussions and valuable suggestions which have contributed greatly to the thesis. He is my primary resource for getting my science questions answered and was instrumental in helping me writing this thesis. The thesis has also benefited from comments and suggestions made by Prof. Pierre Delage, Dr. Jean-Dominique Barnichon and Dr. Xiang-Ling Li. Helps from them are gratefully acknowledged. I also record my appreciation to Prof. Weimin Ye for the constant encouragement.

The experimental work would not have been possible without the constant assistance of the technical team of CERMES. I especially thank Emmanuel De Laure for his uncountable helps. I also thank Xavier Boulay, Hocine Delmi, Baptiste Chabot, Clapies Thomas, who helped me a lot during the experimental work. My gratitude goes also to everybody in CERMES for their encouragement, support and all the nice times I had with them.

I am also grateful to IRSN, ANDRA and SCK/CEN for their support. The support from the PHC Cai Yuanpei project and that of the China Scholarship Council (CSC) are also greatly acknowledged.

My parents and my husband Ma Yongtao watched me from a distance while I worked towards my degree. The completion of this thesis will mean a lot to them, particularly “seeing more of me”. So I dedicate this dissertation to my loving parents and my husband. Without whose love, affection and encouragement this work would not have been possible.

Finally, I am thankful to all my friends who have helped me directly or indirectly in the successful completion of my thesis.

## Publications

### Journal papers

- 1 **Wang, Q.**, Tang, A.M., Cui, Y.J., Delage, P., Gatmiri, B. 2012. Experimental study on the swelling behaviour of bentonite/claystone mixture. *Engineering Geology*, Vol. 124, 59–66
- 2 **Wang, Q.**, Tang, A.M., Cui, Y.J., Delage, P., Barnichon, J.D., Ye, W.M., 2012. The effects of technological voids on the hydro-mechanical behaviour of compacted bentonite-sand mixture. *Soils and Foundations*, Vol.53, No.2
- 3 **Wang, Q.**, Tang, A.M., Cui, Y.J., Delage, P., Gatmiri, B. 2012. Long-term effect of water chemistry on the swelling pressure of a bentonite-based material. Submitted to *Applied Clay Science*
- 4 **Wang, Q.**, Tang, A.M., Cui, Y.J., Li, X.L., Ye, W.M., 2012. Time and density dependent microstructure features of compacted bentonite. Submitted to *Canadian Geotechnical Journal*
- 5 **Wang, Q.**, Tang, A.M., Cui, Y.J., Barnichon, J.D., Ye, W.M., 2012. Hydraulic conductivity and microstructure changes of compacted bentonite/sand mixture during hydration. Submitted to *Engineering Geology*
- 6 **Wang, Q.**, Cui, Y.J., Tang, A.M., Ye, W.M., 2012. Effect of sample preparation on the swelling pressure of compacted bentonite/claystone mixture. Submitted to *Korean Society of Civil Engineers*
- 7 **Wang, Q.**, Tang, A.M., Cui, Y.J., Barnichon, J.D., Ye, W.M., 2012. A comparative study on the hydro-mechanical behaviour of compacted bentonite/sand plug based on laboratory and field infiltration tests. Submitted to *Engineering Geology*
- 8 **Wang, Q.**, Tang, A.M., Cui, Y.J., Barnichon, J.D., Ye, W.M., 2012. Investigation of the HM behaviour of compacted bentonite/sand mixture based on the BExM model. Submitted to *Computers and Geotechnics*
- 9 Ye, W.M., Chen, Y.G., Chen, B., **Wang, Q.**, Wang, J. 2010. Advances on the knowledge of the buffer/backfill properties of heavily-compacted GMZ bentonite. *Engineering Geology*. Volume 116, Issues 1-2, Pages 12-20

### Conference papers

1. **Wang, Q.**, Tang, A.M., Cui, Y.J., Li X.L., Ye, W.M., 2012. Microstructure Features of Compacted MX80 bentonite Used for Hydraulic Seal in PRACLAY Heater Test, *Clays in Natural & Engineered Barriers for Radioactive Waste Confinement*, 5th international meeting, Oct. 22-25 2012, Montpellier, France
2. **Wang, Q.**, Tang, C.S., Tang, A.M., Cui, Y.J. 2012. Effect of suction changes on the microstructure of compacted crushed argillites under constant-volume conditions, *E-UNSAT2012*, June 20-22, Naples, Italy.
3. Ye, W.M., **Wang, Q.**, Pan, H., Chen, B., 2009, Experimental study on the thermal conductivity of compacted GMZ01 bentonite and mixtures, *UNSAT-WASTE 2009*, Shanghai, China, Aug 24-28, 2009: 161-167.

4. Ye, W.M., **Wang, Q.**, Chen, Y.G., Chen, B. 2009. Advances on buffer/backfill properties of heavily compacted gaomiaozi bentonite. Proc. of Int. Symp. on Geo-environmental Eng., ISGE2009, September 8-10, 2009, Hangzhou, China. Springer-Verlag GmbH. P: 370-379.

# CONTENTS

<b>Résumé</b> .....	I
<b>Abstract</b> .....	III
<b>Acknowledgements</b> .....	V
<b>Publications</b> .....	I
INTRODUCTION .....	1
Chapter 1. Experimental study on the swelling property .....	5
INTRODUCTION .....	5
Experimental study on the swelling behaviour of bentonite/claystone mixture .....	6
1 Introduction .....	6
2 Materials and methods .....	8
3 Experimental results .....	12
4 Discussion .....	21
5 Conclusion .....	23
References .....	24
Chapter 2. Long-term effect of water chemistry on the swelling pressure .....	29
INTRODUCTION .....	29
Long-term effect of water chemistry on the swelling pressure of a bentonite-based material .....	30
1 Introduction .....	30
2 Materials and methods .....	31
3 Experimental results .....	35
4 Interpretation and discussion .....	39
5 Conclusion .....	42
References .....	43
Chapter 3. Effect of technological void on the hydro-mechanical behaviour .....	47
INTRODUCTION .....	47
The effects of technological voids on the hydro-mechanical behaviour of compacted bentonite-sand mixture .....	48
1 Introduction .....	48
2 Materials and methods .....	50
3 Experimental results .....	58
4 Interpretation and discussion .....	65
5 Conclusion .....	73
References .....	75
Time and density dependent microstructure features of compacted bentonite .....	78
1 Introduction .....	78
2 Materials and methods .....	79
3 Experimental results and discussions .....	83

4 Conclusion.....	94
References:.....	96
Chapter 4. Hydraulic conductivity and microstructure changes during hydration.....	99
INTRODUCTION.....	99
Hydraulic conductivity and microstructure changes of compacted bentonite/sand mixture during hydration .....	100
1 Introduction .....	100
2 Materials and methods .....	102
3 Experimental results .....	106
4 Interpretation and discussion.....	117
5 Conclusion.....	120
References .....	120
Chapter 5. Comparative study on the hydro-mechanical behaviour based on laboratory and field infiltration tests .....	123
INTRODUCTION.....	123
A comparative study on the hydro-mechanical behaviour of compacted bentonite/sand plug based on laboratory and field infiltration tests .....	124
1 Introduction .....	124
2 Materials and methods .....	126
3 Experimental results .....	131
4 Comparison and discussion .....	138
5 Conclusion.....	141
References .....	142
Chapter 6. Investigation of the HM behaviour of compacted bentonite/sand mixture based on the BExM model .....	145
INTRODUCTION.....	145
Investigation of the HM behaviour of compacted bentonite/sand mixture based on the BExM model.....	146
1 Introduction .....	146
2 Barcelona Expansive Model.....	147
3 Parameters determination .....	150
4 Simulation and interpretation .....	157
5 Conclusion.....	160
References .....	161
CONCLUSION .....	165
REFERENCES.....	169

## **INTRODUCTION**

Deep geological repository has been considered for high-level radioactive waste (HLW) in several countries such as Belgium, China, France, Germany, Japan, Sweden, etc. The safety of this disposal concept is based on the multi-barrier system consisting of the natural barrier (host rock) and engineered barriers (waste container, buffer and sealing elements).

In most cases, bentonite-based materials are chosen as buffer/sealing materials in this system thanks to their low permeability, high swelling and high radionuclide retardation capacities (Pusch, 1979; Yong et al., 1986; Villar et al., 2008). Obviously, these materials, once installed in the repository, will undergo complex thermo-hydro-mechanical loadings. It is therefore essential to well understand their behaviour under such loadings in assessment of the overall repository safety.

In this context, number of laboratory studies has been conducted to study the performance of buffer/sealing materials (e.g. Delage et al., 1998; Lloret et al., 2003; Romero et al., 2005; Lloret & Villar, 2007). Various experiments were also performed in the underground research laboratories (URL) such as TSX at the Manitoba, Canada; FEBEX at Grimsel, Switzerland; RESEAL at Mol, Belgium; KEY at Bure, France, etc.

Recently, The Belgian Agency for Management of Radioactive Waste and Enriched Fissile Materials (ONDRAF/EURIDICE) has launched the PRACLAY in-situ heater experiment in the underground laboratory of Mol, Belgium. The pre-compacted MX80 bentonite is used for the hydraulic seal. This hydraulic seal is of annular shape and made up of compacted bentonite bricks. It is installed between the heated zone and the access gallery to achieve the desired undrained hydraulic boundary condition (Tang et al. 2008, Li et al. 2010). The bentonite bricks are expected to swell upon hydration, filling the initial technological voids and compensating the deformation of the host Boom clay. From a practical point of view, it is important to well understand the swelling behaviour of the compacted bentonite.

In France, ANDRA (Agence Nationale pour la Gestion des Déchets RadioActifs) planned to use the mixture of bentonite and crushed Callovo-Oxfordian (COx) claystone excavated from the Bure site of the URL (-490 m, North-eastern France) as possible sealing and backfill

material. This choice has the advantages of being economical by using local excavated argillite and of ensuring better mineralogical and chemical compatibility between the host rock, mixture and pore-water (Andra, 2005; Tang et al., 2011a; Tang et al., 2011b). Nevertheless, the question of possible interaction between bentonite and claystone remains, at both short and long terms.

In order to identify the key factors related to the long-term performance of bentonite-based sealing systems with consideration of initial technological void, the French institution IRSN (Institut de Radioprotection et de la Sûreté Nucléaire) has launched the SEALEX project. This project consists of a series of in situ experiments performed in natural conditions in Tournemire Underground Research Laboratory. The experimental program was purposefully built allowing systematically exploring the effect of technical specifications, design, construction, deflection, etc. (Barnichon et al. 2009, 2010). Clay seals made of pre-compacted disks of MX80 bentonite/sand mixture were considered. The seals will undergo first the saturation stage. During this process, the injected water volume, total pressure and relative humidity changes are monitored at several positions. Afterwards, hydraulic tests will be performed to determine the overall hydraulic properties (inherent permeability, occurrence of leakage) of the sealing system. The impact of the technical specification and design of the sealing plug will be also investigated by changing the intra-core geometry (jointed vs. monolithic disks), core composition (MX80/sand ratio) and core conditions (pre-compacted vs. in situ compacted). Furthermore, the effect of altered conditions will be also studied by simulating an incidental decrease of swelling pressure caused by a failure of the concrete confining structure. Considering the complexity of the in-situ conditions, it appears important to identify the hydro-mechanical behaviour of compacted mixture in the laboratory condition in order to obtain useful information for interpreting the results obtained in the field condition.

The present work is related to the three projects mentioned above with three materials studied: (1) the pure MX80 bentonite used for the hydraulic seal in the PRACLAY in-situ experiment at Mol (Belgium), (2) the MX80/crushed claystone mixture planned to be used in the underground research laboratory (URL) at Bure site (France), (3) MX80/sand mixture used in the SEALEX in situ experiments performed at Tournemire site (France). Emphasis was put on the effect of technological voids. Both laboratory testing and constitutive modeling were conducted.

The results are subjected to several published and submitted papers. A first paper on the swelling behaviour of bentonite/claystone mixture has been published in the journal *Engineering Geological*; the second paper on the effects of technological voids on the hydro-mechanical behaviour of compacted bentonite/sand mixture has been accepted by the journal *Soils and Foundations*; and five others were submitted to *Applied Clay Science*, *Canadian Geotechnical Journal*, *Engineering Geology*, *Computers and Geotechnics*, respectively. The dissertation is presented in the form of papers/manuscripts, each chapter composing an introduction and the corresponding papers/manuscripts.

The first chapter focuses on the swelling pressure of the bentonite/claystone mixture (Bure URL, ANDRA), which corresponds to the paper published in *Engineering Geology*. The effects of water chemistry, the hydration procedure, the pre-existing technological voids and the experimental methods on the swelling pressure were investigated. Based on the experimental results, the relationship between the swelling pressure and the final dry density of bentonite was proposed.

The second chapter analyses the long-term effect of pore water chemistry on the swelling pressure of bentonite/calystone mixture (Bure URL, ANDRA). Emphasis was put on the physico-chemical interaction between the minerals of claystone, minerals of bentonite and different fluids involved. The kinetics of swelling pressure was also described by comparing a one-step soaking test with multistep soaking test.

The third chapter corresponds to the results presented in two papers. The first, being accepted by *Soils and Foundation*, presents the results of water retention test, hydration test, suction controlled oedometer test and hydraulic test on samples with different voids including the technological void and the void inside the soil (SEALEX prject, IRSN). By introducing the parameters as bentonite void ratio and water volume ratio, the effects of technological voids on hydro-mechanical behaviour were analyzed. The second section characterises the effects of final dry density and hydration time on the microstructure features of the compacted bentonite in case of technological void, which was directly related to the macroscopic hydro-mechanical behaviour (PRACLAY, ONDRAF/EURIDICE).

The forth chapter presents the water retention test and infiltration test as well as the microstructure observation on the bentonite/sand mixture (SEALEX prject, IRSN). Based on the experimental results, the variations of hydraulic conductivity with suction was determined and explained in terms of microstructure changes.

A comparative study on the hydro-mechanical behaviour of compacted bentonite/sand plug based on laboratory and field infiltration tests is presented in the fifth chapter (SEALEX project, IRSN). By comparing the first results from the in situ test, the phenomena identified in the laboratory were used for interpreting and estimating the performance of the bentonite-based plug in the field.

In the sixth and last chapter, the hydro-mechanical behaviour of the MX80 bentonite/sand mixture is interpreted in the framework of the Barcelona Expansive Model (BExM). After determining the parameters based on the experimental results, the hydro-mechanical (H-M) responses of the material identified from other tests with different stress paths were simulated, allowing analysing the performance and limitation of the model (SEALEX project, IRSN).

## **Chapter 1. Experimental study on the swelling property**

### **INTRODUCTION**

The main function of buffer/sealing material is to fill up all the existing voids, creating a relatively impermeable zone around the high-level radioactive waste. This role termed as “self-sealing” (Komine, 2004; Komine and Ogata, 2003) is essential to ensure the overall safety of the geological disposal. Thus, the swelling properties constitute a key factor in the design and development of the sealing/backfill materials and need to be studied in depth.

Previous studies showed that the swelling properties depend strongly on the initial dry density and water content of the soil specimen (Komine et al., 1994; Villar et al., 2008). The swelling properties can be affected by the chemical composition of the saturating fluid: the swelling capacity of the bentonite decreases with the increase in salinity of saturating fluid, although this influence becomes less significant for higher densities (Pusch, 1980; Sugita et al., 2003; Karnland et al., 2005; Castellanos et al., 2008; Siddiqua et al., 2011). Moreover, the swelling potential may decrease with time due to the rearrangement of clay particles with time (Nalzeny et al., 1967; Day et al., 1994; Subba Rao et al., 2003; Delage et al., 2006).

Accounting for these factors, this chapter presents an experimental study on the swelling pressure of the mixture MX80 bentonite/crushed Cox claystone. A series of experiments including determination of the swelling pressure of compacted samples by constant-volume method, pre-swell method, zero-swell method and swell–consolidation method were performed. The influences of water chemistry, hydration procedure and duration, pre-existing technological void and loading-wetting paths on the swelling pressure of compacted samples were analyzed.

This work was published in « Engineering Geology», the article is represented here in its original version.

Wang, Q., Tang, A. M., Cui, Y.J., Delage, P., Gatmiri, B. 2012. Engineering Geology, Vol. 124, 59–66.

## Experimental study on the swelling behaviour of bentonite/claystone mixture

Qiong Wang<sup>1</sup>, Anh Minh Tang<sup>1</sup>, Yu-Jun Cui<sup>1</sup>, Pierre Delage<sup>1</sup>, Behrouz Gatmiri<sup>2</sup>

**Abstract:** A mixture of the MX80 bentonite and the Callovo-Oxfordian (COx) claystone were investigated by carrying out a series of experiments including determination of the swelling pressure of compacted samples by constant-volume method, pre-swell method, zero-swell method and swell–consolidation method. Distilled water, synthetic water and humidity controlled vapour were employed for hydration. Results show that upon wetting the swelling pressure increases with decreasing suction; however, there are no obvious effects of synthetic water chemistry and hydration procedure on the swelling behaviour in both short and long terms. For the same initial dry density, the swelling pressure decreases with increasing pre-swell strain; whereas there is a well defined logarithmic relation between the swelling pressure and final dry density of the sample regardless of the initial dry densities and the experimental methods. It was also found that swelling pressure depends on the loading-wetting conditions as a consequence of the different microstructure changes occurred in different conditions. Furthermore, it was attempted to elaborate a general relationship between the swelling pressure and the final dry density for various reference bentonites.

**Keywords:** bentonite/claystone mixture; swelling pressure; water chemistry effect; long term behaviour; final density; correlation.

---

### 1 Introduction

Deep geological repository is being considered for high-level radioactive waste (HLW) in several countries such as China, Belgium, France, Germany, Japan, Sweden, etc. In most cases, compacted bentonite-based materials are chosen as sealing/buffer materials thanks to their low permeability, high swelling and high radionuclide retardation capacities (Pusch, 1979; Yong et al., 1986; Villar et al., 2008).

Once the repository is closed and local groundwater conditions are re-established, the water in the host rock formation will move to the repository. The bentonite-based material absorbs water and swells, filling the technical voids as the gaps between the bentonite bricks themselves, between the canister and the bricks, between bricks and the host rock, as well as the fractures in the host rock due to excavation. After that, the subsequent swelling is restrained by the host rock and swelling pressure develops. From a mechanical point of view,

---

1. Ecole des Ponts ParisTech, UR Navier/CERMES

2. ANDRA, France

in order to ensure the stability of the system, the swelling pressure must be lower than the in situ minor stress: 7 MPa in the Underground Research Laboratory (URL) of Bure site, France (Delege et al., 2010; Tang et al., 2011a); 3-4 MPa at Tournemire site, France (Barnichon et al., 2009) and 4-5 MPa at Mol site, Belgium (Li et al., 2009), etc. As the compacted bentonite-based material is a key component of a repository system, it governs the overall behaviour of the whole system. Hence, a proper understanding of how the compacted bentonite-based material behaves during hydration process is essential for the assessment of the short and long term performance of the repository system.

The behavior of compacted bentonite-based material upon wetting has been widely investigated, in terms of swelling properties (Pusch, 1982; Komine and Ogata, 1994, 2003, 2004a; Delage et al., 1998; Agus and Schanz, 2005; Komine et al., 2009); hydraulic behaviour under saturated state (Kenney et al., 1992; Dixon et al., 1999; Komine, 2004b;) and unsaturated state (Borgesson et al., 1985, 2001; Kröhn, 2003; Lemaire et al., 2004; Loiseau et al., 2002; Cui et al., 2008). There are also many studies on the effect of temperature (Komine and Ogata, 1998; Romero et al., 2001; Villar and Lloret, 2004; Tang et al., 2005; Tang et al., 2007; Tang et al., 2008a; Tang and Cui, 2009) and water chemistry of the saturating fluid (Pusch 2001a, Karland et al., 2005; Suzuki et al., 2005; Komine et al., 2009) on the hydro-mechanical (HM) behaviour.

For the swelling properties, it has been found that the swelling pressure determined in the laboratory can be affected by the experimental methods (Sridharan et al., 1986; Tang et al., 2011b). Normally, different methods give different values of swelling pressure due to the difference in the loading and wetting conditions in each method (Abdullah et al., 1998, 1999). In addition, the swelling properties depend on the initial dry density and water content of the soil specimen. The higher the initial dry density, the higher the swelling pressure or the higher the swelling strain; the swelling strain decreases with increasing initial water content, but the swelling pressure seems not to be affected by the initial water content (Komine et al., 1994; Villar et al., 2008). The swelling properties can be also affected by the chemical composition of the saturating fluid: the swelling capacity of the bentonite decreases with the increase in salinity of saturating fluid, although this influence becomes less significant for higher densities (Pusch, 1980; Sugita et al., 2003; Karland et al., 2005; Castellanos et al., 2008; Siddiqua et al., 2011). Moreover, Studies on the aging effects on the swelling behavior show that the swelling potential may decrease with time due to the rearrangement of clay particles with time (Nalzeny et al., 1967; Day et al., 1994; Subba Rao et al., 2003; Delage et al., 2006).

Very often, bentonite/sand mixtures are considered for the reasons of good control of swelling pressure, large thermal conductivity and a better mechanical resistance. In France, the mixture of bentonite and crushed Callovo-Oxfordian (COx) claystone excavated from the Bure site of the ANDRA URL (-490 m, North-eastern France) was proposed as a possible sealing and backfill material. This choice has several advantages: (i) it is more economical by using local excavated claystone; (ii) the negative impacts on the environment is reduced by recycling the excavated material; (iii) there is better compatibility of mineralogical and chemical compositions with host rock, allowing reduction of complex physico-chemical interaction with the host rock (Andra, 2005; Tang et al., 2011a; Tang et al., 2011b). On the other hand, unlike relatively inert sand, claystone contains clay minerals and interaction between argillite and bentonite may occur, affecting the hydro-mechanical behaviour of the compacted mixture. Moreover, this interaction can be of long term. Particular attention should be paid to this aspect.

This study focuses on the swelling properties of the mixture MX80 bentonite/crushed Cox claystone. A series of swelling tests were performed under constant temperature ( $20\pm 1^\circ\text{C}$ ). The influences of water chemistry, hydration procedure and duration, pre-existing technical void and loading-wetting paths on the swelling pressure of compacted samples were investigated. Emphasis was put on the relationship between the swelling pressure and the dry density of bentonite.

## 2 Materials and methods

### 2.1 Materials

The commercial MX80 bentonite from Wyoming, USA, was used. Table 1 lists its physical parameters. It appears that the proportion of montmorillonite is dominant in the bentonite (92 %); it has an average specific gravity of 2.76, a liquid limit of 520%, and a plastic limit of 42%. The grain size distribution determined by sedimentation in Figure 1 shows that 84% grains are smaller than  $2\ \mu\text{m}$  (clay fraction).

Table 1 Characteristics of MX80 bentonite (Tang et al., 2008b)

Montmorillonite (%)	Quartz (%)	$w_l$ (%)	$w_p$ (%)	$I_p$	$\rho_s$ (Mg/m <sup>3</sup> )
92	3	520	42	478	2.76

Callovo-Oxfordian (COx) claystone taken from the Bure site of the ANDRA URL was studied. It contains 40–45% clay minerals (mainly interstratified minerals illite–smectite), 20–30% carbonates and 20–30% quartz and feldspar (Hoteit et al., 2000; Lebon and Ghoreychi, 2000; Zhang et al., 2004). The specific gravity is 2.70. The excavated claystone was air-dried ( $w = 2.64\%$ ) and crushed to powder. The grain size distribution determined by sedimentation is presented in Figure 1. It confirms that 40% grains are clays ( $< 2 \mu\text{m}$ ).

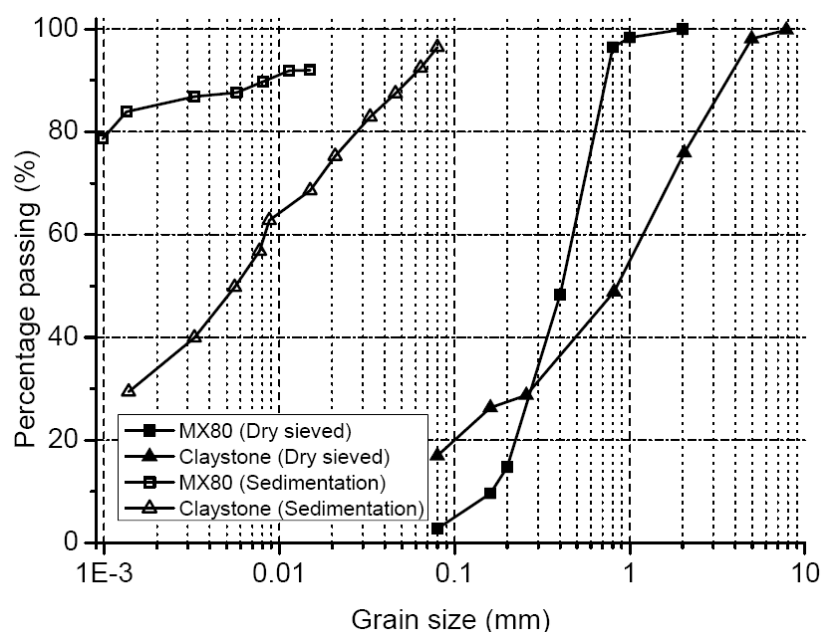


Figure 1. Grain size distribution of MX80 bentonite and crushed COx claystone

Both distilled water and synthetic water having the same chemical composition as the site water (see Table 2) were used.

Table 2 Chemical components of the synthetic water

Components	NaHCO <sub>3</sub>	Na <sub>2</sub> SO <sub>4</sub>	NaCl	KCl	CaCl <sub>2</sub> .2H <sub>2</sub> O	MgCl <sub>2</sub> .6H <sub>2</sub> O	SrCl <sub>2</sub> .6H <sub>2</sub> O
Mass (g) per 1L solution	0.28	2.216	0.615	0.075	1.082	1.356	0.053

## 2.2 Samples preparation

All the tests in this study were performed on samples of compacted bentonite/claystone mixture with a bentonite content of 70 % in dry mass. Bentonite and claystone powders with the initial water contents of 11.8 % and 2.64 % respectively, were used for the samples preparation. Their grain size distributions were determined by sieving and are presented in Figure 1.

Samples were statically compacted in an oedometer cell (38 or 70 mm in internal diameter) at a controlled rate of 0.05 mm/min. A load transducer was used for axial force monitoring, and a micrometer dial gauge was used for axial displacement monitoring. After compaction, the specimen was carefully transferred into the hydration cell (with the same diameter as the oedometer cell) by connecting the bottom of the two cells together. This procedure allows the lateral stress released without significant increase in sample diameter.

### 2.3 Experimental methods

Various methods were used to determine the swelling pressure upon wetting. The stress paths of these methods are presented in Figure 2.

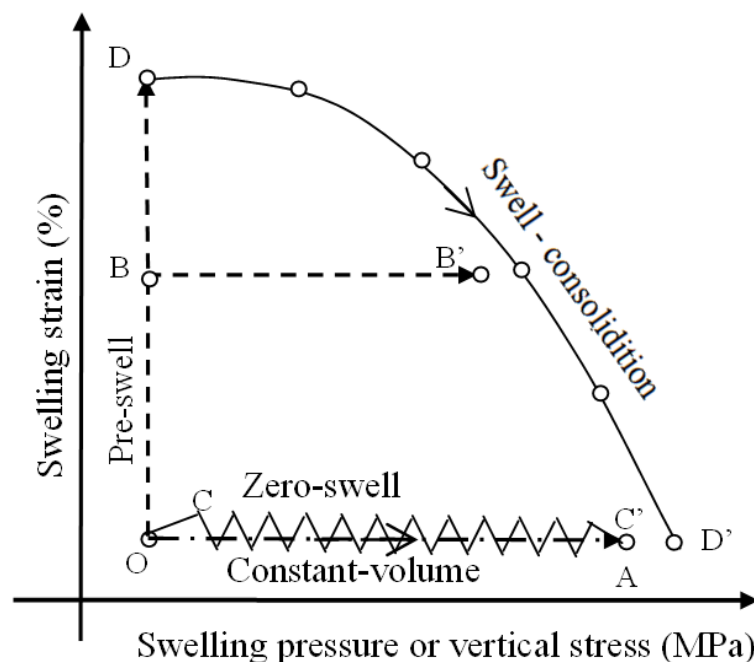


Figure 2. Stress path of various experimental methods used to determine the swelling pressure

For the “constant-volume” method (stress path OA), the devices presented in Figure 3 and Figure 4 were used. The constant-volume cell includes three parts (Figure 3, Tang et al., 2011b): (1) the bottom part containing a porous stone and a drainage system; (2) the middle cell (70 mm inner diameter) used to prevent radial swelling, with two air outlets; (3) the top part incorporating a total pressure sensor to monitor the swelling pressure. Figure 4 presents the setup used to control the suction in the soil sample using the vapour equilibrium technique (see Delage et al., 1998 for more details). When flooding the soil sample, this system was removed and the water inlet was connected to a water reservoir.

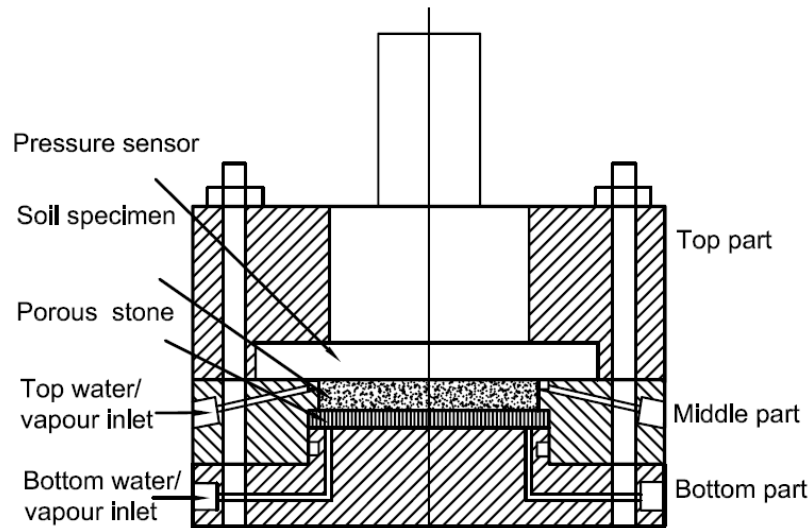


Figure 3. Constant-volume cell

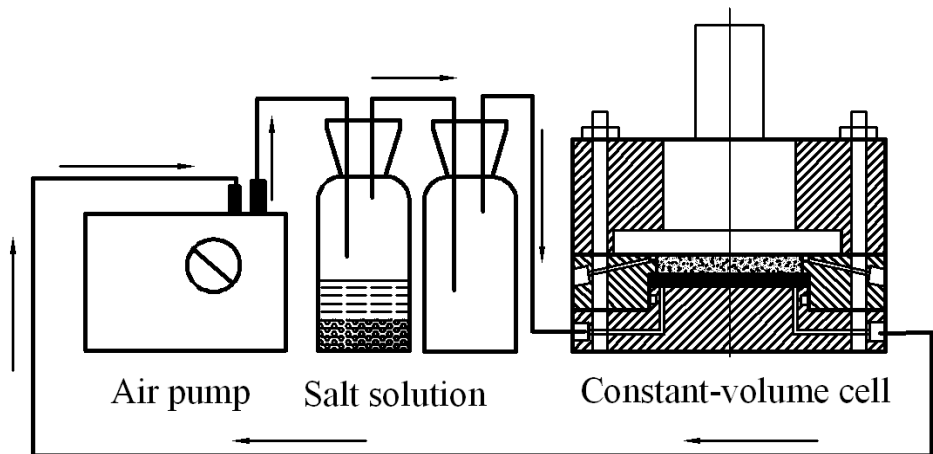


Figure 4. Schematic view of constant volume cell with suction control system

For the “pre-swell” method (stress path OBB’), the sample was first allowed to swell freely in the axial direction to a certain value (Point B, noted as “pre-swell”), then the piston was fixed permitting the generation of swelling pressure that was monitored by the load transducer. This method was used to investigate the effect of pre-existing technical voids (simulated by the pre-swell allowed in the tests) on the swelling pressure.

For the “zero-swell” and “swell-consolidation” methods, the equipment employed was a conventional oedometer (Basma et al., 1995; Nagaraj et al., 2009). Firstly, a low initial load of 0.1 MPa was exerted on the specimen prior to water flooding. As the specimen wetted up it attempted to swell. When the swell exceeded 10  $\mu\text{m}$  (equivalent to 0.1%), additional pressure was added in small increment to bring the volume of soil specimen back to its initial value (Basma et al., 1995; Abdullah et al., 1998, 1999; Attom et al., 2001). This operation was

repeated until the specimen ceased to swell (OCC' in Figure 2). The swelling pressure was defined as the stress where no more swelling strain was observed.

The “swell-consolidation” method consists of re-saturating the soil under a low vertical pressure of 0.1 MPa until full swell was achieved. After swell completion, standard consolidation test was conducted. The pressure required to compress the specimen back to its original void ratio is defined as the swelling pressure (Basma et al., 1995; Abdullah et al., 1998, 1999; Agus, 2005). The corresponding stress path ODD' is shown in Figure 2. In this path, point D also represents the maximum swelling strain of the sample.

The experimental programme is shown in Table 3. Three tests were performed using the constant-volume method to study the effect of water chemistry and the hydration procedure (CV01, CV02 and CV03). Distilled water and synthetic water was used in test CV01 and CV02, respectively. In test CV03, three suctions (57 MPa, 38 MPa and 12.6 MPa) were first applied step by step using vapor equilibrium technique (as shown in Figure 4), prior to distilled water flooding in the last stage.

Four tests were performed by pre-swell method to study the influence of pre-existing technical voids on the swelling pressure (PS01 – PS04). Different pre-swells were allowed before measurement of the swelling pressure. Note that for test PS04 the sample was allowed to swell freely to reach the maximum pre-swell strain.

Two other tests were conducted using zero-swell method (ZSO1) and swell-consolidation method (SCO1), respectively, for analyzing the influence of loading-wetting paths followed in different experimental methods.

As it can be seen in Table 3, the tests conducted have in general long duration, from 80 h to one year.

### **3 Experimental results**

Figure 5 presents the results from tests CV01 and CV02 with distilled water and synthetic water respectively, during the first 100 h. The two curves are very similar, showing negligible effect of water chemistry (in the range considered). With water infiltration, swelling pressure increased first very quickly; after about 20 h the swelling pressure reached a first stability stage. At 32 h, the swelling pressure restarted to increase and it reached a second stability stage at 100 h. The final values are 4.30 MPa and 4.37 MPa for CV01 and CV02, respectively.

Table 3 Test programme

Test No.	Injected water	Method	Initial dry density (Mg/m <sup>3</sup> )	Duration
CV01	Distilled	Constant-volume	1.70	1 year
CV02	Synthetic	Constant-volume	1.70	1 year
CV03	Vapour and distilled	Constant-volume	1.70	1 year
PS01	Synthetic	Pre-swell $\varepsilon = 10\%$	1.90	100 h
PS02	Synthetic	Pre-swell $\varepsilon = 20\%$	1.90	100 h
PS03	Synthetic	Pre-swell $\varepsilon = 25\%$	1.90	100 h
PS04	Synthetic	Pre-swell $\varepsilon = \text{max}$	1.90	80 h
ZSO1	Synthetic	Zero-swell	1.70	80 h
SCO1	Synthetic	Swell-consolidation	1.90	4 months

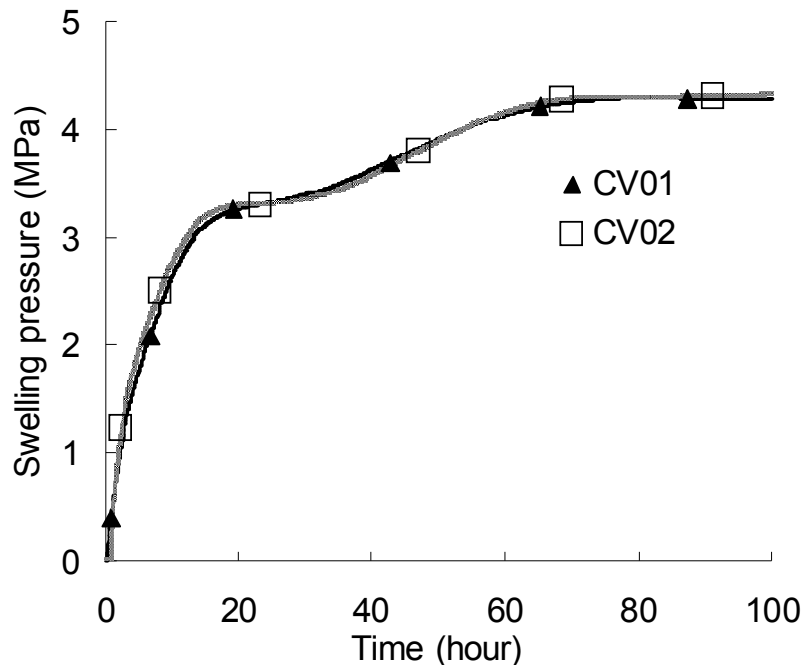


Figure 5. Evolution of swelling pressure for test CV01 and CV02 during the first 100 h.

The results of test CV03 is presented in Figure 6. The initial suction of sample was about 90 MPa (measured by a relative humidity sensor on the soil specimen after the compaction and prior to the installation in the cell). The application of the first suction of 57 MPa resulted in a swelling pressure of 0.57 MPa. Then, the second suction of 38 MPa was applied and the swelling pressure reached 1.43 MPa. With the third suction of 12.6 MPa the swelling pressure increased to 2.61 MPa. The zero suction applied by distilled water led the sample to a maximum value of 4.39 MPa swelling pressure. This value is very close to that from test CV01(4.30 MPa) and CV02(4.37 MPa) in which the samples were flooded directly with water. This means there is no kinematic effect on the swelling pressure for the studied mixture.

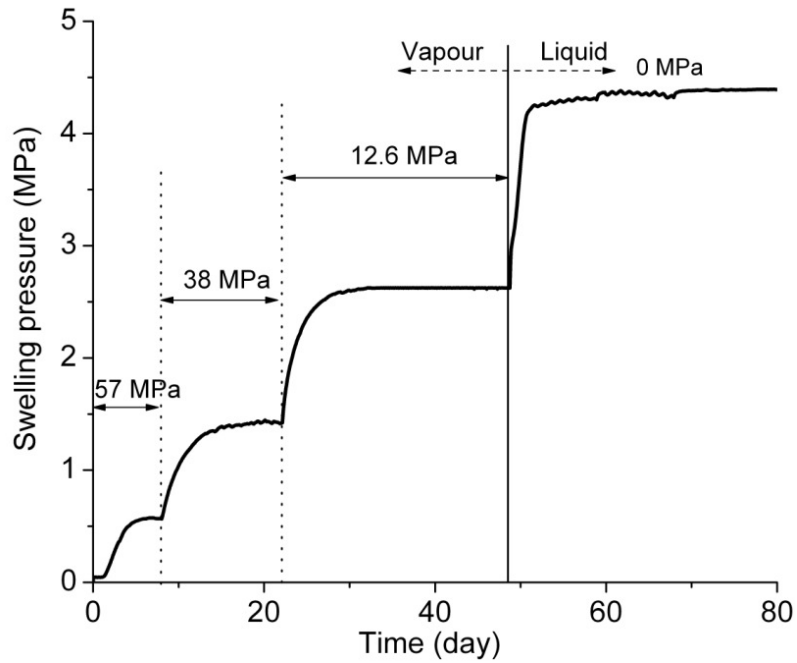


Figure 6. Evolution of swelling pressure for test CV03 during decreasing of suction.

Figure 7 presents the relationship between the swelling pressure ( $\sigma_s$  in MPa) and the suction ( $s$  in MPa), with the values obtained from test CV03. An exponential function can be used to satisfactorily describe this relationship:

$$\sigma_s = 4.9908 \times 10^{-0.0178s} \quad (\text{Eq.1})$$

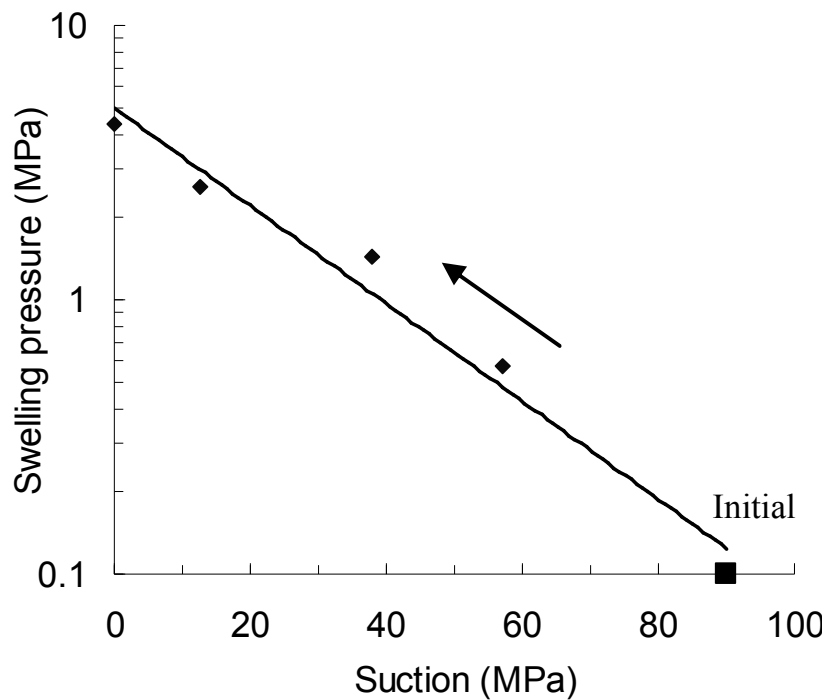


Figure 7. Swelling pressure versus suction of test CV03

In Figure 8, the whole results from the three tests CV01, CV02 and CV03 during one year are presented. It appears that after a long period of one year, there was just a slight decrease of swelling pressure and the values for the three samples still remain very close (4.23MPa, 4.32MPa and 4.29MPa for test CV01, CV02 and CV03, respectively). This shows a negligible effect of any bentonite-claystone interaction on the swelling pressure.

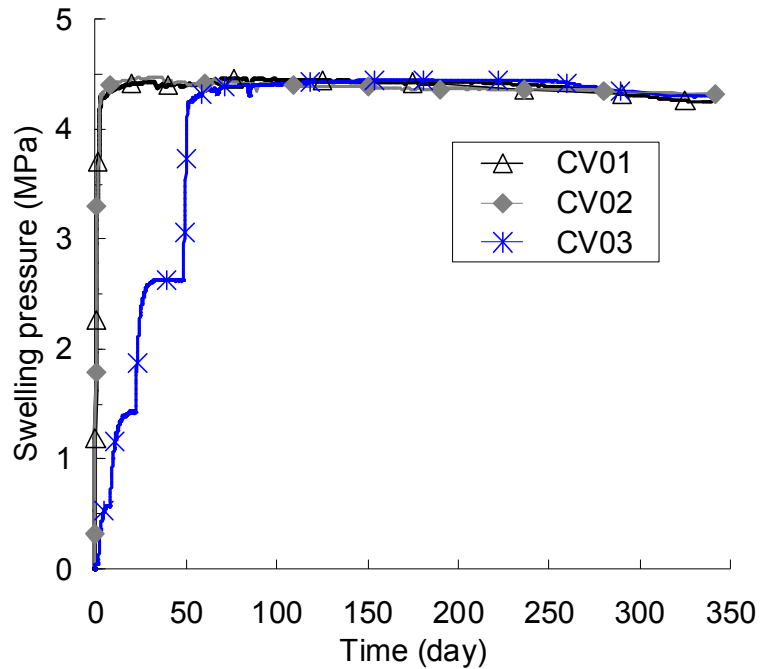


Figure 8. Evolution of swelling pressure for tests CV01, CV02, and CV03 for 1 year

The evolution of swelling pressure for the specimens having the same initial dry density of  $1.90 \text{ Mg/m}^3$  with different pre-swells is presented in Figure 9. An expected significant decrease of swelling pressure with increasing pre-swell is observed. For the pre-swells of 10, 20 and 25%, the swelling pressures obtained are 5.38, 2.03 and 0.7 MPa, respectively. Note that the maximum swelling strain from test PS04 reaches 43 %.

The results from test SCO1 using the swell-consolidation method are presented in Figure 10. As wetting up, the sample swelled under a low vertical pressure of 0.1 MPa and the maximum swelling strain reached 41.76%. Further compression gave a normal consolidation curve that allows the determination of the swelling pressure:  $\sigma_s = 22.20 \text{ MPa}$ .

For test ZSO1 (zero-swell method) on a sample at an initial dry density of  $1.70 \text{ Mg/m}^3$ , a vertical stress of 4.38 MPa was needed to keep the void ratio constant. By definition, this value is the swelling pressure by this method.

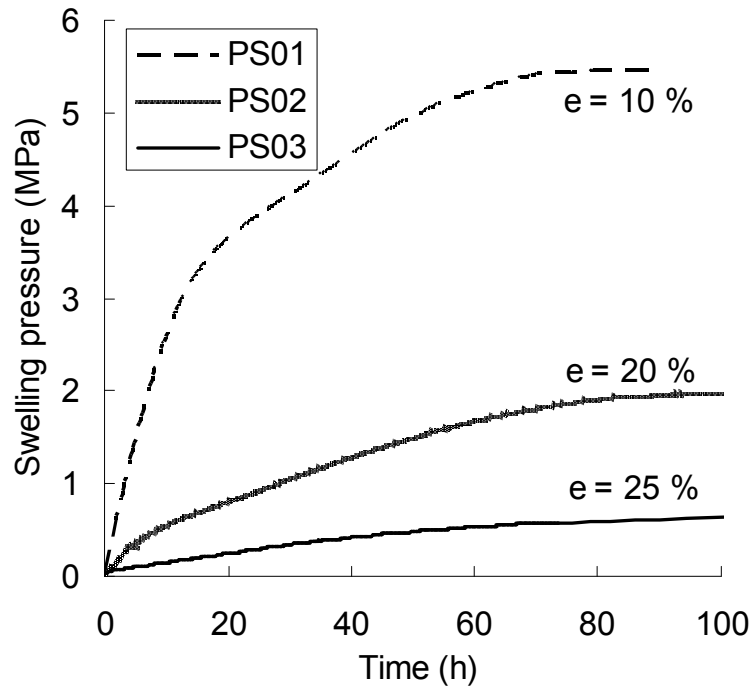


Figure 9. Evolution of swelling pressure with various pre-swells

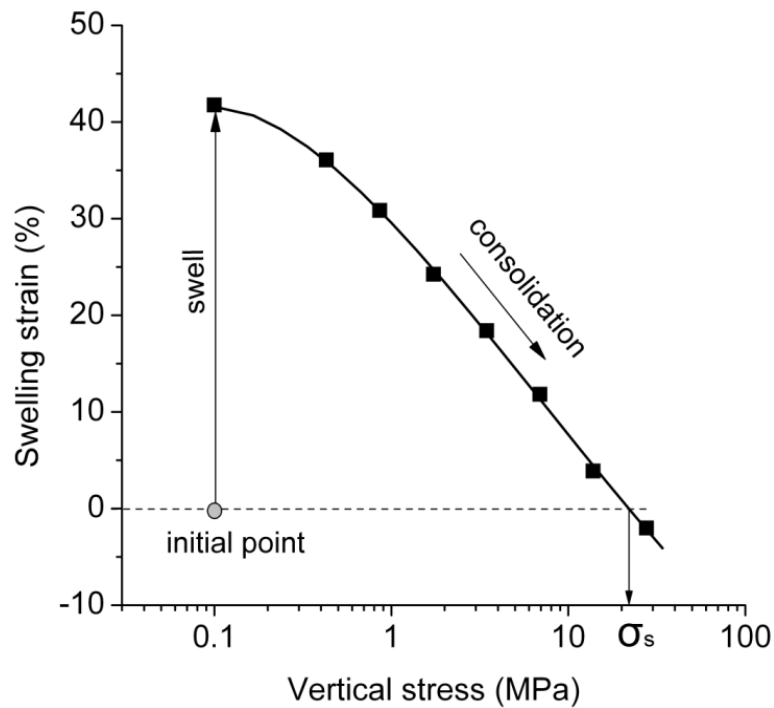


Figure 10. Swelling strain versus vertical stress applied for test SCO1

From the results in Figure 9, the swelling pressure is plotted versus the pre-swell strain in Figure 11. The maximum pre-swell of test PS04 and the swelling strain in SCO1 (swell consolidation method) are also presented in this figure. Note that all specimens had the same initial dry density of  $1.90 \text{ Mg/m}^3$  and all flooded with synthetic water. It appears that the result of SCO1 is close to that of PS04 (free swell) showing a good repeatability of the

free-swell tests. A linear correlation can be obtained between the swelling strain allowed ( $\varepsilon$  in %) and the logarithm of swelling pressure ( $\sigma_s$  in MPa):

$$\varepsilon = -19.32Lg(\sigma_s) + 23.946 \quad (\text{Eq.2})$$

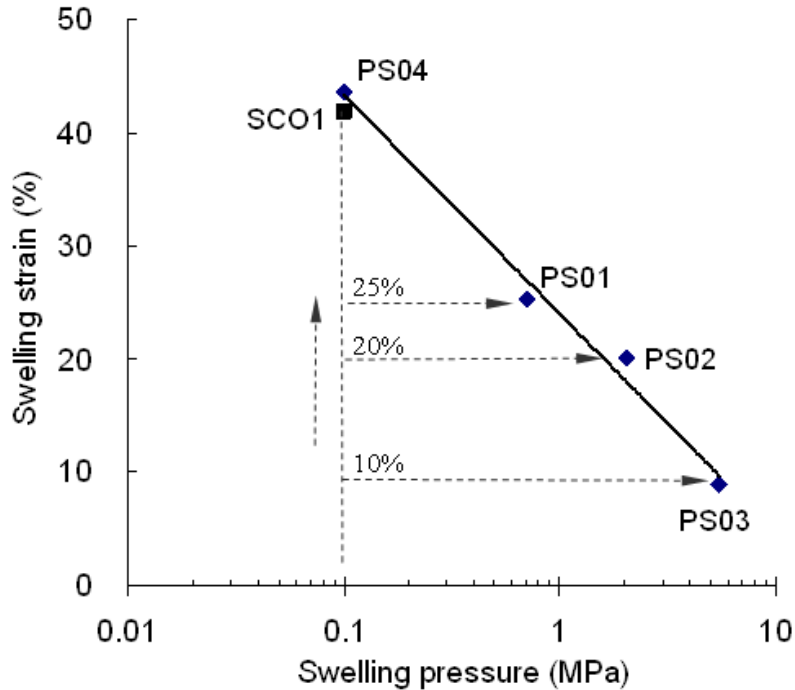


Figure 11. Pre-swell versus swelling pressure

In Figure 12, the swelling pressure determined by the pre-swell method (PS01, PS02, PS03, PS04), constant-volume method (CV02), zero swell method (ZSO1) are plotted in the plane of void ratio/logarithm of vertical stress, together with the consolidation line from test SCO1. Point O and O' correspond to the initial states of the samples at a dry density of  $1.90 \text{ Mg/m}^3$  (PS01, PS02, PS03, PS04 and SCO1) and  $1.70 \text{ Mg/m}^3$  (CV02 and ZSO1), respectively. It can be noted that at the same void ratio, the vertical stress of the consolidation curve (SCO1) is slightly higher than the swelling pressure determined by other methods.

Figure 13 shows the measured swelling pressure versus the final dry density of the bentonite/claystone mixture for all the tests. Note that these tests have been performed with two different initial dry densities ( $\rho_{di} = 1.90 \text{ Mg/m}^3$  for tests PS01, PS02, PS03, PS04, SCO1; and  $\rho_{di} = 1.70 \text{ Mg/m}^3$  for tests CV02, ZSO1), and using various methods (see Table 3). In spite of this, a unique correlation seems enough to describe the relationship between the swelling pressure  $\sigma_s$  (MPa) and the final dry density of the mixture  $\rho_{dm}$  ( $\text{Mg/m}^3$ ):

$$\sigma_s = 4.8 \times 10^{-7} \exp^{9.41\rho_{dm}} \quad \text{Eq.3}$$

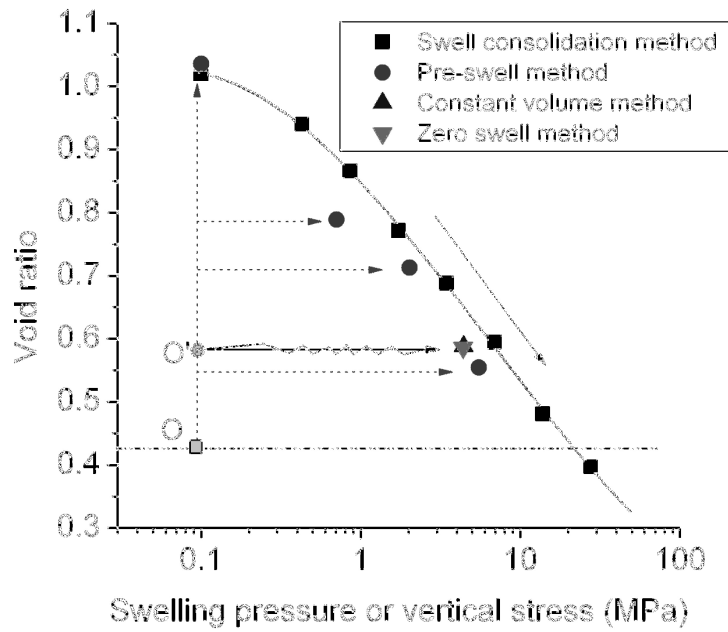


Figure 12. Swelling pressure or vertical pressure versus void ratio of mixture

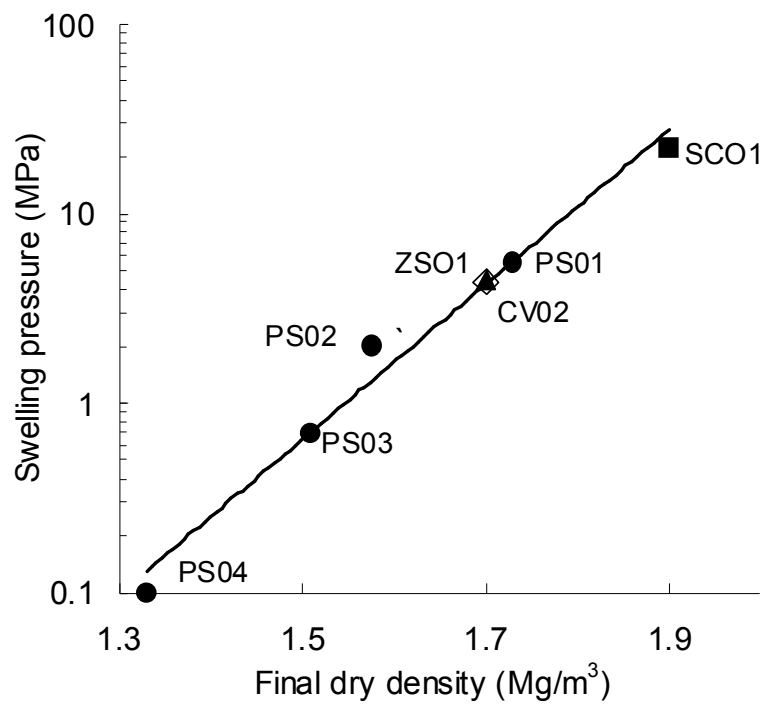


Figure 13. Swelling pressure versus final dry density of bentonite/claystone mixture

This shows that the swelling pressure of the compacted claystone/bentonite mixture is mainly dependent on the final dry density of the mixture. For a deeper analysis on the role of the bentonite itself in the swelling pressure development of the bentonite- based mixutre, the dry density of bentonite ( $\rho_{db}$ ) has been proposed by assuming that the water content of additives (claystone in this study) kept constant, while the water except this part was absorbed by bentonite. It means that the volume of bentonite ( $V_b$ ) is the difference between the total volume ( $V$ ) and the volume of additive (soil particles and water inside). Therefore the bentonite dry density can be calculated by the following equation:

$$\rho_{db} = \frac{(B/100)\rho_m G_{sa}}{G_{sa}(1 + w_m / 100) - \rho_m(1 - B/100)(1 + w_a)} \quad (\text{Eq.4})$$

where  $\rho_m$  ( $\text{Mg/m}^3$ ) is the mixture density;  $B$  (%) is the bentonite content (in dry mass) in the mixture;  $w_m$  is the water content of the mixture;  $w_a$  is the initial water content of the additive (equals zero for sand);  $G_{sa}$  is the specific gravity of additive. In this study,  $w_a = 2.64\%$ ,  $B = 70\%$ ,  $G_{sa} = 2.70$ .

Using Eq. 4, the results shown in Figure 13 were re-analysed and Figure 14 shows the variations of swelling pressure with the final dry density of bentonite. In the same figure, the results collected from other works on the MX80/sand mixture (Karland et al., 2008) and the pure MX80 bentonite (Karnland et al., 2008; Dixon et al., 1996) are also presented. A very similar relationship is obtained for the different data sets, showing that the swelling pressure mainly depends on the final dry density of bentonite, sand and claystone being both inactive components in the mixtures for the swelling pressure development.

To further investigate this point, results on other reference bentonites were collected and analysed in the same fashion. Figure 15 shows the variations of swelling pressure with the final dry density of MX80 (from Figure 14), FoCa7 (Imbert et al., 2006), FEBEX (Villar et al., 2002) and Kunigel V1 (Dixon et al., 1996). It appears that for each bentonite, there is a unique relationship between the swelling pressure and the final dry density of bentonite. However, the relationships are not the same. A general expression can be proposed:

$$\sigma_s = \alpha \times \exp^{\beta \rho_{db}} \quad \text{Eq.6}$$

Where  $\alpha$  and  $\beta$  are the two constants.

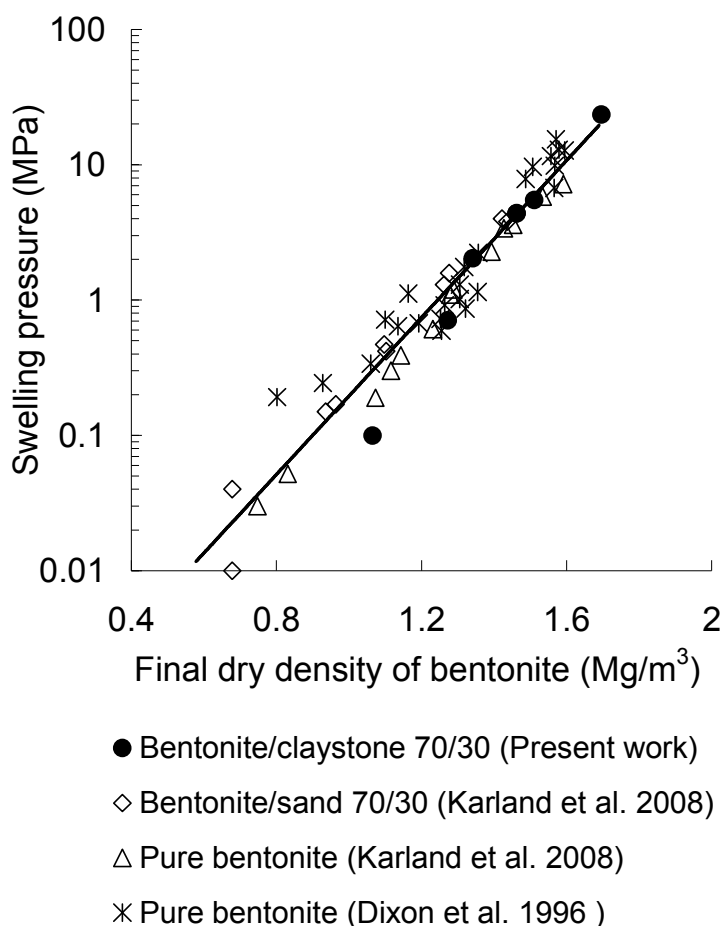


Figure 14. Results of various mixtures using MX80 bentonite - swelling pressure versus final dry density of bentonite

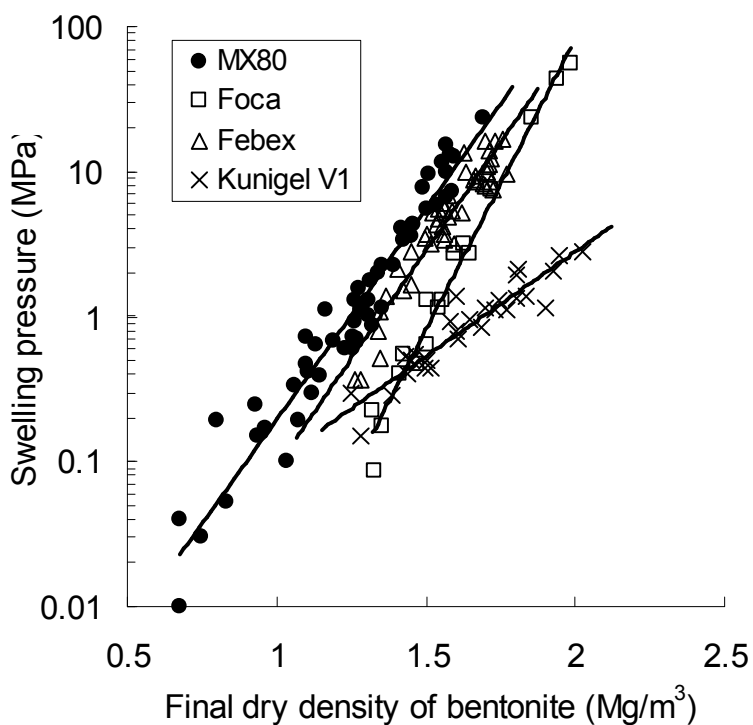


Figure 15. Swelling pressure versus final dry density of bentonite

Table 4 shows the values of  $\alpha$  and  $\beta$  for the four bentonites analysed. In the table, the mineralogy of these materials is also presented. The difference of parameters can be related to the different types of clay (i.e. montmorillonite, beidellite and saponite, etc), montmorillonite content and type of exchangeable cations (i.e. calcium or sodium). In general, the swelling capacity of sodium bentonite is higher than that of calcium bentonite; with the same type of exchangeable cations, a larger montmorillonite content leads to a higher swelling pressure.

Table 4 Montmorillonite content and external cations type of several bentonites

Bentonite	$\alpha$	$\beta$	Montmorillonite Content (%)	Type
MX 80	$1.78 \times 10^{-4}$	6.75	75-90	Na
FEBEX	$9.80 \times 10^{-5}$	6.85	92	Ca
FoCa	$7.83 \times 10^{-7}$	9.24	50 Beidellite, 50 Kaollite	Ca
Kunigel V1	$3.67 \times 10^{-3}$	3.32	48	Na

#### 4 Discussion

It has been observed that the effect of the chemistry of Bure site water on the swelling pressure is negligible. However, it is generally accepted that the swelling pressure decreases with the increase in salinity of the pore-water, although this decrease becomes less significant in case of high density (Karnland et al., 2005; Castellanos et al., 2008; Siddiqua et al., 2011; Komine et al., 2009). Castellanos et al. (2008) reported that the swelling pressure of the FEBEX bentonite compacted to a dry density of  $1.65 \text{ g/cm}^3$  decreases to almost half its initial value when 2 mol/L  $\text{CaCl}_2$  and NaCl/L solutions are used as saturating fluids; At low salinities (0.004 mol/L, granitic water), the swelling pressure of bentonite seems not to be affected by the salinity changes at a dry density ranging from 1.40 to  $1.70 \text{ Mg/m}^3$ . It appears that for the studied bentonite/claystone mixture, the high density and the low salinity of synthetic water together resulted in the negligible effect of water chemistry on the swelling pressure. This can be explained by the theory of cations filtration (Komine et al., 2009). For high dry density of bentonite based materials, the distances between the montmorillonite mineral layers being very small, these layers can filter the cations in the solution; on the contrary, in the case of low dry density, the cations in solution can infiltrate easily into the montmorillonite mineral layers due to the larger distances between them, thus affecting the swelling behaviour.

For the sample wetted with suction control (CV03), an exponential function was found between the swelling pressure and the suction applied. This can be explained as follows. As clay samples are exposed to humid water vapour, water molecules first migrate into the open channels and adsorbed on the exposed mineral surface (Pusch, 2001b; Arifin, 2008), then move to elementary clay layers. The number of water molecules absorbed by the clay layers depends on the relative humidity or suction (Pusch, 2001b; Saiyouri et al., 2004; Delage, 2006), and this water molecules number defines the swelling pressure of the sample. Therefore the swelling pressure is suction or relative humidity dependent. After the sample was flooded with distilled water, the maximum swelling pressure was found close to that obtained by water-flooding the sample directly, indicating the negligible effect of wetting procedure. This phenomenon can be explained by the mechanism identified by Cui et al. (2002): when hydrating by decreasing suction (57-38-12.6 MPa) under confined conditions, the size of macro-pores was progressively decreased, whereas the micro-pores remained almost un-affected. The micro-pores started to change only when the water saturation is approached. This suggests that step-wetting by suction control and direct saturation by water flooding may lead to similar final microstructures, thus similar final swelling pressures.

Yang et al. (2008) reported that the mineralogical composition of the bentonite will not be stable under the chemistry fluid infiltration and its properties may degrade over long time periods. Moreover, for the bentonite/claystone mixture used in this study, interaction of claystone with water and bentonite was suspected. This justifies the long swelling tests kept over one year. However, no any significant effects were observed on the swelling pressure. It is possible that one year test is not long enough and this point should be studied further with longer tests, giving the long-term nature of the nuclear waste disposal.

A linear correlation was observed between the pre-swelling strain and the logarithm of swelling pressure for the samples with the same initial dry density. This line defines the limit of swelling potential: the samples at the same initial state followed different stress-volume paths until reached this limit and then no further expansion occurred. This is consistent with the conclusion of Villar et al. (2008) and Siemens et al. (2009) who found a similar relation between swelling strain and swelling pressure. It can be seen that the final state of specimen controlled the swelling pressure: for the samples with the same initial state, different pre-swelling strains led to different final dry densities and thus resulted in different swelling pressure. Moreover, a unique relationship was observed between the swelling pressure and the final dry density of the samples whatever the initial dry density, the percentage of pre-swell

and the experimental method. This also enhances the conclusion that the final state of the sample controls the swelling pressure. Further analysis showed that the swelling pressure mainly depends on the final dry density of bentonite in the mixture. This observation is in agreement with the conclusion of Lee et al. (1999) and Agus (2005) who noted that the swelling pressure of bentonite/sand mixtures with different bentonite contents is a function of the final bentonite dry density. This suggests that the swelling mechanism of bentonite-based materials is the same as that of pure bentonites.

At the same void ratio, the swelling pressure determined by different methods was found slightly lower than the vertical stress needed to reach the same void ratio following the swell-reload path (swell-consolidation method). This was in agreement with the results by many other authors (Justo et al., 1984; Sridharan et al., 1986; Basma et al., 1995; Abdullah et al., 1998, 1999; Agus, 2005; Villar, 1999; Villar et al., 2008), and can be considered as a consequence of the coupling between the microstructure and macrostructure (Gens and Alonso, 1992; Villar, 1999; Sánchez et al., 2005). For the swell-consolidation oedometer test, wetting took place under a low vertical load and the void ratio increased greatly due to the large microstructural changes which led to more intense breakage of particle aggregates and hence to a more uniform distribution of the expandable component. In this case a higher vertical stress was needed to compensate the large macrostructure deformation. By contrast, smaller microstructure and macrostructure interaction were involved in other methods, giving rise to lower stress at full saturation. Furthermore, the relative larger displacement in the swell-consolidation oedometer test would mobilise higher friction and this friction can also contribute to the phenomenon observed.

## **5 Conclusion**

The swelling pressure of bentonite/claystone mixture was determined by different methods. The effects of the water chemistry, the hydration procedure, the pre-existing technical voids and the experimental methods on the swelling pressure were investigated. From the experimental results the following conclusion can be drawn.

There was no obvious effect of water chemistry on the swelling pressure due to the high density and the low salinity of synthetic water.

An exponential function was found between the swelling pressure and the suction applied; no effect of hydration procedure on the final swelling pressure was observed.

The swell-consolidation method gives higher swelling pressure mainly because of the coupling between the microstructure deformation and macrostructure deformation. The effect of friction is also to be considered for this phenomenon.

The swelling pressure of bentonite-based materials mainly depends on the final dry density of the bentonite in the mixture, suggesting that the swelling mechanism of bentonite-based materials is the same as that of pure bentonites. A general relationship between the swelling pressure and the final dry density of various bentonites was proposed, with two parameters depending on the montmorillonite content and the type of exchangeable cations.

From a practical point of view, the relationship elaborated between the swelling pressure and the final bentonite dry density is helpful in designing the sealing/filling buffers with bentonite-based materials: when the initial state of bentonite-based materials and the technical voids are known, the final swelling pressure can be predicted. Moreover, the crushed Cox claystone can be used to form the bentonite/claystone mixture because it behaves as sand. However it should be noted that this conclusion is based on the results from one year tests and further studies with longer tests are needed to gain more confidence on this aspect.

## **Acknowledgements**

This work was conducted within the framework of GM2 of the French National Agency for Nuclear Waste Management (ANDRA). The conclusions and the viewpoints presented in the paper are those of the authors and do not necessarily coincide with those of ANDRA. The support from the PHC Cai Yuanpei project (24077QE) and that of the China Scholarship Council (CSC) are also greatly acknowledged.

## **References**

- Abdullah, I., Mhaidib, A., 1998. Prediction of swelling potential of an expansive shale. Proceedings Of The Second International Conference On unsaturated soils. 27-30 August. Beijing, China: vol. 1.
- Abdullah, I., Mhaidib, A.I., 1999. Swelling behaviour of expansive shales from the middle region of Saudi Arabia. *Geotechnical and Geological Engineering*. 16(4):291–307.
- Agus, S., 2005. An Experimental study on hydro-mechanical characteristics of compacted bentonite-sand mixtures. PhD thesis. Weimar.
- Agus, S., Schanz, T., 2005. Swelling pressures and wetting-drying curves of a highly compacted bentonite-sand mixture. *Unsaturated Soils: Experimental Studies*, pages 241–256.
- Andra, 2005. Référentiel des matériaux d'un stockage de déchets à haute activité et à vie longue – Tome 4: Les matériaux à base d'argilites excavées et remaniées. Rapport Andra N° CRPASC040015B.

- Arifin, Y.F., 2008. Thermo-hydro-mechanical behavior of compacted bentonite sand mixtures: An Experimental Study. PhD thesis. Weimar.
- Attom, M.; Abu-Zreig, M. & Obaidat, M. 2001. Changes in clay swelling and shear strength properties with different sample preparation techniques. *ASTM geotechnical testing journal*, ASTM, 24, 157-163.
- Barnichon, J.D., and Deleruyelle, F., 2009. Sealing Experiments at the Tournemire URL. Towards convergence of technical nuclear safety practices in Europe, EUROSAFE.
- Basma, A.A., Al-Homoud, A.S., Husein, A., 1995. Laboratory assessment of swelling pressure of expansive soils. *Applied Clay Science*, 9(5):355–368.
- Borgesson, L. 1985. Water flow and swelling pressure in non-saturated bentonite-based clay barriers. *Engineering Geology*, 21(3-4):229–237.
- Borgesson, L., Chijimatsu, M., Fujita, T., Nguyen, T.S., Rutqvist, J., Jing, L., 2001. Thermo-hydro-mechanical characterisation of a bentonite-based buffer material by laboratory tests and numerical back analyses. *International Journal of Rock Mechanics and Mining Sciences*, 38(1):95–104.
- Castellanos, E., Villar, M.V., Romero, E., Lloret, A., Gens, A., 2008. Chemical impact on the hydro-mechanical behaviour of high-density febex bentonite. *Physics and Chemistry of the Earth, Parts A/B/C*, 33(Supplement 1):S516 – S526.
- Cui, Y. J., Loiseau, C., Delage, P., 2002. Microstructure changes of a confined swelling soil due to suction controlled hydration Unsaturated soils: proceedings of the Third International Conference on Unsaturated Soils, UNSAT 2002, 10-13 March 2002, Recife, Brazil, 593.
- Cui, Y.J., Tang, A.M., Loiseau, C., Delage, P., 2008. Determining the unsaturated hydraulic conductivity of a compacted sand-bentonite mixture under constant-volume and free-swell conditions. *Physics and Chemistry of the Earth, Parts A/B/C*, 33(Supplement 1): 462 – S471.
- Day, R.W. 1994. Swell-shrink behaviour of expansive compacted clay. *J. Geotechnical Engineering*, ASCE 120, No. 3, 618–623.
- Delage, P., Howat, M. D. & Cui, Y. J., 1998. The relationship between suction and swelling properties in a heavily compacted unsaturated clay. *Engineering Geology* 50, 31-48.
- Delage, P., Marcial, D., Cui, Y.J., and Ruiz, X., 2006. Ageing effects in a compacted bentonite: a microstructure approach. *Geotechnique*, 56(5):291–304.
- Delage, P. 2006. Some microstructure effects on the behaviour of compacted swelling clays used for engineered barriers. *Chinese Journal of Rock Mechanics and Engineering*, Science Press(Beijing), 16 Donghuangchenggen North St, Beijing, 100717, China., 25, 721-732.
- Delage, P., Cui, Y.J., Tang, A.M., 2010. Clays in radioactive waste disposal, *Journal of Rock Mechanics and Geotechnical Engineering*, Vol (2):111–123.
- Dixon, D.A., Gray, M.N., Graham, J., 1996. Swelling and hydraulic properties of bentonites from Japan, Canada and USA. In *Proceedings of the second International Congress on Environmental Geotechnics*, Osaka, Japan, pages 5–8.
- Dixon, D.A., Graham, J., and Gray, M.N., 1999. Hydraulic conductivity of clays in confined tests under low hydraulic gradients. *Canadian Geotechnical Journal*, 36(5):815–825.
- Gens, A., Alonso, E.E. 1992. A framework for the behaviour of unsaturated expansive clays. *Canadian Geotechnical Journal*, 29(6):1013–1032.
- Hoteit N, Ozanam-O, Su, K. 2000. Geological radioactive waste disposal project in france- conceptual model of a deep geological formation and underground research laboratory in Meuse Haute-Marne site. In *The 4th North American Rock Mechanics Symposium*, Seattle, July 31-August 3.

- Imbert, C., and Villar, M.V., 2006. Hydro-mechanical response of a bentonite pellets-powder mixture upon infiltration. *Applied Clay Science*, 32(3-4):197–209.
- Justo, J.L., Delgado, A., Ruiz, J., 1984. The influence of stress-path in the collapse-swelling of soils at the laboratory. In *Fifth International Conference on Expansive Soils 1984*. Australia. Page 67.
- Karlund, O., Muurinen, A., Karlsson, F., 2005. Bentonite swelling pressure in NaCl solutions-Experimentally determined data and model calculations. *Advances in Understanding Engineering Clay Barriers*. Page 241.
- Karlund, O., Nilsson, U., Weber, H., and Wersin, P., 2008. Sealing ability of Wyoming bentonite pellets foreseen as buffer material-Laboratory results. *Physics and Chemistry of the Earth, Parts A/B/C*, 33:S472–S475.
- Kenney, T.C., Veen, W.A.V., MA Swallow, and Sungaila., M.A., 1992. Hydraulic conductivity of compacted bentonite-sand mixtures. *Canadian Geotechnical Journal*, 29(3):364–374.
- Komine., H., Ogata, N. 1994. Experimental study on swelling characteristics of compacted bentonite. *Canadian geotechnical journal*, 31(4):478–490.
- Komine., H., Ogata, N. 1998. Thermal influence on compacted bentonite for nuclear waste disposal. In *Proceedings of the 3rd International Congress on Environmental Geotechnics*, volume 1, pages 34–39.
- Komine., H., Ogata, N. 2003. New equations for swelling characteristics of bentonite-based buffer materials. *Canadian Geotechnical Journal*, 40(2):460–475.
- Komine., H., Ogata, N. 2004a. Predicting swelling characteristics of bentonites. *Journal of Geotechnical and Geoenvironmental engineering*, 130:818.
- Komine, H., 2004b. Simplified evaluation for swelling characteristics of bentonites, *Engineering geology*, 71(3-4): 265-279.
- Komine, H. Yasuhara, K. and Murakami, S. 2009. Swelling characteristics of bentonites in artificial seawater. *Canadian Geotechnical Journal*, 46(2):177-189.
- Kröhn, K.P. 2003. Results and interpretation of bentonite resaturation experiments with liquid water and water vapour. In: Schanz, T. (Ed.), *Proceedings of the International Conference from Experimental Evidence towards Numerical Modeling of Unsaturated Soils*, Weimar, Germany, vol. 1. 598 Springer, Berlin, pp. 257–272.
- Lebon, P. and Ghoreychi, M. 2000. French underground research laboratory of Meuse, Haute-Marne THM aspects of argillite formation. In *Eurock 2000 Symposium*, March, pages 27–31.
- Lee, J.O., Cho, W.J. and Chun, K.S., 1999. Swelling Pressures of a Potential Buffer Material for High-Level Waste Repository. *Journal of the Korean Nuclear Society*, 31: 139-150.
- Lemaire, T., Moyne, C., and Stemmelen, D., 2004. Imbibition test in a clay powder (MX-80 bentonite). *Applied Clay Science*, 26(1-4):235–248.
- Li, X.L., Bastiaens, W., Van Marcke, P., et al., 2009. Design and Development of the Large Scale In-situ PRACLAY Heater Test and Horizontal HLW Disposal Gallery Seal Test in Belgian URL Hades, *International Symposium on Unsaturated Soil Mechanics and Deep Geological Nuclear Waste Disposal*, Shanghai, China: 24—28.
- Loiseau, C., Cui, Y.J. and Delage, P., 2002. The gradient effect on the water flow through a compacted swelling soil, In: *Proc. 3rd Int Conf Unsaturated Soils, UNSAT 2002*, Recife, Brazil, Balkema 1:395 - 400.
- Nagaraj, H.; MOHAMMED Munnas, M.; Sridharan,A., 2009. Critical Evaluation of Determining Swelling Pressure by Swell-Load Method and Constant Volume Method, *ASTM geotechnical testing journal*, ASTM, 32, 305-314.

- Nalezny, C. L. & Li, M. C., 1967. Effects of soil moisture and thixotropic hardening on the swell behaviour of compacted expansive soils. Highway Res. Rec. Washington, DC: Highway Research Board. No. 209.
- Pusch, R., 1979. Highly compacted sodium bentonite for isolating rock-deposited radioactive waste products. Nuclear Technology. 45(2):153-157.
- Pusch, R. 1980. Swelling pressure of highly compacted bentonite. SKBF/KBS technical report: No.80-13.
- Pusch, R., 1982. Mineral-water interactions and their influence on the physical behavior of highly compacted Na bentonite. Canadian Geotechnical Journal, 19(3):381–387.
- Pusch, R., 2001a. Experimental study of the effect of high porewater salinity on the physical properties of a natural smectitic clay, SKBF/KBS technical report. No.TR01-07.
- Pusch, R. 2001b. The microstructure of MX-80 clay with respect to its bulk physical properties under different environmental conditions, SKBF/KBS technical report. No.TR01-08.
- Romero, E., Gens, A., and Lloret, A., 2001. Temperature effects on the hydraulic behaviour of an unsaturated clay. Geotechnical and Geological Engineering, 19(3):311–332.
- Saiyouri, N., Tessier, D., and Hicher, P.Y., 2004. Experimental study of swelling in unsaturated compacted clays. Clay Minerals, 39(4):469.
- Sanchez, M., Gens, A., Do Nascimento Guimarães, L., Olivella, S., 2005. A double structure generalized plasticity model for expansive materials. International Journal for Numerical and Analytical Methods in Geomechanics, 29(8):751–787.
- Siddiqua, S.; Blatz, J. & Siemens, G. 2011. Evaluation of the impact of pore fluid chemistry on the hydromechanical behaviour of clay-based sealing materials. Canadian Geotechnical Journal, NRC Research Press, 48, 199-213.
- Siemens, G., and Blatz, J.A., 2009. Evaluation of the influence of boundary confinement on the behaviour of unsaturated swelling clay soils. Canadian Geotechnical Journal, 46(3):339–356.
- Sridharan, A., Rao, S., Sivapullaiah, P.V., 1986. Swelling pressure of clays. ASTM geotechnical testing journal, 9(1):24–33.
- Sugita, Y., Chijimatsu, M., and Suzuki, H., 2005. Fundamental properties of bentonite pellet for Prototype Repository Project. Advances in Understanding Engineering Clay Barriers, page 293.
- Suzuki, S.; Prayongphan, S.; Ichikawa, Y. & Chae, B. 2005. In situ observations of the swelling of bentonite aggregates in NaCl solution, Applied Clay Science, Elsevier, 29: 89-98.
- Subba Rao, K. S. & Tripathy, S. 2003. Effect of aging on swelling and swell-shrink behaviour of a compacted expansive soil. ASTM Geotech. Test. J. 26, No. 1, 36–46.
- Tang, A.M., Cui, Y.J., 2005. Controlling suction by the vapour equilibrium technique at different temperatures and its application in determining the water retention properties of MX80 clay. Canadian Geotechnical Journal, 42 (1): 287-296.
- Tang, A.M., Cui, Y.J., Barnel, N., 2007. A new isotropic cell for studying the thermo-mechanical behavior of unsaturated expansive soil. Geotechnical Testing Journal, 30 (5): 341 – 348.
- Tang, A.M., Cui, Y.J., Barnel, N., 2008a. Thermo-mechanical behaviour of a compacted swelling clay. Géotechnique, 58 (1): 45-54.
- Tang, A.M., Cui, Y.J., Le, T.T., 2008b. A study on the thermal conductivity of compacted bentonites. Applied Clay Science, 41 (3-4): 181 – 189.
- Tang, A.M., Cui, Y.J., 2009. Modelling the thermo-mechanical behaviour of compacted expansive clays. Géotechnique, 59 (3): 185-195.

- Tang, C.S., Tang, A.M., Cui, Y.J., Delage, P., Barnichon, J.D., Shi, B., 2011a. A study of the hydro-mechanical behaviour of compacted crushed argillite. *Engineering Geology*, 118 (3-4):93-103.
- Tang, C.S., Tang, A.M., Cui, Y.J., Delage, P., Schroeder, C., De Laure, E., 2011b. Investigating the Swelling Pressure of Compacted Crushed-Callovo-Oxfordian Argillite. *Physics and Chemistry of the Earth*. (accepted)
- Villar, M.V., Lloret, A., 2004. Influence of temperature on the hydro-mechanical behaviour of a compacted bentonite. *Applied Clay Science*, 26(1-4):337 – 350.
- Villar, M.V., 1999. Investigation of the behaviour of bentonite by means of suction-controlled oedometer tests. *Engineering Geology*, 54(1-2):67–73.
- Villar, M.V., 2002. Thermo-hydro-mechanical characterisation of a bentonite from Cabo de Gata. A study applied to the use of bentonite as sealing material in high level radioactive waste repositories. *Publicación Técnica ENRESA 01/2002*, Madrid, 258 pp.
- Villar, M.V., Lloret, A., 2008. Influence of dry density and water content on the swelling of a compacted bentonite. *Applied Clay Science*, 39(1-2):38–49.
- Yang, J., Samper, C., and Montenegro, L., 2008. A coupled non-isothermal reactive transport model for long-term geochemical evolution of a HLW repository in clay. *Environmental Geology*, 53(8):1627–1638.
- Yong, R.N., Boonsinsuk, P., and Wong, G., 1986. Formulation of backfill material for a nuclear fuel waste disposal vault. *Canadian Geotechnical Journal*, 23(2):216–228.
- Zhang, C., and Rothfuchs, T., 2004. Experimental study of the hydro-mechanical behaviour of the Callovo-Oxfordian argillite. *Applied Clay Science*, 26(1-4):325–336.

## **Chapter 2. Long-term effect of water chemistry on the swelling pressure**

### **INTRODUCTION**

Over the long time lifespan of the repository, especially in some geological host formations relatively rich in salts (e.g. salt formation, claystone, granite formations, etc.), site water of certain salinity can interact with bentonite (Herbert et al., 2008); as a result, the hydro-mechanical performance of the bentonite-based material and in turn the safety of the barrier could be notably affected. This effect may be more obvious for the bentonite/ COx claystone mixture which is proposed as a possible sealing/backfill material (Andra, 2005; Tang et al., 2011a; Tang et al., 2011b; Wang et al., 2012a), because of the extra interaction between these two materials. Due to the low permeability of the bentonite-based materials, effects of these interactions could be significant over time. Hence, a particular attention should be paid to their long-term behaviour.

In this context, the swelling pressure of the compacted mixture of MX80 bentonite and crushed COx claystone are investigated. The effects of water chemistry on the swelling pressure are studied in both short and long terms. The results are analysed by considering the physico-chemical interaction between the minerals of claystone, minerals of bentonite and different fluids involved. The kinetics of swelling pressure is also investigated by comparing a one-step soaking test with multistep soaking test. The results are presented in a paper submitted to the journal «Applied Clay Sciences», the manuscript is presented in this chapter.

Wang, Q., Tang, A. M., Cui, Y.J., Delage, P., Gatmiri, B. 2012. Submitted to Applied Clay Science

## Long-term effect of water chemistry on the swelling pressure of a bentonite-based material

Q. Wang<sup>1</sup>, A.M. Tang<sup>1</sup>, Y.J. Cui<sup>1</sup>, P. Delage<sup>1</sup>, B. Gatmiri<sup>2</sup>

**Abstract:** The compacted bentonite-based material was proposed as possible sealing and backfill material in the high-level radioactive waste disposal in several countries. During the long time lifespan of the repository, as the chemical composition of pore water can change, the swelling and sealing capacity of the material could also change. From a point of view of storage safety assessment, it is important to evaluate this possible change of swelling capacity. In this study, a mixture of bentonite and crushed Callovo-Oxfordian claystone is investigated. The long-term effect of pore water chemistry on the swelling pressure was studied at constant-volume conditions for 700 days. Distilled water and synthetic water having the chemical composition similar to that of in-situ pore water were used for hydration. The results obtained during the 100 days show that there is no significant influence of the water nature on the swelling pressure evolution, and the maximum swelling pressures observed were close to 4.30 MPa. For longer time, on the contrary, the swelling pressure decreased for all samples, especially for the sample saturated with synthetic water. In addition, comparison of a one-step soaking test with a multi-step soaking test showed no difference in kinetics of swelling pressure. All the results are analysed by considering the physico-chemical interaction between the minerals of claystone, minerals of bentonite and different fluids involved.

**Keywords:** Radioactive waste disposal; MX80 bentonite; Callovo-Oxfordian claystone; swelling pressure; chemical properties; laboratory test.

---

### 1 Introduction

Compacted bentonite-based materials have been proposed as possible sealing/backfill materials in the deep geological repository for high-level radioactive wastes (HLW) in several countries. Due to their favourable swelling characteristics, these materials are expected to fill up all the voids appeared during the construction process and build up a relatively impermeable zone around the high-level radioactive waste. This role termed “self-sealing” (Komine, 2004; Komine and Ogata, 2003) is essential to ensure the overall safety of the geological disposal: the disposed waste is isolated from the biomass over long periods of time. For this purpose, the swelling properties become a key factor in the design and development of the sealing/backfill materials, and needs to be studied in depth.

The swelling properties (i.e. swelling pressure or swelling potential) of bentonite-based

---

1 Ecole des Ponts ParisTech, UR Navier/CERMES

2. ANDRA, France

materials have been widely investigated (Pusch, 1982; Komine and Ogata, 1994, 2003, 2004a; Delage et al., 1998; Agus and Schanz, 2005; Komine et al., 2009). They depend strongly on the initial state such as dry density and water content (Komine and Ogata, 1994; Villar and Lloret, 2008). After being installed in the field, especially in some geological host formations relatively rich in salts (e.g. salt formation, claystone, granite formations, etc.), site water of certain salinity can interact with bentonite (Herbert et al., 2008); as a result, the hydro-mechanical performance of the bentonite-based material and in turn the safety of the barrier could be notably affected.

Very often, bentonite/sand mixtures are considered for the reasons of good control of swelling pressure, large thermal conductivity and a better mechanical resistance. For example, a 70/30 bentonite-sand mixture was proposed as buffer material in Japan while a 50/50 bentonite/sand mixture was suggested in the Canadian repository concept. In France, Callovo-Oxfordian (COx) claystone is being considered as a possible geological host-rock for high-level radioactive waste disposal, and the mixture of bentonite and crushed Callovo-Oxfordian (COx) claystone is proposed as a possible sealing/backfill material for the economical and environment reason (Andra, 2005; Tang et al., 2011a; Tang et al., 2011b; Wang et al., 2012). If physico-chemical interactions take place only between groundwater and bentonite in the case of sand/bentonite mixture, it is not the case for the bentonite/claystone because of the extra interaction between these two materials. Due to the low permeability of the bentonite-based materials, the effects of these interactions could be significant over time. Hence, particular attention should be paid to their long-term behaviour.

This study focuses on the swelling pressure of the compacted mixture of MX80 bentonite and crushed COx claystone. The long term effect of water chemistry on the swelling pressure and microstructure were investigated after soaking for 700 days. Emphasis was put on the physico-chemical interaction between the minerals of claystone, minerals of bentonite and different fluids involved. The kinetics of swelling pressure was also investigated by comparing a one step soaking test with multistep soaking test.

## **2 Materials and methods**

### **2.1 Materials**

The bentonite used in this study is a commercial MX80 Na-bentonite, which contains large quantities of montmorillonite (75-90%). Silt is the dominant remaining fraction, which mainly consists of quartz and feldspars as well as micas, sulphides, and oxides (Pusch 1982). Table 1

details the main mineralogical components of MX80 bentonite obtained by several authors. The total cation exchange capacity (CEC) is between 0.78 and 0.85 meq/g (Table 2), the cation population at exchange positions is mainly composed of Na<sup>+</sup> (60.0-67.0 meq/100g), other population being much lower: Ca<sup>2+</sup> (5.0-8.0 meq/100g), Mg<sup>2+</sup> (3.0-4.0 meq/100g) and K<sup>+</sup> (0.2-1.3 meq/100g).

Table 1 Mineral components of MX80 bentonite (%)

Researchers	Lajudie et al., 1996	Herbert et al., 2004	Madsen, 1998	Marty, 2010
Montmorillonite	75	90	75.5	84.35
Pyrite	0.3	<1	0.3	0.31
Calcite	1.4	<2	1.4	0.97
Quartz	15.2	4	15	7.03
Feldspars	5-8	2	5-8	4.56
Micas				2.78
Organic matter	0.4		0.4	

Table 2 Exchangeable cations in meq/100g of MX80 bentonite

Researchers	CEC	Na <sup>+</sup>	K <sup>+</sup>	Mg <sup>2+</sup>	Ca <sup>2+</sup>
Pusch (1982)		60.0	-	3.0	5.0
Madsen (1998)		62.4	0.2	3.0	7.4
Herbert (2002)	78-85	62.4-66.8	0.2-1.3	3-4	6.6-7.4
Bradbury (2003)		66.8	1.3	4.0	6.6
Karland (2006)	80	67.0	1.0	5.0	8.0

The grain size distribution (Fig.1) determined by hydrometer (AFNOR NF P94-057) shows that fraction of clay-size particles (< 2 μm) is 84%. The bentonite tested has an average specific gravity of 2.76, a liquid limit of 520%, and a plastic limit of 42%.

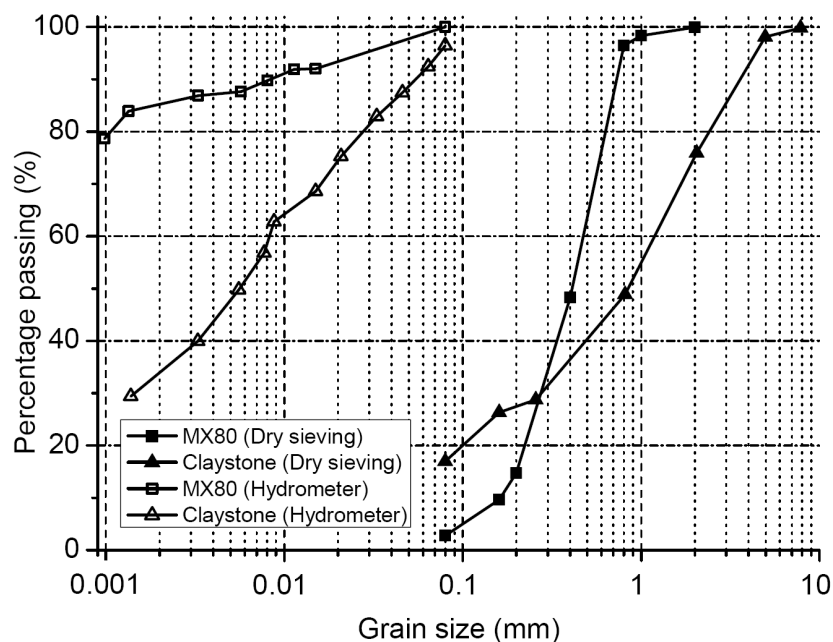


Figure 1. Grain size distribution of MX80 bentonite and crushed COx claystone

Callovo-Oxfordian (COx) claystone was taken at 490-m depth from the Underground Research Laboratory (URL) at Bure in eastern France. It contains 40–45% clay minerals (mainly interstratified minerals of illite–smectite), 20–30% carbonates (mainly calcite) and 20–30% quartz and feldspar (Hoteit et al., 2000; Lebon and Ghoreychi, 2000; Zhang et al., 2004). The in-situ water content is 2.8–8.7 %; the bulk density is 2.32–2.61 Mg/m<sup>3</sup> and the specific gravity is 2.70 (Hoteit et al., 2000; Tang et al., 2011a). The excavated claystone was air-dried and crushed. Fig.1 give the grain size distribution of the crushed powder obtained by dry sieving, it contains 18% of fine grains (0.08 mm). The grain size distribution determined by hydrometer confirms that the content of clay-size particles (< 2 μm) is 40%.

Both distilled water and synthetic water were used for hydration. The chemical composition of the synthetic water (see Table 3) is similar to that of the groundwater at Bure site. The pH values are between 7.00 and 7.28; the concentration of Na<sup>+</sup> is twice that of Ca<sup>2+</sup> and Mg<sup>2+</sup> and four times that of K<sup>+</sup> (Gaucher et al., 2006; Marty et al., 2010).

Table 3 Chemical composition of the synthetic water

Components	NaHCO <sub>3</sub>	Na <sub>2</sub> SO <sub>4</sub>	NaCl	KCl	CaCl <sub>2</sub> ·2H <sub>2</sub> O	MgCl <sub>2</sub> ·6H <sub>2</sub> O	SrCl <sub>2</sub> ·6H <sub>2</sub> O
Mass (g) per 1L solution	0.28	2.216	0.615	0.075	1.082	1.356	0.053

## 2.2 Sample preparation

All tests in this study were performed on samples of compacted bentonite/claystone mixture with a bentonite content of 70 % in dry mass. Bentonite and claystone powders, with the initial water contents of 11.8 % and 2.64 % respectively, were first carefully mixed prior to compaction. Samples were statically compacted to a dry density of  $1.70 \text{ Mg/m}^3$  in a metallic cell (70 mm in internal diameter) at a controlled rate of 0.05 mm/min. The total suction measured in these specimens using a hygrometer was  $s = 90 \text{ MPa}$ . After compaction, the specimen was carefully introduced into the constant-volume cell (having the same diameter as the compaction cell) for the swelling pressure experiment.

## 2.3 Experimental methods and programme

The constant-volume cell used in this study is presented in Fig.2. It includes three parts: (1) the bottom part containing a porous stone and a drainage system; (2) the middle cell (70 mm inner diameter) used to prevent radial swelling, with two air outlets; (3) the top part incorporating a total pressure sensor to monitor the swelling pressure. The soil sample was wetted by connecting the water inlet to a water reservoir or a suction control system using vapour equilibrium technique. More details can be found in Tang et al. (2011b), Wang et al. (2012).

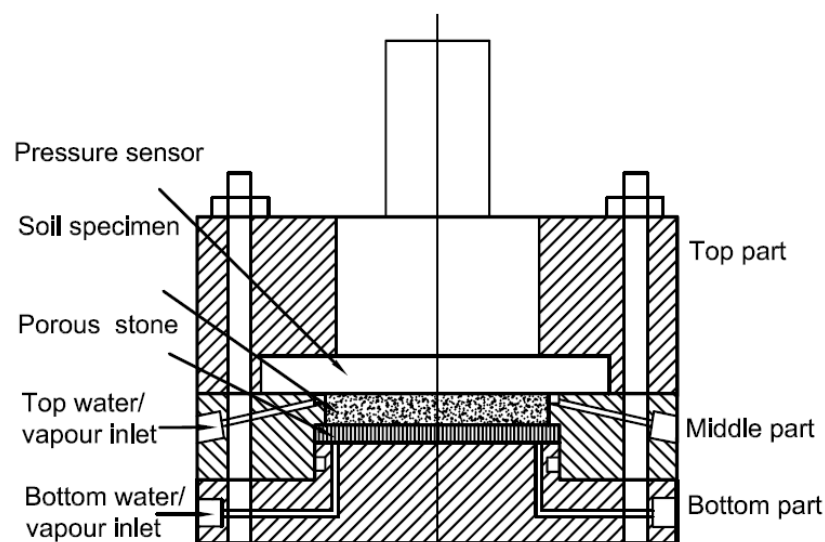


Figure 2. Constant-volume cell for measuring the swelling pressure

Four swelling pressure tests were performed using the constant-volume cell (Table 4). In tests LT01 and LT02 (LT stands for long term), the samples were saturated with synthetic water and distilled water, respectively, and the tests duration was 700 days. They were carried out to

study the long-term effect of water chemistry on the swelling pressure. In test LT03, three suctions (57 MPa, 38 MPa and 12.6 MPa) were first applied in steps using vapour equilibrium technique, prior to distilled water flooding in the last stage. This test also lasted 700 days. This test was performed to compare with test LT02 in order to investigate the kinetics of swelling pressure. Test ST (ST for short term) was performed by directly injecting synthetic water as in test LT01, with a shorter duration of 100 h. At the end of each test, soil specimen was taken out of the cell for the analysis of pore-size distribution by Mercury Intrusion Porosimetry (MIP).

Table.4 Test programme

Test No.	Injected water	Duration
LT01	Synthetic	700 days
LT02	Distilled	700 days
LT03	Vapour-distilled	700 days
ST	Synthetic	100 h

### 3 Experimental results

Fig.3 presents the results from tests LT01, LT02, and ST during the first 100 h after the injection of water. The three curves are very similar, showing negligible effect of water chemistry for this duration and also the good repeatability of the tests. With water infiltration, swelling pressure first increased very quickly; after about 20 h the swelling pressure reached a first stability stage at about 3.4 MPa. At 32 h, the swelling pressure restarted to increase and it reached a second stability stage at 100 h. The final values were in the range of 4.30 – 4.37 MPa for the three tests.

The results of test LT03 is presented in Fig.4. The application of the first suction of 57 MPa resulted in a swelling pressure of 0.57 MPa. Then, the second suction of 38 MPa was applied and the swelling pressure reached 1.43 MPa. With the third suction of 12.6 MPa the swelling pressure increased to 2.61 MPa. The zero suction applied by distilled water led the sample to a maximum value of 4.39 MPa swelling pressure. This value is very close to that from test LT02 (4.37 MPa) in which the procedure did not affect the final swelling pressure for this material.

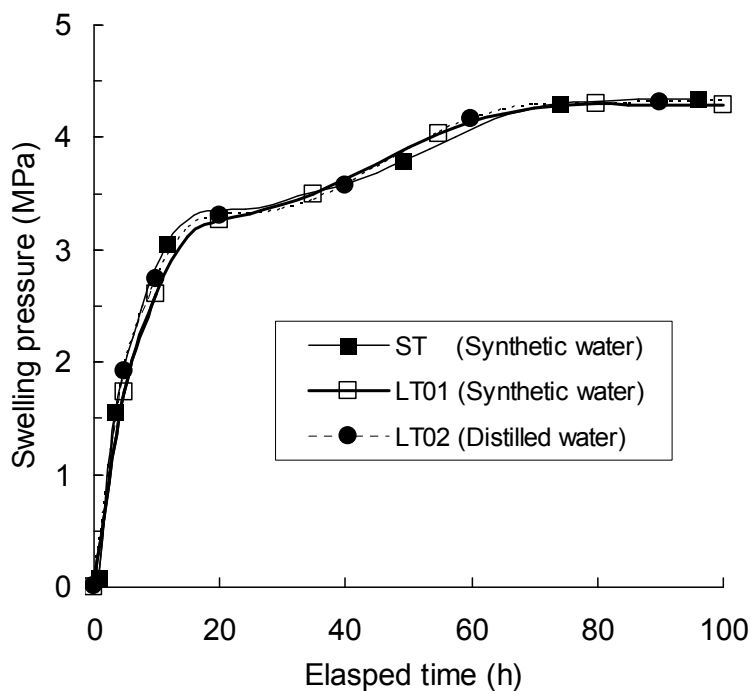


Figure 3. Evolution of swelling pressure for tests LT01, LT02 and ST during the first 100 h

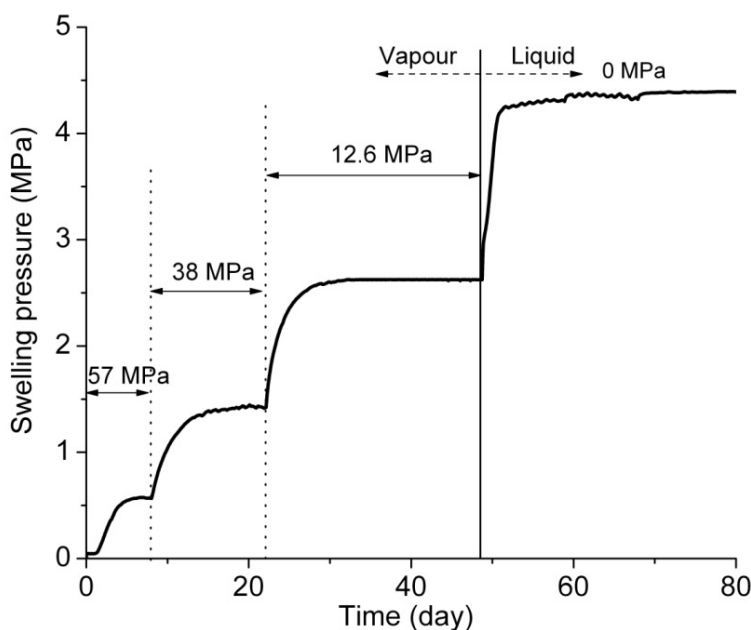


Figure 4. Evolution of swelling pressure for samples wetted with decreasing suction

In Fig.5, the whole results from the three tests LT01, LT02 and LT03 during 700 days are presented. It appears that over this long period, the swelling pressure decreased for all samples, especially for the sample saturated with synthetic water (LT01). The final swelling pressure was 3.95 MPa (corresponding to a decrease of 9%), and 4.19 MPa (decrease of 3%) for samples saturated with synthetic water (LT01) and distilled water (LT02 and LT03), respectively. In addition, the same value was obtained for test LT02 (one-step soaking) and

LT03 (multistep soaking), which were both saturated with distilled water, showing a negligible effect of wetting procedure on the long-term behaviour of swelling pressure.

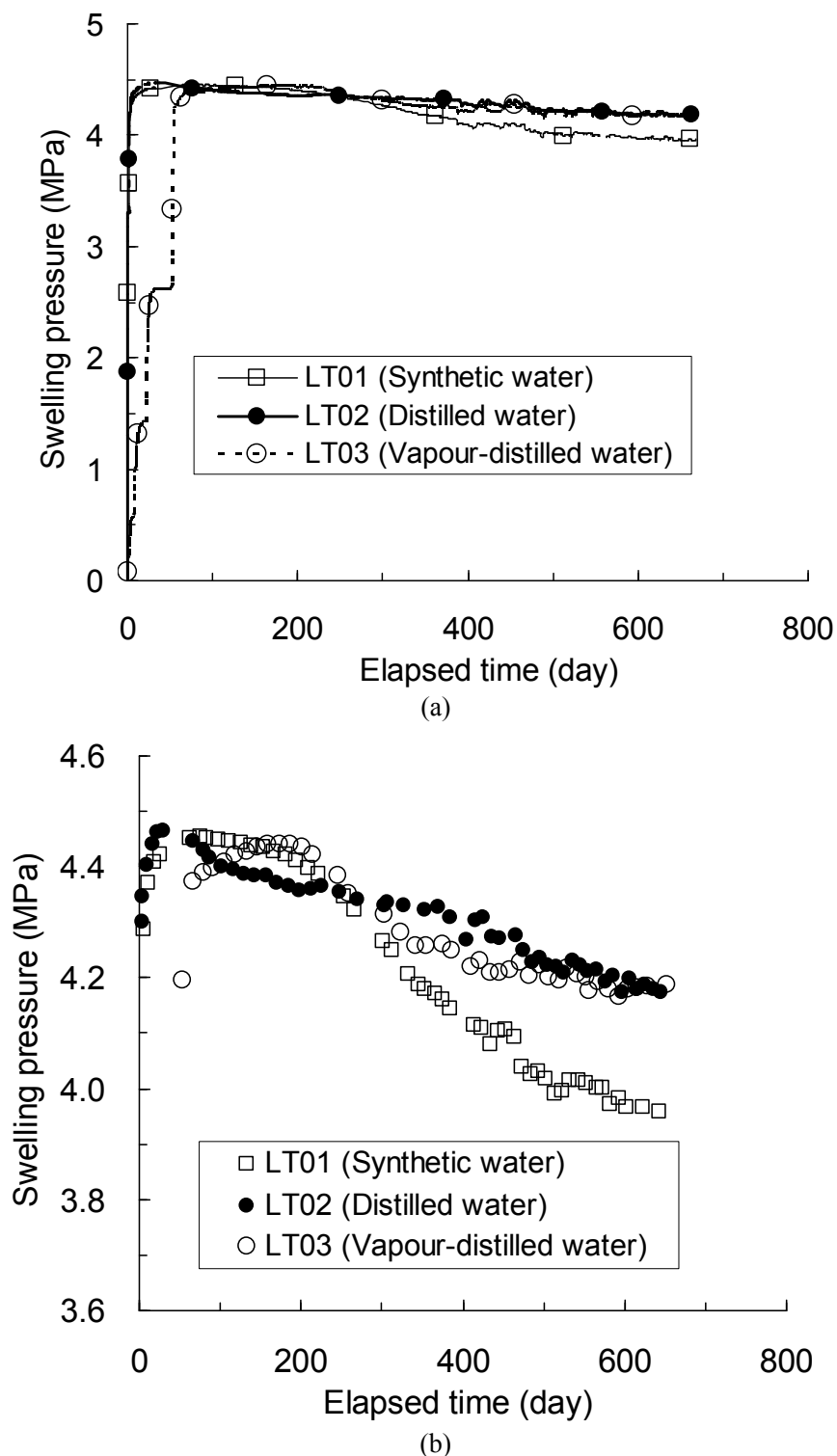


Figure 5. Evolution of swelling pressure for tests LT01, LT02, and LT03 for 700 days

The pore size distribution curve for all the samples taken at the end of the tests are presented in Fig. 6. It is observed in Fig. 6a that the final values of intruded mercury void ratio ( $e_m =$

intruded mercury volume over soil solid volume) are between 0.4 and 0.5, much lower than the soil void ratio ( $e = 0.61$ ). This shows the large amount of inaccessible porosity. Comparison between the curves of different durations clearly shows that the amount of accessible porosity increased after 700 days both for distilled (LT02 and LT03) and synthetic water (LT01), with an increase being larger for synthetic water.

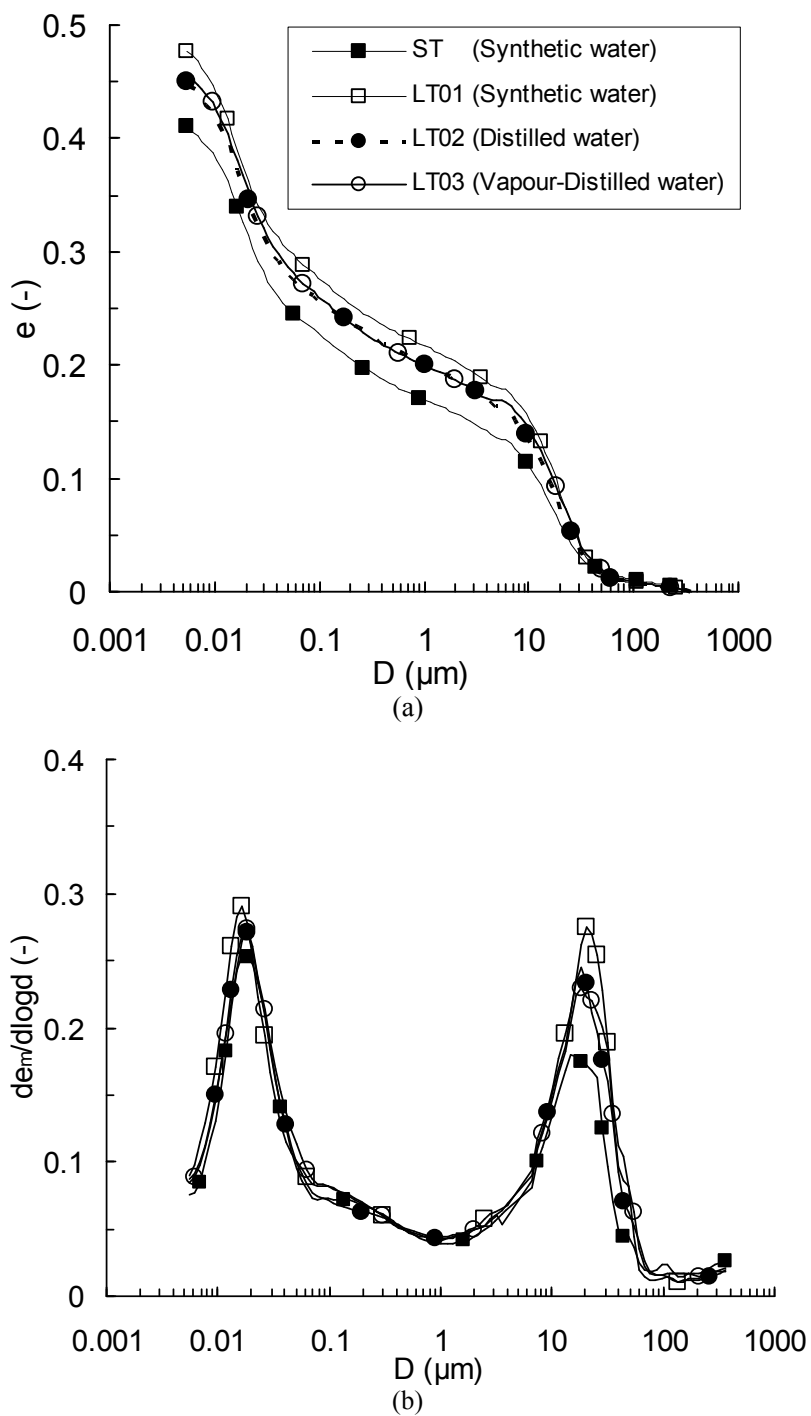


Figure 6. Pore size distribution curves

The incremental pore volume  $de_m/d\log(d)$  (Fig. 6b) refers to the volume of mercury that intrudes into the pores between pressure increments. For all of the samples, a typical bimodal porosity can be observed; thus, two pore groups can be defined: group of micro-pores having a mean size of 0.02  $\mu\text{m}$  and group of macro-pores having a mean size of 20  $\mu\text{m}$ . After 700-day saturation (LT01, LT02 and LT03), the macro-pores and micro-pores quantity increased when comparing to the short-term test (ST). Change in macro-pores is more significant especially for the sample saturated with synthetic water (LT01). For tests LT02 and LT03 which were hydrated with distilled water, very similar microstructure was observed indicating no effect of wetting procedure on the microstructure. As far as changes in pores size are concerned, it can be observed that over time the group of micro-pores had a size slightly decreased, and that, on the contrary, the group of macro-pores had a size slightly increased; changes for test LT01 being more marked.

#### 4 Interpretation and discussion

Various studies showed that the swelling capacity of bentonite is lower in saline water; the higher the salt concentration, the lower the swelling pressure. This phenomenon becomes less pronounced in case of high dry density (Studds et al., 1998; Karland et al., 2005; Suzuki et al., 2005; Karland et al., 2006; Castellanos et al., 2008; Katsumi et al., 2008; Siddique et al., 2011). In general, with a very high void ratios (low dry density) and/or strong salt concentrations, the influence of pore water chemistry on bentonite behaviour is significant and can be qualitatively explained by the diffuse double layer (DDL) theory (Karland, 1997; Mata, 2003; Castellanos et al., 2008). For dense bentonite, since there is little water present between adjacent clay platelets, there can be little or no development of a DDL associated with the clay particles (Dixon, 2000; Pusch and Yong, 2006); thus it becomes difficult even impossible to describe the bentonite behaviour by the DDL theory.

In this regard, Karland et al. (2005) studied the effect of salt concentration on the swelling pressure of MX-80 bentonite, and noted that the effect of the salinity of the saturating fluid was relatively lower with a higher density. For MX80 bentonite, Dixon (2000) also concluded that at a effective bentonite dry density (bentonite dry density in the bentonite/sand mixture) higher than 1.22  $\text{Mg/m}^3$ , changes in water chemistry does not significantly affect the swelling behaviour due to the small number of water layers close to the clay particle. Confirmation was made by Castellanos et al. (2008) on the FEBEX bentonite: an increase in salt concentration reduced the swelling pressure, and this change was much less evident for high density. It

appears that for the studied bentonite/claystone mixture, the high density ( $1.70 \text{ Mg/m}^3$ ) and the low salinity of synthetic water (see Table 3) together resulted in the negligible effect of water chemistry on the swelling pressure in short term.

Basically, the swelling pressure of bentonite is mainly related to the crystalline swelling and double layer swelling. Crystalline swelling is caused by the hydration of exchangeable cations ( $\text{K}^+$ ,  $\text{Na}^+$ ,  $\text{Ca}^{2+}$ ,  $\text{Mg}^{2+}$ ) between mineral layers that have a structure with one alumina octahedral sheet sandwiched between two silica tetrahedral sheets. It is a process which involves the adsorption of maximum number of hydrates depending on the nature of cations. After three to four water monolayers, i.e. at interlayer separation distances  $\geq 1 \text{ nm}$ , surface hydration becomes less important and electrical double-layer repulsion becomes the main swelling mechanism (Bradbury and Baeyens, 2003; Suzuki et al., 2005). For clay at high densities, the low amount of water uptake is to all intents and purposes pseudo-crystalline interlayer water, and insufficient to form the DDL (Pusch and Yong, 2006). Therefore, the swelling pressure is mainly generated by the crystalline swelling (interaction between the layer surfaces and water) and the double layer repulsion makes few contribution. In this case, the exchangeable cations are the key elements that control the clay-water interaction (Abdullah et al., 1997).

As far as the pore water is concerned, it may significantly affect the chemical compositions of clays by means of exchangeable cations (Yukselen et al., 2008). The cation exchange reaction is mainly controlled by the exchange capacity of the clay minerals (Mata, 2003); the ease with which a cation of one type can replace a cation of another type depends mainly on the valence, relative abundance of the different cation types, and the cation size. Other things being equal, the higher the valence of the cation, the higher the replacing power; for cations of the same valence, the replacing power increases with the size of the cation (Laine and Karttunen, 2010). A typical replaceability order is:  $\text{Na}^+ < \text{K}^+ < \text{Mg}^{2+} < \text{Ca}^{2+}$  (Mitchell, 1976; Pusch, 2001; Mata et al., 2003). According to this order, for the Na-bentonite as in this study, it tends to change from sodium (Na-) to other types (i.e. K-, Mg- or Ca-) depending on the cations present in the permeating water.

One of the most common cation exchange reactions in the Na-bentonite is the one involving sodium and calcium (Mata, 2003). Mata (2003) investigated the evolution of  $\text{Ca}^{2+}$  and  $\text{Na}^+$  in a specimen of sodium MX80 bentonite hydrated with saline water (NaCl and CaCl, 50/50 by mass) and distilled water. Analysis of the collected pore fluid showed an enrichment of sodium concentration and a decrease of calcium concentration compared to the injected water.

This means that the sodium bentonite was transformed to a calcium bentonite. Montes-H. et al. (2004, 2005) investigated the chemical transformation of Na/Ca-MX80 bentonite ( $\text{Na}_{0.18}\text{Ca}_{0.10}$ ) in a representative pore water ( $\text{pH} = 7.3$ ) from Bure site (-180 m), the Na/Ca- to Ca-montmorillonite conversion was identified as the main chemical transformation. At a constant temperature, this transformation is affected by the groundwater composition ( $\text{pH}$  and cation concentrations) and solid/liquid ratio as well as the reaction time (Mitchell, 1976; Herbert et al., 2004; Fernández and Villar, 2010; Laine and Karttunen, 2010). For the short term swelling pressure test in this study, it was actually the lower cation concentration (lower salinity of synthetic water mentioned above) and high solid/liquid ratio (i.e. high density) that led to the negligible effect of water chemistry on the swelling pressure. Nevertheless, after a long time period of reactions, the effect became evident because the presence of  $\text{Ca}^{2+}$  in Bure site water (see Table 3) enabled part of Na-montmorillonite to change to Ca-montmorillonite which has a much lower expansibility. This process resulted in a decrease of swelling pressure with time as shown in Fig.5.

The transformation from sodium to calcium montmorillonite is critically dependent on the amount of available calcium ( $\text{Ca}^{2+}$ ) in the pore water (Muurinen and Lehtikoinen, 1999; Fernández et al., 2004, Fernández and Villar, 2010). For the sample saturated with distilled water, as the equilibrium between claystone minerals and pore water may occur over time, it was as if diluted Bure site water that infiltrated to the MX80 bentonite. Therefore, the same mechanism as in synthetic water led to the degradation of swelling pressure in the case of distilled water. However, with a much lower cation concentration (30% percent of claystone in the mixture), the decrease of swelling pressure was significantly less than that with synthetic water.

For the sample first wetted by three steps of suction (LT03), after the sample was flooded with distilled water, the maximum swelling pressure was found close to that obtained by water-flooding the sample directly (LT02), indicating the negligible effect of wetting procedure on the swelling pressure. This phenomenon confirmed the mechanism identified by Cui et al. (2002): when hydrating by decreasing suction (57-38-12.6 MPa) under confined conditions, the macro-pores was progressively clogged, whereas the micro-pores remained almost un-affected. The micro-pores started to change only when the water saturation is approached. This suggests that step-wetting by suction control and direct flooding with water may lead to similar microstructures after saturation, thus similar maximum swelling pressures. After 700- day hydration with distilled water, not only the same swelling pressure, but also

the very close microstructure was observed for tests L02 and L03, which enhanced this conclusion. In addition, the repeatability of swelling pressure test and the MIP test was verified.

It was noted that the chemical effect on the HM behaviour of clayey soils is due to changes at different structural levels and the interaction between them (Mata 2003). From the microstructure observation in this study, it can be seen that the amount of accessible porosity increased after a long time period for both distilled (LT02 and LT03) and synthetic water (LT01), with more increase for synthetic water. If we relate these phenomena to the swelling pressure, it is clear that the sample with lower swelling pressure had a higher intruded mercury void ratio both in micro- and macro-pores. For samples with higher swelling capacity, more interlayer hydration occurred, leading to a constriction of accessible pores. When referring to the incremental pore volume, the same tendency can be identified, for the sample with higher swelling pressure, both the macro-pores and micro-pores decreased. However, most of changes in microstructure occurred in macro-pores family. The same observation can be made in terms of pore size changes. This is in agreement with the observation made by Mata (2003) who conducted MIP test on the compacted sodium bentonite MX80 and sand mixture (70/30) (dry density of 1.37 and 1.67 Mg/m<sup>3</sup>) saturated with distilled water and saline water, and found that the saline water effects were significant on the macropores, the micropores remaining almost unaffected.

## **5 Conclusion**

Long term swelling pressure tests and MIP tests on a bentonite/calystone mixture were performed. The effects of water chemistry as well as the hydration procedure on the swelling pressure were investigated both in short and long term. The results are analysed by considering the physico-chemical interaction between the minerals of claystone, minerals of bentonite and different fluids involved.

There was no obvious effect of water chemistry on the swelling pressure in short term (100 h) due to the high density and the low salinity of synthetic water. However, after a long period of 700 days, the swelling pressure decreased for all samples, especially for the sample saturated with synthetic water.

No effect of hydration procedure on the final swelling pressure was observed due to the similar microstructure obtained after water saturation compared to the one-step soaking test.

The chemical effect on the swelling pressure was closely related to changes in microstructure. The sample with higher swelling pressure showed less macro and micro-pores associated with a higher interlayer hydration.

From a practical point of view, the specification and design of the sealing/backfill material are often made based on the swelling properties measured in short term. However, an ignorable decrease (9%) of swelling pressure was observed after 700 days even with a water of low salinity. In this case, the expected sealing capacity may no longer be ensured in the very long term lifespan of the repository. Therefore, much attention should be paid on this swelling capacity deterioration in long term due to the interaction between bentonite-based materials and pore water.

### **Acknowledgements**

The support from the PHC Cai Yuanpei project (24077QE) and that of the China Scholarship Council (CSC) are greatly acknowledged.

### **References**

- Abdullah, W.S., Al-Zou'bi, M.S., Alshibli, K.A., 1997. On the physicochemical aspects of compacted clay compressibility. *Can. Geotech. J.*, Vol 34, 551–559.
- AFNOR, 1992. AFNOR NF P94-057, Soils: investigation and testing. Granulometric analysis. Hydrometer method. Association Francaise de Normalisation. France.
- Agus, S., Schanz, T., 2005. Swelling pressures and wetting-drying curves of a highly compacted bentonite-sand mixture. *Unsaturated Soils: Experimental Studies*, pages 241–256.
- Andra, 2005. Référentiel des matériaux d'un stockage de déchets à haute activité et à vie longue – Tome 4: Les matériaux à base d'argilites excavées et remaniées. Rapport Andra N° CRPASC040015B.
- Bradbury, M.H., Baeyens, B., 2003. Porewater chemistry in compacted re-saturated MX-80 bentonite. *Journal of Contaminant Hydrology*, 61,329– 338
- Castellanos, E., Villar, M.V., Romero, E., Lloret, A., Gens, A., 2008. Chemical impact on the hydro-mechanical behaviour of high-density febex bentonite. *Physics and Chemistry of the Earth, Parts A/B/C*, 33(Supplement 1):S516 – S526.
- Cui, Y. J., Loiseau, C., Delage, P., 2002. Microstructure changes of a confined swelling soil due to suction controlled hydration *Unsaturated soils: proceedings of the Third International Conference on Unsaturated Soils, UNSAT 2002*, 10-13 March 2002, Recife, Brazil, 593.
- Delage, P., Howat, M. D. & Cui, Y. J., 1998. The relationship between suction and swelling properties in a heavily compacted unsaturated clay. *Engineering Geology* 50, 31-48.
- Dixon, D.A., 2000. Porewater salinity and the development of swelling pressure in bentonite-based buffer and backfill materials. POSIVA Report 2000-04, Posiva Oy, Helsinki, Finland.
- Fernández, A.M., Baeyens, B., Bradbury, M., Rivas, P., 2004. Analysis of the pore water chemical composition of a Spanish compacted bentonite used in an engineered barrier. *Phys. Chem. Earth* 29, 105–118.

- Fernández, A.M., Villar, M.V., 2010. Geochemical behaviour of a bentonite barrier in the laboratory after up to 8 years of heating and hydration. *Applied Geochemistry* 25, 809–824
- Gaucher E. C., Blanc P., Bardot F., Braibant G., Buschaert S., Crouzet C., Gautier A., Girard J.-P., Jacquot E., Lassin A., Negrel G., Tournassat C., Vinsot A., and Altmann S. 2006. Modelling the porewater chemistry of the Callovian-Oxfordian formation at a regional scale. *Comptes Rendus Geosciences* 338(12-13), 917-930.
- Herbert, H.-J., Kasbohm, J., Moog, H.C. & Henning, K.-H. 2004. Long-term behaviour of the Wyoming bentonite MX-80 in high saline solutions. *Applied Clay Science*, 26, 275-291.
- Herbert, H.-J., Kasbohm, J., Sprenger, H., Fernández, A.M. & Reichelt, C. 2008. Swelling pressures of MX-80 bentonite in solutions of different ionic strength. *Physics and chemistry of the earth*, 33, 327-342.
- Hoteit, N., Ozanam, O., Su, K., 2000. Geological Radioactive Waste Disposal Project in France: Conceptual Model of a Deep Geological Formation and Underground Research Laboratory in Meuse/Haute-Marne Site. The 4th North American Rock Mechanics Symposium, Seattle, July 31–August 3, 2000.
- Karland, O., 1997. Bentonite swelling pressure in strong NaCl solutions. Correlation between model calculations and experimentally determined data. SKB Technical Report 97-31. Swedish Nuclear Fuel and Waste Management Co., Stockholm, pp. 1–30.
- Karland, O., Muurinen, A., Karlsson, F., 2005. Bentonite swelling pressure in NaCl solutions-Experimentally determined data and model calculations. *Advances in Understanding Engineering Clay Barriers*. Page 241.
- Karland, O., Olsson, S. & Nilsson, U. 2006. Mineralogy and sealing properties of various bentonites and smectite-rich clay materials. SKB TR-06-30. Swedish Nuclear Fuel and Waste Management Co, Stockholm, Sweden.
- Katsumia, T., Ishimori, H., Onikata, M., Fukagawa, R., 2008. Long-term barrier performance of modified bentonite materials against sodium and calcium permeant solutions *Geotextiles and Geomembranes* 26, 14–30.
- Komine, H., Ogata, N. 1994. Experimental study on swelling characteristics of compacted bentonite. *Canadian geotechnical journal*, 31(4):478–490.
- Komine, H., Ogata, N. 2003. New equations for swelling characteristics of bentonite-based buffer materials. *Canadian Geotechnical Journal*, 40(2):460–475.
- Komine, H., 2004. Simplified evaluation for swelling characteristics of bentonites, *Engineering geology*, 71(3-4): 265-279.
- Komine, H. Yasuhara, K. and Murakami, S. 2009. Swelling characteristics of bentonites in artificial seawater. *Canadian Geotechnical Journal*, 46(2):177-189.
- Laine H., Karttunen P., 2010. Long-Term Stability of Bentonite A Literature Review. POSIVA Report 2010-53, Posiva Oy, Helsinki, Finland.
- Lebon P, Ghoreychi M. French underground research laboratory of Meuse/Haute-Marne: THM aspects of argillite formation. In: EUROCK2000 Symposium. Aachen: [s. n.], 2000: 27–31.
- Marty, N., Fritz, B., Clément, A., Michau, N., 2010, Modelling the long term alteration of the engineered bentonite barrier in an underground radioactive waste repository, *Applied Clay Science* 47 (2010) 82–90
- Mata, C., 2003. Hydraulic behaviour of bentonite based mixtures in engineered barriers: The Backfill and Plug Test at the A<sup>2</sup>spo<sup>2</sup> HRL (Sweden). Ph. D. Thesis. Universitat Politècnica de Catalunya. 257 pp. Barcelona.
- Mitchell, J.K., 1976. *Fundamentals of Soil Behavior*, John Wiley & Sons, New York.
- Montes-H, G., Geraud, Y., 2004. Sorption kinetic of water vapour of MX80 bentonite submitted to different physical-chemical and mechanical conditions. *Colloids and Surfaces A: Physicochemical Engineering Aspects* 235, 17–23.

- Montes-H, G., Geraud, Y., Duplay, J. & Reuschlé, 2005. ESEM observations of compacted bentonite submitted to hydration/dehydration conditions. *Colloids and surfaces A: Physicochem. Eng. Aspects*, 262, 14-22.
- Muurinen, A., Lehtikoinen, J., 1999, Porewater chemistry in compacted bentonite, *Engineering Geology* 54 (1999) 207–214
- Pusch, R., 1982. Mineral-water interactions and their influence on the physical behavior of highly compacted Na bentonite. *Canadian Geotechnical Journal*, 19(3):381–387.
- Pusch, R., 2001. Experimental study of the effect of high porewater salinity on the physical properties of a natural smectitic clay, SKBF/KBS technical report. No.TR01-07.
- Pusch, R., Yong, R.N., 2006, *Microstructure of Smectite Clays and Engineering Performance*, Taylor & Francis, London and New York.
- Siddiqua, S., Blatz, J., Siemens, G., 2011, Evaluation of the impact of pore fluid chemistry on the hydromechanical behaviour of clay-based sealing materials, *Can. Geotech. J.* 48: 199–213.
- Studds, P.G., Stewart, D.I., and Cousens, T.W. 1998. The effects of salt solutions on the properties of bentonite-sand mixtures. *Clay Minerals*, 33: 651–660.
- Suzuki, S.; Prayongphan, S.; Ichikawa, Y. & Chae, B. 2005. In situ observations of the swelling of bentonite aggregates in NaCl solution, *Applied Clay Science*, Elsevier, 29: 89-98.
- Tang, C.S., Tang, A.M., Cui, Y.J., Delage, P., Barnichon, J.D., Shi, B., 2011a. A study of the hydro-mechanical behaviour of compacted crushed argillite. *Engineering Geology*. 118 (3-4):93-103.
- Tang, C.S., Tang, A.M., Cui, Y.J., Delage, P., Schroeder, C., De Laure, E., 2011b. Investigating the swelling pressure of compacted crushed Callovo-Oxfordian argillite. *Physics and Chemistry of the Earth (special issue)*, Volume 36, Issues 17–18, 1857–1866
- Villar, M.V., Lloret, A., 2008. Influence of dry density and water content on the swelling of a compacted bentonite. *Applied Clay Science*, 39(1-2):38–49.
- Wang Q., Tang A. M., Cui Y.J., Delage P., Gatmiri, B., 2012 Experimental study on the swelling behaviour of bentonite/claystone mixture, *Engineering Geology* 124, 59-66.
- Yukselen-Aksoy, Y., Kaya, A., Ören, A.H., 2008, Seawater effect on consistency limits and compressibility characteristics of clays, *Engineering Geology* 102 (2008) 54–61
- Zhang, C., and Rothfuchs, T., 2004. Experimental study of the hydro-mechanical behaviour of the Callovo-Oxfordian argillite. *Applied Clay Science*, 26(1-4):325–336.



## **Chapter 3. Effect of technological void on the hydro-mechanical behaviour**

### **INTRODUCTION**

Engineered barriers are often made up of compacted bricks. When bricks are placed around waste canisters or to form sealing buffers, the so-called technological voids either between the bricks themselves or between bricks, canisters and the host rock are unavoidable. Upon hydration by pore water infiltrating from the host-rock, the bricks swell to fill up all these voids. On the other hand, swelling results in a decrease in dry density that may lead to degradation of the hydro-mechanical performance of engineered barriers (Komine et al., 2009, Komine, 2010). As a result, the safety function expected in the design may no longer be properly ensured.

In order to investigate the effects of technological voids on their hydro-mechanical behaviour, a series of tests was performed on compacted bentonite-based materials. The results are presented in this chapter in the form of two papers.

The first one, being accepted in *Soils and Foundation*, presents the results of water retention test, hydration test, suction controlled oedometer test and hydraulic test on compacted bentonite/sand samples with different voids including the technological void and the void inside the soil. By introducing the parameters such as bentonite void ratio and water volume ratio, the effects of technological voids on the hydromechanical behaviour were analyzed.

The second section characterizes the microstructure features of the compacted MX80 bentonite used for the hydraulic seal in the PRACLAY in-situ experiment. Emphasis was put on the effects of final dry density (density after swelling) and hydration time. This part corresponds to a paper submitted to «*Canadian Geotechnical Journal*».

Wang, Q., Tang, A. M., Cui, Y.J., Delage, P., Barnichon, J.D., Ye, W.M., 2012. Soils and foundations, accepted for publication.

## **The effects of technological voids on the hydro-mechanical behaviour of compacted bentonite-sand mixture**

Qiong Wang<sup>1</sup>, Anh Minh Tang<sup>1</sup>, Yu-Jun Cui<sup>1,3</sup>, Pierre Delage<sup>1</sup>, Jean-Dominique Barnichon<sup>2</sup>,  
Wei-Min Ye<sup>3</sup>

**Abstract:** Compacted bentonite-based materials are often used as buffer materials in radioactive waste disposal. A good understanding of their hydro-mechanical behaviour is essential to ensure the disposal safety. In this study, a mixture of MX80 bentonite and sand was characterized in the laboratory in terms of water retention property, swelling pressure, compressibility and hydraulic conductivity. The effects of the technological voids or the voids inside the soil were investigated. The technological voids are referred to as the macro-pores related to different interfaces involving the buffer material, whereas the voids inside the soil is referred to as the common macro-pores within the compacted bentonite/sand mixture. The results obtained show that at high suctions, the amount of water absorbed in the soil depends solely on suction, whereas at low suctions it depends on both suction and bentonite void ratio. There is a unique relationship between the swelling pressure and the bentonite void ratio, regardless of the sample nature (homogeneous or not) and sand fraction. However, at the same bentonite void ratio, a higher hydraulic conductivity was obtained on the samples with technological voids. The effect of sand fraction was evidenced in the mechanical yield behaviour: at the same bentonite void ratio, the bentonite-sand mixture yielded at a higher pre-consolidation stress.

**Keywords:** Bentonite-sand mixture; Technological voids effects; Water retention property; Swelling pressure; Hydraulic conductivity; Compressibility

---

### **1 Introduction**

Most designs of deep geological repository for high level radioactive wastes (HLW) are based on the multi-barrier concept with isolation of the waste from the environment. The multi-barrier concept includes the natural geological barrier (host rock), engineered barriers made up of compacted sand-bentonite mixtures (placed around waste containers or used as buffer and sealing elements) and metal canister. Compacted bentonite-based materials are relevant materials for this purpose thanks to their low permeability, high swelling and high radionuclide retardation capacities (Pusch, 1979; Yong et al., 1986; Villar and Lloret, 2008; Komine and Watanabe, 2010; Cui et al., 2011).

---

1 Ecole des Ponts ParisTech, Navier/CERMES, France

2 Institut de Radioprotection et de Sûreté Nucléaire (IRSN), France

3. Tongji University, China

Engineered barriers are often made up of compacted bricks. When bricks are placed around waste canisters or to form sealing buffers, the so-called technological voids either between the bricks themselves or between bricks, canisters and the host rock are unavoidable. As an example, 10 mm thick gaps between bentonite blocks and canister and 25 mm thick gaps between the bentonite blocks and the host rock have been considered in the basic design of Finland (Juvankoski, 2010). These technological voids appeared to be equal to 6.6 % of the volume of the gallery in the FEBEX mock-up test (Martin et al., 2006). Fractures that appear in the excavation damaged zone within the host rock in the near field constitute additional voids. In the French concept, the volume of the bentonite/rock gaps is estimated at 9 % of the volume of the gallery by the French waste management agency (ANDRA 2005). This value reaches 14 % in the SEALEX in-situ test carried out in the Tournemire Underground Research Laboratory (URL) run by IRSN (Institut de radioprotection et de sûreté nucléaire, the French expert national organisation in nuclear safety) in South-West of France (Barnichon and Deleruyelle, 2009).

Once placed in the galleries, engineered barriers are progressively hydrated by pore water infiltrating from the host-rock. This water infiltration is strongly dependent on the initial state of the compacted material (water content, suction and density, e.g. Cui et al. 2008). Indeed, it has been shown that water transfer in unsaturated swelling compacted bentonites or sand bentonite mixtures is strongly dependent on the imposed boundary conditions in terms of volume change. As shown in Yahia-Aissa et al. (2001), Cui et al. (2008) and Ye et al. (2009), the degree of swelling allowed significantly affects the amount of infiltrated water, with much water absorbed when swelling is allowed and a minimum amount of water absorbed when swelling is prevented. Volume change conditions also appeared to have, through microstructure changes, significant influence on the hydraulic conductivity.

In this regard, the degree of swelling allowed by the technological voids described above has a significant influence on the hydro-mechanical behaviour of the compacted bentonite and their effects need to be better understood. Swelling results in a decrease in dry density that may lead to a degradation of the hydro-mechanical performance of engineered barriers (Komine et al., 2009, Komine, 2010). As a result, the safety function expected in the design may no longer be properly ensured. Therefore, a better understanding of the effects of the technological voids is essential in assessing the overall performance of the repository.

In this study, a series of tests was performed on a compacted bentonite-sand mixture samples, aiming at investigating the effects of technological voids on their hydro-mechanical behaviour.

Temperature effects were not considered and tests were carried out at constant ambient temperature ( $20\pm 1^\circ\text{C}$ ). Given that the paper deals with the hydration of engineered barriers in the repository, neither the drying process nor hysteresis effects were considered.

Firstly, the water retention curve was determined under both free swell and restrained swell conditions; secondly, the effects of a pre-existing technological void on both the swelling pressure and hydraulic conductivity were investigated; finally, the compressibility at different void ratios was studied by means of suction-controlled oedometer tests. An overall analysis of the effects of voids on the hydro-mechanical response of the engineered barrier was finally performed.

## **2 Materials and methods**

### **2.1 Materials and sample preparation**

A commercial MX80 Na-bentonite from Wyoming, USA was used. The bentonite powder was provided with an initial water content of 12.2% and was stocked in a hermetic container to maintain the water content constant, in a room at  $20\pm 1^\circ\text{C}$ . All tests were performed at this temperature.

This MX80 Na-bentonite is characterised by a high montmorillonite content (80%), a liquid limit of 575%, a plastic limit of 53% and a unit mass of the solid particles of  $2.77 \text{ Mg/m}^3$ . The cation exchange capacity (CEC) is 76 meq/100g (83 % of Na). The grain size distribution (Figure 1) determined using a hydrometer (French standard AFNOR NF P94-057) on deflocculated clay shows that the clay fraction ( $< 2 \mu\text{m}$ ) is 84%. The X-Ray diffractometer diagram of the clay fraction presented in Figure 2 shows a peak at  $12.5 \text{ \AA}$ , typical of montmorillonite (this peak shifted from  $12.5$  to  $16.9 \text{ \AA}$  when treated with glycol and to  $9.5 \text{ \AA}$  when dried). These data are comparable with that provided by Montes-H et al., (2003).

The sand used in the mixture was a quartz sand from the region of Eure and Loire, France, that passed through a 2 mm sieve. Figure 1 shows the sand grain size distribution curve determined by dry sieving (AFNOR NF P94-056). The curve is characterized by a uniformity coefficient  $C_u$  of 1.60 and a  $D_{50}$  close to 0.6 mm. The unit mass of the sand grains is  $2.65 \text{ Mg/m}^3$ .

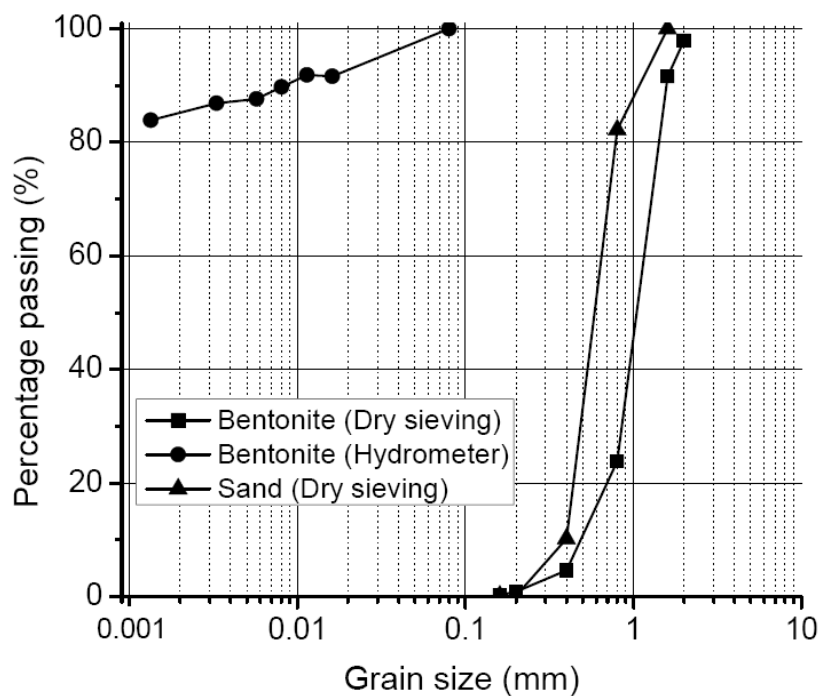


Figure 1. Grain size distribution of the MX80 bentonite and sand

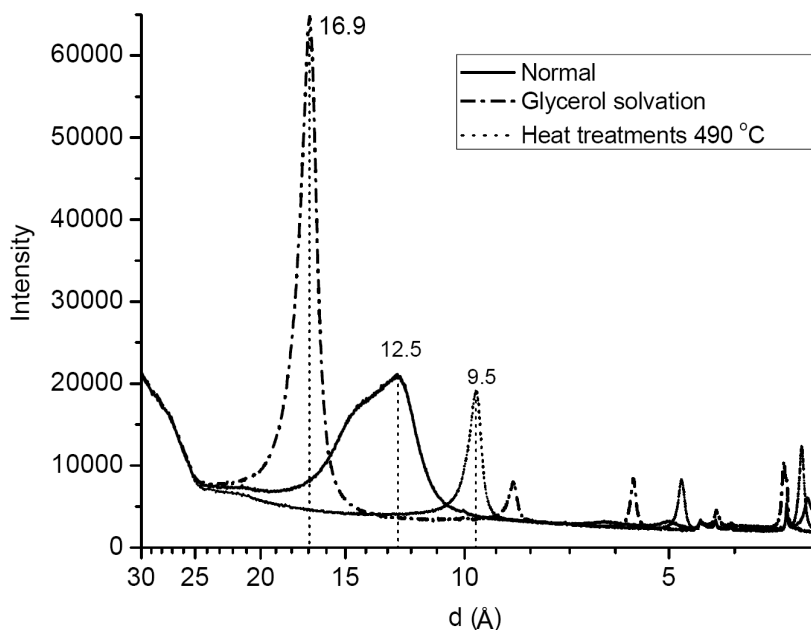


Figure 2. X-Ray curves of the MX80 bentonite

A water having the same chemical composition as the pore water of the Callovo-oxfordian claystone from the ANDRA URL in Bure (France), called synthetic water, was used in the experiments. The corresponding chemical components (see Table 1) were mixed with distilled water in a magnetic stirrer until full dissolution.

Table 1 Chemical composition of the synthetic water

Components	NaHCO <sub>3</sub>	Na <sub>2</sub> SO <sub>4</sub>	NaCl	KCl	CaCl <sub>2</sub> ·2H <sub>2</sub> O	MgCl <sub>2</sub> ·6H <sub>2</sub> O	SrCl <sub>2</sub> ·6H <sub>2</sub> O
Mass (g) per 1L solution	0.28	2.216	0.615	0.075	1.082	1.356	0.053

The grain size distribution of the bentonite powder obtained by “dry” sieving is also presented in Figure 1, showing a well graded distribution around a mean diameter slightly larger than 1 mm. This curve is close to that of sand. The powder was carefully mixed with dry sand (70% bentonite - 30% sand in mass) giving a water content of 8.5% for the mixture. Prior to compaction, the mixture powder was put into a hermetic container connected to a vapor circulation system (see Figure 3) containing free water (100% relative humidity), so as to reach a target water content of 11%. The samples were weighed every two hours until the target water content was attained (after around two days).

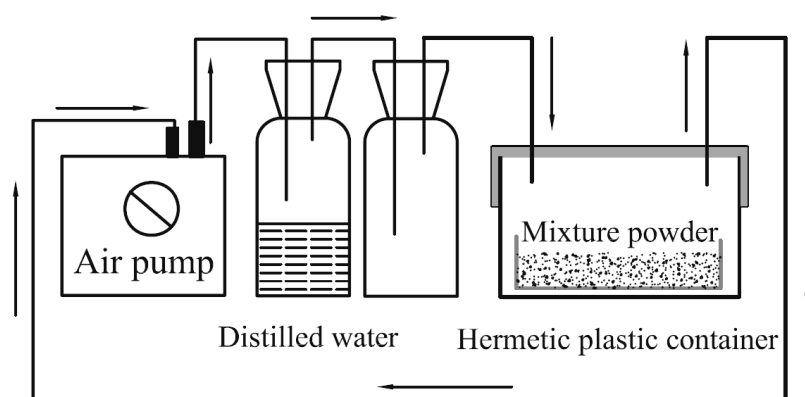


Figure 3. Hermetic plastic container with a vapor circulation system for adjusting water content

A given quantity of mixture was then placed into a rigid ring (35 or 38 mm diameter) and statically compacted using an axial press at a constant displacement rate of 0.05 mm/min to different target dry densities (values given in the following section). Once the target dry density reached, the displacement shaft was fixed for more than 15 h to attain axial stress stabilization (defined by changes in axial stress as low as 0.05 MPa/h). This procedure minimized the sample rebound during unloading.

The results from Mercury intrusion porosimetry (MIP) tests on the bentonite/sand mixtures compacted to dry densities  $\rho_d = 1.67$  and  $1.97 \text{ Mg/m}^3$  and freeze dried are shown in Figure 4. A typical bimodal porosity (e.g. Ahmed et al. 1974, Delage et al. 1996, Romero et al. 1999) was observed in both samples, defining intra-aggregate pores (micro-pores) with a mean size of  $0.02 \text{ }\mu\text{m}$  and inter-aggregate pores (macro-pores) that depend on the dry density and range from  $10 \text{ }\mu\text{m}$  (for  $\rho_d = 1.67 \text{ Mg/m}^3$ ) to  $50 \text{ }\mu\text{m}$  ( $\rho_d = 1.97 \text{ Mg/m}^3$ ). As shown by Delage and

Graham (1995) from the data of Sridharan et al. (1971), this confirms that compaction only affects the largest inter-aggregate pores while intra-aggregate pores remain unaffected (see also Lloret and Villar, 2007). In compacted bentonites, it has been shown that a further smaller sized pore population (ranging between 0.2 and 2 nm) corresponding to the intra-particle (interlayer) pores within the aggregates and not detectable by the MIP had to be also considered (Delage et al., 2006; Lloret and Villar, 2007).

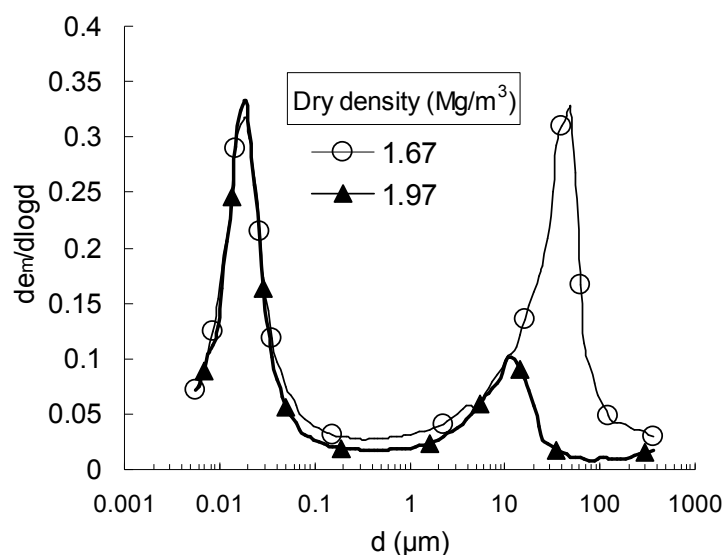


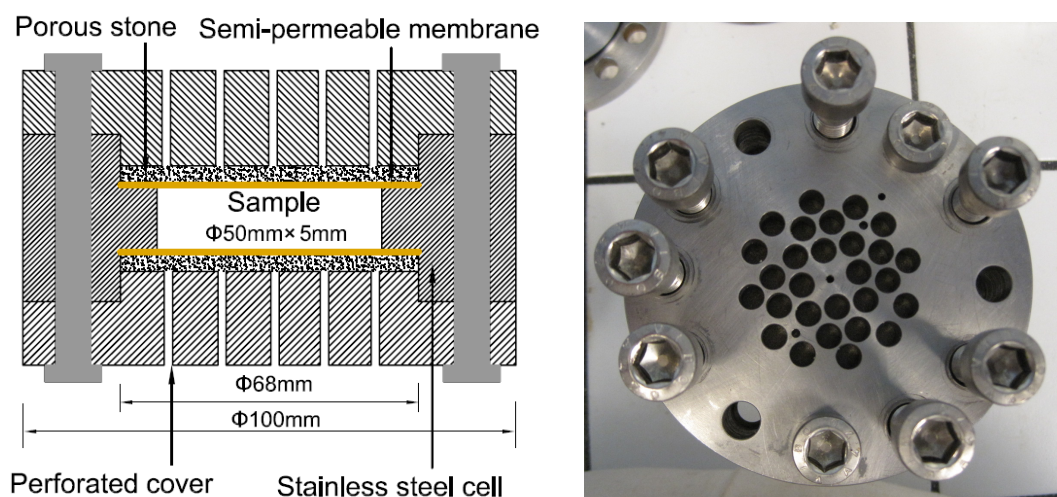
Figure 4. Pore size distribution of bentonite/sand mixture compacted to different dry density with a water content of about 11.0%

## 2.2 Experimental methods

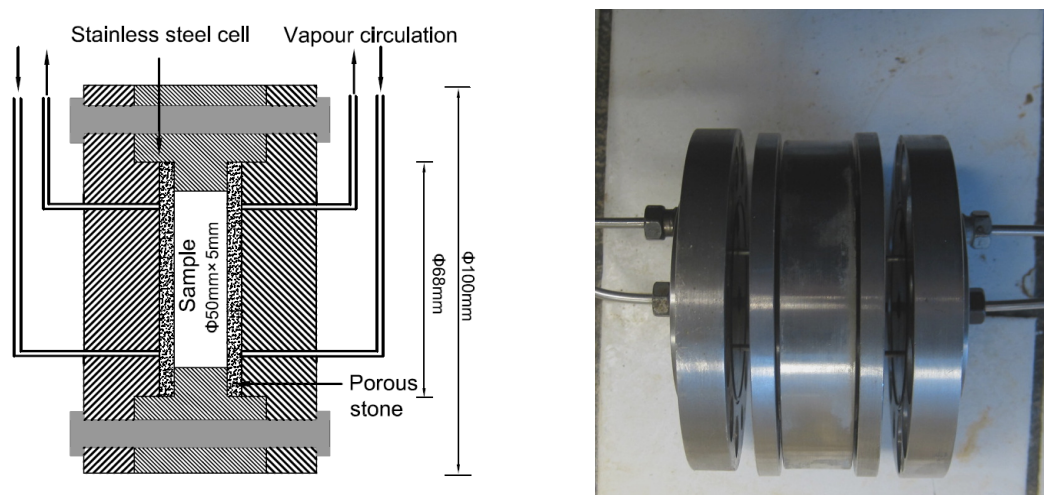
### Water retention test

The water retention curve (WRC) of the bentonite/sand mixture was determined under both free swell and restrained swell conditions by using both the vapour equilibrium technique ( $s > 4.2$  MPa) and osmotic technique ( $s < 4.2$  MPa) for suction control. Three identical samples were used in parallel and the final water content calculated corresponds to the mean value. To apply suction by the vapour equilibrium technique under free swell conditions the as-compacted sample (35 mm diameter and 5 mm height) was placed into a desiccator containing a saturated salt solution at bottom. The sample mass was regularly measured to monitor the water content variation over time. In a standard fashion, equilibrium was considered reached when the mass stabilized. To apply the osmotic technique (Delage et al. 1998; Delage and Cui, 2008a and 2008b), the sample was wrapped by a cylinder-shaped semi-permeable membrane and placed in a PEG 20 000 solution at a concentration corresponding to the required suction. The water content at equilibrium under each suction was determined by weighing.

Following Yahia-Aissa et al. (2001), the determination of the water retention curve under prevented swell conditions (constant volume conditions) was carried out on samples of 50 mm in diameter and 5 mm in height, placed into a specially designed rigid stainless steel cell allowing vapour exchanges through two metal porous disks put on both sides. To apply the osmotic technique, the semi-permeable membrane was placed between the porous stone and the soil sample (Figure 5a); all was then sandwiched between two perforated discs and immersed into a PEG solution at the required concentration. Water infiltrated into the soil through the porous stone and the semi-permeable membrane until the target suction was reached. To apply suction with the vapour equilibrium technique, the sample sandwiched between two porous stones was installed between two external plates with valves (Figure 5b) that were connected to a suction control system using the vapour equilibrium technique. The water content at equilibrium under each suction was determined by weighing.



(a) Osmotic method



(b) Vapour equilibrium technique

Figure 5. Constant volume cell for WRC determination.

All the tests performed and the solutions used for suction control (Delage et al., 1998; Ye et al., 2009) are presented in Table 2. Samples were statically compacted at a dry density of  $1.67 \text{ Mg/m}^3$ , corresponding to the final dry density adopted in the in situ experiment at the Tournemire URL.

Table 2. Test conditions for water retention property

Suction control method		Suction (MPa)	constant volume	Free swell
Saturated salt solution	LiCl	309	–	√
	K <sub>2</sub> CO <sub>3</sub>	113	–	√
	Mg(NO <sub>3</sub> ) <sub>2</sub>	82	–	√
	NaCl	38	√	√
	(NH <sub>4</sub> ) <sub>2</sub> SO <sub>4</sub>	24.9	√	√
	ZnSO <sub>4</sub>	12.6	√	√
	KNO <sub>3</sub>	9.0	√	√
	K <sub>2</sub> SO <sub>4</sub>	4.2	√	√
Concentration of PEG solution (g PEG/g Water)	0.302	1	√	√
	0.095	0.1	√	√
	0.030	0.01	√	√

#### Hydration test with technological void (SP 01 - 04)

The effect of technological void on the swelling behaviour of the compacted sand-bentonite mixture was investigated using the device shown in Figure 6. In this system, a sample is placed inside an oedometer cell placed into a rigid frame comprising a load transducer that allows the measurement of vertical stress during hydration. The small vertical strain due to the deformability of the set-up is measured by a digital micrometer.

A technological void of 14% of the total cell volume that corresponds to the situation of the SEALEX in situ test at the Tournemire URL was set by choosing an initial diameter of the compacted sample smaller than that of the hydration cell. With a ring diameter of 38 mm, the annular technological void selected (14% of the total cell volume representing 17% of the initial sample volume) corresponded to a sample diameter of 35.13 mm.

The sample was hydrated by injecting synthetic water under constant pressure (0.1 MPa) through a porous disk in contact with the bottom face while the top face was put in contact with another porous stone so as to allowed free expulsion of either air or water (see Figure 6). The small water pressure (0.1 MPa) was adopted to avoid any effect on axial pressure measurement. Changes in axial stress, displacement and injected water volume over time

were monitored. Once the axial stress stabilized (after more than 35 h , see Figure 9), water injection under 0.1 MPa was continued for 24 h more in order to determine the hydraulic conductivity under permanent flow condition. Indeed, a linear relationship between flux and time was observed, confirming the observation of Dixon et al. (1992) about the validity of Darcy’s law for saturated compacted bentonites.

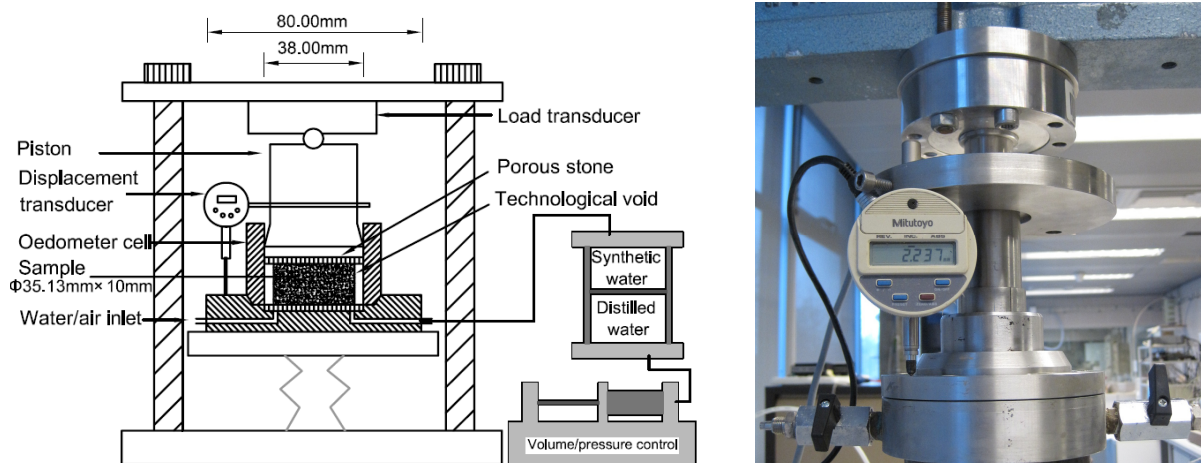


Figure 6. Schematic layout of hydration test with technological void

Four tests with the same technological void of 14% (SP01 - SP04) were conducted on samples with the same initial water content of 11% and various initial dry densities obtained by changing the compaction pressure (between 65 and 85 MPa, giving rise to dry densities comprised between 1.93 and 1.98 Mg/m<sup>3</sup>, see Table 3). An initial axial stress of 0.5 MPa was applied on the specimen before hydration to ensure good contact and satisfactory load measurement (see Figure 6). When water injection started, the piston was fixed and the build-up of axial stress was monitored by the load transducer.

Table 3. Specimens used for swelling pressure test

Tests	Compaction Stress (MPa)	Compacted dry density (Mg/m <sup>3</sup> )
SP01	65	1.93
SP02	70	1.96
SP03	80	1.96
SP04	85	1.98

**Suction controlled oedometer test (SO-01 SO-04)**

Controlled suction oedometer compression tests were carried out on samples of 10 mm in height and 38 mm in diameter by circulating vapour at controlled relative humidity at the base of the sample as shown in Figure 7 (tests SO-02/04). A high pressure oedometer frame was used so as to apply vertical stresses as high as 50 MPa (Marcial et al., 2002). Zero suction was applied by circulating pure water. Vertical strain was monitored using a digital micrometer (accuracy  $\pm 0.001$  mm).

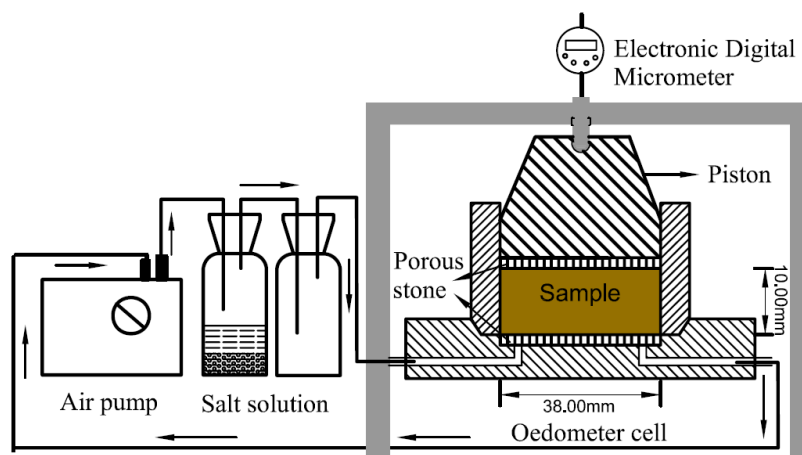


Figure 7. Experimental setup of suction controlled oedometer test

Prior to compression, samples were hydrated under a low vertical stress of 0.1 MPa by applying a suction lower than the initial as-compacted value (estimated at 65 MPa from the water retention curve in Figure 8 at  $w = 11\%$ ).

As seen in Table 4, the testing program includes 3 standard tests (SO-02 to 04) carried out on 38 mm diameter samples with an initial dry density of  $1.67 \text{ Mg/m}^3$  under controlled suctions of 4.2, 12.6 and 38 MPa, respectively. Stabilisation of swelling under the imposed suctions and a vertical stress of 0.1 MPa were waited for prior to compression.

Table 4 Specimens used for suction controlled oedometer test

Tests	$\rho_{di}$ ( $\text{Mg/m}^3$ )	D (mm)	$s$ (MPa)
SO-01	1.97	35.13	0
SO-02	1.67	38.00	4.2
SO-03	1.67	38.00	12.6
SO-04	1.67	38.00	38

The configuration of test SO-01 ( $\rho_{di} = 1.97 \text{ Mg/m}^3$ , internal diameter of 35.13 mm), is similar to that described in Figure 6, with an annular void between the sample and ring corresponding

to a 14% technological void. In this test, the sample was flooded with synthetic water, imposing zero suction through the liquid phase. The higher  $1.97 \text{ Mg/m}^3$  density was chosen so as to correspond to the previous value of  $1.67 \text{ Mg/m}^3$  once the technological void clogged by the lateral sample swelling. Obviously, even though that the global density of sample SO-01 was equal to that of samples SO-02/04 after swelling, the density of sample SO-01 should not be homogeneous and should follow a rather axisymmetrical distribution, with lower values in the zone of former technological void clogged by soil swelling.

### 3 Experimental results

#### 3.1 Water retention curves

Figure 8 presents the wetting path of the water retention curves (WRCs) obtained under both free swell and restrained swell conditions. For suctions higher than 9 MPa, the two curves are very similar while a significant difference can be identified in the range of suction below 9 MPa. When suction reached 0.01 MPa, the water content under free swell condition is 246.0%, a much higher value than that under restrained swell condition (25.4%). This confirms that the prevented swelling condition significantly affects the retention property only in the range of low suctions (Yahia-Aissa et al. 2001, Cui et al. 2008, Ye et al. 2009).

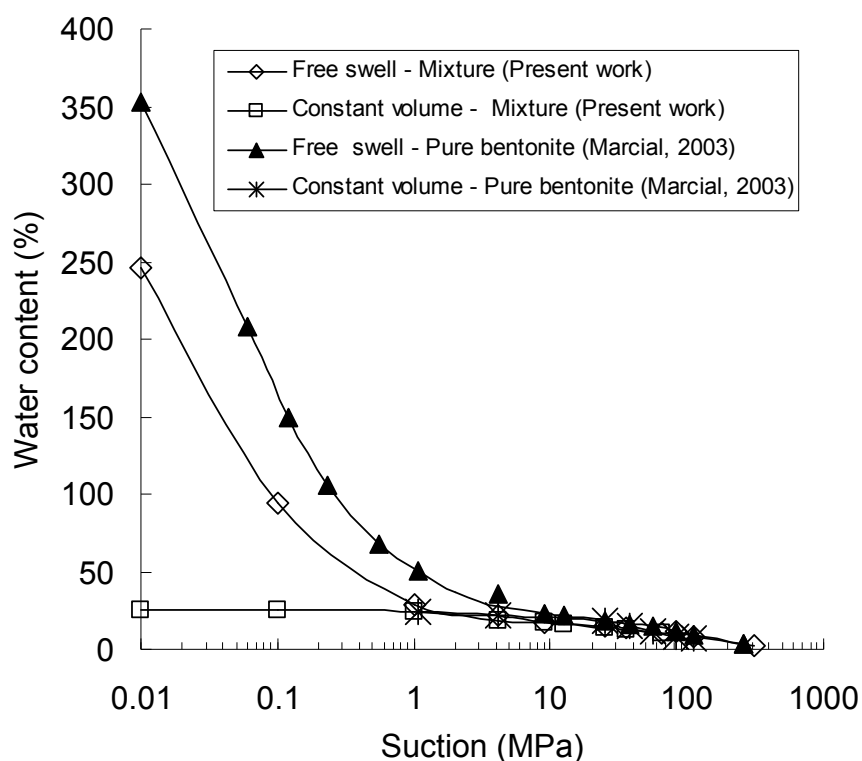


Figure 8. WRCs of bentonite-sand mixture and pure bentonite

The WRCs of samples of pure MX80 bentonite compacted to  $1.7 \text{ Mg/m}^3$  dry unit mass under both free swell and constant volume conditions determined by Marcial (2003) are also presented in Figure 8. In the higher suction range ( $s > 9 \text{ MPa}$ ), all data fall on the same curve, regardless of the imposed condition (swelling allowed or constant volume) and type and density of material (bentonite-sand mixture at  $1.67 \text{ Mg/m}^3$  or pure bentonite at  $1.7 \text{ Mg/m}^3$ ). By contrast, at lower suctions ( $s < 9 \text{ MPa}$ ), the water content of the mixture under free swell condition is lower than that of the pure bentonite at the same suction value.

### 3.2 Effects of the technological void (tests SP01-SP04)

Figure 9 presents the results of the four tests (SP01-SP04) carried out to investigate the effect of technological void on the swelling pressure during water injection under a constant pressure of  $0.1 \text{ MPa}$ . As seen in Photo 1, some water escaping from the top of the cell was observed at the beginning of water injection during the initial increase of vertical stress (Figure 9). This phase of 25-30 min duration corresponded to the circulation of water in the annular gap between the sample and the ring. After this period, the gap was obviously filled by hydrated bentonite with no more outflow observed. After about 35 h, the vertical stress reached stabilization with final values of 2.07, 2.77, 2.44, and  $3.06 \text{ MPa}$  for tests SP01 ( $\rho_{di} = 1.93 \text{ Mg/m}^3$ ), SP02 ( $\rho_{di} = 1.96 \text{ Mg/m}^3$ ), SP03 ( $\rho_{di} = 1.96 \text{ Mg/m}^3$ ) and SP04 ( $\rho_{di} = 1.98 \text{ Mg/m}^3$ ), respectively. Note that even though the piston was fixed (Figure 6), small volume changes (vertical displacements between  $10$  and  $90 \mu\text{m}$ ) were recorded by the displacement transducer because of the deformability of the system.

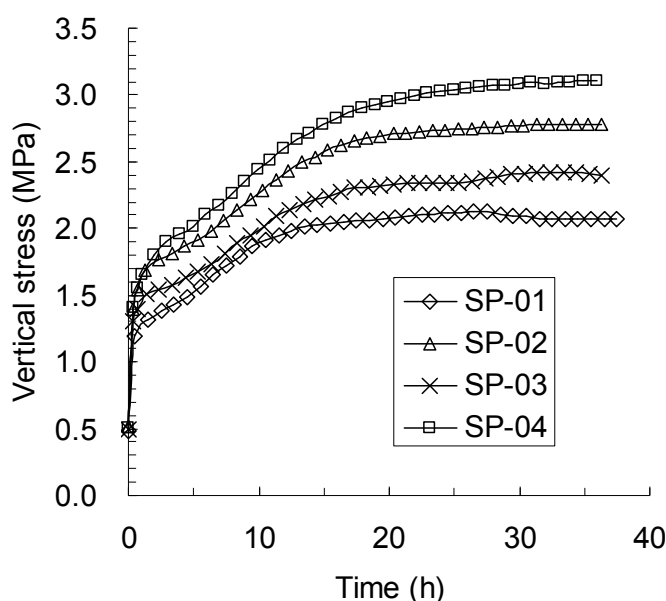


Figure 9. Evolution of the vertical stress for all hydration tests with technological void



Photo 1. Water outflow through the technological void.

### 3.3 Controlled suction compression tests (SO-01, SO-02, SO-03 and SO-04)

The changes in vertical strain with time during suction imposition for tests SO-01, SO-02, SO-03 and SO-04 are presented in Figure 10. In a standard fashion, higher vertical strain rates were observed at smaller suctions with final strains of 1.2% ( $e = 0.69$ ), 5.4% ( $e = 0.73$ ), 6.8% ( $e = 0.75$ ) and 18.0% ( $e = 0.97$ ) obtained for suctions of 38 MPa, 12.6 MPa, 4.2 MPa and 0 MPa, respectively.

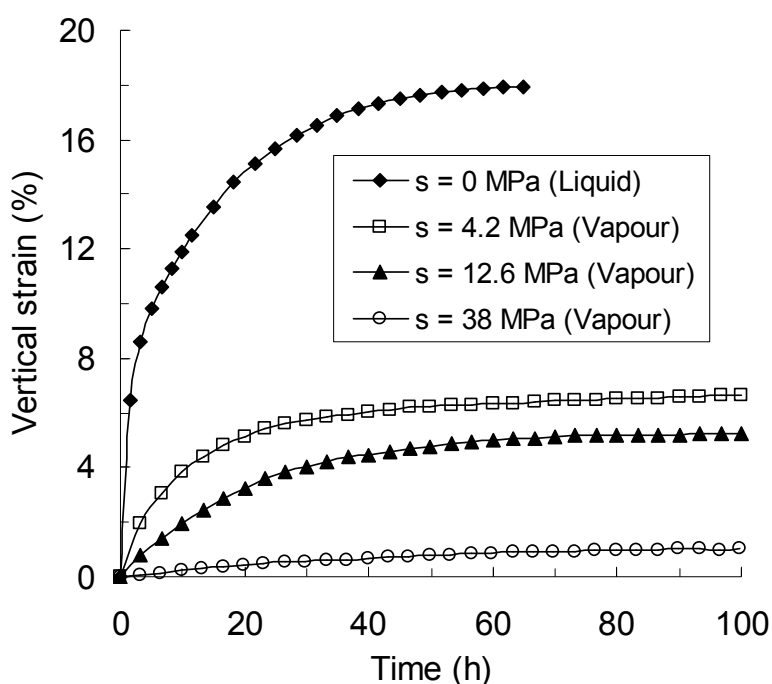


Figure 10. Evolution of vertical strain during suction imposition

The significantly faster hydration observed in test SO-01 (in which liquid water was used imposing a zero suction) was mainly due to the technological void that allowed water circulation around the sample. This first phase was comparable with that of tests SP-02/04 presented in Figure 9.

Figure 11 depicts the final void ratios obtained versus the imposed suctions in a semi-logarithmic plot. The points are reasonably located along a line and the following relationship can be derived:

$$e = -0.048 \ln(s) + 0.848 \quad (\text{Eq.1})$$

where  $e$  is the void ratio at equilibrium and  $s$  is suction in MPa.

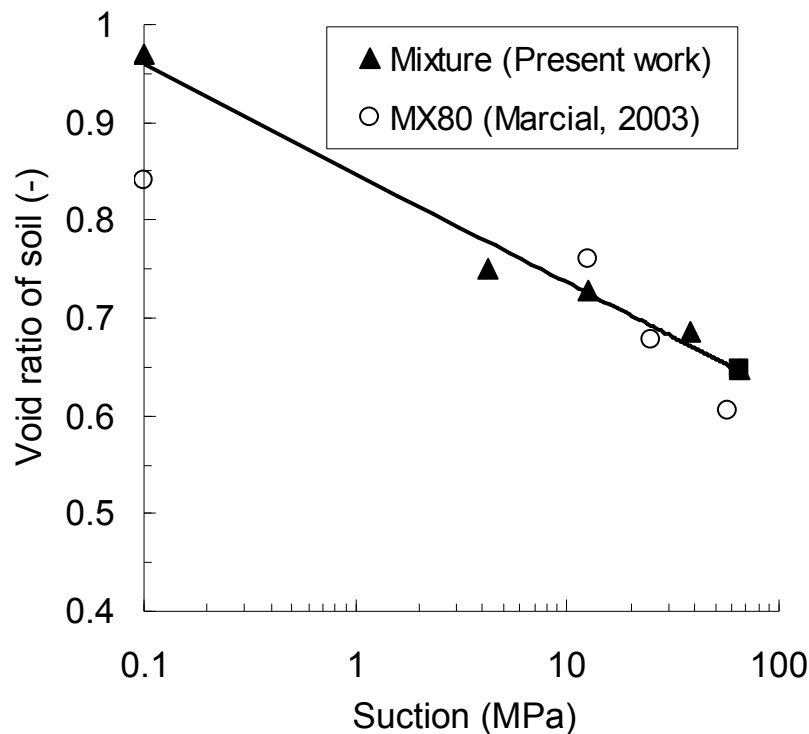


Figure 11. Relationship between void ratio and suction for the compacted sand bentonite mixture.

Once equilibrated at the desired suction, samples were submitted to controlled-suction compression. The compression curves are presented in Figure 12 in a diagram giving the changes in void ratio  $e$  with respect to vertical net stress ( $\sigma_v - u_a$ ) in which  $u_a$  is the air pressure, equal to the atmospheric pressure. Given the significant concerns about the validity of effective stress in unsaturated soils, it was preferred to use the independent variables approach involving the vertical net stress ( $\sigma_v - u_a$ ) and suction ( $s = u_w - u_a$ ), (Coleman 1962, Fredlund and Morgenstern, 1977, Gens 1996).

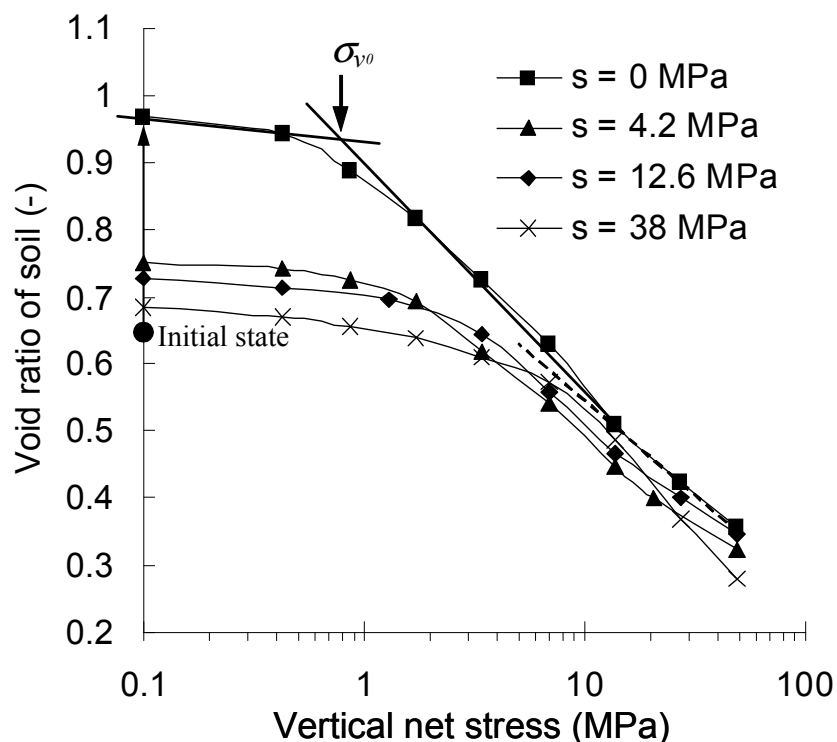


Figure 12. Void ratio of soil versus vertical net stress for different suctions

Initial void ratios were very different because of the significant dependence of initial swelling with respect to the suction imposed. Also, the sample SO-01 was not a homogeneous one, as commented above.

Each sample exhibited a slightly S-shaped compression curve. In a standard fashion, the compression curves are characterized by an initial linear branch with a low compressibility (pseudo-elastic domain) followed by a second branch with a higher compressibility (plastic domain) and a slight upward curvature at higher stresses.

As suggested by other authors (Keller et al., 2004; Tang et al., 2009), the points at high stresses were not used for determining the compression coefficient ( $C_c$ ) and the yield stress ( $\sigma_y$ ) delimitating the pseudo-elastic zone and the plastic one. Figure 13 shows the changes in yield stress with respect to suction. Also plotted in this Figure are the data obtained by Marcial (2003) on pure bentonite samples. Figure 13 confirms that suction decrease significant reduce the yield stress for both the mixture and pure bentonite samples. There is a linear relationship between yield stress and suction, and moreover, both curves are reasonably parallel. At a same suction, smaller yield stresses are observed for the mixture.

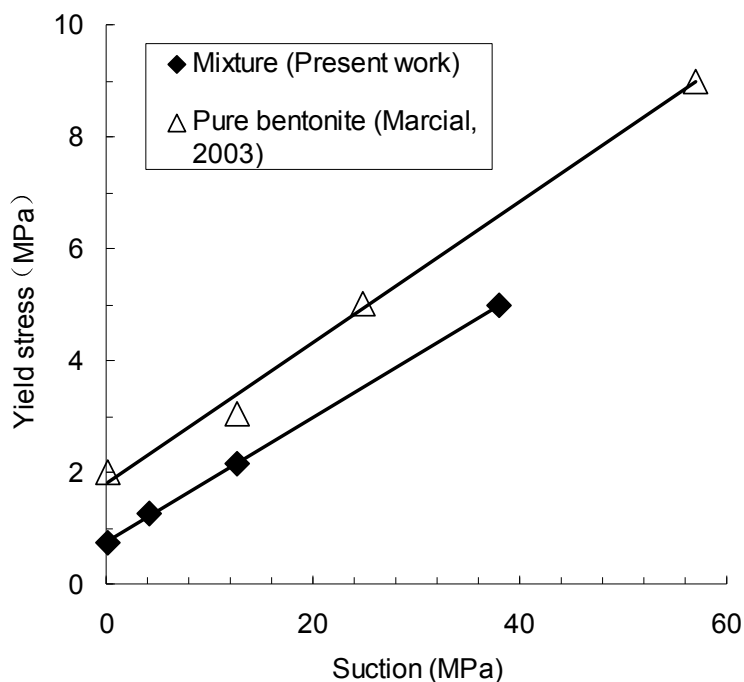


Figure 13. Changes in yield stress with suction

As also observed by Marcial (2003), the change in compression coefficient with respect to suction appeared to be non monotonic (Figure 14) with a decrease when suction was reduced from 38 MPa and 12.6 MPa, followed by an increase when suction was below 12.6 MPa. Comparison between pure bentonite and sand-bentonite mixture shows that at any suction, the latter appears to be more compressible with a larger compression coefficient.

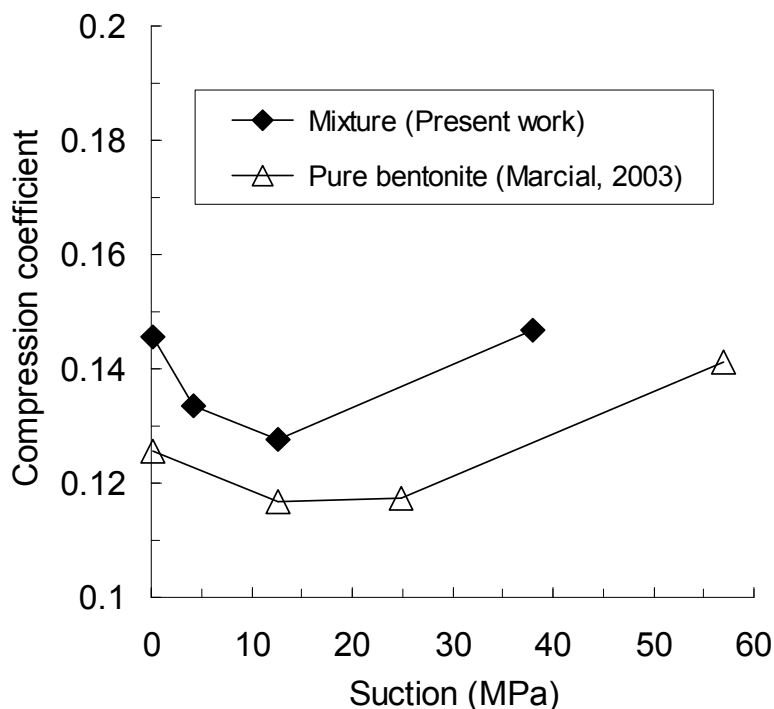


Figure 14. Changes in compression coefficient with suction

### **3.4 Hydraulic conductivity measurements**

The hydraulic conductivity of hydrated samples with initial technological void (tests SP2-SP4) was measured under constant head when applying the 0.1 MPa water pressure by recording the volume of injected water by means of a Pressure/Volume controller (no data were available for test SP01 due to a technical problem with the Pressure/Volume controller). The determination of hydraulic conductivity was done over the last 24 h once swelling stabilised. The hydraulic conductivity was also determined indirectly based on the consolidation curves during different compression stages of test SO-01 (see Figure 12) using Casagrande's method. As mentioned before, the sample density was not homogeneous in those samples. Therefore, a non uniform hydraulic conductivity can be expected for each sample. The measured values correspond to the global hydraulic conductivity.

The changes in hydraulic conductivity with respect to dry density obtained from both methods are presented in Figure 15 and compared with constant head permeability measurements obtained by Gatabin et al. (2008) on homogeneous samples at similar densities. The data obtained for the heterogeneous samples with both methods are in good agreement. In a standard fashion, the hydraulic conductivity decreases with density increase following a slope comparable to that obtained by Gatabin et al. (2008). An in-depth examination shows that the samples tested here exhibit higher hydraulic conductivity than that by Gatabin et al. (2008), with a difference of one order of magnitude. This difference is suspected to be due to a preferential water flow in the looser zone (initial technological voids) around the samples.

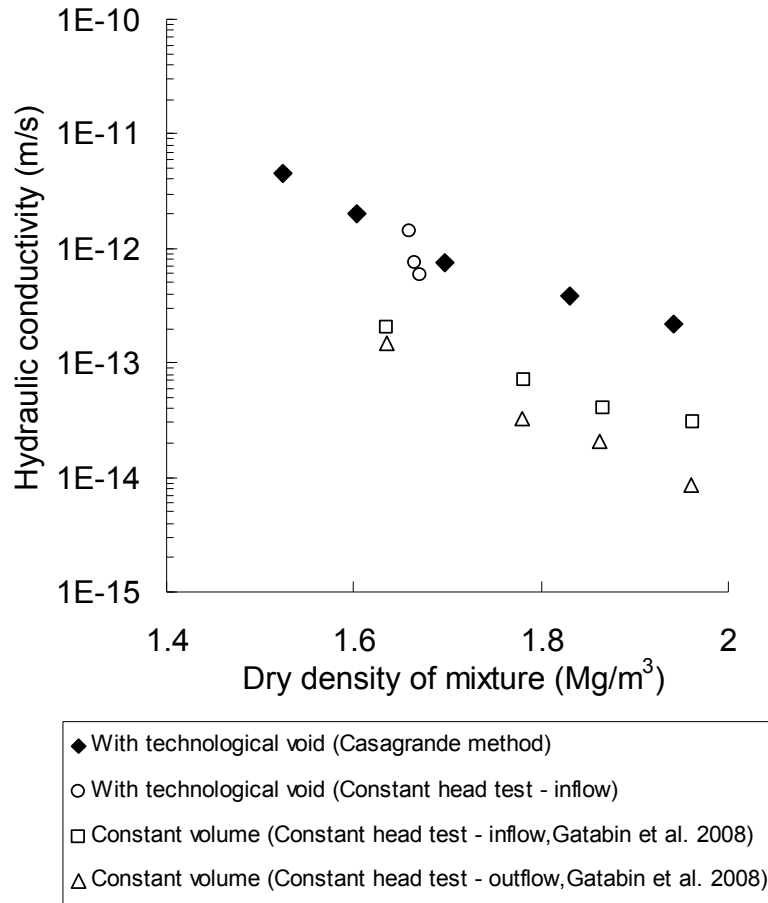


Figure 15. Hydraulic conductivity versus dry density of mixture

#### 4 Interpretation and discussion

In order to further analyse the effects of the technological void, various constitutive parameters of the compacted mixture are now defined (see Figure 16), such as for instance the bentonite void ratio ( $e_b$ ). It is supposed that the volume of bentonite ( $V_b$ ) in the mixture is equal to the difference between the total volume ( $V$ ) and the volume of sand ( $V_s$ ).  $V_b$  is equal to the sum of the bentonite particle volume ( $V_{bs}$ ) and the volume of void, namely intra-void volume ( $V_i$ ). The parameter  $e_b$  consists of two parts (Eq.2), the intra-bentonite void ratio inside the soil ( $e_{bi}$ ) and the void ratio corresponding to the technological void ( $e_{tech}$ ). Eq.3 and Eq. 4 define these two voids, respectively.

$$e_b = e_{bi} + e_{tech} \quad (\text{Eq.2})$$

$$e_{bi} = \frac{V_i}{V_{bs}} \quad (\text{Eq.3})$$

$$e_{tech} = \frac{V_{tech}}{V_{bs}} \quad (\text{Eq.4})$$

where  $V_{tech}$  is the volume of technological void. The value of  $e_{bi}$  can be deduced from the initial dry unit mass of the mixture ( $\rho_{dm}$ ) using Eq.5 and Eq.6.

$$e_{bi} = \frac{G_{sb}\rho_w}{\rho_{db}} - 1 \quad (\text{Eq.5})$$

$$\rho_{db} = \frac{(B/100)\rho_m G_{ss}\rho_w}{G_{ss}\rho_w(1+w_m/100) - \rho_m(1-B/100)} \quad (\text{Eq.6})$$

where  $\rho_w$  is the water unit mass,  $G_{sb}$  is the specific gravity of bentonite,  $\rho_{db}$  is the initial dry unit mass of bentonite in the mixture, which was calculated using Eq.6 (Dixon et al., 1985; Lee et al., 1999; Agus and Schanz, 2008; Wang et al., 2012),  $\rho_m$  is the unit mass of the mixture,  $B$  (%) is the bentonite content (in dry mass) in the mixture,  $G_{ss}$  is the specific gravity of sand,  $w_m$  is the water content of the mixture. In this study the decrease of water unit mass ( $\rho_w$ ) during hydration (e.g. Skipper et al., 1991; Villar and Lloret, 2004) was not considered and the value was assumed to be constant ( $1.0 \text{ Mg/m}^3$ ),  $B = 70\%$ ,  $G_{ss} = 2.65$ .

To analyse the water retention property under free swell condition, a parameter namely water volume ratio ( $e_w$ ) defined as the ratio of water volume ( $V_w$ ) to the bentonite volume ( $V_{bs}$ ) is also adopted (Romero et al., 2011). This parameter can be deduced from the water content of the mixture ( $w_m$ ) using the following equation:

$$e_w = \frac{w_m G_{sb}}{B} \quad (\text{Eq.7})$$

In the following, the two parameters  $e_b$  and  $e_w$  are used to analyze all experimental results obtained in order to evidence the effects of voids on the water retention capacity, the swelling pressure, the compressibility and the hydraulic conductivity.

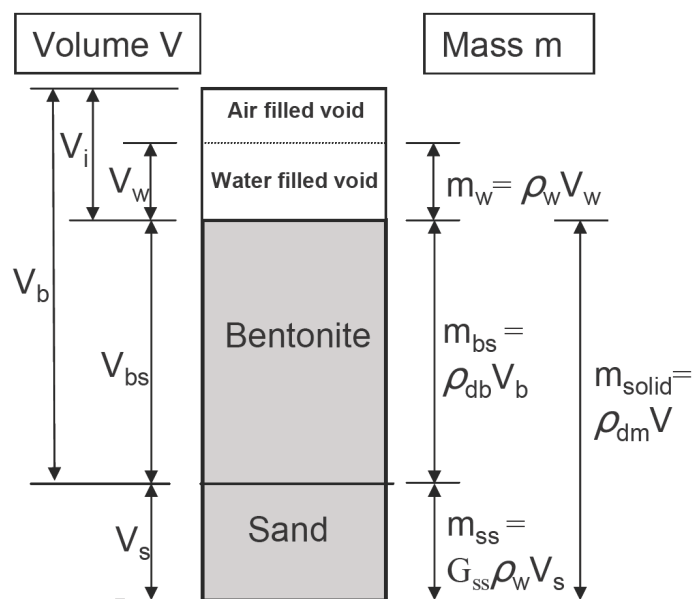


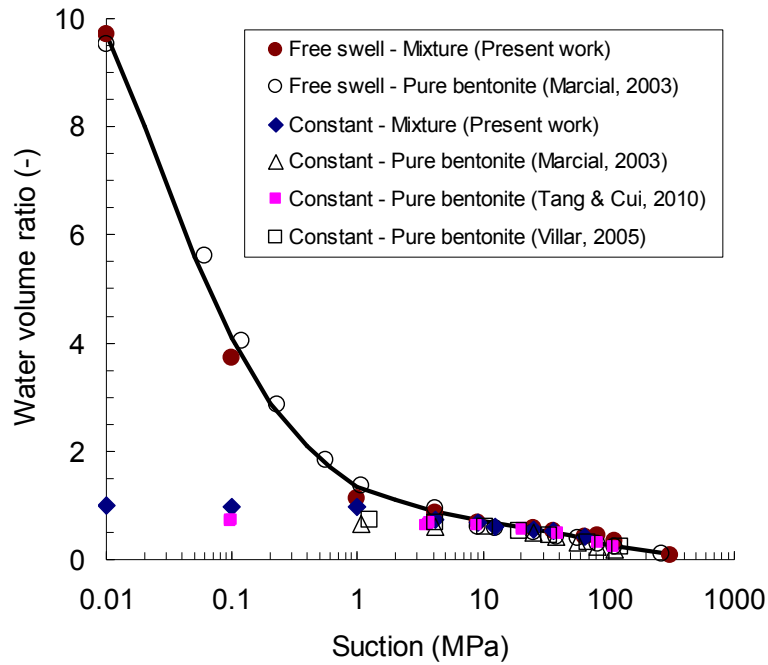
Figure 16. Composition of the bentonite/sand mixture

#### 4.1 Water retention curves

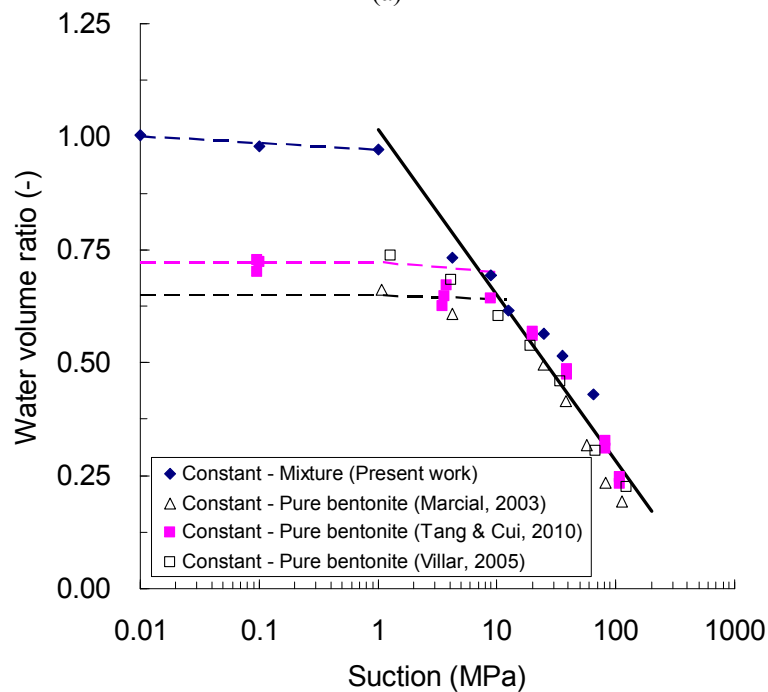
Figure 17a shows the changes in water volume ratio  $e_w$  of both the mixture and the pure bentonite with respect to suction under free swell condition. Unlike in the water content/suction plot (Figure 8), Figure 17a shows an excellent agreement with Marcial (2003)'s data on pure bentonite, with a unique relationship between  $e_w$  and suction along the wetting path with swelling. It confirms that water was only adsorbed in the bentonite (volume  $V_{bs}$ ) and that the lower water content observed in the mixture at same suction (Figure 8) is related to the lower volume of bentonite in the mixture.

The results from the hydration tests on pure compacted bentonites under restrained swell condition with different void ratios (Marcial, 2003; Tang and Cui, 2010; Villar, 2005) are also presented in Figure 17. A phenomenon similar to that observed in the water content/suction plane (Figure 8) can be identified: in the range of low suctions ( $<9$  MPa for the MX80 bentonite), the water retention property of bentonite depends strongly on the confining conditions; conversely, all curves become almost the same in the range of high suctions (as also observed by Agus 2005 and Agus et al. 2010) As suggested by Cui et al. (2002, 2008) and Ye et al. (2009), this confirms that the exfoliation of clay particles from the aggregates into inter-aggregate pores caused by hydration is moderate and can be accommodated at high suctions. By contrast, at lower suctions, available pores become completely full by hydrated clay particles and no more water can be adsorbed. This is not the case when swelling is allowed with much more water adsorbed. Figure 17b is a zoom of Figure 17a at small water

volume ratios (between 0 and 1.5). The difference observed in the curves at constant volume is due to differences in bentonite dry density  $\rho_{db}$ . When the full saturation is approached, samples with a higher bentonite void ratio (lower dry density) logically absorb more water for a given suction.



(a)



$\rho_{db} = 1.43 \text{ Mg/m}^3$  (Present work);  
 $\rho_{db} = 1.60 \text{ Mg/m}^3$  (Tang et al., 2010; Villar, 2005);  $\rho_{db} = 1.70 \text{ Mg/m}^3$  (Marcial, 2003).  
 (b)

Figure 17. Water volume ratio (ew) Versus suction. a) full range of water volume ratio; b) zoom on the range of low water volume ratio

## 4.2 Hydration test with technological void

The values of vertical stress measured on heterogeneous samples at the end of the hydration tests on samples with technological voids (SP 01-04) are presented in Figure 18 with respect to the bentonite void ratio. Note that the bentonite void ratios for tests SP 01-04 were determined by taken into account the system deformation mentioned above (i.e. vertical displacements between 10 and 90  $\mu\text{m}$ ). The data of swelling stresses measured in homogeneous samples under the same conditions of constant volume by other authors are also plotted for comparison (MX80 70/30 bentonite/sand mixture from Karnland et al., 2008 and pure MX80 bentonite from Börgesson et al., 1996; Dixon et al., 1996; Karnland et al., 2008; Komine et al., 2009).

All data remarkably agree, providing a unique relationship between the vertical pressure and the bentonite void ratio, regardless of the sample nature (homogeneous or not). The correspondence with data from Karnland (pure bentonite and 70/30 bentonite sand mixture) at bentonite void ratio close to 1 is particularly good. The following expression can be deduced for the relationship between the axial stress ( $\sigma_s$  in MPa) and the bentonite void ratio  $e_b$  for the material studied here:

$$\sigma_s = 2.250e_b^{-1.149} \quad (\text{Eq.8})$$

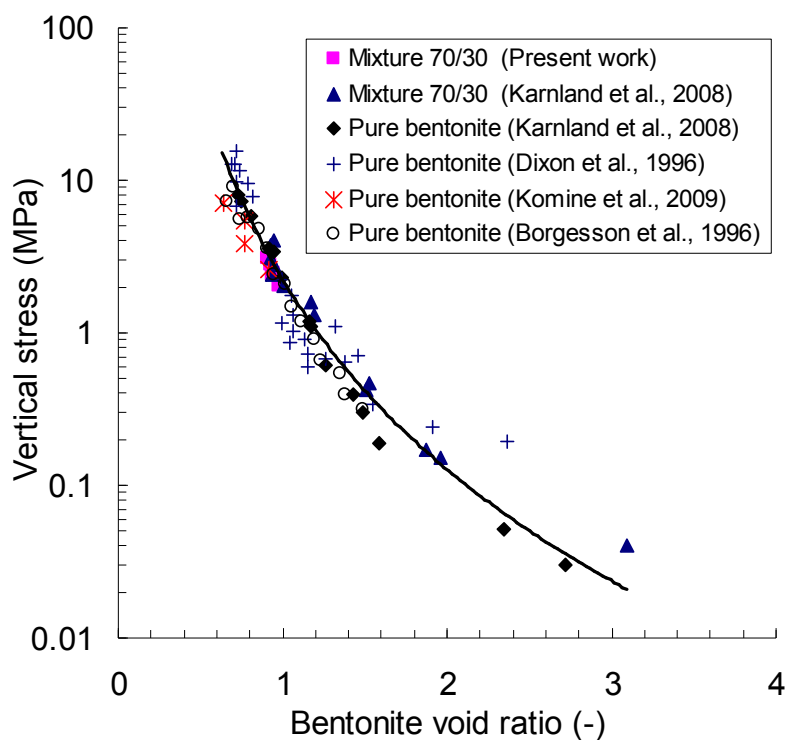


Figure 18. Relationship between vertical stress and bentonite (MX 80) void ratio

This good correspondence between the response in swelling stress of homogeneous samples and that in axial stress of a hydrated heterogeneous sample indeed confirms that the stress at equilibrium is not affected by the heterogeneity of the samples. The pressure ( $\sigma_s$  in MPa) only depends on the global bentonite void ratio ( $e_b$ ), regardless of the technological void and of the presence of sand.

In other words, during the hydration under constant global volume and in spite of their significant difference in form and dimension, the technological voids play the same role as the macro-pores of the homogeneous compacted bentonite in terms of filling voids by particle exfoliation, as commented above. The global final bentonite void ratio (or density) appears to be a relevant parameter allowing predicting the final axial stress obtained.

### 4.3 Compressibility

The interpretation of the compressibility data was based on the well known features of the aggregate microstructure of compacted soils that have been recalled above, showing in particular that the compression at constant water content of unsaturated compacted soils initially occurs by the collapse of large inter-aggregate pores full of air with little effect on the aggregates themselves. As a consequence, it was observed that the changes in suction during compression at constant water content are negligible, since suction changes are governed by intra-aggregate clay water interactions that are little affected during compression (Li, 1995; Gens et al., 1995; Tarantino and De Col, 2008).

The compression curves of the homogeneous samples in Figure 12 (SP2 to 4) are further interpreted by an approximated estimation of the changes in degree of saturation during compression. This estimation is based on the assumption that the order of magnitude of the initial water contents of the samples hydrated from the initial as-compacted suction (65 MPa) at given suctions (38, 12.6 and 4.2 MPa) prior to compression can be obtained from the wetting path of the water retention curve in Figure 17. Based on this assumption, the water contents after hydration were determined, equal to 12.8, 16.8 and 18.6 % for suctions of 38, 12.6 and 4.2 MPa, respectively. The corresponding degrees of saturation are 52, 63 and 68%, respectively.

The application of suctions as high as 4.2, 12.6 and 38 MPa generated a moderate swelling of the samples, with void ratio increasing from the initial value of 0.64 to 0.75 at 4.2 MPa suction. In terms of microstructure, the changes corresponds to a moderate swelling of the aggregates within a structure still significantly desaturated with a maximum degrees of

saturation of 68% at 4.2 MPa suction, indicating that the inter-aggregates pores remained full of air. During compression, the water content that was controlled within the aggregates did not suffer from any significant changes and the changes in degree of saturation could be estimated, as shown in Figure 19. The data show how the degree of saturation increase with increased stress and provide an estimation of the stress values at which saturation was reached (9, 14 and 27 MPa at  $s = 4.2$ , 12.6 and 38 MPa respectively). Once reported on the compression curves of Figure 12, we can observe that these stress values are located close to the inflection points observed on the curves, indicating that these points correspond to the saturation of the samples. In other words, the change in slope of the curves corresponds to the transition between two physical mechanisms, namely from the collapse of dry inter-aggregate pores to the expulsion of inter-aggregate adsorbed water. This is in agreement with the observation by Kochmanová and Tanaka (2011).

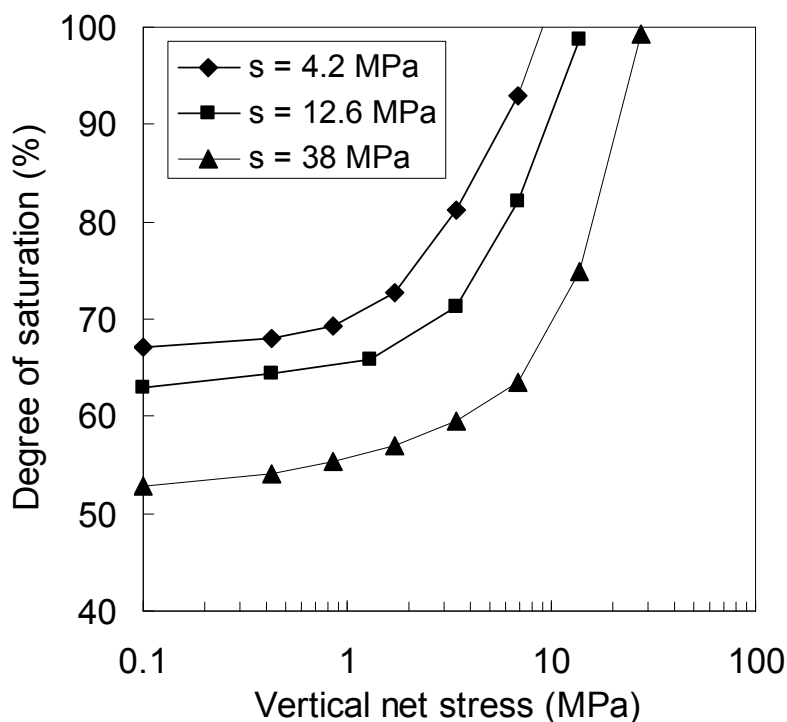


Figure 19. Changes in degree of saturation during compression

When the yield stress ( $\sigma_{v0}$ ) in Figure 13 is plotted versus the corresponding bentonite void ratio ( $e_b$ ) at the yield point (Figure 20), it appears that for both the mixture and pure bentonite, the yield stress increases sharply with decreasing bentonite void ratio. However, the curve of the mixture lies in the right of the pure bentonite's one, evidencing the role of sand in the compression behaviour. It can be concluded from Figure 20 that at the same bentonite void ratio, the mixture yields at a higher pre-consolidation stress.

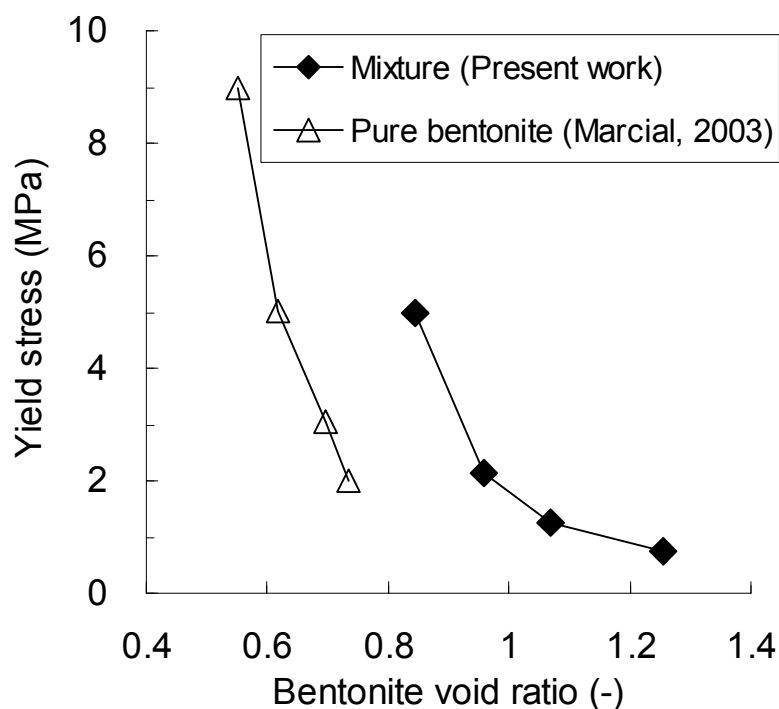


Figure 20. Relationship between yield stress and bentonite void ratio

#### 4.4 Hydraulic conductivity

The values of global hydraulic conductivities presented in Figure 15 showed possible preferential flow pathway in the case of heterogeneous samples with initial technological voids. This observation can be made also in Figure 21 in which the data of Figure 15 are re-plotted versus the bentonite void ratio and compared to other data of the pure MX80 bentonite (Karnland et al., 2008; Dixon et al., 1996) and of the 70/30 bentonite-sand mixture (Gatabin et al., 2008). The good agreement observed also confirms a negligible effect of sand on the hydraulic conductivity.

Note that the looser zone corresponding to the initial technological void is a weak zone with poorer mechanical resistance, at least on the short term. The question of the possible further changes that could occur on the long term is opened, given that some observations already showed that ageing effects are significant in compacted bentonite, both at microscopic scale (Delage et al. 2006) and macroscopic scale (Stroes-Gascoyne, 2010), showing a tendency towards density homogenisation. Further studies are needed to investigate the long term change in hydraulic conductivity of samples with initial technological voids.

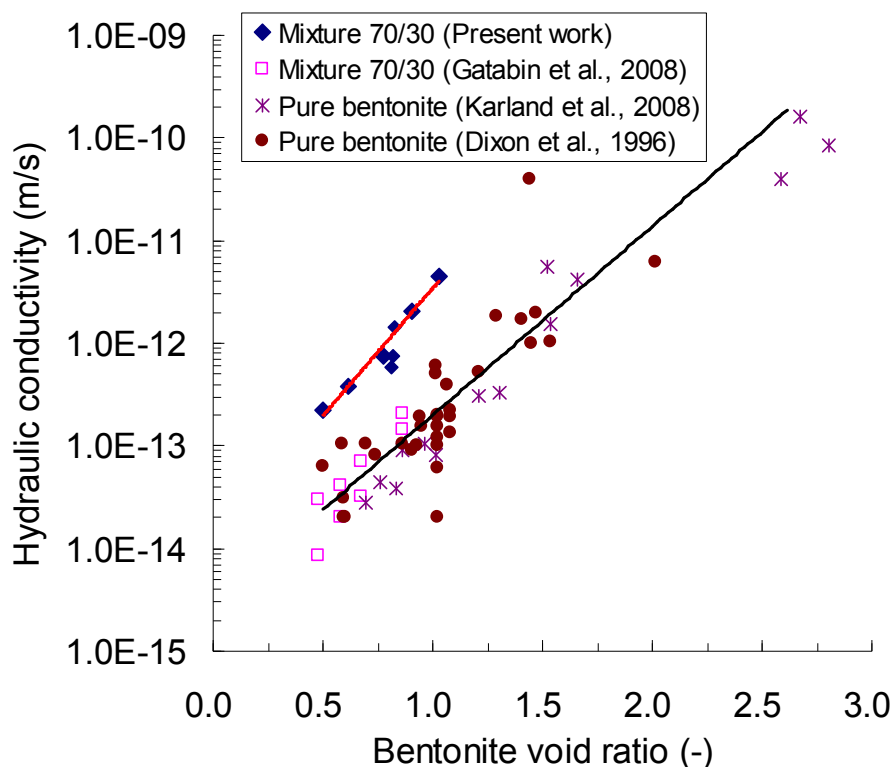


Figure 21. Hydraulic conductivity versus bentonite void ratio

## 5 Conclusion

The effects of voids on the hydro-mechanical properties of a compacted bentonite-sand mixture were studied. Water retention test, hydration test, suction controlled oedometer test and hydraulic test were performed on samples with different voids including the technological void and the void inside the soil. By introducing the parameters as bentonite void ratio and water volume ratio, the effects of voids on the water retention property, the swelling pressure, the compressibility and the hydraulic conductivity were analyzed.

Under different conditions (free swell and restrained swell), different water retention properties were observed depending on the suction value: at high suctions, the relation between the water volume ratio and the suction is unique, independent of the test conditions, indicating that the relatively limited exfoliated clay particles are mainly accommodated by the macro-pore of the soil. On the contrary, in the range of low suctions, the macro-pores available for accommodating exfoliated particles becomes limited in the case of restrained swell condition, explaining why less water is adsorbed in this case.

There is a unique relationship between the axial stress (for samples with technological void) or swelling pressure (constant volume condition) and the bentonite void ratio, regardless of

the sample nature (homogeneous or not) and presence of sand, suggesting that the technological voids play the same role as the macro-pores of the homogeneous compacted bentonite. It also reveals that the swelling mechanisms of bentonite-sand mixture are the same as that of pure bentonite.

The change in slope of the compression curves corresponds to the transition between two physical mechanisms, namely from the collapse of dry inter-aggregate pores to the expulsion of inter-aggregate adsorbed water.

At the same bentonite void ratio, bentonite/sand mixture yields at a higher pre-consolidation stress, evidencing the effect of sand on the compression behaviour.

Similar relationship between hydraulic conductivity and bentonite void ratio was observed for the bentonite-sand mixture and the pure bentonite without technological void; however, with the technological void in this study, the measured hydraulic conductivity for the same bentonite void ratio is generally higher, indicating the possible preferential flow pathway formed by the swollen soil that occupied the initial technological void.

From a practical point of view, the relationship elaborated between the hydro-mechanical behaviour with bentonite void ratio is helpful in designing the buffers/sealing elements with bentonite-based materials: if the bentonite proportion and the technological void are known, the specification of the buffer elements could be determined using the correlations elaborated in this study, according to the requirements in terms of swelling pressure and hydraulic conductivity. Then the water retention property and compressibility of the selected material can be evaluated. It should be however noted that the conclusion drawn here was based on the results of the bentonite/sand mixture with 70% of MX80 bentonite. Further experimental studies on other proportions and other bentonites are needed to generalise it.

## **Acknowledgements**

The work was conducted in the framework of the SEALEX project of IRSN and the PHC Cai Yuanpei project (24077QE). The support of the National Nature Science Foundation of China (41030748) and that of the China Scholarship Council (CSC) are also greatly acknowledged.

## References

- AFNOR, 1992. AFNOR NF P94-057, Soils: investigation and testing. Granulometric analysis. Hydrometer method. Association Francaise de Normalisation. France.
- AFNOR, 1996. AFNOR NF P94-056, Soils: investigation and testing. Granulometric analysis. Dry sieving method after washing. Association Francaise de Normalisation. France.
- Agus, S.S., 2005. An Experimental study on hydro-mechanical characteristics of compacted bentonite-sand mixtures. PhD thesis. Weimar.
- Agus, S.S., and Schanz, T., 2008. A method for predicting swelling pressure of compacted bentonites. *Acta Geotechnica*, 3(2), 125-137.
- Agus, S.S., and Schanz, T., and Fredlund, D.G., 2010. Measurements of suction versus water content for bentonite-sand mixtures. *Can. Geotech. J.*, 47, 583-594.
- Ahmed, S., Lovell, C.W. & Diamond, S. 1974. Pore sizes and strength of compacted clay. *ASCE Journal of the Geotechnical Engineering Division* 100, 407-425.
- Andra, 2005. Référentiel des matériaux d'un stockage de déchets à haute activité et à vie longue - Tome 4: Les matériaux à base d'argilites excavées et remaniées. Rapport Andra N° CRPASC040015B.
- Barnichon, J.D. and Deleruyelle, F., 2009. Sealing Experiments at the Tournemire URL. EUROSAFE.
- Börjesson, L., Karnland, O., Johannesson L.E., 1996. Modelling of the physical behaviour of clay barriers close to water saturation.pdf: Modelling of the physical behaviour of clay barriers close to water saturation. *Engineering Geology* 41, 127-144.
- Coleman, J.D. 1962. Stress-Strain relations for partially saturated soils. *Géotechnique* 12 (4), 348-350.
- Cui, Y.J., Loiseau, C. and Delage, P., 2002. Microstructure changes of a confined swelling soil due to suction controlled hydration. *Unsaturated soils: proceedings of the Third International Conference on Unsaturated Soils*, 10-13, March 2002, Recife, Brazil, 593-598.
- Cui, Y.J., Tang, A.M., Loiseau, C., Delage, P., 2008. Determining the unsaturated hydraulic conductivity of a compacted sand-bentonite mixture under constant-volume and free-swell conditions. *Physics and Chemistry of the Earth, Parts A/B/C*, 33 (Supplement 1), S462 - S471.
- Cui, Y.J., Tang, A.M., Qian, L.X., Ye, W.M., Chen, B., 2011. Thermal-mechanical behavior of compacted GMZ Bentonite. *Soils and Foundations*, Vol. 51, No. 6, 1065-1074.
- Delage P. & Graham J. 1995. The mechanical behaviour of unsaturated soils. *Proceedings of the 1st International Conference on Unsaturated soils*, Vol. 3, 1223-1256, Paris, E.E. Alonso and P. Delage eds, Balkema.
- Delage, P., Audiguier, M., Cui, Y.J. & Howat, M.D. 1996. Microstructure of a compacted silt. *Canadian Geotechnical Journal*, 33 (1), 150-158.
- Delage, P., Howat, M.D., Cui, Y.J., 1998. The relationship between suction and swelling properties in a heavily compacted unsaturated clay. *Engineering Geology*, 50(1-2), 31-48.
- Delage, P., Marcial, D., Cui, Y.J., Ruiz, X., 2006. Ageing effects in a compacted bentonite: a microstructure approach. *Géotechnique* 56 (5), 291-304.
- Delage, P. and Cui, Y.J. 2008a. An evaluation of the osmotic method of controlling suction. *Journal of Geomechanics and Geoengineering* 3 (1), 1-11.
- Delage, P. and Cui, Y.J. 2008b. A novel filtration system for polyethylene glycol solutions used in the osmotic method of controlling suction. *Canadian Geotechnical Journal* 45, 421-424.
- Dixon, D.A., Gray, M.N. and Thomas, A.W., 1985. A study of the compaction properties of potential clay-sand buffer mixtures for use in nuclear fuel waste disposal. *Engineering Geology*, 21, 247-255.
- Dixon, D.A., Gray, M.N., Hnatiw, D., 1992. Critical gradients and pressures in dense swelling clays. *Canadian Geotechnical Journal* 29 (6), 1113-1119.

- Dixon, D.A., Gray, M.N., Graham, J., 1996. Swelling and hydraulic properties of bentonites from Japan, Canada and USA. In Proceedings of the second International Congress on Environmental Geotechnics, Osaka, Japan, 5-8.
- Fredlund D.G. & Morgenstern N.R. 1977. Stress state variables for unsaturated soils. ASCE J. Geotech. Eng. Div. GT5, 103, 447-466.
- Gatabin, C., Touze, G., Imbert, C., Guillot, W., Billaud, P., 2008. ESDRED Project, Module 1-Selection and THM characterization of the buffer material. In International conference underground disposal unit design&emplacement processes for a deep geological repository, 16-18 June, Prague.
- Gens, A., Alonso, E.E., Suriol, J., Lloret, A., 1995. Effect of structure on the volumetric behaviour of a compacted soil. In: Alonso, Delage (Eds.), Proc. 1st Int. Conf. on Unsaturated Soils, Paris, vol. 1. Balkema, Rotterdam, 83-88.
- Gens, A., 1996. Constitutive modelling : Application to compacted soils . Proc. 1st Int. Conf on Unsaturated Soils UNSAT' 95, Vol. 3, 1179-1200, Paris.
- Juvankoski, M., 2010. Description of basic design for buffer (working report 2009-131). Technical report, EURAJOKI , FINLAND.
- Karland, O., Nilsson, U., Weber, H., and Wersin, P., 2008. Sealing ability of Wyoming bentonite pellets foreseen as buffer material-Laboratory results. Physics and Chemistry of the Earth, Parts A/B/C, 33, S472-S475.
- Keller, T., Arvidsson, J., Dawidowski, J.B., Koolen, A.J., 2004. Soil precompression stress. II. A comparison of different compaction tests and stress - displacement behaviour of the soil during wheeling. Soil Till. Res. 77, 97-108.
- Kochmanová, N., Tanaka, H., 2011. Influence of the Soil Fabric on the Mechanical Behaviour of Unsaturated and Saturated Clay. Soils and Foundations, Vol. 51, No. 2, 275-286.
- Komine, H. and Yasuhara, K. and Murakami, S. 2009. Swelling characteristics of bentonites in artificial seawater. Canadian Geotechnical Journal. 46, 177-189
- Komine, H., 2010. Predicting hydraulic conductivity of sand bentonite mixture backfill before and after swelling deformation for underground disposal of radioactive wastes. Engineering Geology. 114, 123-134
- Komine, H., Watanabe, Y., 2010. The past, present and future of the geo-environment in Japan. Soils and Foundations, Vol. 50 (2010) No. 6 977-982.
- Lee, J.O., Cho, W.J. and Chun, K.S., 1999. Swelling Pressures of a Potential Buffer Material for High-Level Waste Repository. Journal of the Korean Nuclear Society, 31, 139-150.
- Li, Z.M., 1995. Compressibility and collapsibility of compacted unsaturated loessial soils. In: Alonso, Delage (Eds.), Proc. 1st Int. Conf. on Unsaturated Soils, Paris, vol. 1.Balkema, Rotterdam, 139-144.
- Lloret, A., Villar, M., 2007. Advances on the knowledge of the thermo-hydro-mechanical behaviour of heavily compacted FEBEX bentonite. Physics and Chemistry of the Earth, 32, 701-715
- Marcial, D., Delage, P. and Cui, Y.J. 2002. On the high stress compression of bentonites. Canadian Geotechnical Journal 39, 812-820.
- Marcial, D., 2003. Comportement hydromécanique et microstructural des matériaux de barrière ouvragée, thèse ENPC.
- Martin, P.L., Barcala, J.M., and Huertas, F., 2006. Large-scale and long-term coupled thermo-hydro-mechanic experiments with bentonite: the febex mock-up test. Journal of Iberian Geology, 32(2), 259-282.
- Montes-H, G., Duplay, J., Martinez, L., and Mendoza, C. 2003. Swelling–shrinkage kinetics of MX80 bentonite. Applied Clay Science, 22, 279-293.
- Pusch, R., 1979, Highly compacted sodium bentonite for isolating rock-deposited radioactive waste products. Nucl. Technol.:(United States), 45(2).

- Romero, E., Gens, A. & Lloret, A., 1999. Water permeability, water retention and microstructure of unsaturated compacted Boom clay. *Engineering Geology*, 54, 117-127.
- Romero, E., Della Vecchia, G., and Jommi, C., 2011. An insight into the water retention properties of compacted clayey soils. *Geotechnique* 61, No. 4, 313-328.
- Skipper, N.T., Refson, K., McConnell, J.D.C., 1991. Computer simulation of interlayer water in 2:1 clays. *J. Chem. Phys.* 94 (11), 7434-7445.
- Sridharan, A., Altschaeffle, A. G. and Diamond, S. (1971), Pore size distribution studies, *Journal of the Soil Mechanics and Foundations Division, Proceedings of the ASCE*, vol. 97, SM 5, 771-787
- Stroes-Gascoyne, S. 2010. Microbial occurrence in bentonite-based buffer, backfill and sealing materials from large-scale experiments at AECL's underground research laboratory. *Applied Clay Science*, 47(1-2), 36-42.
- Tang, A.M., Cui, Y.J., Eslami, J. Defossez, P., 2009. Analysing the form of the confined uniaxial compression curve of various soils . *Geoderma* vol (148)3-4, 282-290.
- Tang, A.M and Cui, Y.J., 2010, Effects of mineralogy on thermo-hydro-mechanical parameters of MX80 bentonite, *Journal of Rock Mechanics and Geotechnical Engineering*. 2 (1), 91-96.
- Tarantino, S. and De Col, E., 2008. Compaction behaviour of clay. *Géotechnique*, vol. 58 (3), 199-213.
- Villar, M.V. and Lloret, A., 2004. Influence of temperature on the hydro-mechanical behaviour of a compacted bentonite. *Applied Clay Science*, 26(1-4), 337-350.
- Villar, M.V., 2005, MX-80 Bentonite. Thermo-Hydro-Mechanical Characterisation Performed at CIEMAT in the Context of the Prototype Project. CIEMAT Technical Report: CIEMAT/DIAE/54540/2/04.
- Villar, M.V., Lloret, A., 2008. Influence of dry density and water content on the swelling of a compacted bentonite. *Applied Clay Science*, 39(1-2), 38-49.
- Wang Q., Tang A.M., Cui Y.J., Delage P., Gatmiri B. 2012. Experimental study on the swelling behaviour of bentonite/claystone mixture. *Engineering Geology* 124, 59-66.
- Yahia-Aissa, M., Delage, P., & Cui, Y.J. 2001. Suction-water relationship in swelling clays. *Clay science for engineering*, IS-Shizuoka International Symposium on Suction, Swelling, Permeability and Structure of Clays, 65-68, Adachi & Fukue eds, Balkema.
- Ye, W.M., Cui, Y.J., Qian, L.X., and Chen. B., 2009. An experimental study of the water transfer through confined compacted gmz bentonite. *Engineering Geology*, 108(3-4), 169-176.
- Yong, R.N., Boonsinsuk, P., and Wong, G., 1986. Formulation of backfill material for a nuclear fuel waste disposal vault. *Canadian Geotechnical Journal*, 23(2), 216-228.

Wang, Q., Tang, A. M., Cui, Y.J., Li X.L., Ye, W.M., 2012. submitted to Canadian Geotechnical Journal

## Time and density dependent microstructure features of compacted bentonite

Qiong WANG<sup>1</sup>, Anh Minh TANG<sup>1</sup>, Yu-Jun CUI<sup>1,3</sup>, Xiang-Ling LI<sup>2</sup>, Wei-Min YE<sup>3</sup>

**Abstract:** Pre-compacted bentonite bricks are often considered as sealing/backfill elements in deep geological repository for high level radioactive waste. A good understanding of its microstructure changes upon hydration is essential as it is directly related to the macroscopic hydro-mechanical behaviour. In this study, the microstructure features of the compacted MX80 bentonite used as a sealing material in a field heating experiment were characterized by means of both mercury intrusion porosimetry (MIP) and scanning electron microscopy (SEM). Emphasis was put in the effects of final dry density (density after swelling) and hydration time. The results obtained show that the changes in soil porosity upon swelling is mainly due to the increase in macro-pores of about 50  $\mu\text{m}$  diameter and the meso-pores of 1  $\mu\text{m}$  diameter. In addition, the microstructure changed over time due to the water re-distribution that occurred among each pores level: both the macro-pores and micro-pores volume decreased along with an increase in the volume of meso-pores. A uniform microstructure can be then expected in long term. Furthermore, it was observed that the higher the final dry density the slower the evolution of microstructure changes.

**Keywords:** radioactive waste disposal; compacted bentonite; microstructure; final dry density; hydration time

---

### 1 Introduction

In the conception of deep geological repository for high-level radioactive wastes (HLW), compacted bentonite are often considered as buffer and sealing material. During its long lifetime, this material will be subjected to thermo-hydro-mechanical loadings, and it is therefore important, for the safety of the storage system, to well understand its behaviour under such complex and coupled loadings. On the other hand, as the thermo-hydro-mechanical behaviour of bentonite is strongly related to its microstructure changes, a good understanding of its microstructure changes is essential. For this reason, the microstructure of compacted bentonite has been widely investigated. A typical bi-model porosity is usually observed on the as-compacted unsaturated samples (Ahmed et al. 1974, Delage et al. 1996, Romero et al. 1999, Cui et al. 2002, Delage 2007), corresponding to the intra-aggregate pores and inter-aggregate pores, respectively. Increase of dry density reduces the macro-pores quantity (Delage and Graham 1995, Sridharan et al. 1971), but does not

---

1 Ecole des Ponts ParisTech, Navier/CERMES , France

2 Euridice Group, SCK/CEN, Belgium

3 Tongji University, China

change the micro-pores. Upon hydration, Cui et al. (2002) observed that wetting by decreasing suctions under constant volume condition leads to deformation of aggregates; as a result, the macro-pores are progressively clogged. This was confirmed by Thom et al. (2007) on unsaturated compacted kaolin.

The microstructure of compacted bentonite can also change over time. Indeed, Delage et al. (2006) investigated the time-dependent microstructure changes of the MX80 bentonite compacted at various dry densities and water contents, and they observed that under constant volume condition, the microstructure of soil changed over time because of the equilibration of water potential between micro- and macro-pores. Their work was however limited to the as-compacted state which corresponds to an unsaturated state. To the authors' knowledge, there has been no investigation of microstructure changes during different hydration time when the soil samples were fully saturated, even though this corresponds to the situation in a real repository system.

This effect of hydration time on microstructure changes was investigated in this study. The soil studied is the pre-compacted MX80 bentonite which is used for the hydraulic seal in the PRACLAY in-situ experiment performed in the underground laboratory of Mol, Belgium. This hydraulic seal is of annular shape and made up of compacted bentonite bricks. It is installed between the heated zone and the access gallery to achieve the desired undrained hydraulic boundary condition (Tang et al. 2008, Li et al. 2010). The bentonite bricks are expected to swell upon hydration, filling the initial technological voids and compensating the deformation of the host Boom clay. Thus, its dry density decreases as a result of the swelling. From a practical point of view, it is important to understand the microstructure changes due to the density evolution.

In the present work, the microstructure features of MX80 bentonite were investigated by means of both mercury intrusion porosimetry (MIP) and scanning electron microscopy (SEM). To study the final density effect (density after swelling), saturated samples with different final dry densities were prepared. To study the hydration time effect, samples of different dry densities were, after saturation, maintained for various time periods, and then subjected to microstructure investigation.

## **2 Materials and methods**

Samples used in this study were cut from the pre-compacted MX80 bentonite blocks identical to that used for the construction of the hydraulic seal in the PRACLAY heater experiment.

The initial dry density of the soil is  $1.80 \text{ Mg/m}^3$  and the initial water content is 15.22%. The MX80 bentonite has a soil particle density of  $2.77 \text{ Mg/m}^3$  and a montmorillonite content as high as 80%. Its high montmorillonite content explains its high Atterberg limits (liquid limit  $w_L = 520$ , plastic limit  $w_P = 46$ , plasticity index  $I_p = 474$ ). Its cation exchange capacity (CEC) is 76 meq/100g of which  $\text{Na}^+$  represents 83 %.

The pore size distribution (PSD) curve obtained from MIP tests on the as-compacted bentonite ( $\rho_d = 1.80 \text{ Mg/m}^3$ ,  $e = 0.54$ ) is shown in Figure 1. A typical bimodal porosity (Ahmed et al. 1974, Delage et al. 1996, Romero et al. 1999) was identified, defining a family of intra-aggregate pores of  $0.015 \text{ }\mu\text{m}$  diameter and a family of inter-aggregate pores of  $10 \text{ }\mu\text{m}$  diameter. The macro-pore quantity which depends on the dry density (Delage and Graham 1995, Delage et al. 1996, Sridharan et al. 1971) appears quite limited. Note that in compacted bentonite, a smaller size pore population ( $< 2 \text{ nm}$ ) corresponding to the intra-particle (interlayer) pores within the aggregates can also be identified by transmission electronic microscope (Ben Rhaïem, H. 1985, Saiyouri 1998). This population is not detectable by the MIP (Delage et al. 2006, Lloret et al. 2003, Lloret and Villar 2007, Nowamooz and Masrouri 2010).

In order to investigate the effects of final dry density and hydration time on the microstructure features of compacted MX80, a constant volume cell (50 mm in diameter and 5 mm in height) was developed (Figure 2). The choice of final dry density values referred to the technological voids (different gaps involving the bentonite bricks) and the deformation of host Boom clay. Preliminary numerical analysis showed that the value is around  $1.6 \text{ Mg/m}^3$ . In order to evidence experimentally the final dry density effect, four values ranging from  $1.80$  to  $1.40 \text{ Mg/m}^3$  (see Table 1) were considered, which correspond to a swelling in the range from 0 to 17.6 % in the field conditions. To investigate the hydration time effect, for each final dry density, three identical samples were prepared and hydrated for 15, 30 and 90 days, respectively (Table 1).

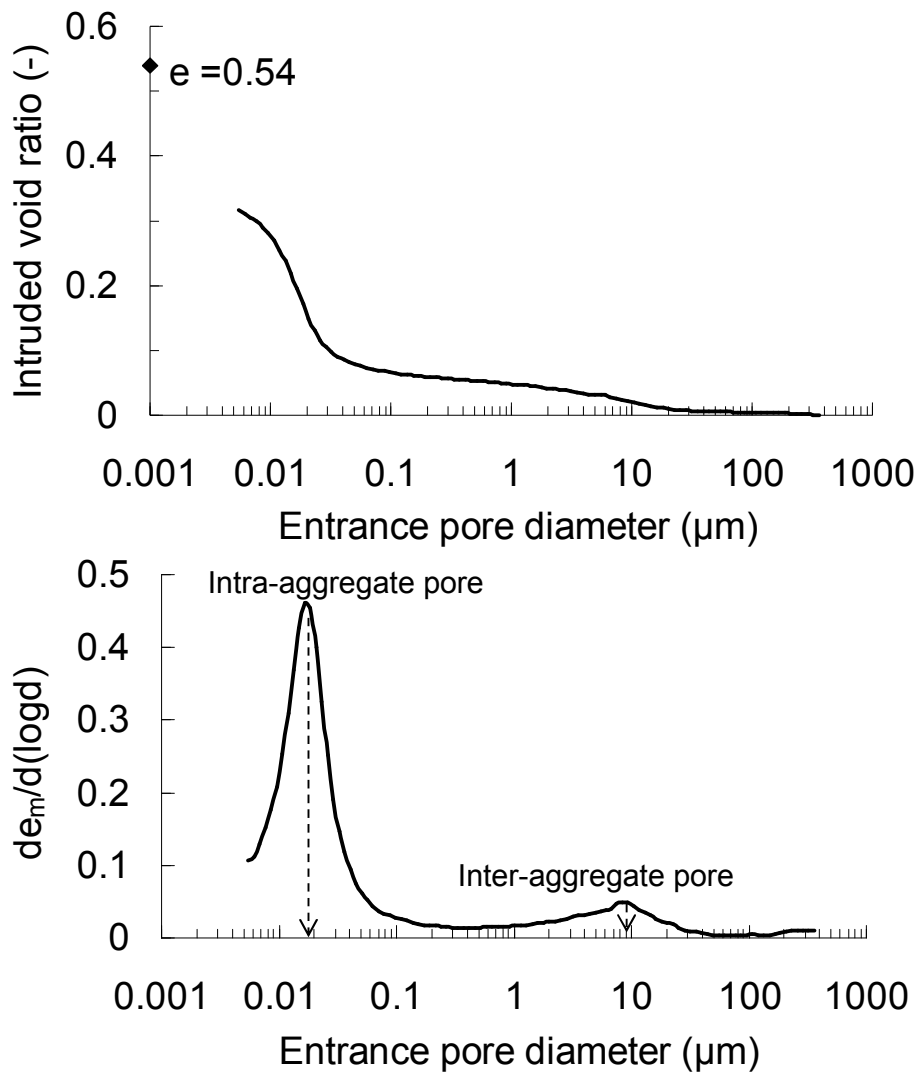


Figure 1 Pore size distribution of the as-compacted sample with dry density of  $1.80 \text{ Mg/m}^3$

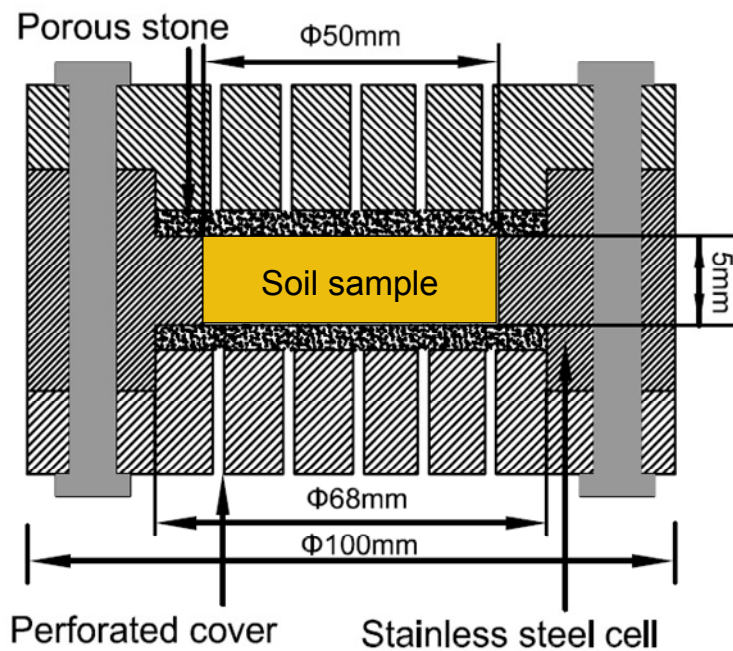


Figure 2 Constant volume cell used for hydration

To prepare samples of different final dry densities from the same pre-compacted block, it was decided to prepare the samples with the same height (5 mm) but various diameters (50.00, 48.63, 47.18 and 45.37 mm) by trimming. This implied that there was an initial gap between the soil sample and the cell inner wall. It was this gap that simulated different technological voids as well as the deformation of Boom clay (0-17.6 % of the total volume) appeared in the field conditions. Figure 3 shows that the samples were well positioned at the centre of the cell. Two porous disks were put at both sides of the sample allowing water flow. The whole was then sandwiched between two perforated discs (Figure 2) and immersed in distilled water for hydration. After the full saturation of the soil (verified after hydration), with the assumption that the density is uniform in each sample, the dry densities of the four samples were calculated, equal to 1.80, 1.70, 1.60 and 1.40 Mg/m<sup>3</sup>, respectively.

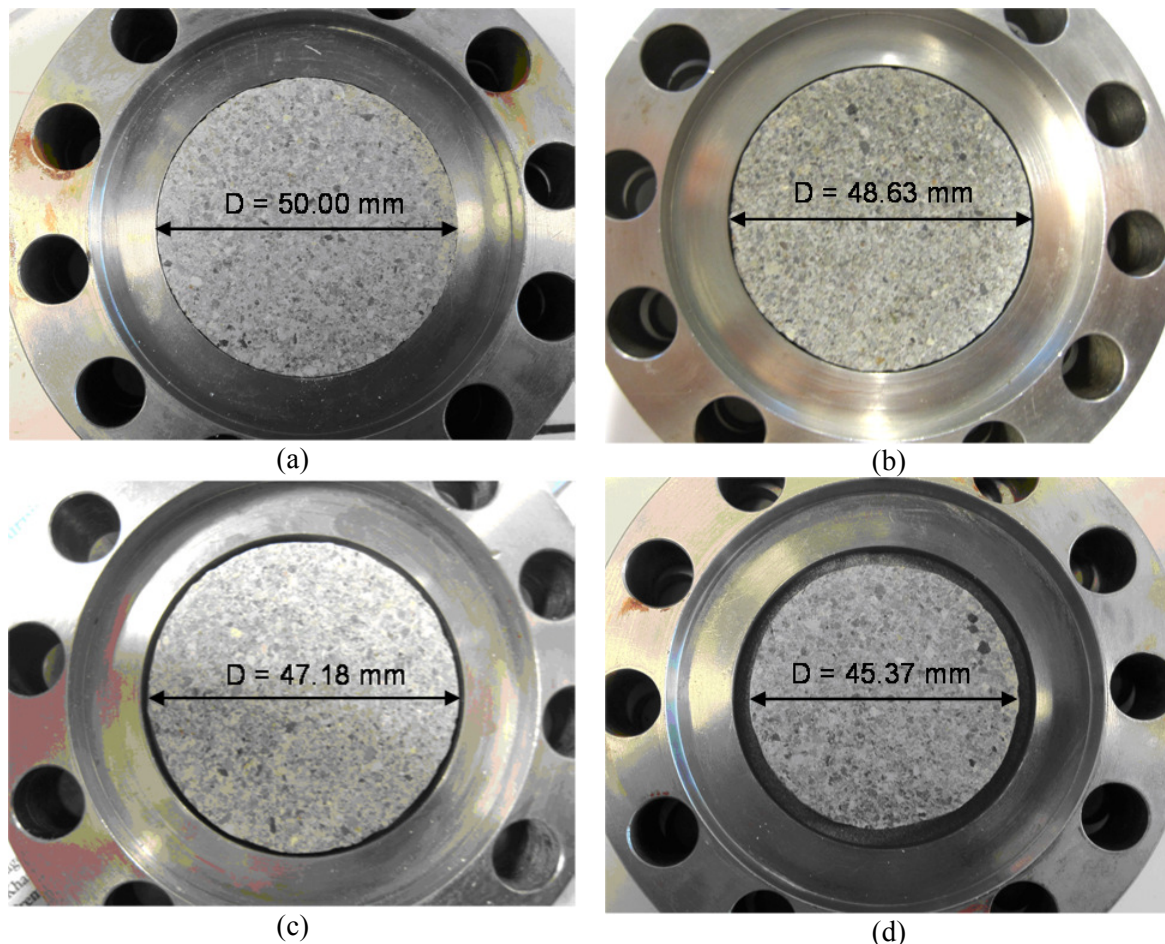


Figure 3 Samples preparation with lateral gaps

For the samples subjected to different hydration times (15, 30 and 90 days), they were extracted from the cell and each was divided into two parts, one for water content determination and the other for the microstructure observation. Note that the water content of

all samples was measured to verify the saturation of samples. To prepare the samples for microstructure observation, the soil was cut into small pieces and freeze-dried using liquid nitrogen previously vacuum-cooled below its boiling temperature (-196°C). This procedure allows optimizing the preservation of the microstructure during dehydration (Delage et al. 2006). Afterwards, the MIP and SEM tests were conducted.

Table 1 lists the MIP and SEM tests that were performed for the microstructure observation. MIP tests have been performed on all the samples, but the results of T30-2 and T90-2 (dry density of 1.70 Mg/m<sup>3</sup>) were unfortunately not available due to some technical problems that occurred during the test. For the SEM tests, only the three samples hydrated for 15 days were investigated. This test program was motivated by the comparison of the pore size distributions obtained from MIP tests. Indeed, the first comparison showed that the microstructure changes over time (30 and 90 days) would be too small to be identified by the SEM technique.

Table 1. Experimental program

Test	$\rho_{d-final}$ (Mg/m <sup>3</sup> )	Duration (Day)	MIP	SEM
T15-1	1.80	15	√	√
T15-2	1.70		√	-
T15-3	1.60		√	√
T15-4	1.40		√	√
T30-1	1.80	30	√	-
T30-2	1.70		-	-
T30-3	1.60		√	-
T30-4	1.40		√	-
T90-1	1.80	90	√	-
T90-2	1.70		-	-
T90-3	1.60		√	-
T90-4	1.40		√	-

### 3 Experimental results and discussions

The water content was determined after hydration for all samples, and the results are presented versus the final dry density in Figure 4, together with the saturation lines. The water contents measured at different hydration times (15, 30 and 90 days) were similar for the same final dry density. In addition, the measured water contents were higher than that defined by

the saturation line which was calculated by assuming that the water density ( $\rho_w$ ) is equal to  $1.00 \text{ Mg/m}^3$  (Figure 4). The difference can be attributed to the low water density considered in the determination of the saturation line. Indeed, for high plasticity materials as the MX80 bentonite, the water density can be much higher than  $1.00 \text{ Mg/m}^3$  (Marcial 2003, Villar and Lloret 2004, Lloret and Villar 2007, Jacinto et al. 2012). Skipper et al. (1991) reported an interlayer water density of  $1.38 \text{ Mg/m}^3$  for a Mg-smectite and  $1.14 \text{ Mg/m}^3$  for a Na-smectite. Villar & Lloret (2004) found that the average density of the water in the saturated compacted FEBEX bentonite depends also on the samples global density and gravimetric water content. They found that the values ranged from  $1.05 \text{ Mg/m}^3$  to  $1.22 \text{ Mg/m}^3$  for bentonite dry densities comprised between  $1.30 \text{ Mg/m}^3$  and  $1.80 \text{ Mg/m}^3$ . Based on the specific surface and basal spacing, Jacinto et al. (2012) calculated the average water density. They found that the values changes from 1.17 to  $1.09 \text{ Mg/m}^3$  when increasing the relative humidity from 40 to 99% for the MX 80 bentonite compacted at  $1.60 \text{ Mg/m}^3$  dry density. In Figure 4, if considering a water density of  $1.09 \text{ Mg/m}^3$ , it can be seen that the experimental results are close to that defined by the saturation line for the soil dry density lower than  $1.6 \text{ Mg/m}^3$ . For higher dry densities ( $1.7$  and  $1.8 \text{ Mg/m}^3$ ), it appears clearly that higher water densities must be considered to match the experimental results and values defined by the saturation line. This is consistent with the phenomenon of increase of water density with the increasing soil dry density, identified by Villar & Lloret (2004).

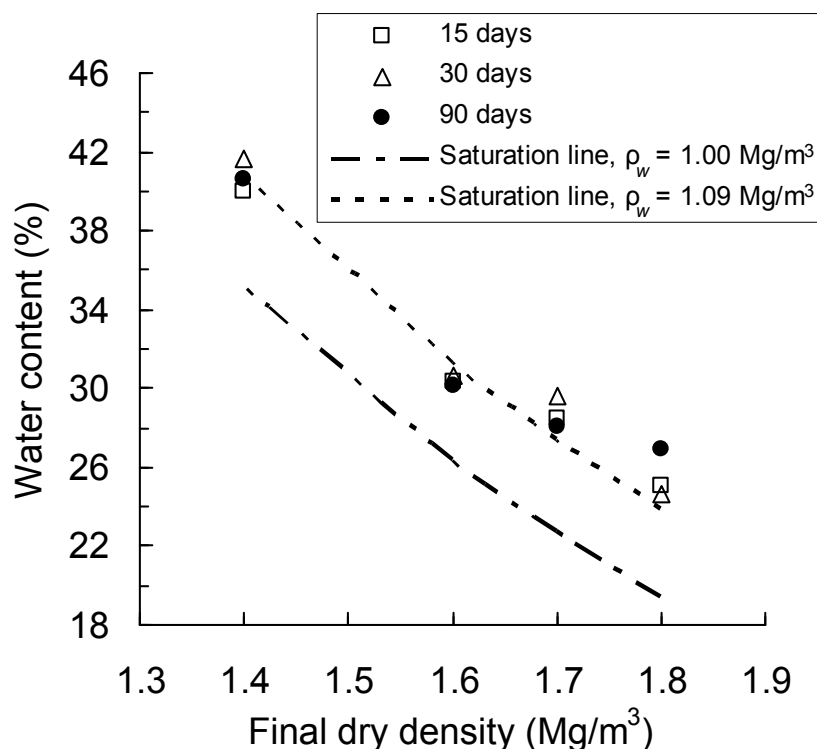


Figure 4 Relationship between water content and final dry density after different hydration times

Figure 5 presents the results from the MIP tests on the samples hydrated for 15 days, together with that of the as-compacted sample. The cumulative curves (Figure 5a) shows that the final values of intruded mercury void ratio ( $e_m$ ) are lower than the soil void ratio ( $e$ ). The difference can be mainly related to the limited pressure range of the MIP technique: for the high-plasticity soils, there is a significant pore volume (entrance diameter smaller than 6  $\mu\text{m}$ , depending on the porosimeter capacity in terms of maximum mercury pressure) that the mercury could not penetrate to (Lloret et al. 2003, Delage et al. 2006, Monroy et al. 2010). A typical bimodal porosity was observed for the as-compacted state ( $\rho_d = 1.80 \text{ Mg/m}^3$ ), with two pore families defined: (i) intra-aggregate pores (micro-pores) having a mean size of 0.015  $\mu\text{m}$ ; (ii) inter-aggregate pores (macro-pores) having a mean size of 10  $\mu\text{m}$ . The pore size function curve in Figure 5b shows that water saturation increased the size of dominant macro-pores to 30-50  $\mu\text{m}$ , without significantly changing in the size of micro-pores. Moreover, a new pore family with pore size of 0.04-2  $\mu\text{m}$  appeared (defined as meso-pores) for the final dry densities of 1.70, 1.60 and 1.40  $\text{Mg/m}^3$  (Figure 5b), displaying a tri-modal porosity.

To provide a quantitative analysis of the final dry density effect on the various pores, the following pores families were defined according to the entrance diameter: nano-pore (< 0.006  $\mu\text{m}$ ), micro-pore (0.006  $\mu\text{m}$  – 0.04  $\mu\text{m}$ ), meso-pore (0.04  $\mu\text{m}$  – 2  $\mu\text{m}$ ) and macro-pore (> 2  $\mu\text{m}$ ). Using these limit values, the void ratios corresponding to these four pore families can be derived from the cumulative curves (Figure 5a). Taking the PSD curve of 1.40  $\text{Mg/m}^3$  for an example, the nano-pores void ratio (0.257) corresponds to the difference between the global void ratio (0.98) and the intruded void ratio at the entrance diameter of 0.006  $\mu\text{m}$  (0.723); the micro-pores void ratio (0.181) corresponds to the difference of intruded void ratio between the entrance diameter of 0.006  $\mu\text{m}$  (0.723) and 0.04  $\mu\text{m}$  (0.542); the meso-pore void ratio (0.256) corresponds to the difference of intruded void ratio between the entrance diameter of 0.04  $\mu\text{m}$  (0.542) and 2  $\mu\text{m}$  (0.286); the macro-pore void ratio corresponds to the intruded void ratio at the entrance diameter of 2  $\mu\text{m}$  (0.286).

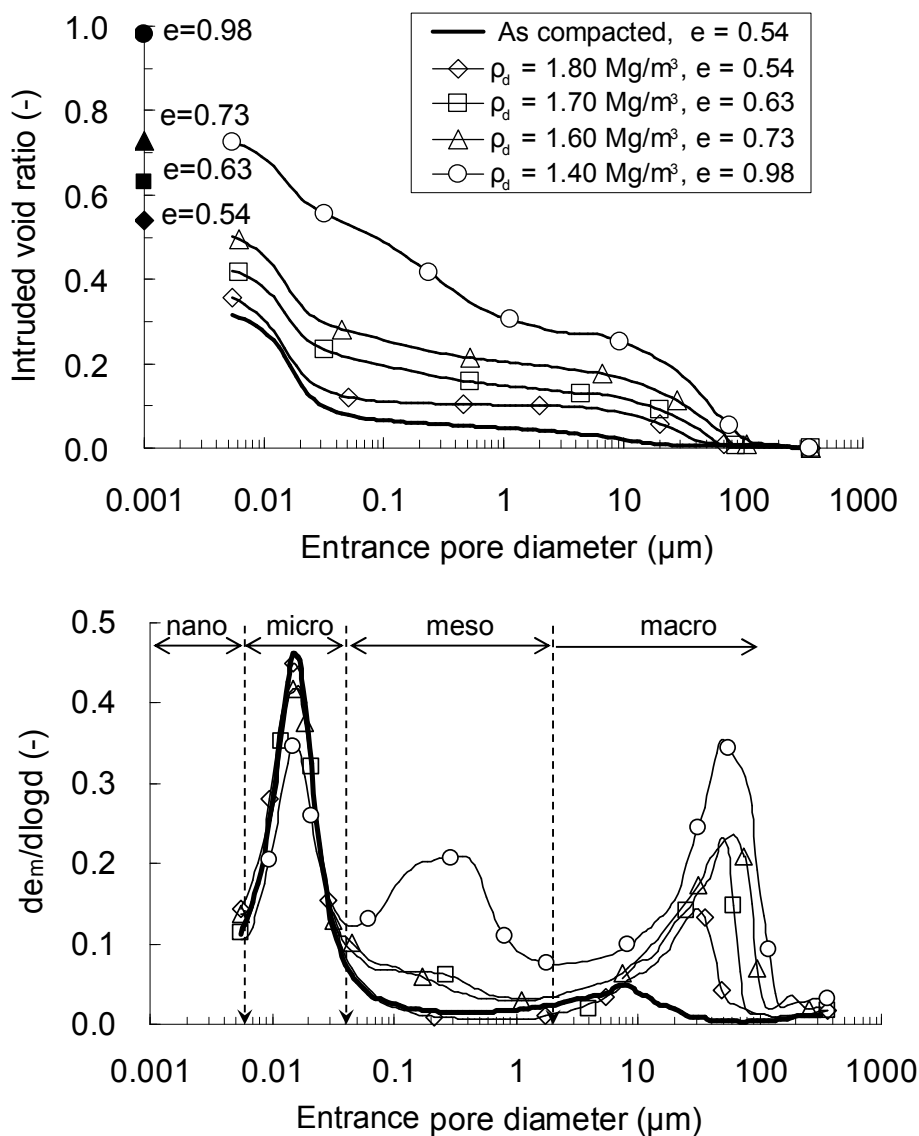


Figure 5 Results of MIP tests on saturated samples having different final dry densities and hydrated for 15 days

The void ratios determined for all four pore families and for all final dry densities are plotted in Figure 6. It clearly shows that both the macro-pores and meso-pores volume increased significantly with decreasing final dry density (increasing global void ratio), while the micro-pores quantity decreased slightly. This means that the main change in soil porosity when passing from the denser state to the looser state by hydration is due to changes in macro-pores and meso-pores. As far as the nano-pore is concerned, it can be observed that the amount of this unidentifiable porosity is higher for samples of lower final dry density. This can be explained as follows: in the montmorillonite, hydration initially occurred on the mineral surface and around the ex-changeable cations in the interlayer space, by the ordered and progressive placement of water molecules along the clay surface, layer after layer up to

four layers. This results in soil swelling (Saiyouri et al. 2000). In case of constant volume conditions, this swelling is not allowed to be fully developed; a lower final dry density (higher void ratio) normally allows more water infiltration into the interlayer space, resulting thereby in a higher unidentifiable porosity by MIP.

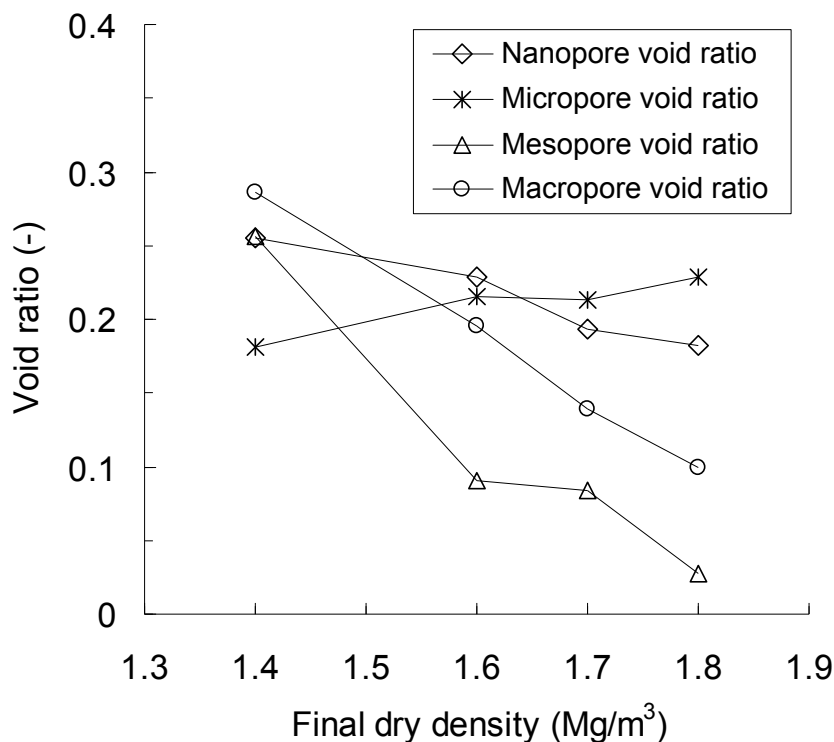


Figure 6 Nano-pore, micro-pore, meso-pore and macro-pore void ratio versus final dry density of samples hydrated for 15 days

It should be noted that several methods have been proposed in the literature to quantify the volume changes at different microstructure levels for compacted clays. As mentioned previously, the microstructure of this kind of clays is characterised by a bimodal PSD (Romero et al. 1999, Lloret et al. 2003, Agus and Schanz 2005, Delage et al. 1996, 2006). The as-compacted PSD curve is normally used to separate the intra-aggregate porosity from the inter-aggregate porosity by an entrance pore size (Romero et al. 2011). Delage and Lefebvre (1984) and Delage et al. (1996) proposed another method based on the data from a mercury intrusion/extrusion cycle. If these methods have been successfully applied for unsaturated soils (Delage et al. 2006, Lloret and Villar 2007), it is not the case for saturated soils in which the different levels of structure within the compacted clay interact in a more complex fashion (Monroy et al. 2010). The present study confirms this complexity: a new pore family of meso-pores appeared after saturation, between the micro- and macro-pores defined from the PSD of as-compacted sample.

Figure 7 presents the SEM pictures taken on the soil samples saturated for 15 days along with that of as-compacted samples. Note that the micro-pores observed in MIP test ( $0.015\ \mu\text{m}$ ) cannot be distinguished by the SEM technique. In the as-compacted state, the SEM picture clearly shows the clay aggregates which are densely assembled (Figure 7a). The macro-pores that were observed on the MIP test ( $10\ \mu\text{m}$  of entrance diameter) can be related to the voids existing between the clay aggregated. Observation on the surface of a clay aggregate (Figure 7b) shows that the clay aggregated is made up of thin clay lamella. Saturation at constant volume conditions induced swelling of clay aggregates, making the aggregates hardly identifiable (Figure 7c). Nevertheless, the gaps between the aggregates still exist. These gaps are called 2D pores by Audiguier et al. (2008), identified on a natural expansive clay after free swelling. These gaps become larger when the final dry density of soil is lower (Figure 7e and Figure 7g). Observation on the clay aggregates surface shows that it was not significantly affected by hydration when the dry density was kept constant (Figure 7d). When swelling was allowed, it seems that the clay lamella were progressively separated (Figure 7f and Figure 7h). In the case of  $\rho_d = 1.40\ \text{Mg/m}^3$  (Figure 7h), this lamella separation created a new void family inside the clay aggregate. This new void family corresponds to the meso-pore that was observed from the MIP test (Figure 5).

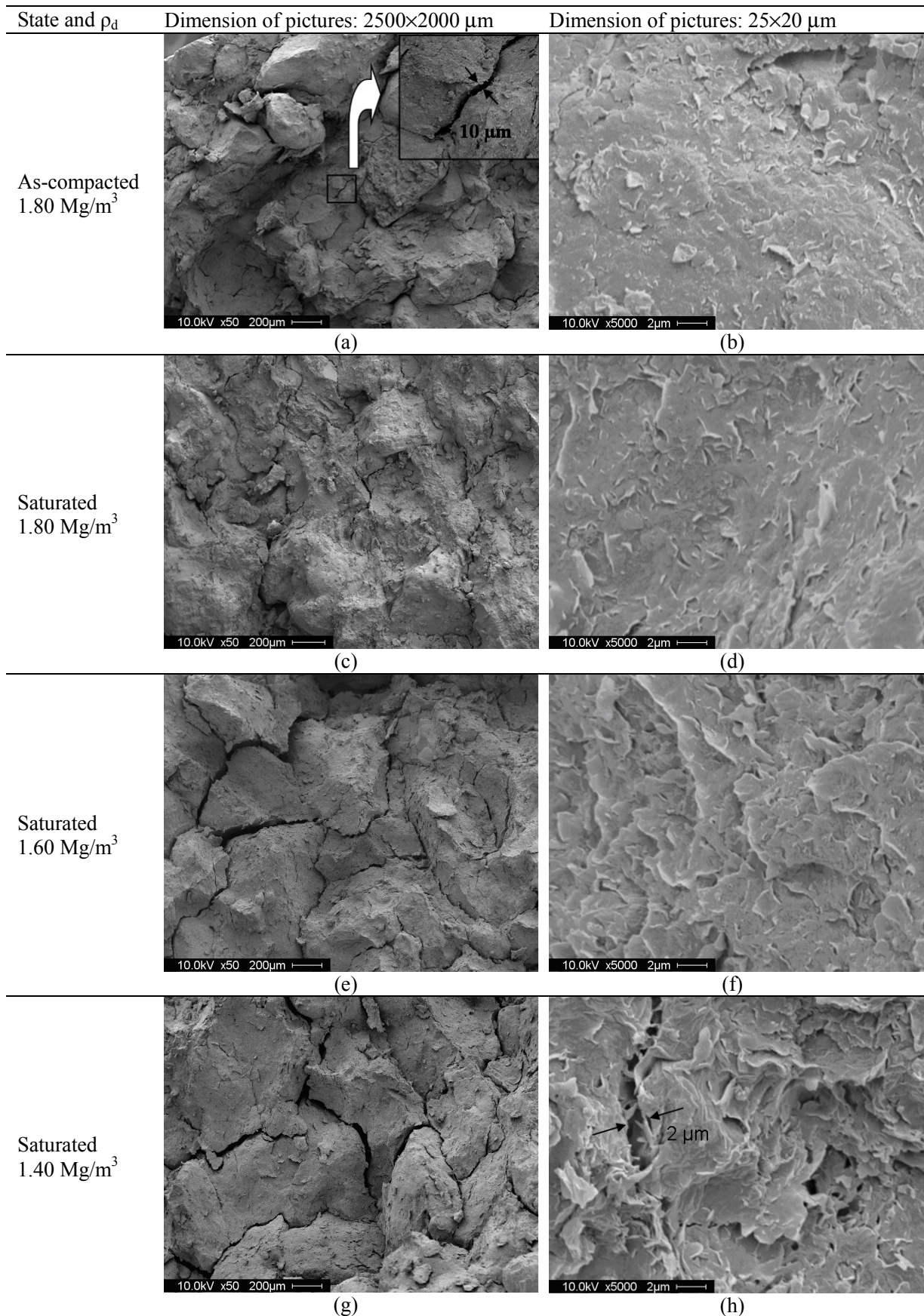
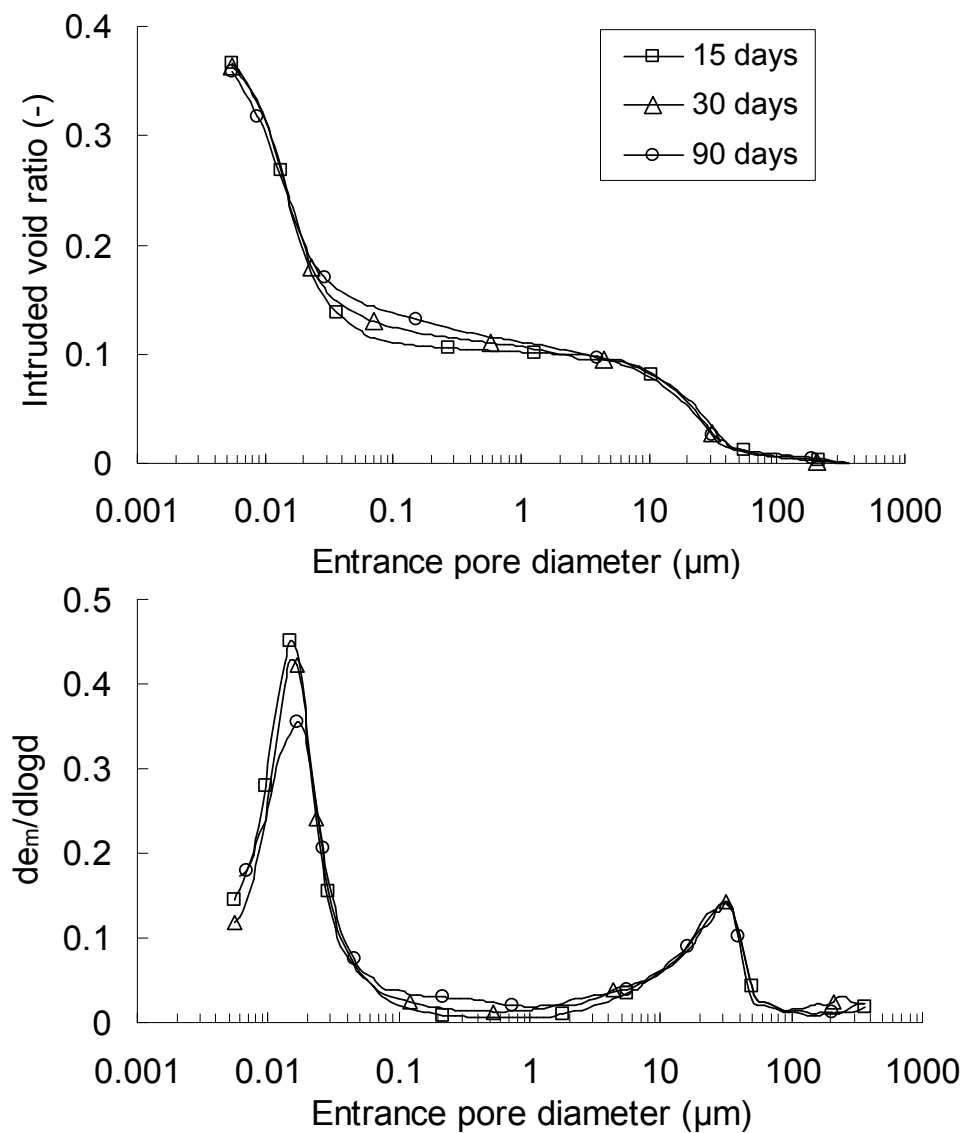
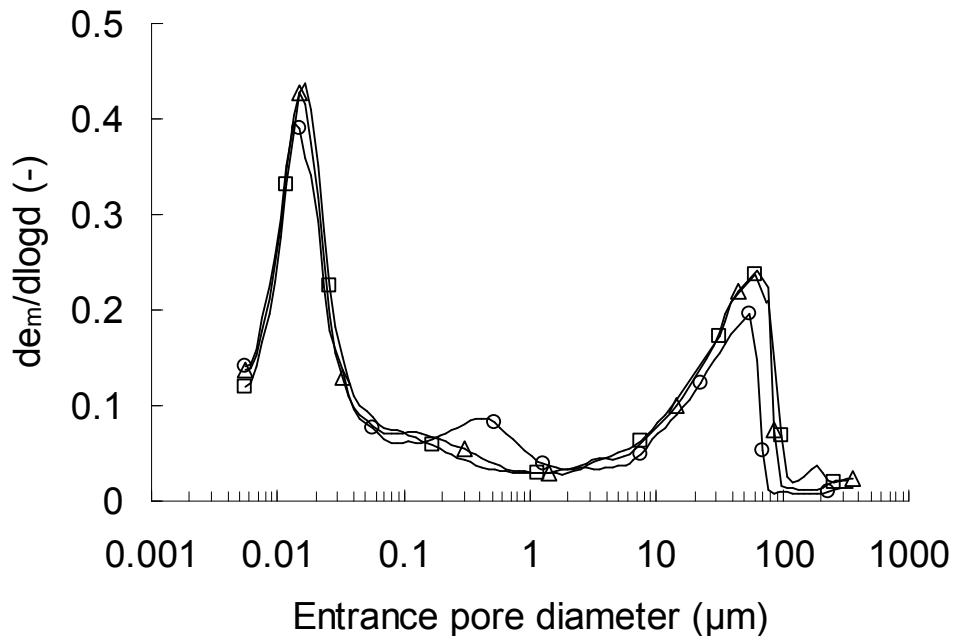
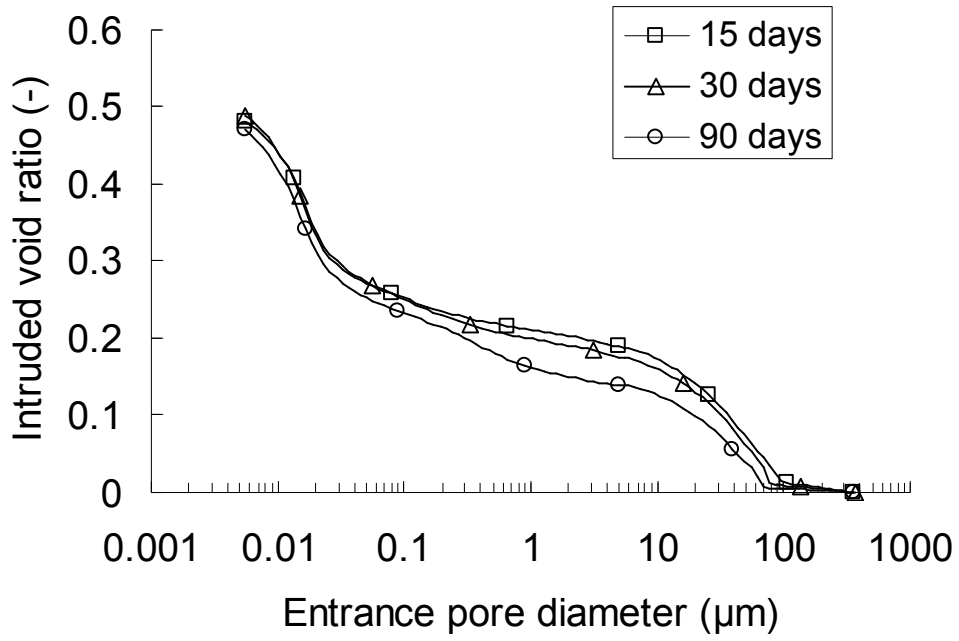


Figure 7 SEM pictures of soil samples at different states

Figure 8 presents the MIP tests results obtained on the soil samples hydrated at various periods (15, 30 and 90 days). For the samples having  $\rho_d = 1.80 \text{ Mg/m}^3$  (Figure 8a), the results obtained for the three periods are quite similar. For the samples having  $\rho_d = 1.60 \text{ Mg/m}^3$  (Figure 8b), the results obtained at 15 and 30 days of hydration are similar, showing in both cases a double-porosity structure (with micro- and macro-pore families). For the results obtained on the sample after 90-day hydration, the meso-pore family appeared. As mentioned previously, for the sample having  $1.40 \text{ Mg/m}^3$  this meso-pore appeared much earlier: after 15-day hydration (Figure 5). Figure 8c shows that the volume of this pore family continued to increase over time.



(a)  $\rho_d = 1.80 \text{ Mg/m}^3$



(b)  $\rho_d = 1.60 \text{ Mg/m}^3$

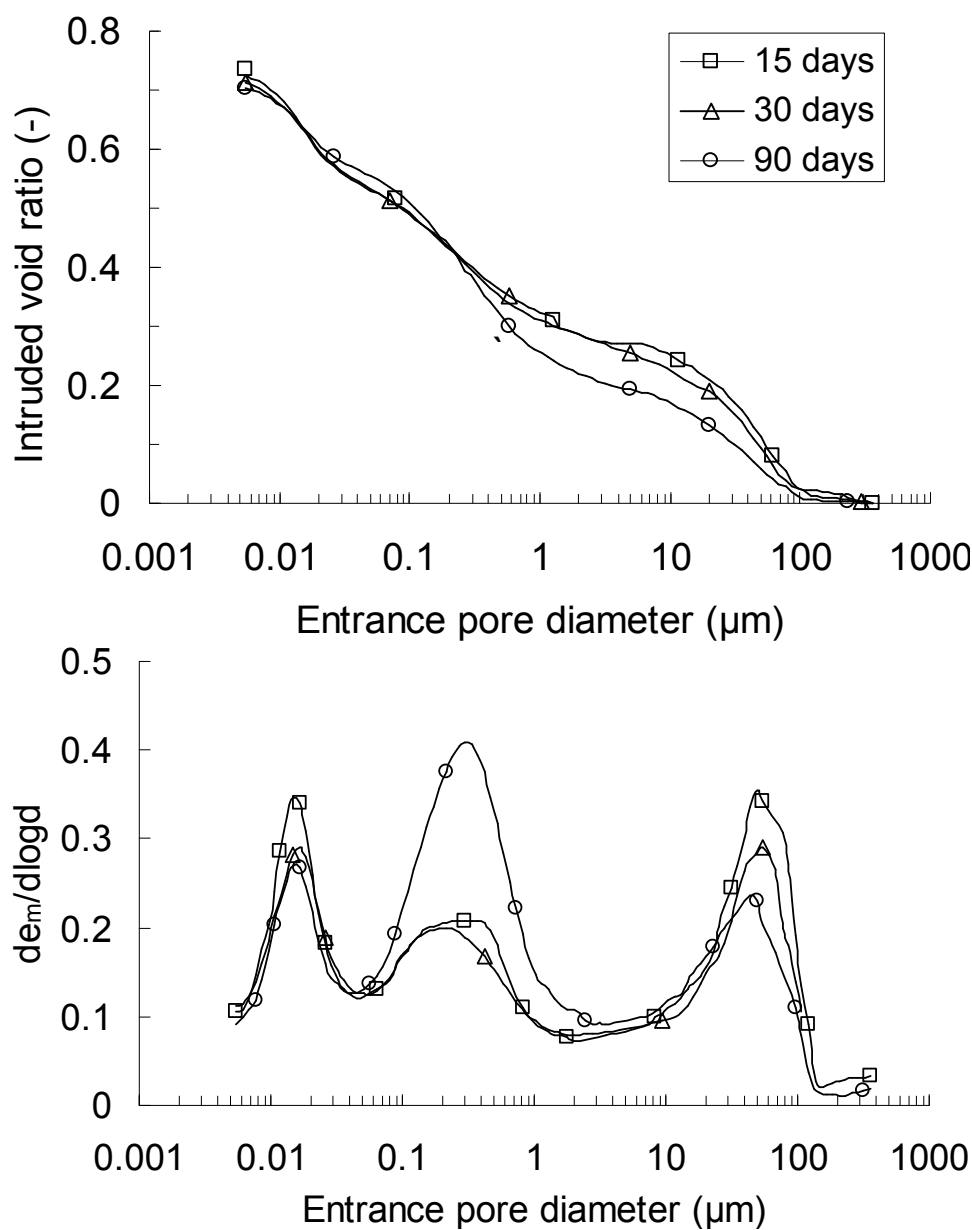
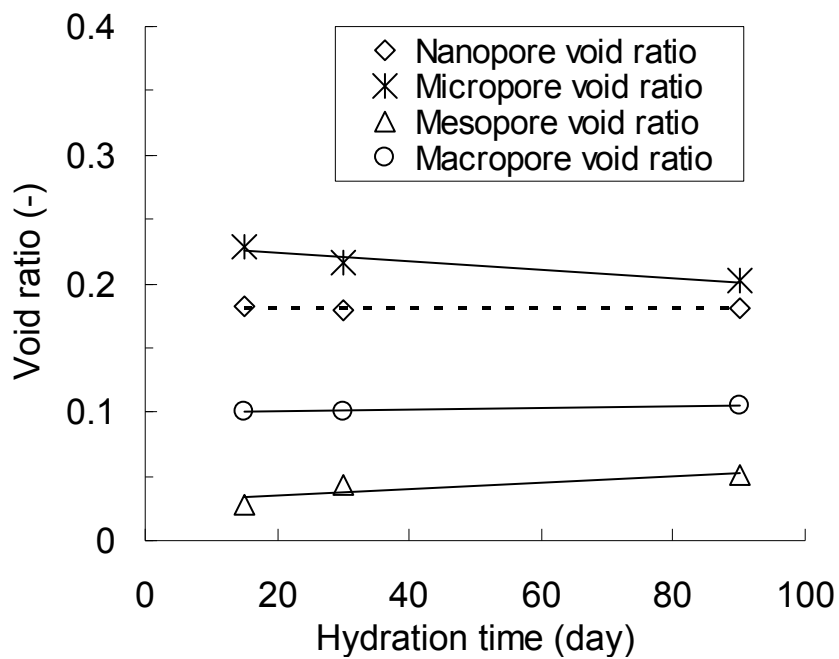
(c)  $\rho_d = 1.40 \text{ Mg/m}^3$ 

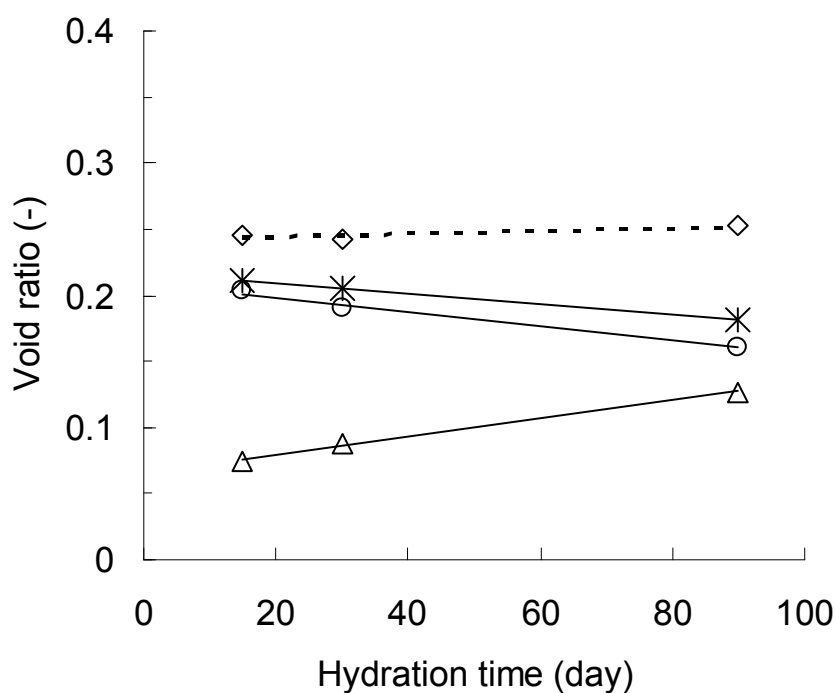
Figure 8 Evolution of PSD curves for various dry densities

The values of void ratio corresponding to the four pore families were determined following the definitions made previously and plotted versus hydration time in Figure 9. It can be seen that over time the nano-pore void ratio kept almost constant for all final dry densities. For the final dry density of  $1.80 \text{ Mg/m}^3$  (Figure 9a), the meso-pores void ratio increased slightly, while the micro-pores void ratio decreased slightly, with no obvious changes in macro-pores void ratio. For the final dry densities of  $1.60$  and  $1.40 \text{ Mg/m}^3$ : both the macro-pore void ratio and micro-pore void ratio decreased over time, resulting in an increase in the volume of the meso-pores (Figure 9b and c). Moreover, the change in meso-pore void ratio with time at the

density of  $1.40 \text{ Mg/m}^3$  was found higher than that at  $1.60 \text{ Mg/m}^3$ :  $1.63 \times 10^{-3}/\text{day}$  against  $0.69 \times 10^{-3}/\text{day}$ .



(a)  $\rho_d = 1.80 \text{ Mg/m}^3$



(b)  $\rho_d = 1.60 \text{ Mg/m}^3$

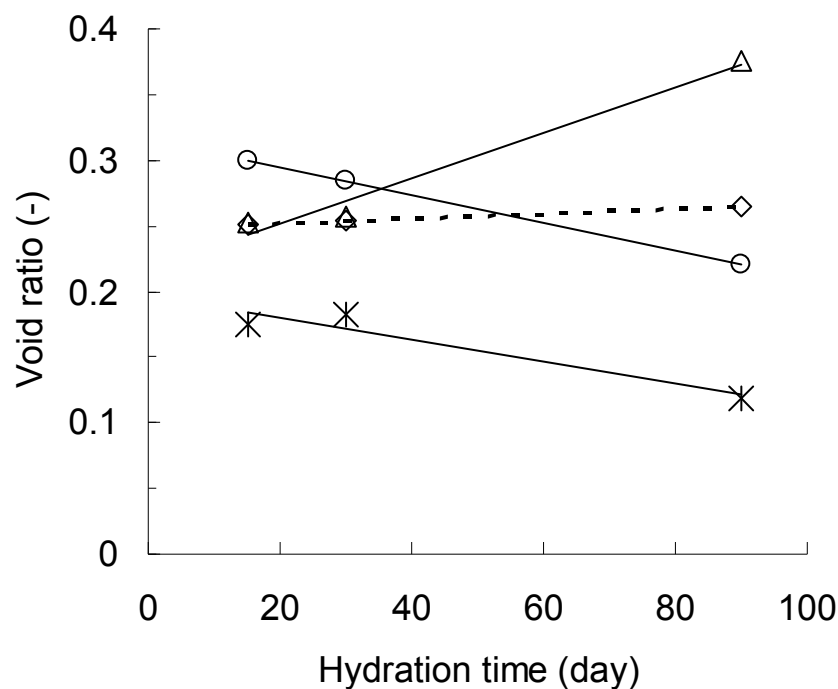
(c)  $\rho_d = 1.40 \text{ Mg/m}^3$ 

Figure 9 Evolution of nano-pore, micro-pore, meso-pore and macro-pore void ratio over time

As a first attempt, the re-organization of microstructure over time can be related to the water distribution occurred inside the soil at constant water content (saturation state in this study). When compacted clays are wetted by liquid water, water fills the open channels first; however, this quantity of water in the macropores is not necessarily in equilibrium with the water inside the aggregates in terms of water potential (Alonso et al. 2011). Over time, water is driven from the open connected macro-porosity to the intra-aggregate voids until equilibrium is reached. This process is accompanied by swelling/deformation of aggregates, corresponding to macrostructure changes. Obviously, this process is strongly dry density dependent especially under constant volume conditions: larger macro-pore volume exists in a sample at low final dry density (for instance, in the case of  $\rho_d = 1.40 \text{ Mg/m}^3$ ), making the swelling/deformation of aggregates easier; on the contrary, at high final dry density (for instance, in the case of  $\rho_d = 1.80 \text{ Mg/m}^3$ ), the limited macro-pore volume does not allow significant swelling/deformation of aggregates, thereby limiting the microstructure changes.

#### 4 Conclusion

The effects of final dry density and hydration time on the microstructure features of compacted MX80 bentonite in saturated state were characterized by means of both MIP and SEM techniques.

On the whole, four pore families can be distinguished: (1) nano-pore ( $< 0.006 \mu\text{m}$ ) corresponding to the inter-lamella pore that cannot be detected by the MIP technique employed, (2) micro-pore ( $0.006 \mu\text{m} - 0.04 \mu\text{m}$ ) corresponding to the intra-aggregated pore, (3) meso-pore ( $0.04 \mu\text{m} - 2 \mu\text{m}$ ) and (4) macro-pore ( $> 2 \mu\text{m}$ ) corresponding to the inter-aggregated void.

Hydration for 15 days created a new meso-pore family when the soil was let swell from its initial dry density of  $1.80$  to  $1.40 \text{ Mg/m}^3$ . This swelling was found to correspond to the increase in nano-pore, meso-pore and macro-pore void ratios but in a decrease in micropore void ratio.

When the soil was hydrated under constant volume conditions, the microstructures identified after various periods of hydration (15 days to 90 days) were found similar. When swelling was allowed during hydration, a new pore family (meso-pore) can appear. In the case of final dry density of  $1.60 \text{ Mg/m}^3$ , this new pore family appeared only after 90-day hydration. However, in the case of final dry density of  $1.40 \text{ Mg/m}^3$ , it was identified much earlier, after 15-day hydration. Moreover, the meso-pore volume was found to be increasing over time in the case of final dry density of  $1.40 \text{ Mg/m}^3$ . This increase seemed to be contributed by both the micro- and macro-pores: both pore families decreased in volume.

As a first attempting explanation, the final dry density and time dependent features of the microstructure of compacted MX80 can be attributed to the process of equilibration of water potential between water in the open macroscopic voids and water inside the aggregates. It is the water movement during this process that leads to the swelling/deformation of aggregates or macrostructure changes.

## **Acknowledgements**

The authors are grateful to the SCK/CEN for its support. The supports from the PHC Cai Yuanpei project (24077QE), the National Nature Science Foundation of China (41030748), the China Atomic Energy Authority (Project [2011]1051), the Program for Changjiang Scholars and Innovative Research Team in University (PCSIRT, IRT1029) and the China Scholarship Council (CSC) are also greatly acknowledged.

**References:**

- Agus, S. and Schanz, T. 2005. Swelling pressures and wetting-drying curves of a highly compacted bentonite-sand mixture, *Unsaturated Soils: Experimental Studies*, 241–256.
- Ahmed, S., Lovell, C.W. & Diamond, S. 1974. Pore sizes and strength of compacted clay. *ASCE Journal of the Geotechnical Engineering Division* 100, 407-425.
- Alonso, E.E., Romero, E., Hoffmann, C. 2011, Hydromechanical behaviour of compacted granular expansive mixtures: experimental and constitutive study, *Geotechnique*, Vol(61), NO.4, 329-334.
- Audiguier, M., Geremew, Z., Cojean, R. 2008. Relations entre les microstructures de deux sols argileux de la région parisienne et leur sensibilité au retrait gonflement. SEC2008, Paris, France, 1-3 sept. Editions du LCPC, 235-243.
- Ben Rhaïem, H., Pons, C.H., Tessier, D. 1985. Factors affecting the microstructure of smectites: role of cations and history of applied stresses, In: Schultz et al. (eds) *Proc Int Clay Conf*, Denver, The Clay Mineralogical Soc, 292–297
- Cui, Y. J., Loiseau, C., Delage, P. 2002. Microstructure changes of a confined swelling soil due to suction controlled hydration *Unsaturated soils: proceedings of the Third International Conference on Unsaturated Soils, UNSAT 2002, 10-13 March 2002, Recife, Brazil*, 593-598
- Delage, P. & Lefebvre, G. 1984. Study of the structure of a sensitive Champlain clay and its evolution during consolidation. *Can. Geotech. J.* Vol(21), No. 1, 21–35.
- Delage, P. & Graham, J. 1995. The mechanical behaviour of unsaturated soils. *Proc. 1st Int. Conf. on Unsaturated Soils*, Paris 3, 1223–1256.
- Delage, P., Audiguier, M., Cui, Y.J. & Howat, M.D. 1996. Microstructure of a compacted silt. *Canadian Geotechnical Journal*, 33 (1), 150-158.
- Delage, P., Marcial, D., Cui, Y.J., Ruiz, X. 2006. Ageing effects in a compacted bentonite: a microstructure approach. *Géotechnique* 56 (5), 291-304.
- Delage, P. 2007, Microstructure features in the behaviour of engineered barriers for nuclear waste disposal, *SPRINGER PROCEEDINGS IN PHYSICS*, 112 (11), 11-312
- Jacinto, A. C., Villar, M. V., and Ledesma, A. 2012. Influence of water density on the water-retention curve of expansive clays, *Géotechnique* 62, No. 8, 657–667
- Li, X.L., Bastiaens, W., Van Marcke, P., Verstricht, J., Chen, G.J., Weetjens, E., Sillen, X. 2010. Design and development of large-scale in-situ PRACLAY heater test and horizontal high-level radioactive waste disposal gallery seal test in Belgian HADES, *Journal of Rock Mechanics and Geotechnical Engineering*. 2 (2), 103–110
- Lloret, A., Villar, M.V., Sánchez, M., Gens, A., Pintado, X. & Alonso, E. E. 2003. Mechanical behaviour of heavily compacted bentonite under high suction changes. *Géotechnique* 53, No. 1, 27–40
- Lloret, A., Villar, M., 2007. Advances on the knowledge of the thermo-hydro-mechanical behaviour of heavily compacted FEBEX bentonite. *Physics and Chemistry of the Earth*, 32, 701-715
- Marcial, D., 2003. Comportement hydromécanique et microstructural des matériaux de barrière ouvragée, thèse ENPC.
- Monroy, R. And Zdravkovic, L. And Ridley, A. 2010. Evolution of microstructure in compacted London Clay during wetting and loading, *Geotechnique*, Vol(60),: 105--119
- Nowamooz, H. and Masroufi, F. 2010, Relationships between soil fabric and suction cycles in compacted swelling soils, *Engineering Geology*, Vol (114), 444-455
- Romero, E., Gens, A. & Lloret, A., 1999. Water permeability, water retention and microstructure of unsaturated compacted Boom clay. *Engineering Geology*. 54, 117-127.
- Romero, E., Della Vecchia, G., and Jommi, C. 2011. An insight into the water retention properties of compacted clayey soils. *Geotechnique* 61, No. 4, 313-328.

- Saiyouri, N., Hicher, P.Y., and Tessier, D. 2000. Microstructural approach and transfer water modelling in highly compacted unsaturated swelling clays. *Mechanics of cohesive-frictional materials*, 5, 41-60.
- Skipper, N.T., Refson, K., McConnell, J.D.C. 1991. Computer simulation of interlayer water in 2:1 clays. *J. Chem. Phys.* 94 (11), 7434-7445.
- Sridharan, A., Altschaeffle, A. G. and Diamond, S. 1971, Pore size distribution studies, *Journal of the Soil Mechanics and Foundations Division, Proceedings of the ASCE*, vol. 97, SM 5, 771-787
- Tang, A.M., Munoz, J.J., Cui, Y.J., Delage, P., Li, X.L. 2008. Experimental Evaluation of the Hydraulic Resistance of Compacted Bentonite/Boom Clay Interface, In: *Proceedings of the International Technical Conference on the Practical Aspects of Deep Geological Disposal of Radioactive Waste*, Prague, Czech Republic, June 2008, 16-18
- Thom. R., Sivakumar, R., Sivakumar, V., Murray, E.J., Mackinnon, P. 2007. Pore size distribution of unsaturated compacted kaolin: the initial states and final states following saturation. *Geotechnique* 57(5), 469-474
- Villar, M.V. and Lloret. A. 2004. Influence of temperature on the hydro-mechanical behaviour of a compacted bentonite. *Applied Clay Science*, 26(1-4), 337-3



## **Chapter 4. Hydraulic conductivity and microstructure changes during hydration**

### **INTRODUCTION**

As mentioned in the previous chapter, one of the most important functions of the engineering barrier is to create a zone of low permeability for separating the high-level radioactive waste from its surrounding environment (Komine, 2010). Thus, a proper understanding of its hydraulic conductivity changes is essential.

Upon suction decrease, the hydraulic conductivity of the bentonite-based materials has been found to first decrease and then increase below a given suction threshold (Cui et al. 2008, Ye et al. 2009). This is different from the common results showing that the hydraulic conductivity of unsaturated soils increases monotonously with suction decrease (van Genuchten, 1980; Fredlund and Rahardjo, 1993). The particular trend observed for the bentonite-based materials adds a degree of complexity while dealing with the long term behaviour of these materials.

In order to understand the phenomenon of this particular hydraulic conductivity changes with suction decrease for bentonite-based materials, infiltration test and water retention test as well as microstructure observation are carried out on the MX80 bentonite/sand mixture. The results obtained allow relating the variation of hydraulic conductivity to the microstructure changes.

The work presented in this chapter has been submitted to «Engineering Geology».

Wang, Q., Tang, A. M., Cui, Y.J., Barnichon, J.D., Ye, W.M., 2012, submitted to Engineering Geology

## Hydraulic conductivity and microstructure changes of compacted bentonite/sand mixture during hydration

Qiong Wang<sup>1</sup>, Anh Minh Tang<sup>1</sup>, Yu-Jun Cui<sup>1,3</sup>,  
Jean-Dominique Barnichon<sup>2</sup>, Wei-Min Ye<sup>3</sup>

**Abstract:** Compacted bentonite-based materials are often considered as sealing/backfill materials in deep geological repository for high level radioactive waste. A good understanding of their hydration process is essential as this process is directly related to over-pack corrosion and nuclide migration. In this study, the unsaturated hydraulic properties of MX80 bentonite/sand mixture were characterized by carrying out a series of experiments including water retention test, infiltration test as well as microstructure observation. It was found that with suction decrease under constant volume condition, the hydraulic conductivity decreased followed by an increase after a suction threshold. At suctions higher than 12.6 MPa, hydration led to progressive macro-pores clogging by exfoliation of clay particles. On the contrary, when saturation was approached (suction lower than 4.2 MPa), the macro-pores quantity increased due to the creation of two-dimensional pores. It was also observed that the soil hydraulic conductivity changed following the same tendency as the macro-pores quantity during hydration. In other words, water transfer was primarily governed by the network of macro-pores.

**Keywords:** bentonite/sand mixture; suction; constant-volume condition; hydraulic conductivity; microstructure; macro-pores

---

### 1 Introduction

Most concepts of deep geological repository for high level radioactive waste are based on the multi-barrier system consisting of the natural barrier (host rock) and engineered barriers (waste container, buffer and sealing elements). One of the most important functions of the engineering barrier is to create a zone of low permeability for separating the high-level radioactive waste from the surrounding environment (Komine, 2010). Bentonite-based materials are often chosen as sealing/backfill materials in this multi-barrier system thanks to their low permeability, high swelling and high radionuclide retardation capacities (Pusch, 1979; Yong et al., 1986; Villar et al., 2008).

Once emplaced in the repository, the bentonite-based materials start to be hydrated by the pore water infiltrating from the host-rock. These materials absorb water and swell, first filling up all technological voids and then developing swelling pressure under the quasi-constant

---

1 Ecole des Ponts ParisTech, Navier/CERMES, France

2 Institut de Radioprotection et de Sûreté Nucléaire (IRSN), France

3 Tongji University, China

volume conditions. Note that the hydration under quasi-constant volume condition corresponds to a coupled hydro-mechanical process with involvement of microstructure changes. A proper understanding of this process is essential for well controlling the water transfer-related phenomena as over-pack corrosion, nuclide migration, etc.

Number of studies have been performed to study the water transfer in bentonite-based materials both in saturated state (Kenney et al., 1992; Dixon et al., 1999; Komine, 2004, etc) and unsaturated state (Börgesson, 2001; Loiseau et al., 2002; Kröhn, 2003a, 2003b; Lemaire et al., 2004; Cui et al., 2008). The saturated hydraulic conductivity has been found to be strongly dependent on the initial state defined by the water content (or suction) and density (Dixon, 1999; Karnland et al., 2008, etc.). Under unsaturated conditions where water flow is suction dependent, the hydraulic conductivity was often determined using the instantaneous profile method (Daniel, 1982). Following this method, Cui et al. (2008) investigated the unsaturated hydraulic conductivity of the Kunigel bentonite/sand mixture and observed that with suction decrease under constant volume condition, the hydraulic conductivity decreased followed by an increase after certain suction threshold. Ye et al. (2009) obtained similar results on GMZ bentonite. This is different from the common results showing that the hydraulic conductivity of unsaturated soils increases with suction decrease (van Genuchten, 1980; Fredlund and Rahardjo, 1993). The particular trend observed for bentonite-based materials adds a degree of complexity when dealing with the long term behaviour of these materials. Without considering this phenomenon, the water transfer in bentonite-based materials will be over-estimated. Thus, it is of great importance to go in depth of this phenomenon by considering the coupled hydro-mechanic changes during the hydration process.

If the phenomenon of the particular hydraulic conductivity changes with suction decrease for bentonite-based materials was revealed experimentally (Cui et al., 2008; Ye et al., 2009), the explanation has been not yet confirmed by microstructure analysis. The present study aims at completing this lack by investigating the hydraulic properties of a compacted bentonite-sand mixture and the microstructure changes during the hydration process. Infiltration test and water retention test were first conducted under constant volume conditions allowing the determination of hydraulic conductivity by the instantaneous profile method. The study was then completed with the microstructure observation allowing analysing the effect of microstructure change on the variations of hydraulic conductivity.

## 2 Materials and methods

### 2.1 Materials and samples preparation

The soil studied is a mixture of MX80 bentonite and quartz sand with a proportion of 70/30 in dry mass. The bentonite is from Wyoming, USA, with a high content of montmorillonite (80%). It has a liquid limit of 575%, a plastic limit of 53% and a unit mass of  $2.77 \text{ Mg/m}^3$ . The cation exchange capacity (CEC) is  $76 \text{ meq/100g}$  (83 % of  $\text{Na}^+$ ). The grain size distribution (Figure 1) determined by hydrometer (AFNOR NF P94-057) shows that the fraction of clay-size particles ( $< 2 \mu\text{m}$ ) is 84%. The sand used in the mixture was from Eure and Loire (France) with a unit mass of the sand grains is  $2.65 \text{ Mg/m}^3$ . It was sieved at 2 mm prior to being mixed with the bentonite. Figure 1 also shows the grains size distribution curve determined by the dry sieving method (AFNOR NF P94-056). The curve for sand is characterized by a uniformity coefficient  $C_u$  of 1.60.

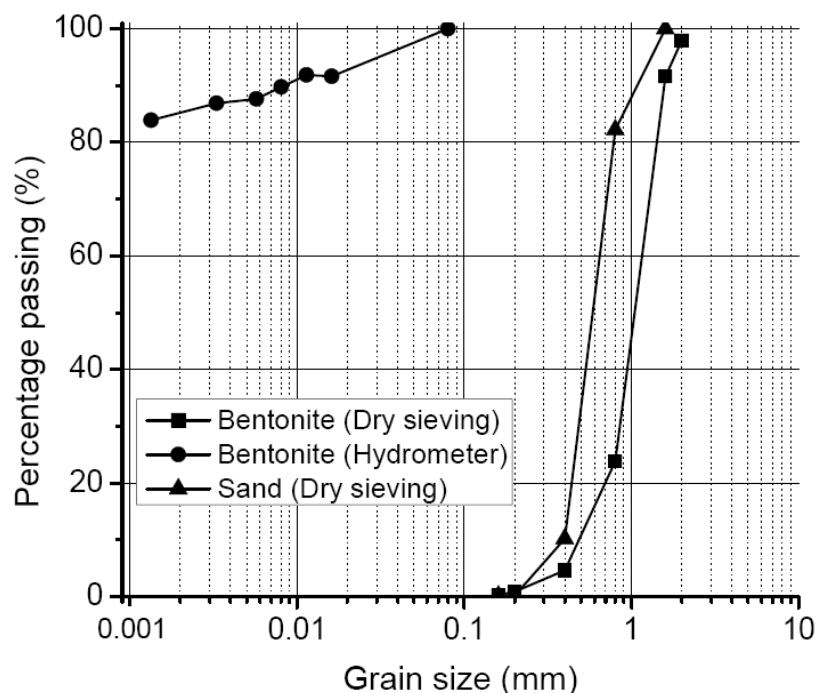


Figure 1. Grain size distribution of the MX80 bentonite and sand

Synthetic water having similar chemical composition to that of the pore water of the Callovo-Oxfordian claystone from the ANDRA URL in Bure (France) was used for the infiltration test (Table 1). For the preparation of the synthetic water, the chemical components in powder were mixed with distilled water using a magnetic stirrer until full dissolution.

Table 1. Chemical composition of the synthetic water

Components	NaHCO <sub>3</sub>	Na <sub>2</sub> SO <sub>4</sub>	NaCl	KCl	CaCl <sub>2</sub> .2H <sub>2</sub> O	MgCl <sub>2</sub> .6H <sub>2</sub> O	SrCl <sub>2</sub> .6H <sub>2</sub> O
Mass (g) per litre of solution	0.28	2.216	0.615	0.075	1.082	1.356	0.053

Soil specimens for water retention test were prepared by compaction of the bentonite/sand mixture at its initial water content of 11.0%. A given quantity of the mixture was placed in a metallic mould and statically compacted to a dry density of 1.67 Mg/m<sup>3</sup> that corresponds to the dry density adopted in the design of sealing plug at the French Tournemire site. The initial suction of the compacted samples was about 65 MPa (measured using a relative humidity sensor).

For the infiltration test, the specimen (250-mm long and 50 mm in diameter) was compacted in 5 layers of 50-mm thickness each. The same dry density as for the water retention test was adopted (1.67 Mg/m<sup>3</sup>). After compaction, the specimen was carefully introduced into the testing cell (having the same diameter as the compaction cell) by connecting the ends of the two cells.

## 2.2 Experimental method

The hydraulic conductivity of the unsaturated bentonite/sand mixture was determined using the instantaneous profile method. This method requires both suction and volumetric water content profiles (Daniel, 1982; Cui et al., 2008; Ye et al., 2009). The infiltration test was performed using the cell presented in Figure 2. After compaction, the soil specimen was introduced into the cylindrical cell (50 mm in inner diameter and 80 mm in outer diameter) which hindered any lateral volume changes. Four relative humidity (RH) sensors were installed every 50 mm along the sample (h = 50, 100, 150, 200 mm from the wetting end) through the ports in the wall of the cell. The two ends of the cell were covered by metallic discs of 40 mm thickness each. Water supply was done through the water inlets in the bottom base. The top base contains an outlet for air expulsion. To avoid water evaporation, a deflated balloon-shaped membrane was used to cover the air outlet. The air in the membrane was released regularly in order to keep a air pressure close to the atmospheric one. The water volume injected into the sample was also monitored during the test.

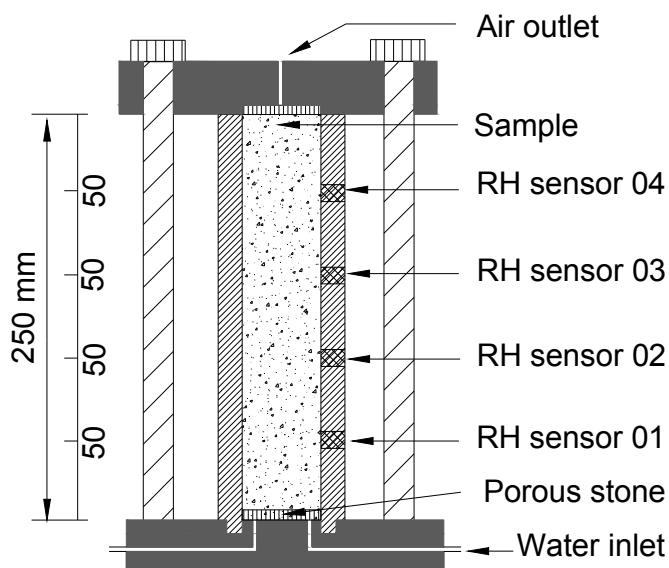


Figure 2. Schematic setup of the infiltration cell

The suction profiles were obtained using the data of relative humidity (RH), whereas the volumetric water content profiles were obtained indirectly from the water retention curve (WRC) and the suction profiles. The water retention curve of the bentonite/sand mixture under constant volume condition was determined by controlling the suction using both the vapour equilibrium technique (for suctions higher than 4.2 MPa) and osmotic technique (for suctions of 1 and 0.1 MPa). The zero suction was imposed by injecting water into the sample.

For the determination of the water retention properties, the sample (50 mm in diameter and 5 mm in height) was placed in a stainless steel cell. Two porous disks were put at both sides of the sample allowing vapour or water flow. To apply the osmotic technique, a semi-permeable membrane was placed between the porous stone and the soil sample (Figure 3a), the whole was then sandwiched between two perforated discs and immersed in a PEG (Polyethylene Glycol) solution. To apply suction with the vapour equilibrium technique, the sample sandwiched between two porous stones was installed between two external plates with valves (Figure 3b) that were connected to a device containing a saturated salt solution for relative humidity control (see Wang et al., 2012 for more details). Following this technique, 2-4 weeks was required to reach the equilibrium (Marcial, 2003; Tang & Cui, 2005). However, the equilibration time was much shorter for the osmotic technique as it allows liquid water exchanges between the soil sample and the PEG solution (Blatz et al., 2008). In this study, the equilibration time was extended to 2 months for both the vapour equilibrium technique and osmotic technique and the water content of all samples was determined by weighing at the end.

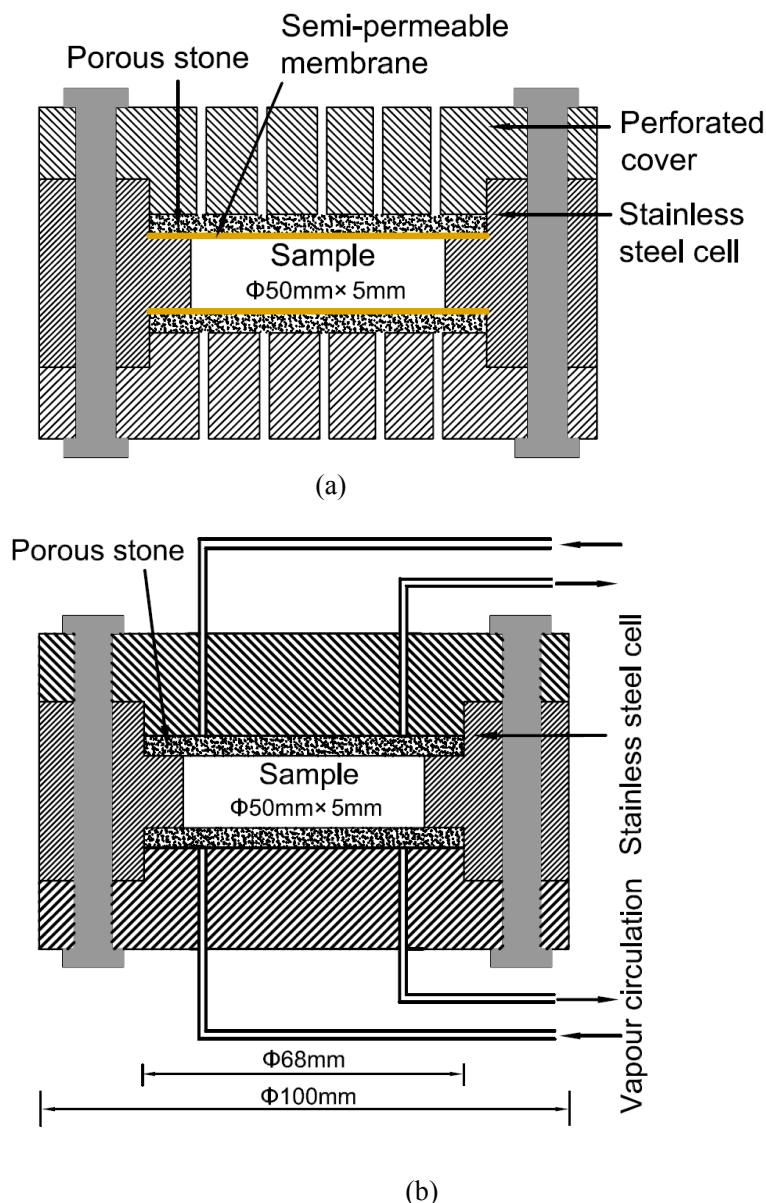


Figure 3. Constant volume cell for WRC determination; (a) osmotic method; (b) vapour equilibrium technique

All water retention tests performed and the solutions used for suction control are presented in Table 2. As shrinkage may occur upon drying, it was not possible to control sample volumes along drying paths. Thus, only the wetting curve was determined under restrained-swell conditions. This was enough for the purpose of hydraulic conductivity determination based on the infiltration test under constant volume conditions.

Mercury Intrusion Porosity (MIP) and Scanning Electron Microscope (SEM) tests were carried out on samples equilibrated at different suctions under constant volume conditions. The suction values considered ranged from 65 MPa (as-compacted state) to zero (saturated state). For as-compacted samples, it was cut to small slices and freeze-dried (see Delage &

Lefevbre, 1984; Cui et al., 2002., Delage et al., 2006; Tang et al., 2011 for more details). Samples for other suctions were taken from the water retention test under constant volume condition (Table 2 for details). Each sample was cut to two parts, one for the preparation of samples for the microstructure observation and another for water content determination by weighing (for water retention curve).

Table 2. Tests performed for water retention property and microstructure observation

Suction (MPa)	Suction control method and duration	Microstructure	
		MIP	SEM
38	Vapour (2 months)	√	√
24.9		√	
12.6		√	
9.0			
4.2		√	√
1	Osmotic (2 months)	√	
0.1			
0	Distilled water (2 months)	√	√
65	Initial suction	√	√

### 3 Experimental results

Figure 4 depicts the water retention curve (suction versus the gravimetric water content) obtained along the wetting path under constant-volume conditions. It is observed that in a semi-logarithmic plane, water content increases linearly with suction decrease when this latter is higher than 1 MPa. At lower suctions the water content increase almost ends and the water retention curve is almost horizontal.

The results of the infiltration test is shown in Figure 5 where the RH changes over time is plotted for all measurement positions ( $h = 50, 100, 150$  and  $200$  mm). The initial RH was  $62 \pm 1\%$  corresponding to a suction of  $64.5 \pm 1.5$  MPa. Once the infiltration started, the value of the RH at  $h = 50$  mm increased rapidly and reached 90% after 500 h, then increased gradually to 98.30% after 1900 h. The value of the sensors at  $h = 100, 150$  and  $200$  mm started to increase after about 200 h, 500 h and 1900 h respectively. The larger the distance from the wetting end the lower the increasing rate of RH. Loiseau et al. (2002) and Cui et al. (2008) performed similar infiltration tests on the bentonite/sand mixture (70/30 in dry mass,  $\rho_d = 1.70$  Mg/m<sup>3</sup>) and obtained similar results.

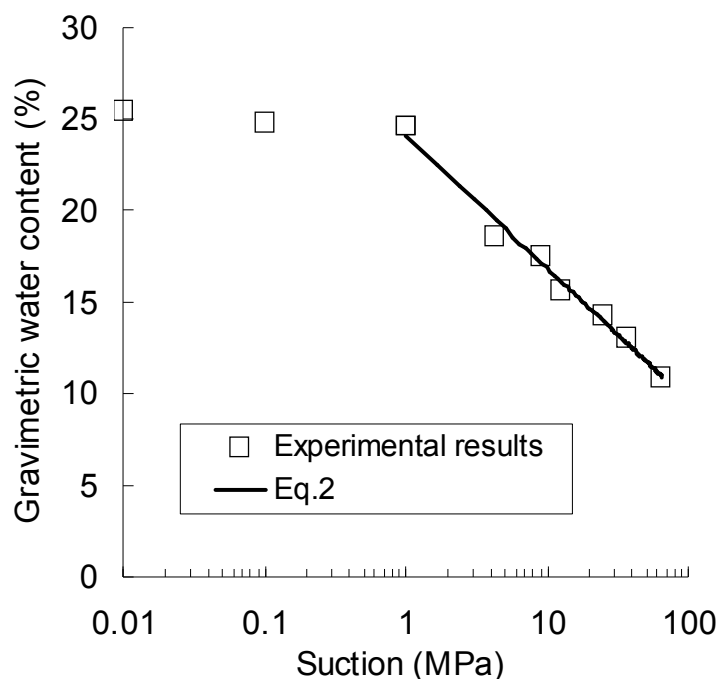


Figure 4. WRC of bentonite/sand mixture under constant-volume conditions

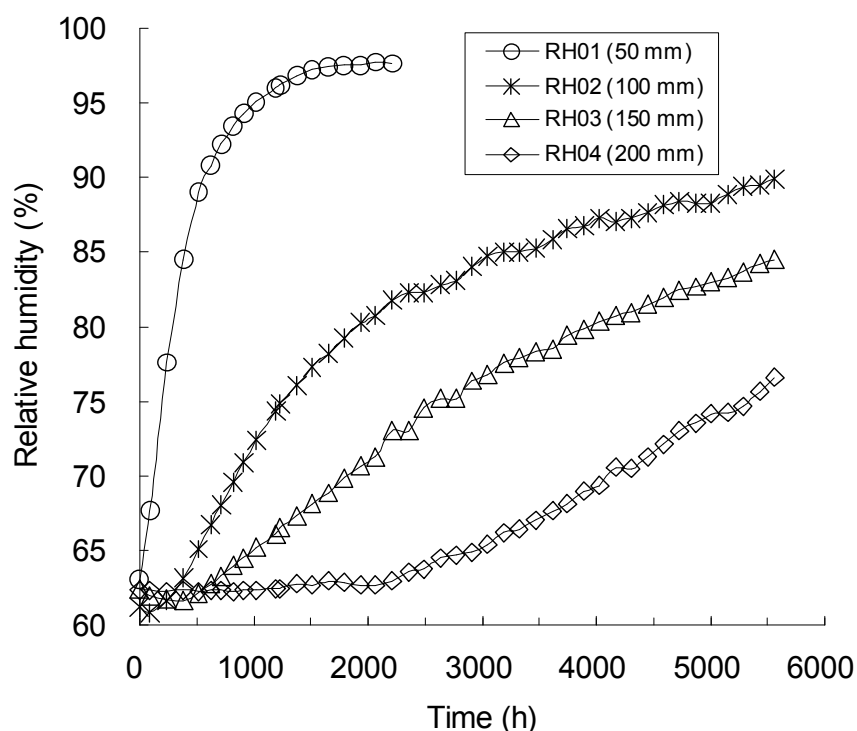


Figure 5. Evolution of relative humidity during water infiltration

The total suction ( $s$ ) was then calculated from RH value using Kelvin's law:

$$s = -(\rho_w RT / M_w) \ln(RH / 100) \quad \text{Eq. (1)}$$

where  $\rho_w$  is the water unit mass ( $1 \text{ Mg/m}^3$ ),  $R$  is the universal (molar) gas constant ( $8.31432 \text{ J/mol K}$ ),  $T$  is the absolute temperature (K),  $M_w$  is the molecular mass of water vapour ( $18.016 \text{ kg/kmol}$ ).

Figure 6 depicts the suction isochrones for every 400 h. Note that the suction value at  $h = 250$  mm was not monitored and it was estimated by linearly extending the curves between  $h = 150$  mm and  $h = 200$  mm. At  $t = 0$ , the initial suction of the sample was quite homogeneous, with a mean value of  $64.5 \pm 1.5$  MPa. It was supposed that after starting the infiltration, the suction at the wetting face  $h = 0$  mm decreased rapidly to zero. The total suction at  $h = 50$  mm decreased to 2.37 MPa at  $t = 2200$  h while the total suction at  $h = 200$  mm started to increase  $t = 1900$  h, and remained high ( $s = 33.84$  MPa) at  $t = 6000$  h.

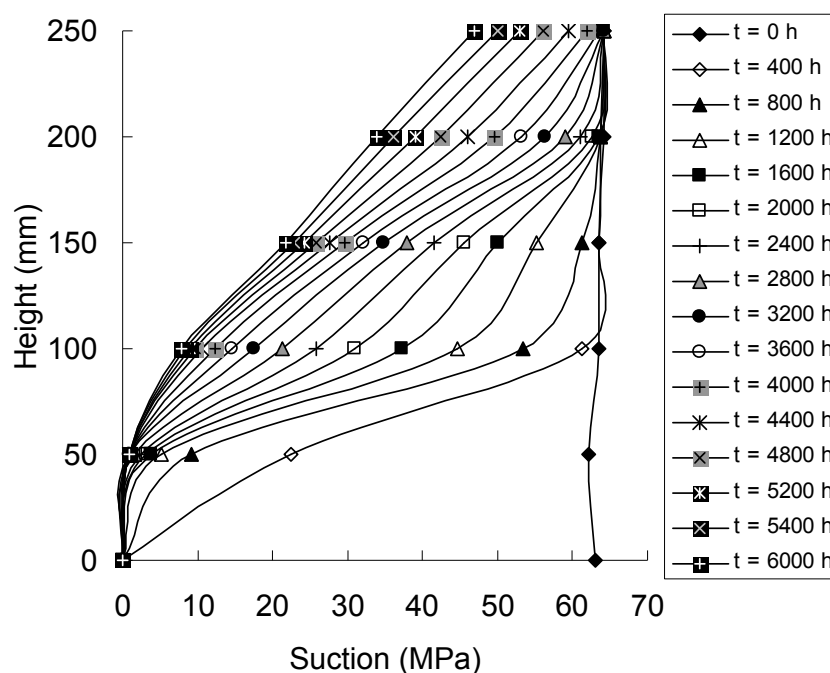
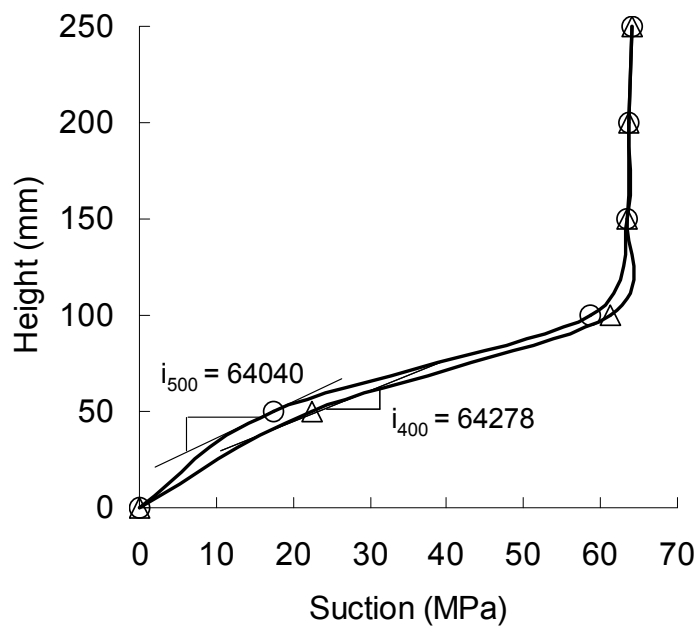
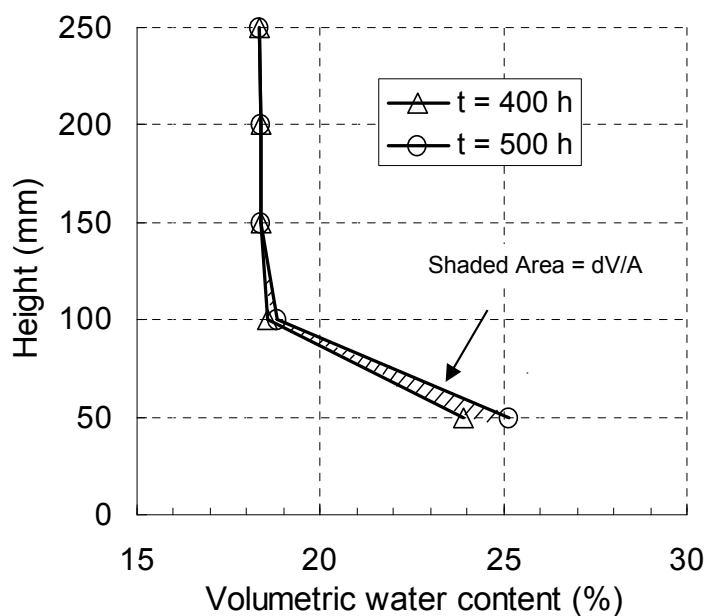


Figure 6. Suction profiles at different times

Based on the suction profiles (Figure 6), the hydraulic gradients ( $i$ ) and water fluxes ( $q$ ) at each measurement section ( $h$ ) and time ( $t$ ) were deduced following the methods shown in Figure 7. The hydraulic gradients was calculated as the tangent of suction profiles ( $s$  and  $h$  are expressed in m) as indicated in Figure 7a and the water fluxes was determined by integrating the difference in the volumetric water content profiles at a time interval ( $\Delta t$ ) as indicated in Figure 7b.



(a)



(b)

Figure 7. Determination of hydraulic gradient and water flux: (a) hydraulic gradient; (b) rate of water flow

To calculate the water flux, the volumetric water content of the mixture was deduced from the total suction using the water retention curve obtained at constant-volume conditions (Figure 4). As the suction measured by RH sensors in the infiltration test ranges from 2.37 MPa to 65 MPa, Eq. 2 (see also Figure 4) was used to calculate the gravimetric water content from suction, and the volumetric water content ( $\theta$ ) can be then calculated using Eq.3:

$$w = -7.261 \text{Log}(s) + 24.102 \quad (\text{Eq. 2})$$

$$\theta = w \rho_d / \rho_w \quad (\text{Eq. 3})$$

Note that  $\rho_d$  is assumed to be constant ( $1.67 \text{ g/m}^3$ ) during infiltration under constant volume conditions.

In order to verify the validity of these calculations, the total volume of water passing through each section was calculated from the volumetric water content profiles. The sum of these volumes from  $h = 0 \text{ mm}$  to  $h = 250 \text{ mm}$  corresponds to the volume of water absorbed by the soil specimen during infiltration. Figure 8 shows the comparison between the injected volume of water and that estimated from the water content profiles. It can be observed that there is a good agreement between the measured and calculated values, confirming the validity of the analyses performed.

Using the suction profiles presented in Figure 6, the hydraulic gradient ( $i$ ) and water fluxes ( $q$ ) at the four measurement sections  $h = 50 \text{ mm}$ ,  $100 \text{ mm}$ ,  $150 \text{ mm}$  and  $200 \text{ mm}$  for each  $100 \text{ h}$  were obtained, and used to calculate the hydraulic conductivity by applying Darcy's law:

$$k_w = -\frac{1}{A} \cdot \frac{q}{\frac{1}{2}(i_t + i_{t+\Delta t})} \quad (\text{Eq. 4})$$

where,  $k_w$  is the hydraulic conductivity;  $i_t$  and  $i_{t+\Delta t}$  are the hydraulic gradients at instant  $t$  and  $t+\Delta t$ , respectively.

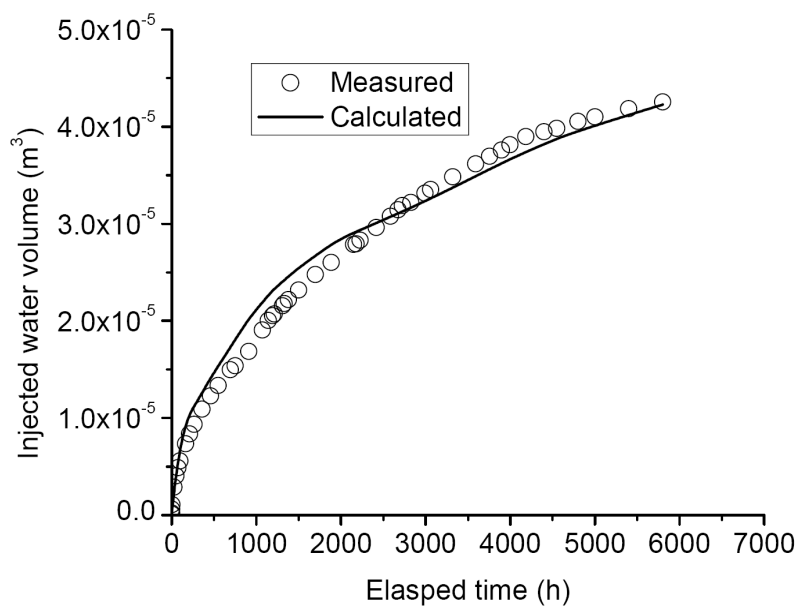


Figure 8. Calculated and measured water volume into the sample

In Figure 9, the hydraulic conductivity determined is plotted versus suction. It can be seen that at different measurement sections different relationships were obtained. As reported by Loiseau et al. (2002), Cui et al., (2008) on the Kunigel/sand mixture and Marcial (2003) on the pure MX80 bentonite, this phenomenon is related to the effect of hydraulic gradient. For clarifying this effect, the water fluxes ( $q$ ) and hydraulic gradient ( $i$ ) for each suction level (suction from 62 to 32 MPa) are plotted in Figure 10. Bi-linear relationships can be observed for each suction value, indicating the existence of “critical gradients”, their values ranging from 8000 to 38000. To apply Darcy’s law, the water flow is considered only when the linear segment at higher water flux is reached (details about this method can be found in Dixon et al., 1992).

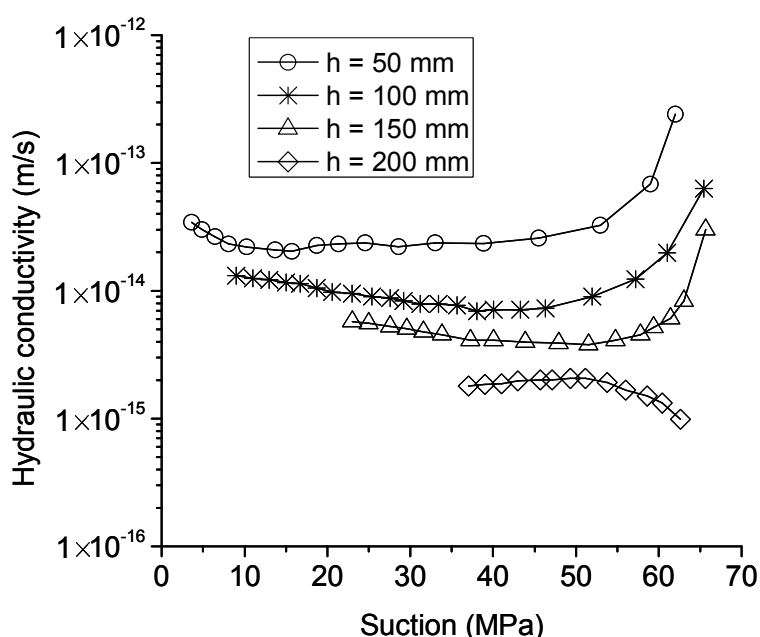


Figure 9. Hydraulic conductivity versus suction for different measurement sections

Taking into account the gradient effect, a unique relationship was obtained between hydraulic conductivity and suction, independent of the measurement sections (Figure 11). In Figure 11, the hydraulic conductivity determined by Karland et al. (2008) for the same material in saturated state is also presented: a much higher value of  $10^{-13}$  m/s was observed. Unlike the non swelling soils for which the hydraulic conductivity is increasing upon wetting, a “U-shape” relationship was observed: the hydraulic conductivity decreased when suction decreased from 65 to about 15 MPa, then increased for further suction decrease. Similar observations were made on the Kunigel-V1/sand mixture (JNC, 2000; Cui et al., 2008) and GMZ bentonite (Ye et al., 2009).

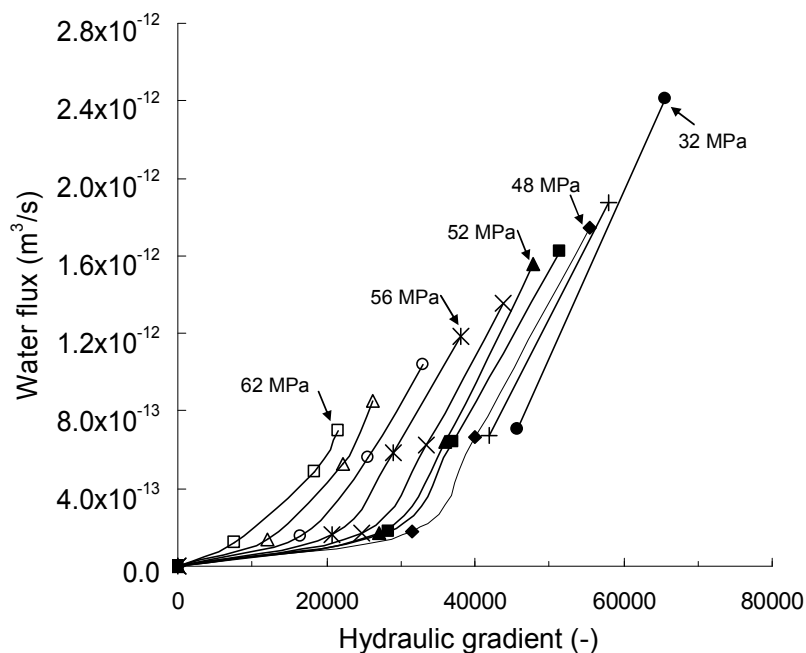


Figure 10. Water flux versus hydraulic gradient for different suctions

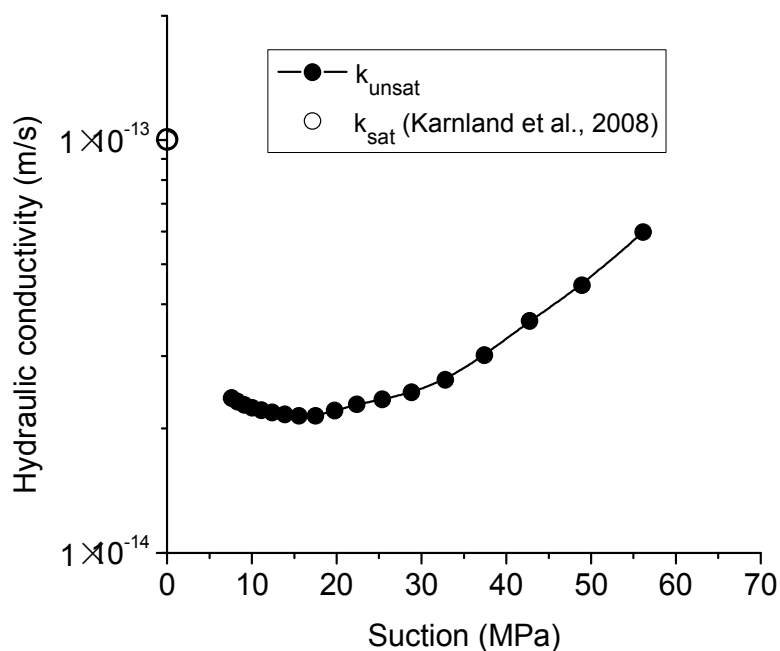
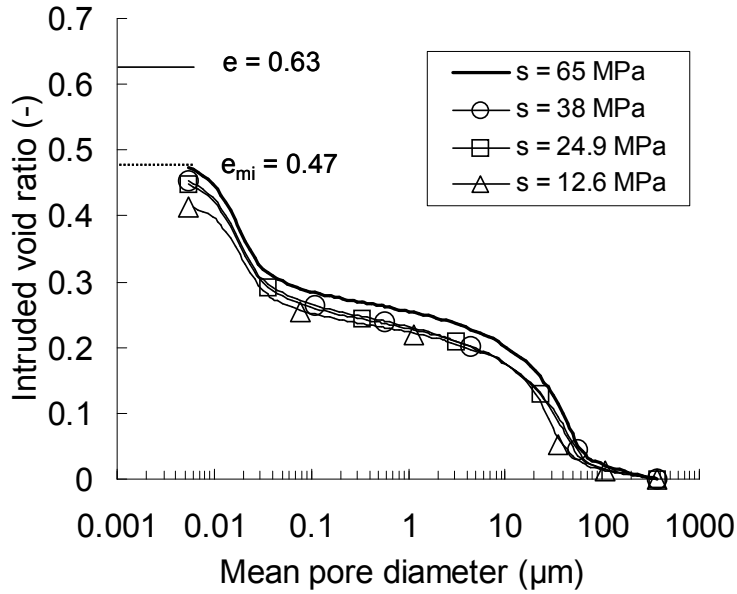


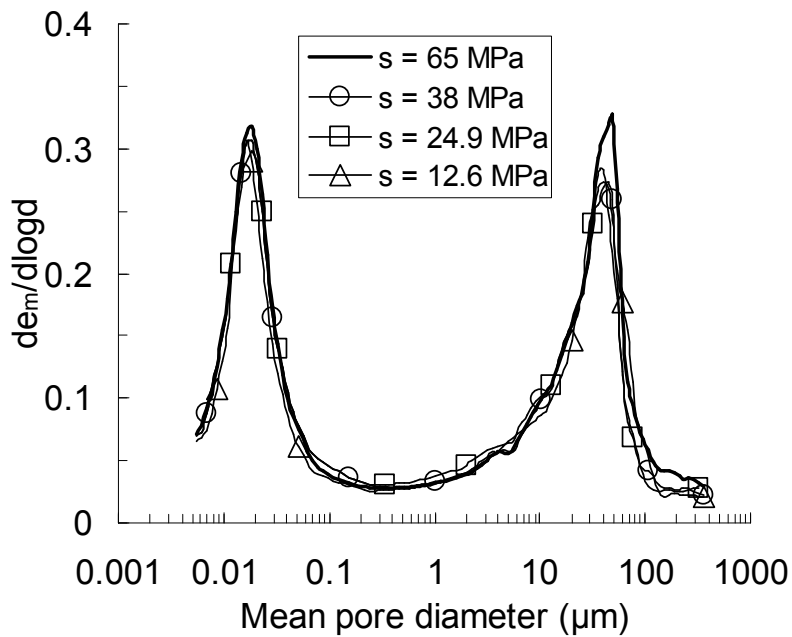
Figure 11. Hydraulic conductivity versus suction

The pore size distribution curves for suctions ranging from 65 MPa (initial state) to 12.6 MPa are presented in Figure 12a and Figure 12b. It was observed in Figure 12a that the final values of intruded mercury void ratio ( $e_{mi}$ ) were lower than the global soil void ratio ( $e = 0.63$ ). This can be explained by the limited pressure range of the MIP technique: for the high-plasticity soils, there is a significant pore volume (entrance diameter smaller than 6 nm) that the mercury could not penetrate to (Lloret et al., 2003; Delage et al., 2006). Figure 12a also shows that the amount of identifiable porosity ( $e_{mi} = 0.47$  in the initial state) decreased with

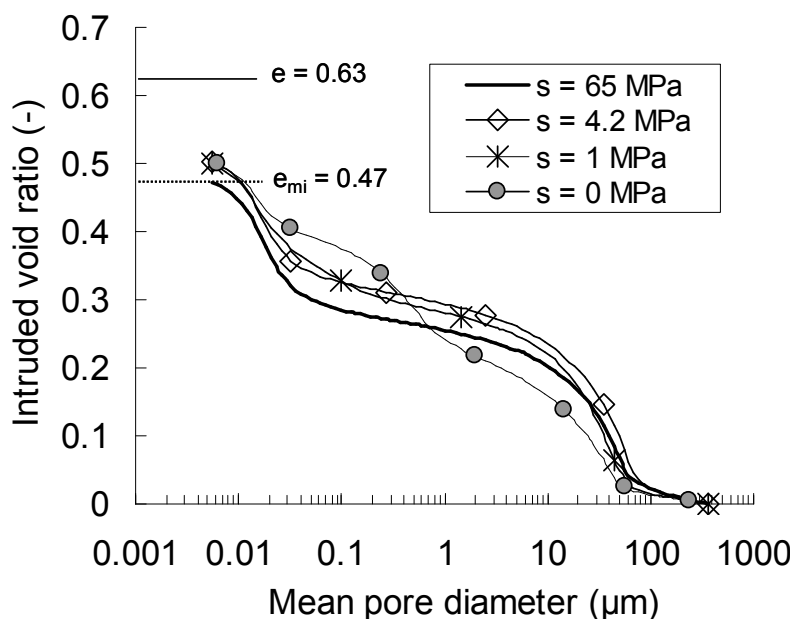
suction decrease. From the derived curves (Figure 12b), a typical bimodal porosity was observed in the initial state ( $\rho_d = 1.67 \text{ Mg/m}^3$ ,  $s = 65 \text{ MPa}$ ), and two pore groups can be defined: micro-pores (intra-aggregate pores having a mean size of  $0.02 \text{ }\mu\text{m}$ ) and macro-pores (inter-aggregate pores having a mean size of  $50 \text{ }\mu\text{m}$ ). The application of  $38 \text{ MPa}$  suction resulted in significant decrease of macro-pores quantity (Figure 12b), and little changes in micro-pores. However, no obvious further changes in both the macro-pores and micro-pores can be observed for the subsequently decrease of suction ( $38 - 24.8 - 12.6 \text{ MPa}$ ).



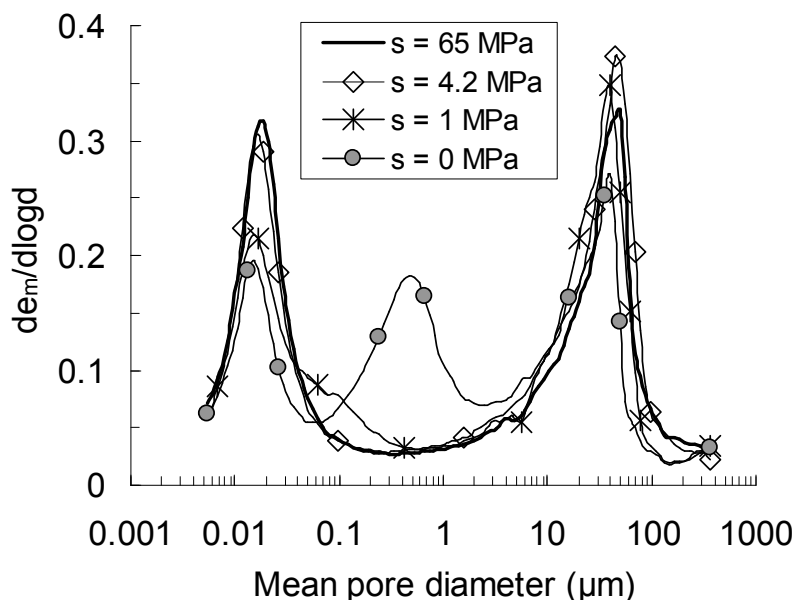
(a) 65 - 12.6 MPa suction



(b) 65 - 12.6 MPa suction



(c) 4.2 – 0 MPa suction



(d) 4.2 – 0 MPa suction

Figure 12. Pore size distributions of the bentonite-sand mixture wetted with different suctions under constant volume conditions

Figures 12c and 12d show the curve for 4.2, 1 and 0 MPa suction, lower values of identifiable void ratio  $e_{mi}$  were also obtained compared to the global void ratio of the soil (Figure 12c). However, it was found that the intruded porosity at these suctions were slightly higher than that in the initial state ( $s = 65$  MPa,  $e_{mi} = 0.47$ ). From the derived curves (Figure 12d), it was clearly seen that this increased intruded porosity corresponded to the difference in macro-pores volume, as the micro-pores volume decreased with decreasing suction. Moreover,

a third pore family (with pore size of 0.1-2  $\mu\text{m}$ ) appeared for the saturated sample.

The pore size distribution analyse was completed using the SEM technique (Figure 13). The photos were taken at two scales which focused on the behaviour of mixture (1250 x 1000  $\mu\text{m}$ ) and bentonite aggregates (25 x 20  $\mu\text{m}$ ), respectively. The sand grains were confused with aggregates in the photos at lower magnification (picture size of 1250 x 1000  $\mu\text{m}$ ) and cannot be identified. The photograph taken at the initial state ( $s = 65$  MPa) clearly shows the macro-pores (inter-aggregate pores) with a maximum diameter of about 100  $\mu\text{m}$  (Figure 13a), which is in agreement with the MIP results from Figure 12a. Figure 13b shows that the aggregates were densely assembled. Note that the micro-pores (intra-aggregate pores) observed in the MIP test (0.02  $\mu\text{m}$ ) cannot be detected by the SEM technique. Comparison of the photographs of 38 MPa suction (Figure 13d) and 65 MPa suction (Figure 13b) shows that the clay particles exfoliation occurred when suction decreased. The photographs at saturated state (Figure 13e and 13f) show that the macro-pores observed at higher suctions (Figure 13a and 13c) were filled by the swollen bentonite; however, there are 2-dimensional pores (2-D pores) appeared which may correspond to the pore group with a mean diameter of 50  $\mu\text{m}$  and 1  $\mu\text{m}$  observed in Figure 12d. Note that Audiguier et al. (2008) observed similar 2-D pores of a diameter between 0.1 and 1  $\mu\text{m}$  from a natural clay after free swelling.

In order to quantify the suction effect on the macro-pores, a macro-pores radius larger than 2  $\mu\text{m}$  was defined based on the curves in Figure 12 where it can be observed that the pores larger than 2  $\mu\text{m}$  changed with decreasing suction. Using this limit value that separates macro-pores from micro-pores, the MIP results at different suctions were re-analysed and the relationship between the calculated macro-void ratio ( $e_{\text{macro}}$ ) and applied suction are presented in Figure 14. It can be observed that the macro-pores quantity was progressively reduced with decreasing suction in the range of 65 to 12.6 MPa (zone I). For suctions in the range of 4.2 MPa to 1 MPa, the macro-pores quantity was increasing with suction decrease. This can be explained by the creation of the 2-D pores described above; a significant decrease followed when suction decreased from 1 MPa to zero (zone II).

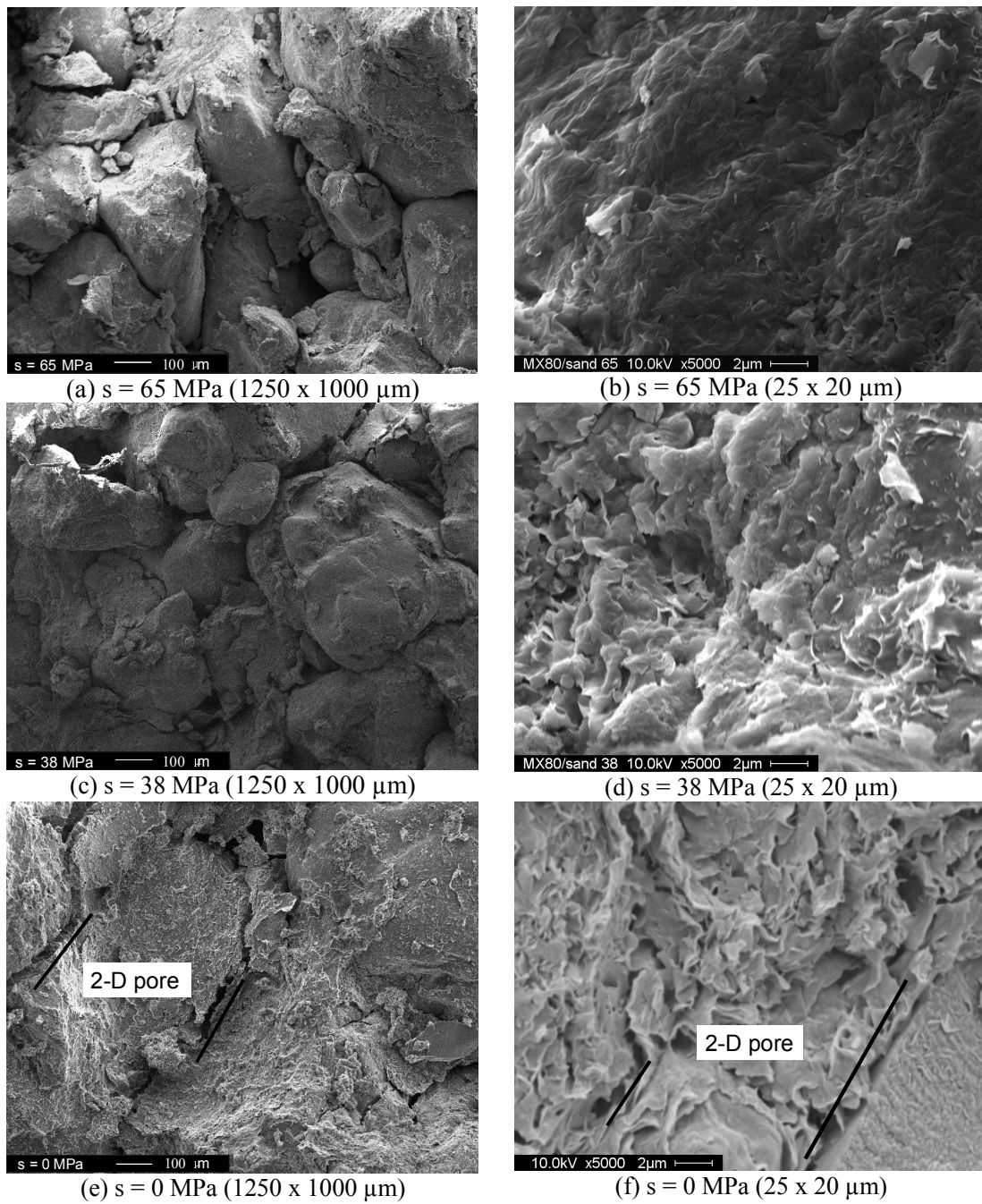


Figure 13. SEM photographs of bentonite/sand mixture samples equilibrated at different suctions

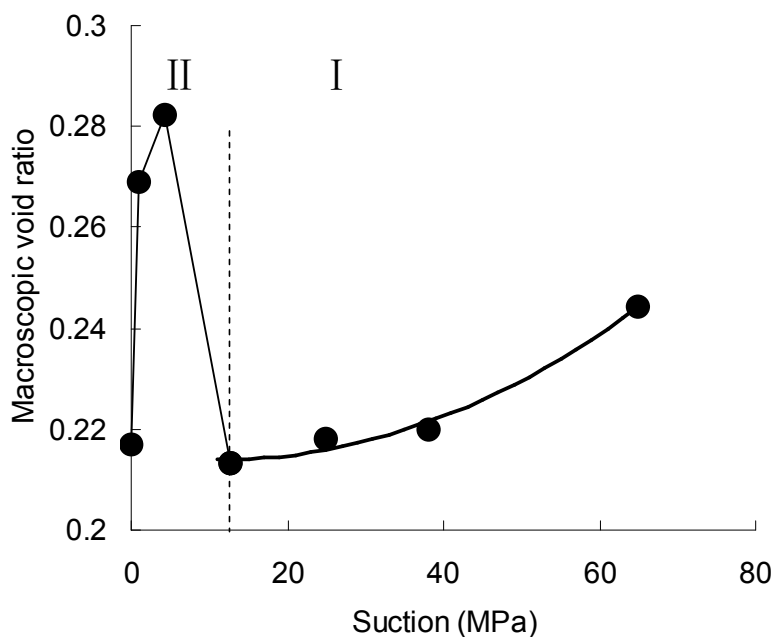


Figure 14. Changes of macroscopic void ratio

#### 4 Interpretation and discussion

From the shape of the suction isochrones shown in Figure 6, it can be observed that suction changes mainly occurred in the lower part of the sample below 100 mm, and in the upper part less changes were identified. As mentioned by Ye et al. (2009), this phenomenon could be explained by separating the liquid water transfer from the water vapour transfer. In the zone near the wetting face, the water transfer involves mainly the liquid water which has low permeability. By contrast, water vapour diffusion prevails in the zone far from the wetting face, and vapour transfer is relatively quicker through the macro-pores. Indeed, many researchers considered that the infiltration process is a vapour diffusion-controlled process rather than a convection process (Kröhn, 2003a, 2003b; Pusch and Yong, 2003; Ye et al. 2009). Kröhn (2003a, 2003b) proposed a vapour diffusion model for the re-saturation of bentonite and a good correspondence between the model prediction and the experimental data was obtained. This confirmed that the compacted bentonite in contact with liquid water was hydrated mainly by evaporation in the pore network and subsequently by vapour diffusion.

Comparison of the curves at different suctions in Figure 12a shows that with decreasing suction (65-38-24.9-12.6 MPa), the amount of identifiable porosity decreases, which can be related to the interaction between macro- and micro-pores. During suction decrease under constant-volume conditions the size of unidentifiable pores increased with increasing interlayer space, while the macro-pores was filled by small clay particles (Pusch, 1999; Cui et al., 2002).

Figure 12b showed that suction decrease did not change the micro-pores group, whereas a decrease of macro-pores quantity was observed - it was significant when suction decreased from 65 MPa to 38 MPa and much less for the subsequent suction decrease (38-24.8-12.6 MPa). This confirms the previous conclusion that during suction decrease the macro-pores was clogged by exfoliated clay particles (although in different rate) which were also visible in the SEM photograph for 38 MPa suction (Figure 13d).

For suction lower than 4.2 MPa (Figure 12c), a lower value of  $e_{mi}$  was also obtained compared to the global void ratio ( $e = 0.63$ ). However, the identified porosity at these suctions (4.2, 1 and 0 MPa) was slightly higher than that in the initial state ( $s = 65$  MPa,  $e_{mi} = 0.47$ ). This phenomenon can be attributed to the larger pore quantity of the pore group having a mean size of 50  $\mu\text{m}$  (for 4.2 and 1 MPa suction) and 1  $\mu\text{m}$  (for zero suction) compared with the initial state (Figure 12d). These two pores groups were identified as 2-D pores of about 50 and 1  $\mu\text{m}$  diameter for the saturated sample in Figure 13e and 13f, respectively. Audiguier et al. (2008) explained the formation of the 2-D pores by the division of clay aggregates due to swelling. Moreover, it should be noted that the small deformation induced by the release of swelling pressure before freeze-drying may also play a role in the macro-pores increase. However, this slight effect could not be identified by the current samples preparation technique, and new methods without stress state changes are needed to obtain more accurate microstructure observations.

It appeared that the micro-pores changed only when the saturation was approached (1 MPa and 0 MPa in Figure 12 and Figure 13). This phenomenon is in agreement with the conclusion by Cui et al. (2002) for the Kunigel clay/sand mixture: when water infiltrated into the soil, clay aggregates hydration started first on the surface giving rise to the clay particles exfoliation and resulting in the clogging of macro-pores, whereas the micro-pores remained almost un-affected; the micro-pores started to change only when the water saturation was approached (suction lower than 9 MPa). When saturation was reached, the clay aggregates disappeared (Figure 13f) and a new pore group of about 1  $\mu\text{m}$  diameter was formed, visible from both MIP and SEM tests. The micro-pores seemed to be compressed by the swelling pressure, whereas 2-D pores of 1  $\mu\text{m}$  in diameter appeared due to the separation of clay sheets within the aggregates (Saiyouri et al., 2000).

Generally, when experimentally determining the hydraulic conductivity by Darcy's law, a linear relationship between water flow rate ( $q$ ) and hydraulic gradient ( $i$ ) is obtained. However, non-linear relationships are often observed for clayey soils (Lutz & Kemper, 1959; Miller &

Low, 1963; Zou, 1996), and there is a “critical gradient” below which flow occurs in non-Darcian mode (Yong and Warkentin, 1975; Dixon et al., 1987). This can be explained by the high energy of the water adsorbed in clays, which increases with the clay fraction and activity (Dixon et al., 1987). When the hydraulic gradient increases, this energy is overcome locally and the adsorbed water can be mobilised. For soils containing highly active clay minerals, as smectite in this study, this critical gradient effect can be significant leading to different  $k - s$  relationships obtained at different measurement sections in Figure 9. To apply Darcy’s law, only water flow at higher hydraulic gradient should be considered (when the linear segment in Figure 10 is reached).

Considering the critical gradient effect (Figure 10), the hydraulic conductivity was corrected and shown in Figure 11. It was observed that the suction decrease resulted in a first decrease then an increase of hydraulic conductivity. As explained by Cui et al. (2008) and Ye et al. (2009), in the beginning water transfer was primarily governed by the network of macro-pores, which were progressively clogged by the expanding hydrated aggregates, leading to the hydraulic conductivity decrease. When the macro-pores clogging ended and water transfer was controlled by the suction gradient, the common hydraulic conductivity increase with suction decrease was observed.

It is interesting to note that if we relate the macro-pore changes (Figure 14) to the hydraulic conductivity changes (Figure 11), it seems that the hydraulic conductivity changed following the same trend as the macro-pores quantity during hydration. In other words, water transfer was primarily governed by the network of macro-pores in the full suction range, but not be controlled by the suction gradient in the lower suction range as mentioned above. The macro-pores decreased progressively in quantity due to the clay particles exfoliation occurred on the aggregates surface in the suction range from 65 to 12.6 MPa, leading to a decrease of hydraulic conductivity. When saturation was approached (4.2 - 1 MPa), water transfers through the 2-D pores appeared, leading to an increase in hydraulic conductivity; in saturated state the value can reach as high as  $10^{-13}$  m/s as reported by Karnland et al. (2008). It should be noted that after saturation, the hydraulic conductivity has been found to be time dependent (Loiseau et al., 2002; Cui et al., 2008). It decreased with time due to the re-organization of microstructure over time in the soil sample. This is probably related to the closure of the 2-D pores in long term, that leads to a uniform microstructure (Stroes-Gascoyne et al., 2010).

## 5 Conclusion

The hydraulic properties of a compacted bentonite-sand mixture were investigated in the laboratory by carrying out water retention test and infiltration test as well as the microstructure observation. The results obtained allowed relating the variation of hydraulic conductivity to the microstructure changes.

During suction decrease (suction higher than 12.6 MPa) the macro-pores were clogged progressively by the exfoliated clay particles (although at different rates); however, when saturation was approached (suction lower than 4.2 MPa) macro-pores quantity increased again due to the appearance of 2-D pores. The micro-pores changed only when saturation was approached.

With suction decrease under constant volume condition, the hydraulic conductivity decreased followed by an increase after certain suction threshold. This change followed the same tendency as the macro-pores quantity. In other words, water transfer was primarily governed by the network of macro-pores. Over time, the hydraulic conductivity is expected to decrease due to the re-organization of microstructure that leads to the closure of 2-D pores.

## Acknowledgements

The work was conducted in the framework of the SEALEX project of IRSN and the PHC Cai Yuanpei project (24077QE). The support of the National Nature Science Foundation of China (41030748) and that of the China Scholarship Council (CSC) are also greatly acknowledged.

## References

- AFNOR, 1992. AFNOR NF P94-057, Soils: investigation and testing. Granulometric analysis. Hydrometer method. Association Francaise de Normalisation. France.
- AFNOR, 1996. AFNOR NF P94-056, Soils: investigation and testing. Granulometric analysis. Dry sieving method after washing. Association Francaise de Normalisation. France.
- Audiguier, M., Geremew, Z., Cojean, R., 2008. Relations enter les microstructures de deux sols argileux de la région parisienne et leur sensibilité au retrait gonflement. SEC2008, Paris, France, 1-3 sept. Editions du LCPC.2008: 235-243.
- Blatz, J.A., Cui, Y. J., Oldecop. L., 2008. Vapour Equilibrium and Osmotic Technique for Suction Control. *Geotech Geol Eng* (2008) 26:661–673.
- Börgesson, L., Chijimatsu, M., Fujita, T., Nguyen, T.S., Rutqvist, J., Jing, L., 2001. Thermo-hydro-mechanical characterisation of bentonite-base buffer material by laboratory tests and numerical back analyses. *International Journal of Rock Mechanics & Mining Sciences* 38, 95-104.
- Cui, Y. J., Loiseau, C., Delage, P., 2002. Microstructure changes of a confined swelling soil due to suction controlled hydration Unsaturated soils: proceedings of the Third International Conference on Unsaturated Soils, UNSAT 2002, 10-13 March 2002, Recife, Brazil, 593.

- Cui, Y.J., Tang, A.M., Loiseau, C., Delage, P., 2008. Determining the unsaturated hydraulic conductivity of a compacted sand-bentonite mixture under constant-volume and free-swell conditions. *Physics and Chemistry of the Earth, Parts A/B/C*, 33(Supplement 1):S462 – S471.
- Daniel, D.E., 1982. Measurement of hydraulic conductivity of unsaturated soils with thermocouple psychrometers. *Soil Science Society of America Journal* 20 (6):1125–1129.
- Delage, P., Lefebvre, G., 1984. Study of the structure of a sensitive Champlain clay and its evolution during consolidation. *Canadian Geotechnical Journal* 21 (1), 21–35.
- Delage, P., Marcial, D., Cui, Y.J., Ruiz, X., 2006. Ageing effects in a compacted bentonite: a microstructure approach. *Géotechnique* 56 (5), 291–304.
- Dixon, D.A., Cheung, S.C.H., Gray, M.N., Davidson, B.C., 1987. The hydraulic conductivity of dense clay soils. *Proc. 40th Canadian Geotechnical Conference, Regina, Saskatchewan - Canada*, pp. 389–396.
- Dixon, D.A., Gray, M.N., Hnatiw, D., 1992. Critical gradients and pressures in dense swelling clays. *Canadian Geotechnical Journal* 29 (6), 1113–1119.
- Dixon, D.A., Graham, J., Gray, M.N., 1999. Hydraulic conductivity of clays in confined tests under low hydraulic gradients. *Canadian Geotechnical Journal* 36 (5), 815- 825.
- Fredlund, D.G., Rahardjo, H., 1993. *Soil mechanics for unsaturated soils*. John Wiley and Sons, New York
- JNC, 2000. H12: Project to establish the scientific and technical basis for HLW disposal in Japan, report TN1410 2000-001, Tokai-Mura.
- Karnland, O., Nilsson, U., Weber, H., and Wersin, P., 2008. Sealing ability of Wyoming bentonite pellets foreseen as buffer material-Laboratory results. *Physics and Chemistry of the Earth, Parts A/B/C*, 33:S472–S475.
- Kenney, T.C., van Veen, W.A., Swallow, M.A., Sungaila, M.A., 1992. Hydraulic conductivity of compacted bentonite-sand mixtures. *Canadian Geotechnical Journal* 29 (3): 364–374.
- Komine, H., 2004. Simplified evaluation on hydraulic conductivities of sand-bentonite mixture backfill. *Applied Clay Science* 26 (1–4), 13–19.
- Komine, H., 2010. Predicting hydraulic conductivity of sand bentonite mixture backfill before and after swelling deformation for underground disposal of radioactive wastes. *Engineering Geology*.
- Kröhn, K. P., 2003a. New conceptual models for the resaturation of bentonite. *Applied Clay Science* 23 (1-4), 25-33.
- Kröhn, K. P., 2003b. Results and interpretation of bentonite resaturation experiments with liquid water and water vapour. In: Schanz, T. (Ed.), *Proceedings of the International Conference from Experimental Evidence towards Numerical Modeling of Unsaturated Soils*, Weimar, Germany, vol. 1. Springer, Berlin, pp. 257–272.
- Lemaire, T., Moyne, C., Stemmelen, D., 2004. Imbibition test in a clay powder (MX-80 bentonite). *Applied Clay Science* 26: 235-248.
- Lloret, A., Villar, M.V., Sanchez, M., Gens, A., 2003. Mechanical behaviour of heavily compacted bentonite under high suction changes. *Géotechnique*, 53(1):27–40.
- Loiseau, C., Cui, Y.J., Delage, P., 2002. The gradient effect on the water flow through a compacted swelling soil. *Proc. 3rd Int Conf Unsaturated Soils, UNSAT'2002 Recife, Brazil, Balkema*, vol. 1, pp. 395-400.
- Lutz, J.F., Kemper, W.D., 1959. Intrinsic permeability of clay as affected by clay-water interaction. *Soil science* 88: 83-90.
- Marcial, D., 2003. *Comportement hydromécanique et microstructural des matériaux de barrière ouvragée*. Ph.D. thesis, École nationale des ponts et chaussées, Paris, France
- Miller, R.J., Low, P.F., 1963. Threshold Gradient for Water Flow in Clay Systems. *Soil Science Society of America Journal*. 27 (6):605-609.
- Pusch, R., 1979. Highly compacted sodium bentonite for isolating rock-deposited radioactive waste products. *Nucl. Technol. (United States)*, 45(2).

- Pusch, R., 1999. Microstructural evolution of buffers. *Engineering geology*. 54:33-41.
- Pusch, R., Yong, R., 2003. Water saturation and retention of hydrophilic clay buffer-microstructural aspects. *Applied Clay Science*, 23:61-68.
- Saiyouri, N., Hicher, P.Y., Tessier, D., 2000. Microstructural approach and transfer water modeling in highly compacted unsaturated swelling clays. *Mechanics of Cohesivefrictional Materials* 5, 41–60.
- Stroes-Gascoyne, S., 2010. Microbial occurrence in bentonite-based buffer, backfill and sealing materials from large-scale experiments at AECL's underground research laboratory. *Applied Clay Science*, 47(1-2):36–42.
- Tang, A. M. & Cui, Y. J., 2005. Controlling suction by the vapour equilibrium technique at different temperatures and its application in determining the water retention properties of MX80 clay. *Can. Geotech. J.* 42 (1): 287-296.
- Tang, C.S., Tang, A.M., Cui, Y.J., Delage, P., Barnichon, J.D., Shi, B., 2011. A study of the hydro-mechanical behaviour of compacted crushed argillite. *Engineering Geology*. 118 (3-4):93-103.
- Van Genuchten, M.T., 1980. A closed-form equation for predicting the hydraulic conductivity of unsaturated soils. *Soil Science Society of America Journal*, 44: 892-898.
- Villar, M.V., Lloret, A., 2008. Influence of dry density and water content on the swelling of a compacted bentonite. *Applied Clay Science*, 39(1-2):38-49.
- Wang, Q., Tang, A. M., Cui, Y. J., Delage, P., Gattmiri, B., 2012. Experimental study on the swelling behaviour of bentonite/claystone mixture. *Engineering Geology*. 124:59-66.
- Ye, W.M., Cui, Y.J., Qian, L.X., Chen, B., 2009. An experimental study of the water transfer through confined compacted GMZ bentonite. *Engineering Geology*, 108(3-4):169–176.
- Yong, R.N., Warkentin, B.P., 1975. *Soil properties and behaviour*. Elsevier, Amsterdam.
- Yong, R.N., Boonsinsuk, P., and Wong, G., 1986. Formulation of backfill material for a nuclear fuel waste disposal vault. *Canadian Geotechnical Journal*, 23(2):216-228.
- Zou, Y., 1996. A non-linear permeability relation depending on the activation energy of pore liquid. *Géotechnique* 46 (4), 769-774.

## **Chapter 5. Comparative study on the hydro-mechanical behaviour based on laboratory and field infiltration tests**

### **INTRODUCTION**

IRSN has launched the SEALEX project aiming at identifying the key factors related to the long-term performance of bentonite-based sealing systems when considering an initial technological void. This project consists of a series of in situ experiments performed in natural conditions in Tournemire.

A mock-up test (1/10) was carried out in controlled conditions in the laboratory aiming at providing useful information for analyzing the in situ tests in terms of saturation time and sealing effectiveness.

In this chapter, the results of the small scale test are presented along with the results from one of the in situ test (PT-N1). By comparing the injected water volume and axial swelling pressure evolution during saturation in two cases, an up-scaling ratio was obtained. Accordingly, the time needed to reach the stabilization of axial swelling pressure for the in situ test (PT-N1) as well as the evolution of swelling strain and swelling pressure in the case of failure of the confining structure were estimated.

This comparative study is subjected to a paper submitted to « Engineering Geology». The manuscript is presented in this chapter.

Wang, Q., Tang, A. M., Cui, Y.J., Barnichon, J.D., Ye, W.M., 2012

## **A comparative study on the hydro-mechanical behaviour of compacted bentonite/sand plug based on laboratory and field infiltration tests**

Qiong Wang<sup>1</sup>, Anh Minh Tang<sup>1</sup>, Yu-Jun Cui<sup>1,3</sup>,  
Jean-Dominique Barnichon<sup>2</sup>, Wei-Min Ye<sup>3</sup>

**Abstract:** SEALEX is a research project aiming at identifying the key factors that affect the long-term performance of bentonite-based sealing systems with an initial technological void. In this framework, a series of in situ experiments are being performed in situ. Meanwhile, a small scale test (1/10) was carried out in controlled conditions in the laboratory, aiming at providing useful information for analyzing the in situ tests in terms of saturation time and sealing effectiveness. In this paper, the results of the small scale test are presented along with the results from the first in situ test (PT-N1). It was observed that during the saturation process, the evolution of injected water volume followed a hyperbolic relationship in both cases. A decrease in axial swelling pressure occurred due to the filling process of technological void in the laboratory. By contrast, this decrease is not observed in the in situ condition. Comparison of the injected water and axial swelling pressure obtained from different scales gave the same time up-scaling ratio of 2.5 (in situ experiment /small scale test). Accordingly, the saturation duration of the in situ experiment was estimated to be equal to two years. For the small scale test, a swelling strain evolution rate of 0.588 mm/day was identified in the case of infiltration from the two sides of sample. This is useful when predicting the evolution of swelling strain in the case of failure of the sealing plug. After filling an additional 20% void, a swelling pressure of 0.18 MPa was obtained, indicating the favorable sealing capacity after filling the technological void.

**Keywords:** mock up test; in situ experiment; bentonite/sand mixture; technological void; swelling pressure; swelling stain

---

### **1 Introduction**

In the design of deep geological repository for High Level Long Lived radioactive Wastes (HLLW), compacted bentonite-based materials are often considered as buffer/sealing materials. These materials are expected to exhibit a swelling pressure high enough to fulfil their buffer/sealing functions.

Numerous laboratory studies have been conducted to study the performance of buffer/sealing materials (e.g. Delage et al., 1998; Lloret et al., 2003; Romero et al., 2005; Lloret & Villar, 2007). Various experiments were also performed in underground research laboratories (URL)

---

1 Ecole des Ponts ParisTech, Navier/CERMES , France

2 Institut de Radioprotection et de Sûreté Nucléaire (IRSN), France

3 Tongji University, China

(TSX at Manitoba, Canada; FEBEX at Grimsel, Switzerland; RESEAL at Mol, Belgium; KEY at Bure, France, etc.). Recently, IRSN (Institut de Radioprotection et de Sûreté Nucléaire) has launched the SEALEX project aiming at identifying and quantifying the key factors related to the long-term performance of bentonite-based sealing systems taking into account an initial technological void. This project consists of a series of in situ experiments performed in situ in the Tournemire URL, and a small scale test (1/10) in the laboratory.

The in situ experimental program was purposefully built allowing systematically exploring the effect of technical specifications, design, construction, defect, etc., by changing a single parameter each time. As a reference case (see Barnichon et al. 2009, 2012 for more details), the first test PT-N1 with a clay core made of pre-compacted monolithic disks of MX80 bentonite/sand mixture (70/30 in dry mass) has been conducted in the Tournemire Underground Research Laboratory. Due to the low permeability of this material, saturation is expected to be reached in several years (see Barnichon et al., 2012). During this process, the injected water volume, total pressure, pore pressure and relative humidity changes have been monitored at several positions within the plug. After the re-saturation stage, hydraulic tests will be performed to determine the overall hydraulic properties (permeability, occurrence of leakage) of the sealing system. In addition to this reference case, three tests are designed to quantify the impact of the technical specification and design of the sealing plug by changing the intra-core geometry (jointed against monolithic disks), core composition (MX80/sand ratio) and core conditions (pre-compacted against in situ compacted). Moreover, to investigate the effect of altered conditions, an additional test is designed to simulate an incidental decrease of swelling pressure caused by a failure of the confining structure.

Based on the design of in situ experiments, a laboratory small scale test (1/10) was performed, focusing on the recovery capacity of the bentonite-based seal with technological voids. The same material as for test PT-N1 (MX80 bentonite/sand mixture) was used. A stainless steel confining cell was used to better define the boundary conditions. After the initial saturation process as in the PT-N1 in situ experiment, the seal evolution upon a confinement failure (failure of the confining plug) was simulated by allowing a given amount of free swell. This free swell was followed by a last stage of wetting under constant volume condition. To assess the sealing capacity, the injected water volume, axial swelling pressure and swelling strain were monitored in different stages. It was expected to obtain useful information from the laboratory small scale test for analysing the field tests in terms of saturation time and sealing effectiveness.

In this paper, the results of the small scale test are presented along with the results from the in situ test (PT-N1). An up-scaling ratio was obtained by comparing the injected water volume and axial swelling pressure evolution during saturation process in two cases. The time needed to reach the stabilization of axial swelling pressure for the in situ test (PT-N1) as well as the evolution of swelling strain and swelling pressure in the case of failure of the confining structure were estimated accordingly.

## 2 Materials and methods

### 2.1 Materials

The soil studied is a compacted MX80/sand mixture with a proportion of 70/30 in dry mass. The bentonite is from Wyoming, USA, with a high content of montmorillonite (80%). It has a liquid limit of 575%, a plastic limit of 53% and a unit mass of  $2.77 \text{ Mg/m}^3$ . The cation exchange capacity (CEC) is 76 meq/100g (83 % of  $\text{Na}^+$ ). The quartz sand used in the mixture comes from Eure and Loire (France) with a unit mass of  $2.65 \text{ Mg/m}^3$ . It was sieved at 2 mm prior to being mixed with the bentonite.

The water having the same chemical composition as the pore water of the Callovo-oxfordian claystone from the ANDRA URL in Bure (France), namely synthetic water (Wang et al., 2012a, 2012b), was used. It was obtained by mixing the corresponding chemical compounds (see Table 1) with distilled water using a magnetic stirrer until full dissolution.

Table 1. Chemical composition of the synthetic water.

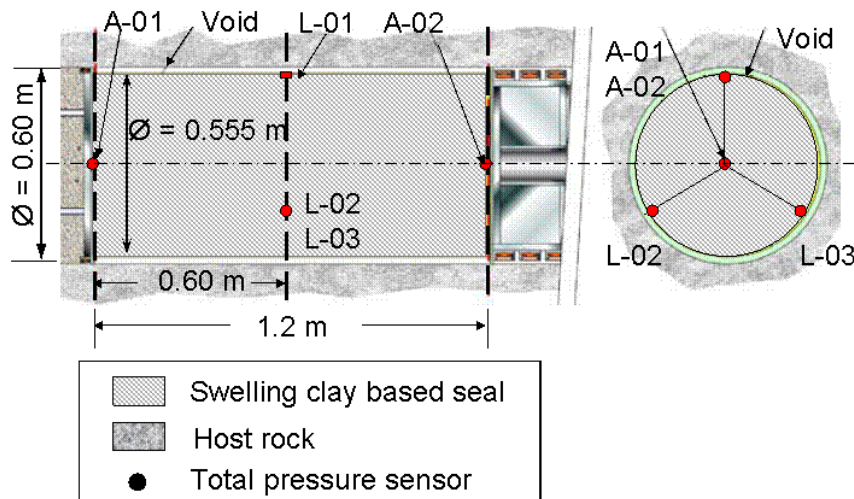
Compound	$\text{NaHCO}_3$	$\text{Na}_2\text{SO}_4$	$\text{NaCl}$	$\text{KCl}$	$\text{CaCl}_2 \cdot 2\text{H}_2\text{O}$	$\text{MgCl}_2 \cdot 6\text{H}_2\text{O}$	$\text{SrCl}_2 \cdot 6\text{H}_2\text{O}$
Mass (g) per Litter of solution	0.28	2.216	0.615	0.075	1.082	1.356	0.053

### 2.2 SEALEX in situ test (PT-N1)

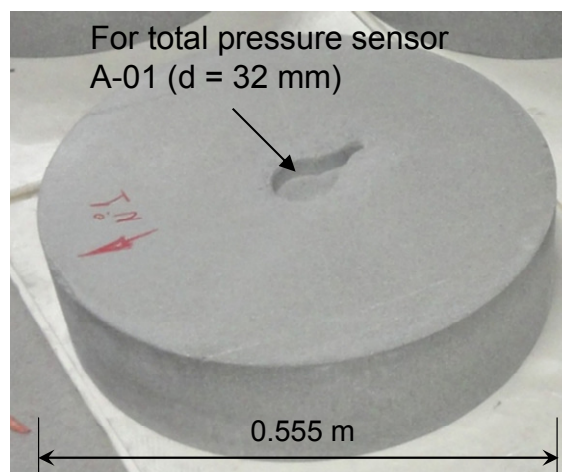
As mentioned above, the in situ experiment (PT-N1) has been conducted in the Tournemire Underground Research Laboratory excavated in Toarcian argillite. A horizontal borehole (0.60 m in diameter) was drilled for this purpose. Figure 1 shows the layout of the experiment. A seal made of compacted MX80/sand mixture is sandwiched between two porous plates, allowing water inflow from two water reservoirs (i.e. upstream and downstream). The 14.33% annular technological void (volume of void/volume of borehole) adopted originated from a smaller initial diameter (0.555 m) of the pre-compacted clay seal compared to the borehole diameter (0.60 m). The upstream plate is in direct contact with host-rock while the downstream one is retained by a confining system maintaining a constant volume condition. A



saturation system, L-01, L-02, L-03) to measure the radial swelling pressure; two total pressure sensors were installed at section 0 and 1.20 m to measure the axial swelling pressure (A-01, A-02). For each sensor, a hole as shown in Figure 3b was prepared at their pre-assigned positions before the assemblage of blocks, keeping the hole to a minimum size. Wireless sensors ( $d = 32$  mm) were used to limit preferential flow along cables and a wireless transmitter was installed at each measurement section. Data were recorded automatically by a data acquisition system.



(a) Distribution of the total pressure sensors



(b) Hole machined for installation of wireless sensor

Figure 3. Distribution and installation of the total pressure sensors.

Regarding the test operational phases, 49 L of water were first injected, which corresponds to the volume of the technological void designed. This process ended in one hour. Afterwards, the water supply was stopped because the side packer was not properly inflated; it restarted after 20 days with a water pressure of 0.1 MPa. As the saturation proceeded, the swelling

pressure, pore pressure, water content or water saturation within the plug were monitored. The injected water volumes at both upstream and downstream chambers were also measured. After completion of the saturation process (which may likely last several years), hydraulic tests will be performed to determine the overall hydraulic properties (permeability, occurrence of leakage) of the corresponding sealing systems.

### 2.3 Laboratory small scale test

The experimental devices used for the laboratory small scale test (1/10) are shown in Figure 4. A stainless steel cell of 60 mm in inner diameter and 200 mm long is used. As in the in situ test, an annular technological void is simulated by adopting a smaller initial diameter (55.5 mm) for the pre-compacted sample compared to the diameter of the hydration cell (60 mm). Note however that the hydration cell is placed in the vertical direction (see Figure 4) and it is different from the in situ test which is performed in a horizontal borehole (Figure 1 and Figure 2). Water supply is achieved through the water inlets in the bottom base, which is connected to burettes. This allows measuring the total amount of water taken up by the sample. A piston of 60 mm diameter is used to simulate the confining structure. On the bottom of the piston, there is drainage with two inlets (upside inlet in Figure 4) and a porous stone of 50 mm diameter, allowing water/air flow. A mechanical press is used to restrain the axial deformation and a force transducer is used to monitor the axial swelling pressure. A displacement transducer fixed on the piston allows monitoring the axial displacement to an accuracy of 1  $\mu\text{m}$ . The axial pressure and axial displacement are recorded automatically to a data logger, while the inlet water volume is measured manually by determining the water level in the burettes. Note that in this small scale test, the radial swelling pressure is not measured.

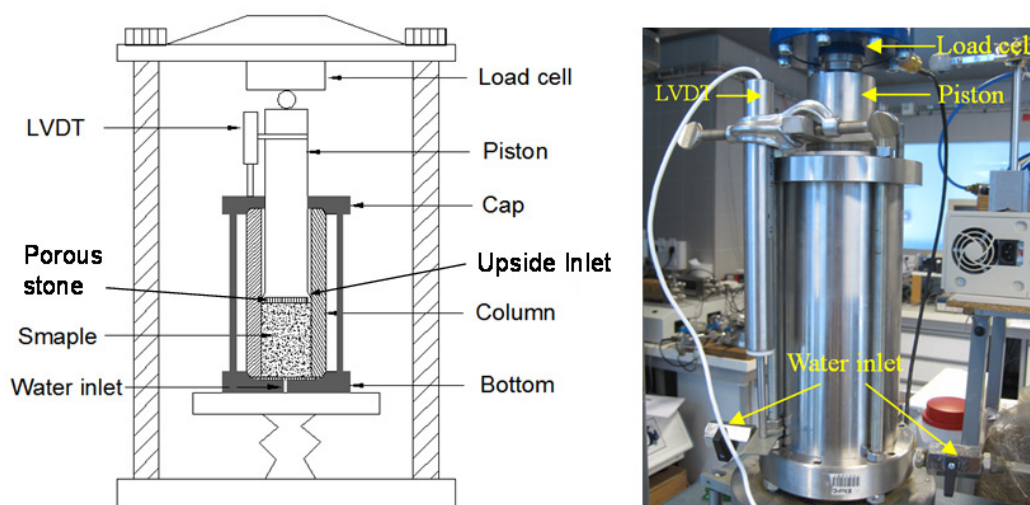


Figure 4. Experimental devices.

A monolithic cylindrical sample (55.5 mm in diameter, 120 mm high) is used in the test. It was statically compacted in a mould to the same dry density as for the in situ test ( $1.97 \text{ Mg/m}^3$ ). In order to ensure the homogeneity of the specimen, the compaction was carried out in two layers. The surface of the first compacted layer was carefully scarified before the next layer was added to ensure a good junction between both. Figure 5a shows the pre-compacted specimen with the hydration cell. After compaction, the specimen (55.5 mm in diameter) was inserted into the center of the cell (60 mm in inner diameter) letting an annular void (2.25 mm) between the specimen and cell wall (Figure 5b). An initial axial stress of 0.1 MPa was applied on the specimen before hydration to ensure a good contact (i.e. between the load cell and piston, between the piston and the sample, between the sample and the bottom) and satisfactory load measurement. After stabilization under the axial stress, the upside inlets (see Figure 4) were sealed and vacuum was applied to evacuate all air in the voids (technological void mainly). The synthetic water was then injected from the bottom.

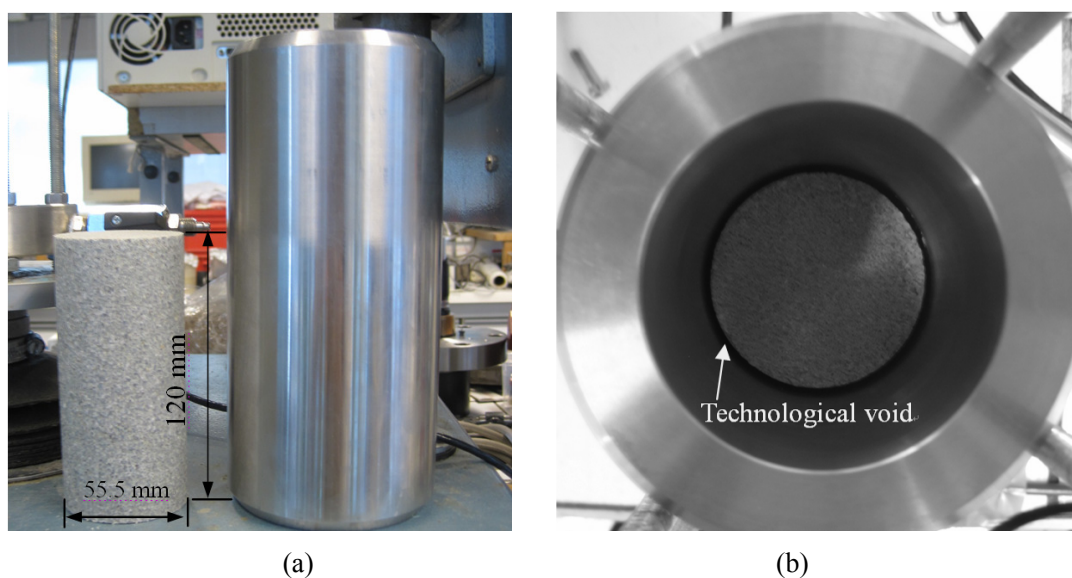


Figure 5. Sample preparation.

As described in Figure 6, hydration is carried out in three stages. First, the axial deformation is restrained and water injected towards the sample; during this stage (Stage 1. initial saturation phase), the evolution of the vertical swelling pressure is monitored. Once the hydration ends, the confining pressure in the axial direction is removed by unloading, allowing a free swell of 20% (Stage 2. recovery of the void phase). To reduce the test duration in this stage, two-side infiltration is applied by injecting water from both the bottom and the top, while recording changes in axial swelling strain over time. This stage aims at simulating the case of a saturation defect or a failure of confining structure that may occur in the field during its long term lifespan. The free swell of 20% represents the sealing capacity required

after filling the technological void. When the axial swelling strain reaches the desired value of 20%, the piston automatically blocks itself thanks to a reserving distance of 24 mm (corresponding to 20% of swelling strain) between the piston and load cell (Figure 7), and the evolution of swelling pressure is monitored again (Stage 3. confinement phase).

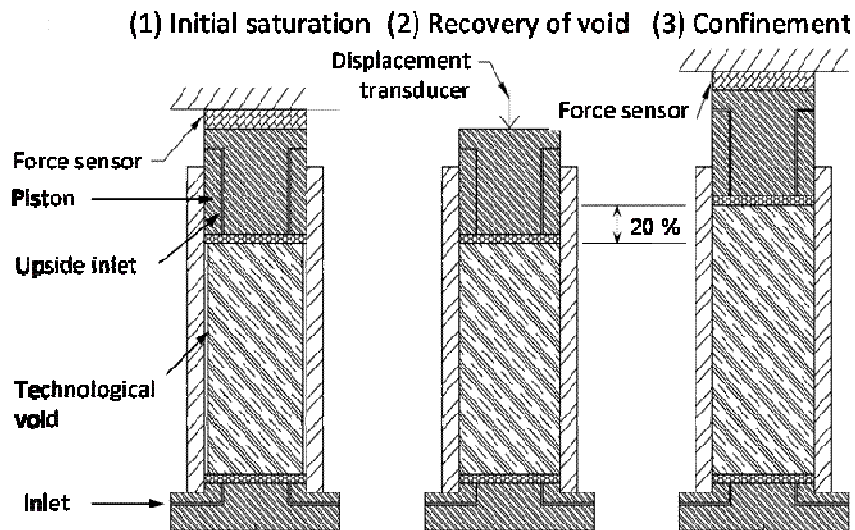


Figure 6. A schematic description of three stages of the small scale test.

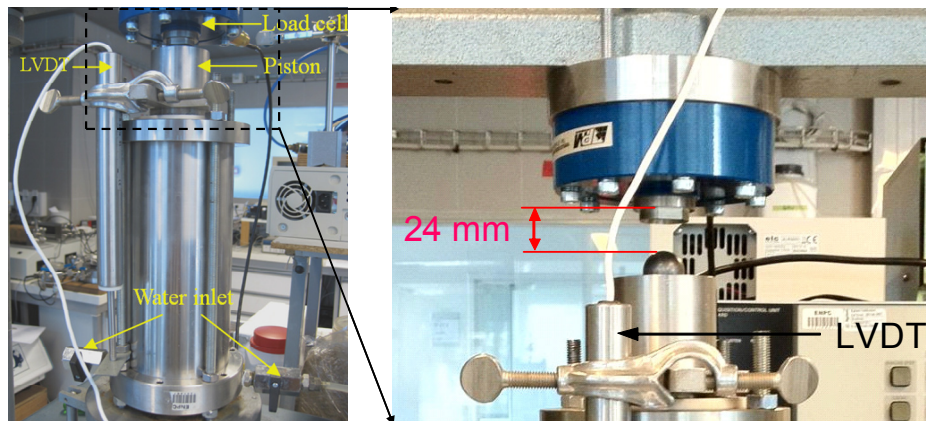


Figure 7. Lifting of load cell for free swell.

### 3 Experimental results

#### 3.1 In situ test (PT-N1)

Figure 8 shows the injected water volume over time. As mentioned above, a volume of 49 L was first injected to fill the technological void and the injection was stopped for 20 days due to a technique problem related to the packer. After the restoration of injection, the increase rate of water volume was followed by an asymptotic curve with a decreasing rate. After 367

days, the total injected water volume was 71.39 L (Figure 8). Examination of the curve shows that the shape of water volume versus time (after rejection) is similar to that of a hyperbolic function. Figure 9 presents the time/water volume (day/L) data plotted versus time. A good linear relationship is obtained, confirming that the shape of the water volume-time curve is of a hyperbolic shape. Thus, the following equation can be written:

$$\frac{t}{V} = a + bt \quad \text{Eq.1}$$

where  $t$  is time,  $V$  is injected water volume,  $a$  and  $b$  are the intercept and the slope of the straight line, respectively (Figure 9).

According to this hyperbolic relationship, the maximum volume of water volume can be calculated by  $1/b$  (Eq.2), equal to 72.46 L. This is to be compared with the total volume of voids including technological void and the soil porosity: 69.1 L.

$$V_{max} = \lim_{t \rightarrow \infty} V(t) = \lim_{t \rightarrow \infty} \left( \frac{1}{a/t + b} \right) = \frac{1}{b} \quad \text{Eq.2}$$

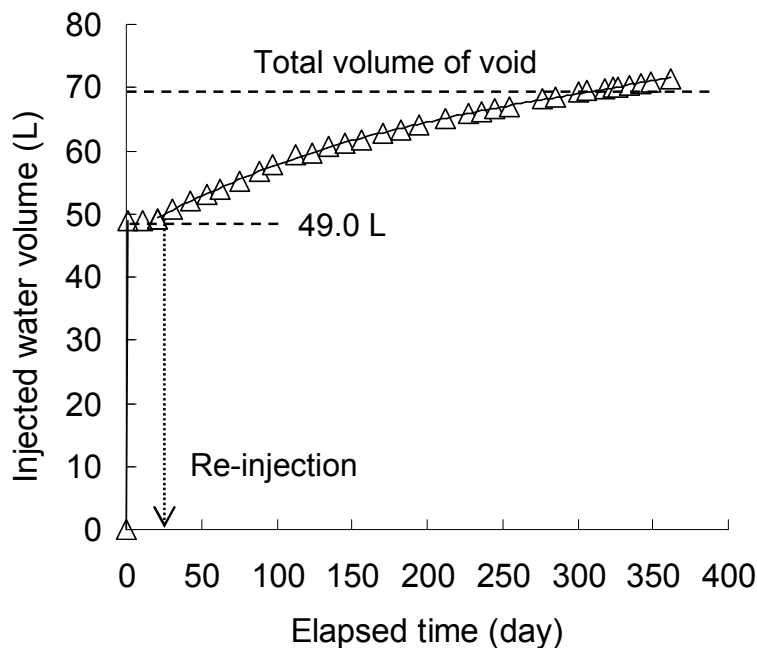


Figure 8. Injected water volume versus time.

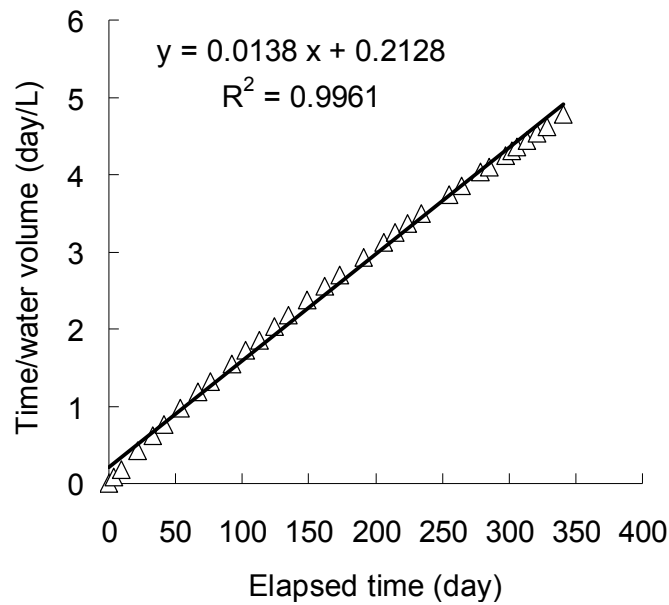


Figure 9. Time/water volume versus elapsed time after water rejection.

During hydration, both the axial and radial swelling pressure were recorded by the total pressure sensors (see Figure 3) and shown in Figure 10. The data by the sensor located at 1.20 m section for the axial swelling pressure measurement were unfortunately not available; only the axial swelling pressure values at 0 m section are presented. This pressure increased at an almost constant rate, and reached 1.63 MPa after 367 days. For the radial swelling pressure, the evolution rates were very different for the three sensors (see Figure 3), and reached 1.78 MPa, 0.56 MPa and 1.05 MPa for sensor L-01, L-02 and L-03, respectively. This indicates the heterogeneous radial swelling under the in situ conditions.

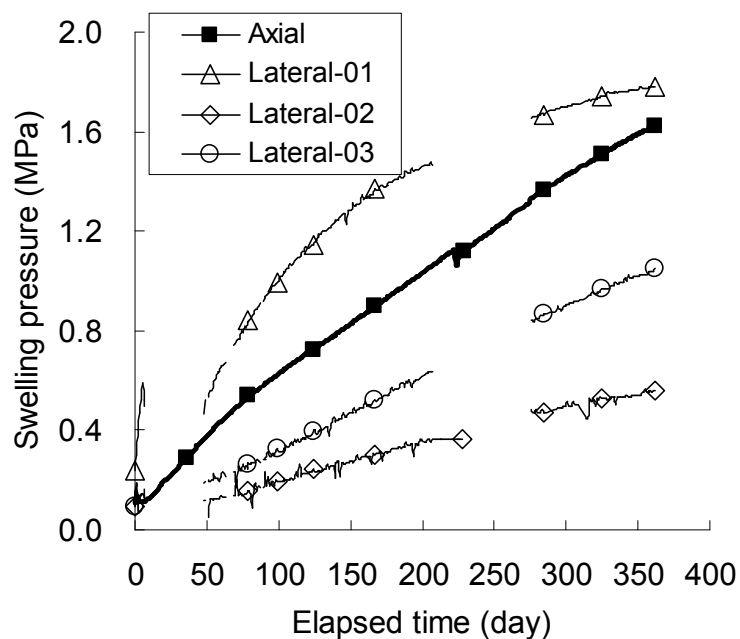


Figure 10. Evolution of swelling pressure.

### 3.2 Small scale test

Figure 11 shows the measured water inflow over time. Once the water supply was connected to the bottom inlet, water volume increased rapidly and reached 49 mL in a few minutes. This value corresponds exactly to the volume of technological void (49 mL). Afterwards, water volume increased gradually to reach a maximum water volume of 70.6 mL. No more water can infiltrate after about 200 days. The total volume of void (including the technological void  $V_{tech}$  and void inside the soil  $V_{v-s}$ ) that could be filled with water was estimated at 69.1 mL. The result shows that a little more water was injected with respect to the estimated one (70.6 mL against 69.1 mL).

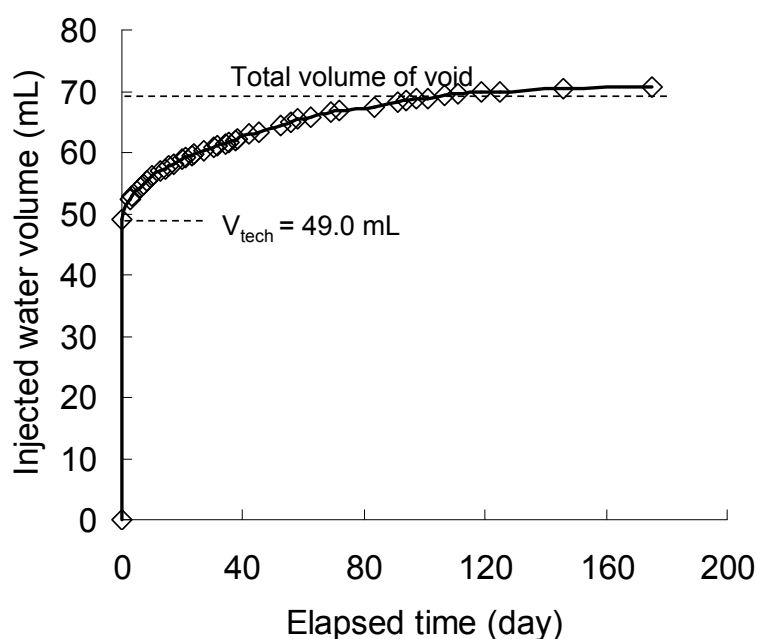


Figure 11. Water volume injected into the specimen

For further analyzing the evolution of water volume, the time/water volume (day/mL) data were plotted versus time in Figure 12. As in the case of in situ test, a straight line was obtained justifying a hyperbolic relationship between the water volume and elapsed time (Eq.1). The reciprocal of the slope of the straight line gives the theoretical maximum volume of water:  $1/b = 71.43$  mL, which is very close to the measured water volume (70.6 mL).

Figure 13 and Figure 14 depict the evolution of swelling pressure in the first stage (i.e. initial saturation phase). Once water was injected into the specimen, the axial swelling pressure increased very quickly (Figure 14). After about 2 days, the swelling pressure reached a first stability stage (1.30 MPa) and it restarted to increase on the 4<sup>th</sup> day. When the swelling pressure reached 1.45 MPa after about 12 days, a significant decrease of swelling pressure occurred towards a minimum value of 0.70 MPa. Afterwards, the swelling pressure increased

again after about 33 days (Figure 13), but at a slower rate. In addition, the evolution curve shows fluctuating pattern. It reached a mean value of 1.80 MPa after 300 days and then fluctuated in the range of 1.75-1.95 MPa.

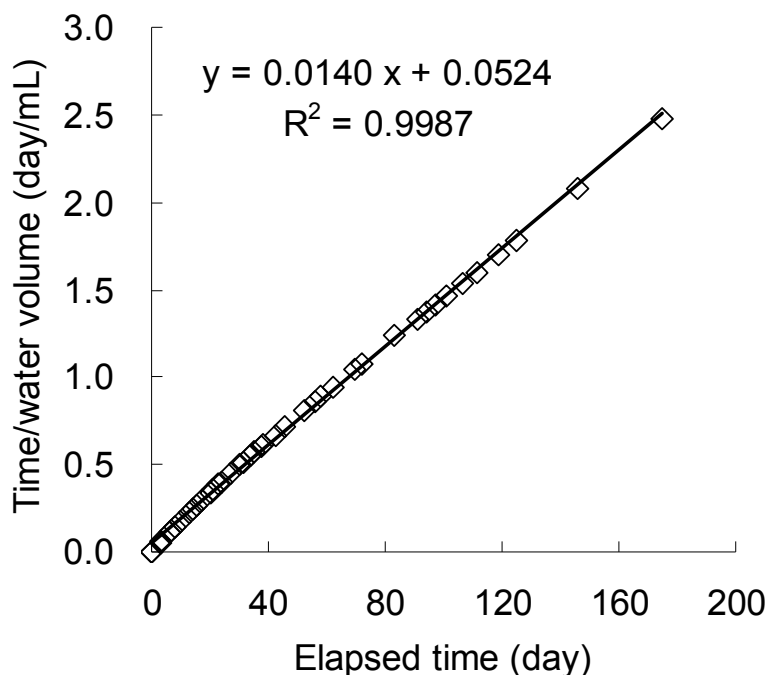


Figure 12. Time/water volume versus elapsed time.

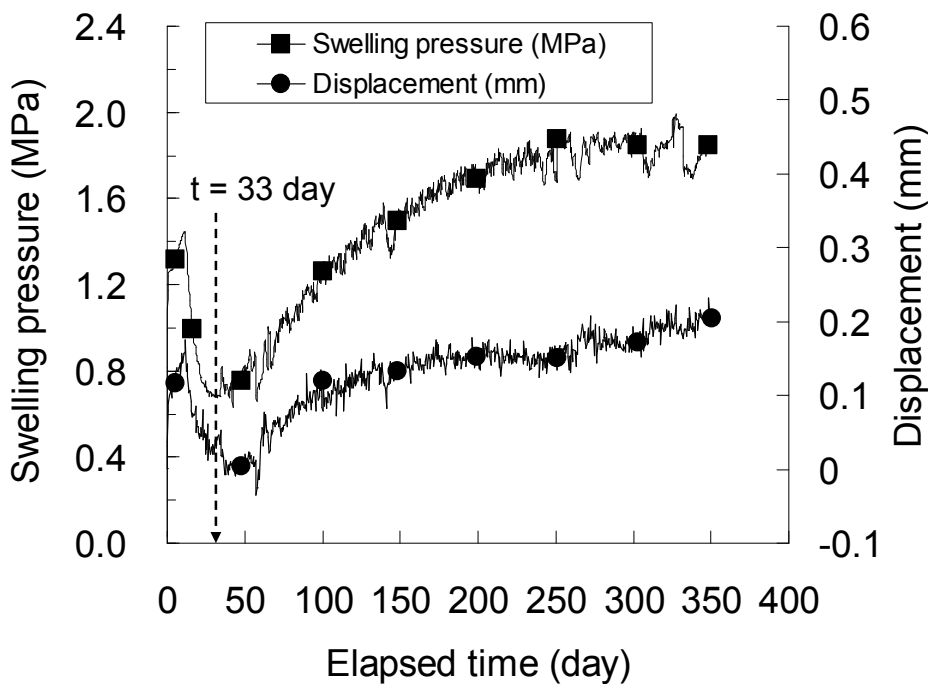


Figure 13. Evolution of axial swelling pressure and displacement in the first stage.

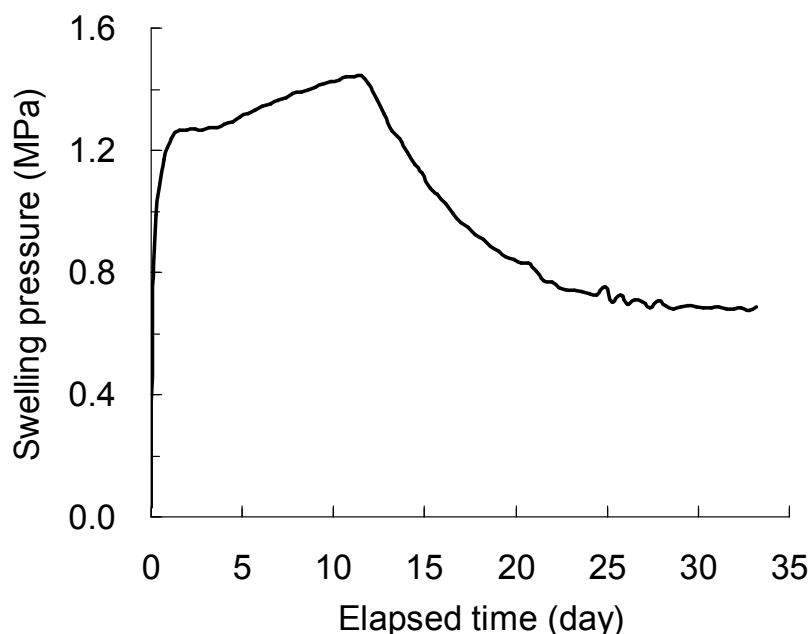
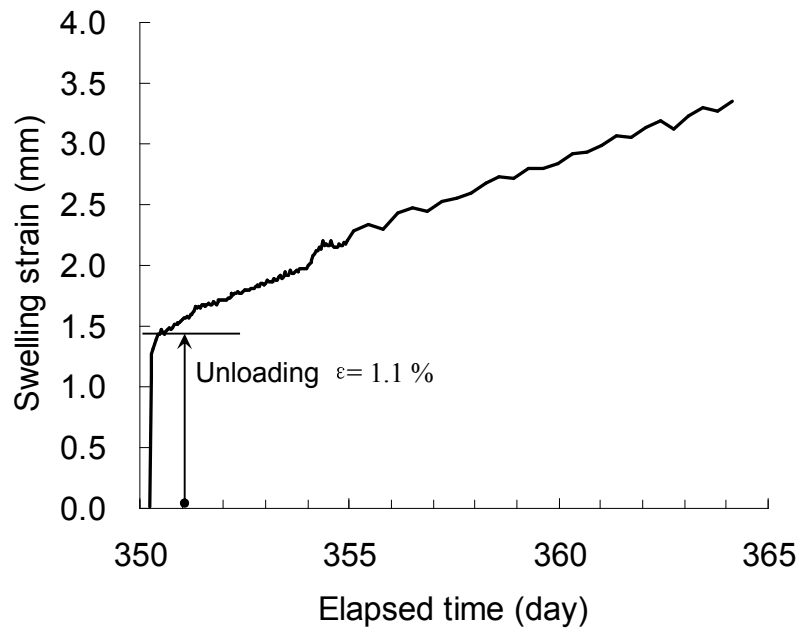


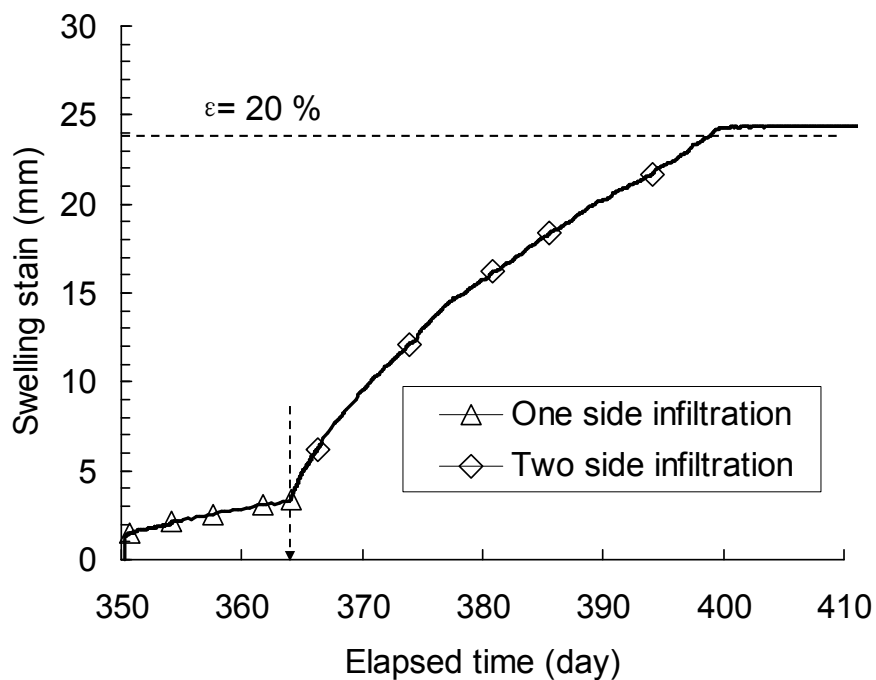
Figure 14. Evolution of swelling pressure during the first 33 days.

The axial deformation during swelling pressure development was also recorded, and shown in Figure 13. It followed the same trend as the swelling pressure kinetics. Note however that the variation of displacement was lower than 0.2 mm. It represents 0.16% of the specimen height (120 mm), indicating a satisfactory control of axial displacement in this stage.

According to the data obtained in the first stage (Figure 13), no obvious swelling pressure increase occurred during a period of 50 days from day 300 to day 350. Thus, it was decided to start the second stage. The confining pressure was then removed on day 350, allowing the free swell. Changes in axial swelling strain were recorded and presented in Figure 15. The uplifting of load cell led to an instantaneous rebound of 1.1% (1.4 mm / 120 mm). Following, the axial swelling strain increased almost linearly at a rate of 0.145 mm/day. Following this rate, 20% of swelling strain was expected to be reached after 157 days. In order to reduce the test duration, two sides infiltration was applied on day 364. This resulted in an increase of the swelling strain rate to 0.588 mm/day, which is four times faster than that with one-side infiltration. The expected value of 20% (24 mm) was reached at day 400. The piston was then re-blocked automatically to start Stage 3. Note that the measured axial swell was 24.4 mm.



(a) Evolution of axial swelling strain during the first 15 days after unloading.



(b) Evolution of axial swelling strain

Figure 15. Evolution of axial swelling strain during Stage 2.

The evolution of swelling pressure was then measured again and the results are presented in Figure 16. Small fluctuation was observed and this fluctuation can be attributed to the daily temperature variations. As expected, the evolution curve follows an asymptotic curve with a decreasing rate over time. It reached stabilization on day 520 with a final swelling pressure of 0.18 MPa.

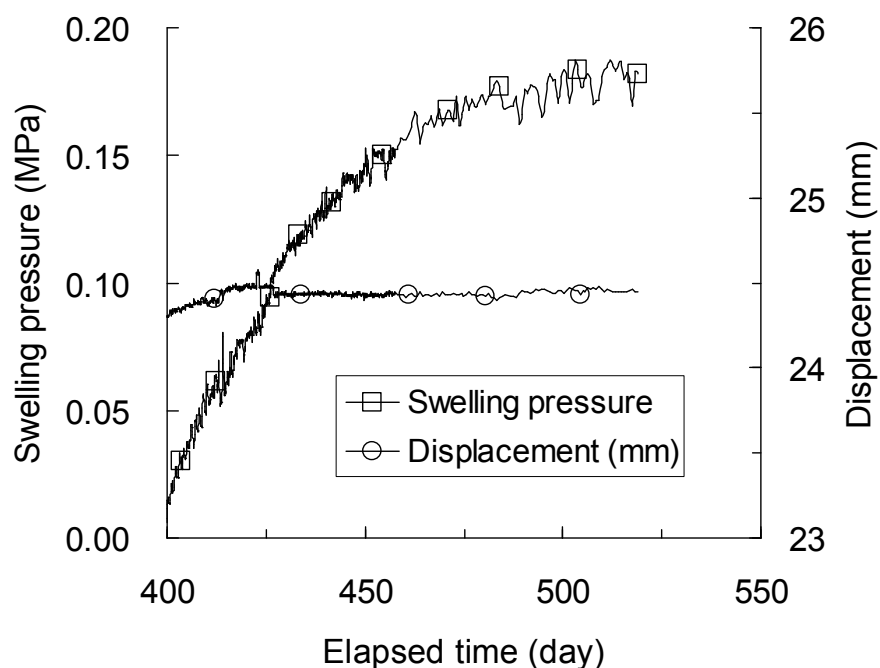


Figure 16. Evolution of axial swelling pressure during Stage 3.

#### 4 Comparison and discussion

It was observed that more water infiltrated into the soil than that calculated by considering the technological void and the soil porosity in both the in situ test (71.39 L) and laboratory small scale test (70.60 mL). Even though the water volume has been not yet reached the stabilization in the in situ condition, the discrepancy was found to be larger than in the small scale test. This can be related to the natural conditions of the in situ test, where some water intake by the host rock does occur. With a well controlled condition in the small scale test, the larger infiltrated water obtained in this study may be related to the low water density ( $1.00 \text{ Mg/m}^3$ ) considered in the determination of soil void ratio. Indeed, for high plasticity materials as the MX80 bentonite, the water density can be much higher than  $1.00 \text{ Mg/m}^3$  (Marcial 2003, Villar and Lloret 2004, Lloret and Villar 2007, Jacinto et al. 2012). This is in agreement with the observation from the KBS-3H mock up test (Börgesson et al. 2005).

Regarding the evolution of water volume, a hyperbolic relationship between the injected water volume and elapsed time was obtained in both tests. Accordingly, the maximum water volume was estimated at 72.46 L and 71.43 mL for the in situ and small scale test, respectively. To compare the evolution curve at different scales, the water volume was normalized by using these two values. The normalized water volume is equal to the ratio of water volume at time  $t$  ( $V_t$ ) to the maximum water volume that can be injected (72.46 L and 71.43 mL for the in situ and small scale test, respectively). In terms of time scale, an

up-scaling ratio of 2.5 (in situ test/small scale test) was found from the normalized water volume shown in Figure 17, where very similar evolution curves (normalized water volume versus normalized time) were obtained for the two tests (i.e. in situ and small scale tests).

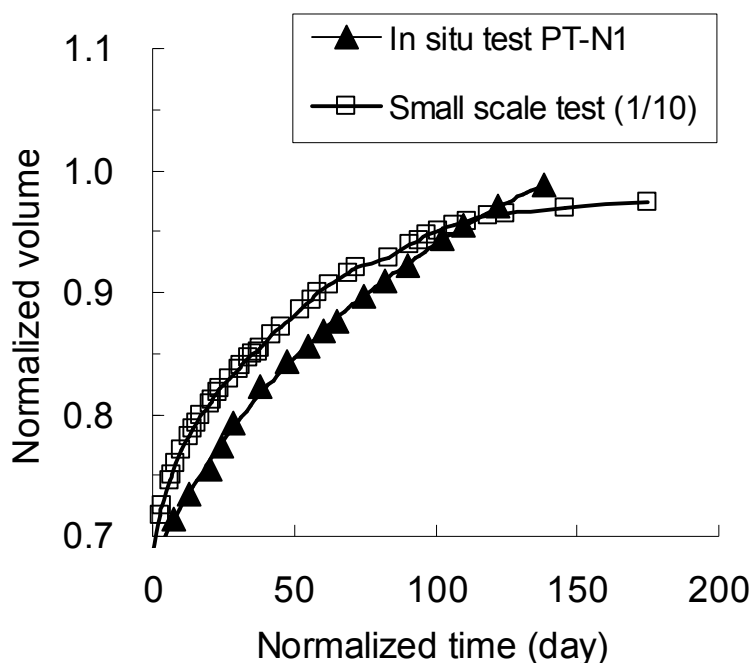


Figure 17. Normalized water volume versus normalized time.

This up-scaling ratio is much smaller than that estimated from the consolidation theory by considering the experiment scale and hydration conditions: according to the infiltration length, the hydration rate of in situ test should be 100 times ( $10^2$ ) lower than in the small scale test (1/10). As the two-side infiltration applied in the in situ test increases the hydration rate by 4 times, the up-scaling ratio should be equal to 25 (in situ test / small scale test), still ten times larger than the rate identified from the measurements. In fact, under the in situ conditions, water may fill some voids between the pre-compacted disks at the first minutes (0.15 m thick, see Figure 2). This infiltration length of 0.15 m can reduce the up-scaling ratio to 0.56. The up-scaling ratio of 2.5 observed is possibly related to the combined effect of these two phenomena.

Using this up-scaling ratio, the axial swelling pressure evolution curve obtained from the in situ test (Figure 10) was normalized and depicted in Figure 18, together with the axial swelling pressure measured in the first stage of the small scale test. Except for the first 33 days (see Figure 13), where significant decrease of swelling pressure occurred in the small scale test, the normalized evolution of swelling pressure for the in situ test join the curve of the small scale test, confirming the up-scaling ratio of 2.5. Based on the results of small scale

test, this ratio allows estimating the time needed to reach the stabilization of swelling pressure in the in situ test. It can be observed in the small scale test that the swelling pressure reached the stability after about 300 days. Thus, 155 days more is needed to reach the maximum swelling pressure in the normalized time scale for the in situ test. Accordingly, it can be estimated that the maximum swelling pressure in the in situ test should be reached after 388 days, corresponding to 754 days from the time of water injection.

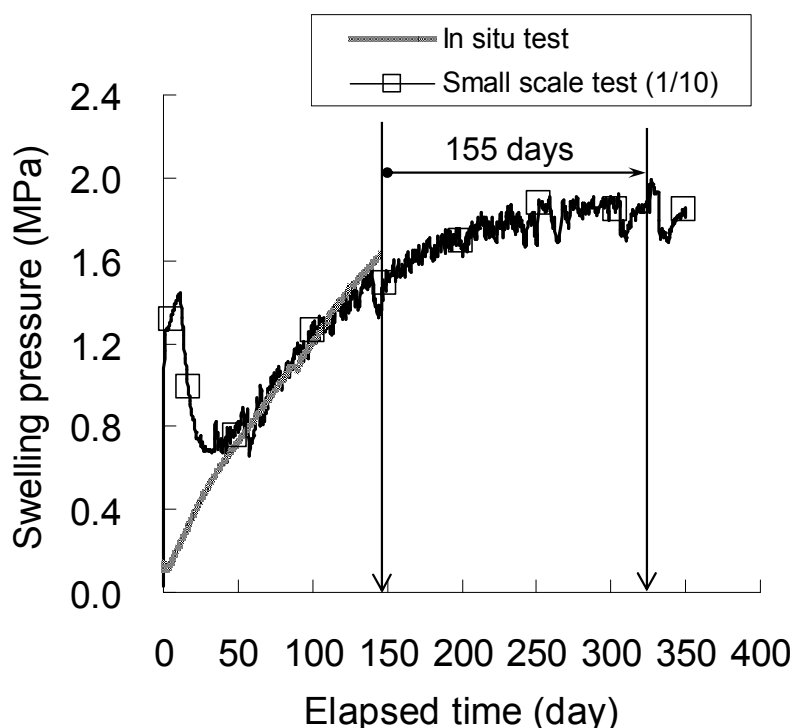


Figure 18. Swelling pressure versus normalized time.

As regards the kinetics of the axial swelling pressure in the first 33 days of small scale test, stabilization was attained after about 2 days (1.30 MPa) and restarted to increase from day 4 (Figure 14). Wang et al. (2012b) observed similar phenomenon in the swelling pressure test on small samples (35 mm in diameter, 10 mm high) with the same percentage of technological void. This is related to the changes in microstructure of the soil. With the progress of hydration, the effect of the microstructure changes is reduced, resulting in the re-increase in swelling pressure (Cho et al., 2000; Baille et al., 2010). When the swelling pressure reached 1.45 MPa around day 12, a significant decrease of swelling pressure occurred, towards a minimum value of 0.70 MPa. This decrease could be attributed to the filling of the technological void. Afterwards, the swelling pressure increased again from day 33. However, the evolution curve showed fluctuation due to the reorganization of the microstructure under the effect of technological void.

On the contrary, the axial swelling pressure measured in the in situ test increased constantly without any fluctuation. This can be related to a coupled effect of large scale and pressure sensor location. In the small scale test, the axial swelling pressure was measured on the whole cross section and any changes in axial pressure could be monitored. However, in the in situ test, the total pressure sensor was installed in the centre of the cross section (Figure 3) and the axial swelling pressure herein corresponded to the local one. Therefore, the axial swelling pressure changes occurred in the technological void zone could not be detected by this sensor.

After the axial swelling pressure of small scale test reached stabilization, removing the confining pressure led to a very small rebound of 1.1% (1.4 mm/ 120 mm). This observation provides valuable information for the confinement removal phase of the in situ test. During the free swelling process (Stage 2), a swelling strain evolution rate (swelling strain/time) of 0.588 mm/day was observed under two-side infiltration condition. Combined with the up-scaling ratio, this result (0.588 mm/day) allows the prediction of swelling strain evolution in the in situ test when simulating an incidental decrease of the swelling pressure caused by a failure of the concrete confining structure.

As the piston was re-blocked automatically in the small scale test (Stage 3), swelling pressure developed again. It indicates the favorable sealing capacity after filling of the technological void. If a saturation defect or a confining structure failure occurred in the field, a 20% additional void could be sealed. A final swelling pressure of 0.18 MPa was attained, which is in accordance with the swelling pressures measured in laboratory on small samples (Wang et al., 2012b): after 20% of free swell (24.5 mm), the dry density decreased to a final value of 1.39 Mg/m<sup>3</sup>; this corresponds to a swelling pressure of 0.23 MPa.

## 5 Conclusion

In the framework of the SEALEX project, a laboratory small scale test (1/10) was performed to investigate the recovery capacity of bentonite-based plug with technological void. By comparison with the first results from the in situ test PT-N1, the phenomena identified in the laboratory were used for interpreting and estimating the performance of the bentonite-based plug in the in situ experiment.

During the saturation process, a hyperbolic relationship between the injected water volume and elapsed time was obtained in both tests. However, a little more water was injected compared to the value estimated from the consideration of total porosity. Larger discrepancy was found for the in situ test due to the effect of natural conditions.

Decrease of axial swelling pressure was observed in the small scale test due to the filling of technological void. In contrast, the axial swelling pressure measured increased continually in the in situ test. This can be attributed to the effect of both the scale and pressure sensors locations.

Comparison of the injected water volume and axial swelling pressure obtained from different scales gave the same up-scaling ratio of 2.5 (in situ experiment / small scale test). Using this up-scaling ratio, the time needed to reach the swelling pressure stabilization in the in situ experiment was estimated to 754 days.

After removal of the confining pressure, a swelling strain evolution rate (swelling strain/time) of 0.588 mm/day was observed in the case of two-side infiltration. Combined with the up-scaling ratio, this rate allows the prediction of swelling strain evolution in the case of a confining structure failure. A swelling pressure of 0.18 MPa was obtained after filling an additional 20% void, indicating the favorable sealing capacity after filling the technological void.

## Acknowledgements

The work was conducted in the framework of the SEALEX project carried out by IRSN, with collaboration of the Canadian Nuclear Safety Commission. The supports of the China Scholarship Council (CSC) and from the PHC Cai Yuanpei project (24077QE) are also greatly acknowledged.

## References

- Baille, W., Tripathy, S. & Schanz, T. 2010. Swelling pressures and one-dimensional compressibility behaviour of bentonite at large pressures. *Applied Clay Science*, Vol 48, 324-333
- Barnichon, J.D. & Deleruyelle, F. 2009. Sealing Experiments at the Tournemire URL. EUROSAFE.
- Barnichon, J.D., Dick, P. & Bauer, C. 2012. The SEALEX in situ experiments: performance test of repository seals. *Harmonising Rock Engineering and the Environment – Qian & Zhou (eds) Taylor & Francis Group, London*. ISBN 978-0-415-80444-8, pages 1391-1394.
- Börgesson, L., Sandén, T., Fälth, B., Åkesson, M. & Lindgren, E. 2005. Studies of Buffers Behaviour in KBS-3H Concept: Work During 2002-2004, SKB, R-05-50.
- Cho, W.J., Lee, J.O., & Kang, C.H. 2000. Influence of temperature elevation on the sealing performance of a potential buffer material for a high-level radioactive waste repository. *Annals of Nuclear Energy*, Vol 27, 1271-1284
- Delage, P., Howat, M.D. & Cui., Y.J. 1998. The relationship between suction and swelling properties in a heavily compacted unsaturated clay. *Engineering Geology*, 50(1-2), 31-48.
- Jacinto, A.C., Villar, M.V. & Ledesma, A. 2012. Influence of water density on the water-retention curve of expansive clays, *Geotechnique* 62, No. 8, 657–667

- Lloret, A., Villar, M.V., Sánchez, M., Gens, A., Pintado, X. & Alonso, E.E. 2003. Mechanical behaviour of heavily compacted bentonite under high suction changes. *Geotechnique* 53, No. 1, 27–40
- Lloret, A. & Villar, M. 2007. Advances on the knowledge of the thermo-hydro-mechanical behaviour of heavily compacted FEBEX bentonite. *Physics and Chemistry of the Earth*, 32, 701-715
- Marcial, D. 2003. Comportement hydromécanique et microstructural des matériaux de barrière ouvragée, PHD thesis, École Nationale des Ponts et Chaussées, Paris, France.
- Romero, E., Villar, M. V. & Lloret, A. 2005. Thermo-hydro-mechanical behaviour of heavily overconsolidated clays. *Engng Geol.* 81(3): 255 – 268.
- Villar, M.V. & Lloret, A. 2004. Influence of temperature on the hydro-mechanical behaviour of a compacted bentonite. *Applied Clay Science*, 26(1-4), 337-350.
- Wang, Q., Tang, A. M., Cui, Y.J., Delage, P. & Gatmiri, B. 2012a. Experimental study on the swelling behaviour of bentonite/claystone mixture, *Engineering Geology*, Vol. 124, 59–66.
- Wang, Q., Tang, A. M., Cui, Y.J., Delage, P., Barnichon, J.D. & Ye, W.M. 2012b. The effects of technological voids on the hydro-mechanical behaviour of compacted bentonite-sand mixture. *Soils and Foundations*, accepted for publication.



## **Chapter 6. Investigation of the HM behaviour of compacted bentonite/sand mixture based on the BExM model**

### **INTRODUCTION**

To describe the behaviour of compacted bentonite-based materials under complex hydromechanical loadings, a relevant constitutive model is required. For this reason, a number of constitutive models have been developed such as the model of Gens and Alonso (1992), the model of Alonso et al. (1999) and the model of Cui et al. (2002), etc. Among them, the elasto-plastic model developed by Alonso et al. (1999), namely Barcelona Expansive Model (BExM), is the most widely used to describe the mechanical behaviour of unsaturated expansive soils.

Based on the BExM model, the hydro-mechanical behaviour of compacted MX80 bentonite/sand mixture is investigated in this study. The determination of the model parameters are first determined by matching the model equations with the laboratory experimental results. These parameters are then used to simulate the hydromechanical behaviour of material during swelling pressure test and water retention test. The performance and limitation of the model are further analysed by comparing the model and experimental results, and by considering the microstructure changes upon wetting or suction decrease.

The results are presented in a paper submitted to «Computers and Geotechnics», this chapter corresponds to the manuscript.

Wang, Q., Tang, A. M., Cui, Y.J., Barnichon, J.D., Ye, W.M., 2012

## **Investigation of the HM behaviour of compacted bentonite/sand mixture based on the BExM model**

Qiong Wang<sup>1</sup>, Anh Minh Tang<sup>1</sup>, Yu-Jun Cui<sup>1,3</sup>,  
Jean-Dominique Barnichon<sup>2</sup>, Wei-Min Ye<sup>3</sup>

**Abstract:** This study focuses on the hydro-mechanical behaviour of a MX80 bentonite/sand mixture. Barcelona Expansive Model (BExM) was used to describe this behaviour. For this purpose, experimental data obtained in the laboratory were analysed, allowing determination of the parameters used in the model. These parameters were then used to simulate the hydro-mechanical (H-M) responses of the material from other tests with different stress paths. It was observed that the model reproduced well the main feature of swelling pressure development, micro-structural volume change during suction decrease as well as the water retention property. On the other hand, the simulations also showed some limitations of the model which is based on the consideration of two levels of soil structure or double structure: the pore size distribution curve determined by the technique of mercury intrusion porosimetry (MIP) in the range of low suctions (4.2 and 1 MPa) being revealed to be tri-modal, the BExM model cannot capture this aspect to correctly describe the macro-structural and micro-structural void ratio changes. Moreover, because the BExM model lumps clay intra-particle spaces and inter-particles voids together as micro-pores, it leads to overestimation of the micro-structural water content compared to the experimental value.

**Keywords:** bentonite-sand mixture; hydro-mechanical behaviour; constitutive modeling; volume change; microstructure

---

### **1 Introduction**

Compacted bentonite-based materials have been proposed as engineering barriers in the deep geological repository for high-level radioactive wastes (HLW) in several countries. Thanks to their low permeability, high swelling and high radionuclide retardation capacities (Pusch, 1979; Yong et al., 1986; Villar et al., 2008), they are expected to limit the release of radionuclide to the surrounding host rock (Cho et al., 2010). After the installation in the repository, the engineering barriers will simultaneously undergo the intrusion of groundwater from the host rocks or geological barriers, and the stress changes due to mainly the bentonite swelling. Therefore, the hydro-mechanical performance of engineering barriers is a key issue in assessment of the overall repository safety.

Various laboratory studies (e.g. Delage et al., 1998; Lloret et al., 2003; Romero et al., 2005;

---

1 Ecole des Ponts ParisTech, Navier/CERMES, France

2 Institut de Radioprotection et de Sûreté Nucléaire (IRSN), France

3 Tongji University, China

Lloret & Villar, 2007) have been conducted on the H-M behaviour of bentonite-based materials. Based on the experimental results, a number of constitutive models have been developed such as the model of Gens and Alonso (1992), the model of Alonso et al. (1999) and the model of Cui et al. 2002, etc. To the authors' knowledge, the elasto-plastic model developed by Alonso et al. (1999), namely Barcelona Expansive Model (BExM), is the most widely used one in describing the mechanical behaviour of unsaturated expansive soils.

In the BExM model, the authors incorporate the microstructure effects by introducing two levels of soil structure: a microstructure level that corresponds to the active clay minerals with prevailing physico-chemical effects, and a macrostructure level that accounts for the larger scale structure of the soil. The coupling between the two levels is described by means of the interaction functions, capable of describing, in a phenomenological fashion, the occurrence of macro-structural elasto-plastic strains as a consequence of micro-structural strains.

Because of the complexity of the model, there have been few experimental works that allow the determination of the full set of its parameters, especially for the bentonite-based materials. In this study, the hydro-mechanical behaviour of compacted MX80 bentonite/sand mixture was investigated based on the BExM model. The determination of the model parameters was first conducted by matching the model equations with the laboratory experimental results. The parameters thus determined were then used to simulate the H-M behaviour of the material in the swelling pressure and water retention tests. The performance and limitation of the model were further analysed by comparing the model and experimental results and by considering the microstructure changes upon wetting or suction decrease.

## 2 Barcelona Expansive Model

As mentioned previously, Barcelona Expansive Model (BExM) proposed by Alonso et al. (1999) accounts for two levels of soil structure (Gens & Alonso, 1992): micro- and macro-structural levels. The micro-structural level corresponds to the aggregates of active clay particles with intra-aggregate pores, whereas the macro-structural level corresponds to the larger-scale soil structure (Kröhn, 2003; Alonso et al., 2005). Following this concept, the void ratio ( $e$ ) can be divided to two parts:

$$e = e_m + e_M \quad \text{Eq.1}$$

where  $e_m$  and  $e_M$  are micro- and macro-structural void ratios, respectively.

The micro-structural pores are assumed to be always saturated, thus the effective stress

concept holds: any changes in suction ( $s$ ) induce the same volume change as that induced by a change in mean net stress ( $p$ ). The volume change in this level is reversible and independent of macro-structural effects (Gens & Alonso, 1992). Thereby, the micro-structural elastic volumetric strain is calculated as follows:

$$d\mathcal{E}_{vm}^e = \frac{de_m}{1 + e_m} = \frac{d(p + s)}{K_m} \quad \text{Eq.2}$$

$$\text{with } K_m = \frac{\exp[\alpha_m(p + s)]}{\beta_m} \quad \text{Eq.3}$$

where  $K_m$  is the micro-structural modulus; it increases with increase in  $p$  or  $s$ .

In the macro-structural level, both elastic and plastic strains can develop as a result of stress/suction changes. The macro-structural elastic volumetric strain is expressed as a function of mean net stress and suction:

$$d\mathcal{E}_{vM}^e = \frac{de_M}{1 + e_M} = \left( \frac{\kappa}{1 + e_M} \right) \frac{dp}{p} + \left( \frac{\kappa_s}{1 + e_M} \right) \frac{ds}{s + p_{atm}} \quad \text{Eq.4}$$

where  $\kappa$  and  $\kappa_s$  are the macro-structural elastic compressibility parameters for changes in net mean stress and in suction, respectively,  $p_{atm}$  is the atmospheric pressure.

The variation of pre-consolidation mean net stress ( $p_0$ ) with suction is given by an LC (Loading Collapse) yield curve function in the ( $p, s$ ) plane (Figure 1):

$$\frac{p_0}{p_c} = \left( \frac{p_0^*}{p_c} \right)^{\frac{\lambda(0) - \kappa}{\lambda(s) - \kappa}} \quad \text{Eq.5}$$

$$\text{with } \lambda(s) = \lambda(0)[r + (1 - r)\exp(-\beta s)] \quad \text{Eq.6}$$

where  $p_c$  is a reference stress,  $p_0^*$  is the net mean yield stress at zero suction,  $\lambda(0)$  is the macro-structural compressibility parameter for changes in  $p$  at zero suction (saturated state),  $\lambda(s)$  is the macro-structural compressibility parameter for changes in  $p$  at suction  $s$ ,  $r$  is a parameter that defines the minimum compressibility of soil and  $\beta$  is a parameter that controls the rate of compressibility decrease with increasing suction.

The micro-structural deformations induced - plastic strains are described by two additional yield curves SI (suction increase) and SD (suction decrease) in Figure 1. The SI yield curve is defined by the expression  $p + s_I = 0$  and the SD yield curve is defined by the expression  $p + s_D = 0$  where  $s_I, s_D$  are hardening parameters. For a reason of simplification, it was assumed in this study that the SI and SD yield curves are always activated thereby inducing irreversible macro-structural deformations. Under this assumption the SI and SD curves are masked by

the NL (Neutral Line). Note that Alonso et al. (2005), Sanchez et al. (2007), Tang and Cui (2009) also considered the NL solely to separate micro-structural swelling from micro-structural compression. Upon hydro-mechanical loadings, the NL moves following the current net mean stress ( $p$ ) and current suction ( $s$ ). Therefore, the following two parts of irreversible volumetric strains are taken into account:

1) When the yield curve LC is reached by a mechanical loading:

$$d\epsilon_{vML}^p = \frac{\lambda(s) - \kappa}{1 + e_M} \frac{dp_0}{p_0} \quad \text{Eq.7}$$

2) When SI or SD surfaces are activated, the macro-structural plastic strain induced by micro-structural strain is:

$$d\epsilon_{vMSI}^p = f_I d\epsilon_{vm}^e \quad \text{Eq.8}$$

$$d\epsilon_{vMSD}^p = f_D d\epsilon_{vm}^e \quad \text{Eq.9}$$

where  $f_I$  and  $f_D$  are the interaction functions between micro- and macro-structural levels in case of suction increase and suction decrease, respectively.

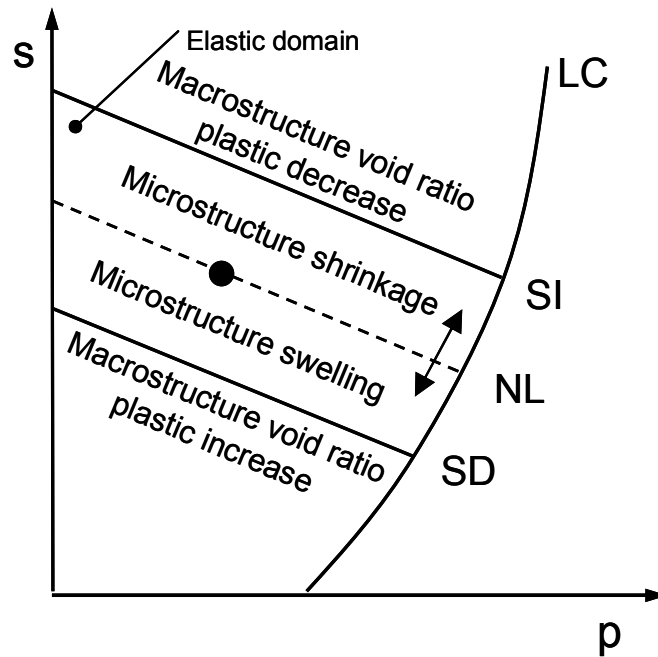


Figure 1. BExM yield loci in the  $p$ - $s$  plane (after Alonso et al. 2005)

Regarding the hardening law for the mechanical yield curve (LC), the net mean yield stress at zero suction ( $p_0^*$ ) is expressed as a function of the total macro-structural strain ( $\epsilon_{vM}^p$ ). Note that the increment of the total macro-structural plastic strain ( $d\epsilon_{vM}^p$ ) is the sum of the increment of the macro-structural plastic strain resulted by hydraulic and mechanic loading

( $d\epsilon_{vML}^p$ ) and that resulted by the micro-structural interactions ( $d\epsilon_{vMSI}^p$  or  $d\epsilon_{vMSD}^p$ ), as follows:

$$d\epsilon_{vM}^p = d\epsilon_{vML}^p + d\epsilon_{vMSI}^p + d\epsilon_{vMSD}^p \quad \text{Eq.10}$$

### 3 Parameters determination

The model parameters were determined on the basis of the experimental results obtained on the MX80 bentonite/sand mixture. The soil microstructure was investigated using mercury intrusion porosimetry (MIP) by Wang et al. (2012b), and the results allow determining the initial micro- and macro-structural void ratios ( $e_m$  and  $e_M$ ). Montes-H et al. (2003) investigated the swelling of a single clay aggregate under relative humidity changes using the technique of environmental scanning electron microscopy (ESEM) in conjunction with a digital image analysis. The observed volume changes were used to calibrate the variation of  $e_m$  with suction changes. The volume changes upon wetting and loading were studied by carrying out suction controlled oedometer tests (Wang et al., 2012b). The results obtained were used for the determination of the model parameters related to the hydro-mechanical behaviour.

Figure 2 depicts the pore size distribution (PSD) curve of the compacted MX80 bentonite/sand mixture having an initial suction of 65 MPa and a void ratio of 0.635. The incremental pore volume was represented by the change of void ratio  $e$  divided by the change of the logarithm of pore diameter  $d$ :  $de/d\log d$ , corresponding to the total volume of the pores having similar entrance pore diameter  $d$ . A clear double structure can be observed, defining a population of intra-aggregate pores (micro-pores) with a mean size of 0.02  $\mu\text{m}$  and a population of inter-aggregate pores (macro-pores) with a mean size of 50  $\mu\text{m}$ . The inter-aggregate pores were found to be dependent on dry density, while the intra-aggregate pores remain unaffected by the compaction [8]. Based on this evidence, a delimiting value of 2  $\mu\text{m}$  between macro-pores and micro-pores for the MX80 bentonite/sand mixture was defined by Wang et al. (2012b) from the PSD curves of different dry densities. Thus, the micro-structural and macro-structural void ratios can be determined using the limit pore diameter of 2  $\mu\text{m}$ :  $e_m = 0.391$  and  $e_M = 0.244$ , as noted in Figure 2.

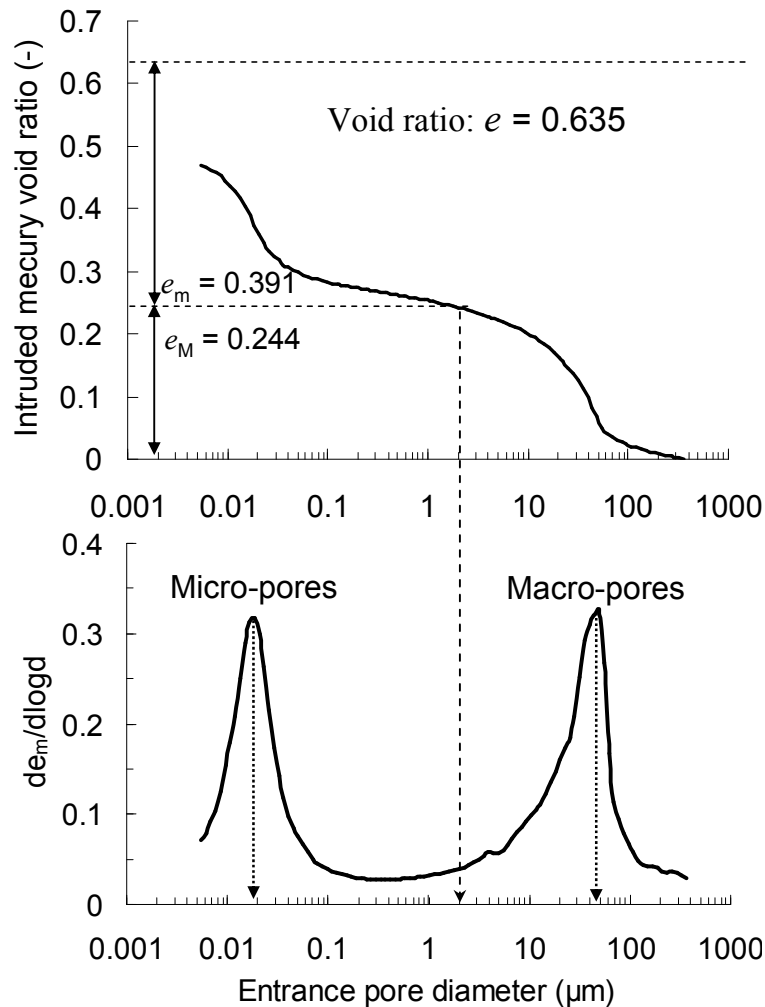


Figure 2. Pore size distribution of the compacted MX80/sand mixture

Regarding the micro-structural volume change, Montes-H et al. (2003) examined the swelling/shrinkage potential of a single MX80 aggregate at different relative humidity states using environmental scanning electron microscopy (ESEM) and the technique of digital image analysis. The deformations are shown in Figure 3 versus suction (deduced from the corresponding relative humidity and temperature applied). Note that the result at the relative humidity of 95% was not taken into account due to the “water over-saturation of aggregate” appeared in the experiment (Montes-H et al. 2003). The data show that wetting from the initial suction of 537 MPa to a suction of 13.5 MPa (90% relative humidity) induced a micro-structural volumetric swelling of 21%.

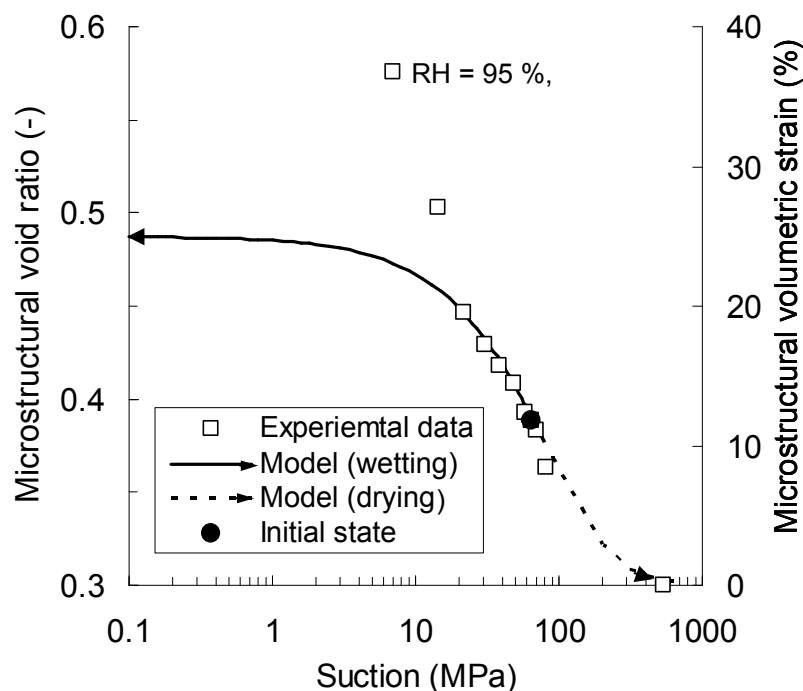


Figure 3. Micro-structural volumetric strain of MX80 bentonite and micro-structural void ratio of mixture versus suction

Based on the evidence that the swelling of mixture is totally controlled by bentonite and sand being inert (Karlund et al. 2008, Wang et al. 2012a, 2012b), the experimental data obtained from MX80 bentonite (Montes-H et al. 2003) were used to calibrate parameters  $\alpha_m$  and  $\beta_m$  which define the micro-structural bulk modulus  $K_m$  (Eq. 2 and Eq. 3). The changes of mixture void ratio were determined from the corresponding void ratio of pure bentonite based on the expressions shown in Wang et al. 2012b, (Eq.5 and Eq.6). The following parameters were used to fit the micro-structural volumetric strain to the experimental data:  $\alpha_m = 0.083 \text{ MPa}^{-1}$  and  $\beta_m = 0.011 \text{ MPa}^{-1}$ . Starting from the initial suction of  $s_0 = 65 \text{ MPa}$  with the initial micro-structural void ratio of  $e_m = 0.391$ , both the wetting and drying paths were considered:  $e_m$  reduced to 0.301 at suction = 537 MPa and increased to 0.474 at suction = 0.1 MPa. With the parameters thus determined, the model can satisfactorily fit the experimental results (Figure 3).

The volume changes of compacted MX80 bentonite/sand mixture upon wetting and loading were investigated by carrying out suction controlled oedometer tests (Wang et al. 2012b). The stress paths followed are presented in Figure 4. Three tests were conducted on samples with an initial dry density of  $1.67 \text{ Mg/m}^3$  ( $e = 0.635$ ) under controlled suctions. From the initial state ( $p_{ini} = 0.1 \text{ MPa}$ ,  $s = 65 \text{ MPa}$ ), suctions of 38 MPa, 12.6 MPa, 4.2 MPa were first applied by the vapour equilibrium technique under a low vertical stress of 0.1 MPa, allowing the development of vertical swelling strain. After completion of the swelling strain at each suction,

loading (up to 30 MPa) was applied under constant suction condition. An additional test at zero suction was conducted by considering an annular void between sample and ring (see Wang et al. 2012b for more details).

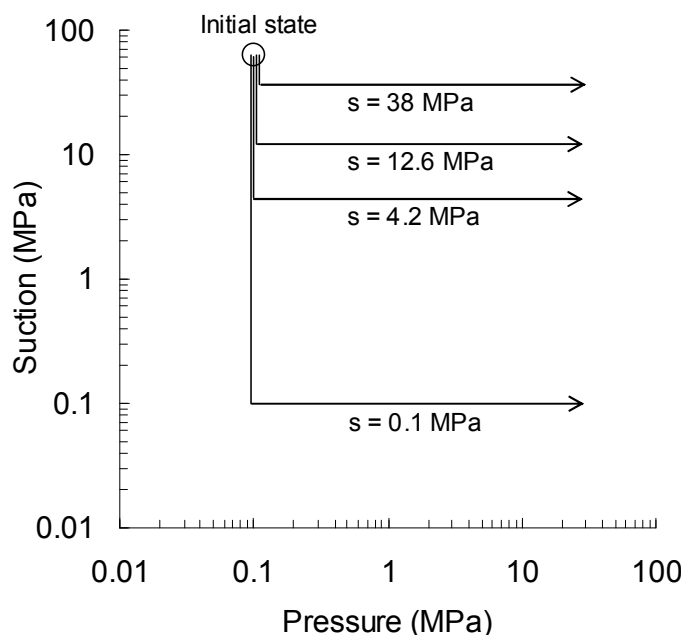


Figure 4. Stress paths followed in the suction controlled oedometer tests

The final void ratio values after suction equilibrium following wetting path are presented in Figure 5. Due to the annular void that allowed water circulation around the sample at zero suction, gel was formed in this zone and the water quantity absorbed was larger than that of the sample without void. Therefore, these results for 38 MPa, 12.6 MPa, 4.2 MPa suction were used to calibrate the parameters related to the macro-structure changes due to suction decrease. Upon wetting, the macro-structural behaviour involves two mechanisms: (i) elastic volumetric strain (Eq. (4)) which depends on parameter  $\kappa_s$ ; (ii) plastic volumetric strain induced by the micro- and macro-structural interaction (Eq. 9) which depends on  $f_D$ . The micro-structural void ratio was calculated using the parameters determined above ( $\alpha_m$  and  $\beta_m$ ). The  $\kappa_s$  and  $f_D$  were then determined by matching the void ratio values in Figure 5 with Eq. 4 and Eq.9:  $\kappa_s = 0.001$  and  $f_D = 0.8 - 1.1 \tanh [20 \times (p/p_0 - 0.25)]$ .

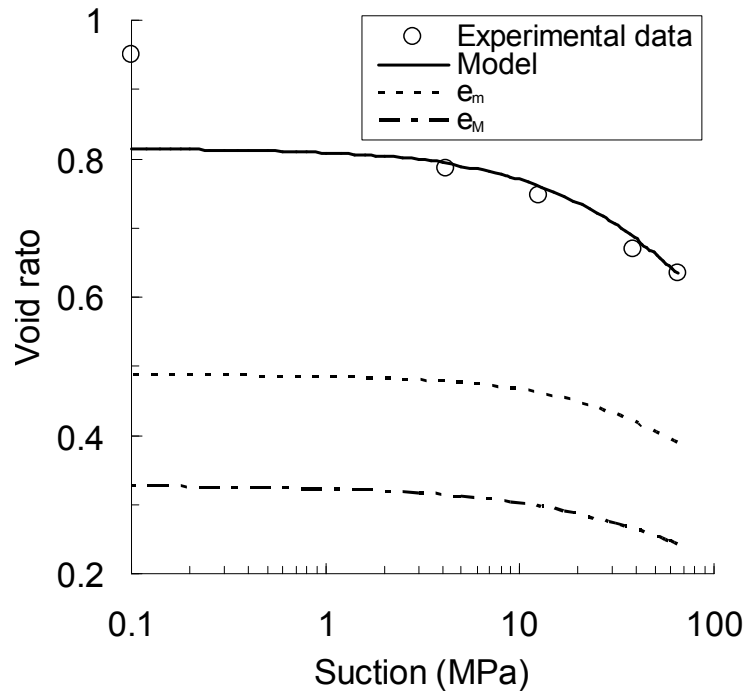
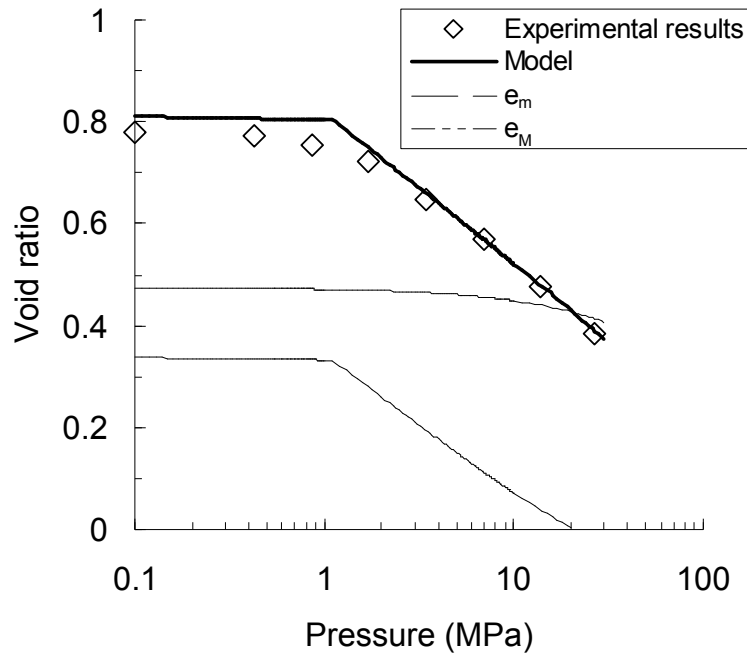
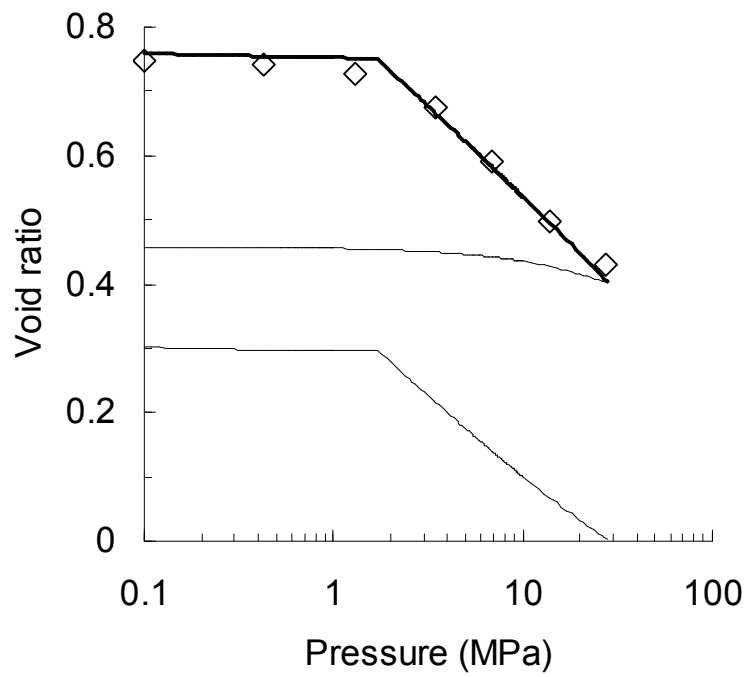


Figure 5. Void ratio changes upon wetting under a vertical stress of 0.1 MPa

The parameters that control the hydro-mechanical behaviour can be obtained based on the compression curves at different constant suctions. The compression curves at 4.2 MPa, 12.6 MPa and 38 MPa suction are depicted in Figure 6. From these curves the values of  $\lambda(4.2)$ ,  $\lambda(12.6)$ ,  $\lambda(38)$ ,  $p_0(4.2)$ ,  $p_0(12.6)$ ,  $p_0(38)$  and  $\kappa$  can be determined. After substitution of these values in Eq. (5) and (6), parameters  $\lambda(0)$ ,  $\gamma$ ,  $\beta$ ,  $p_0^*$ ,  $p_c$  were determined. Afterwards, the  $f_I$  (in Eq.8) was obtained by fitting the experimental compression curves. The following values were found from this operation:  $\lambda(0) = 0.14$ ,  $\gamma = 0.82$ ,  $\beta = 0.07$ ,  $p_0^* = 0.92$ ,  $p_c = 0.005$ ,  $f_I = 0.05 - 1.1 \tanh [20 \times (p/p_0 - 0.25)]$ . Note that during the mechanical loading, the following volumetric strains were taken into account:  $\varepsilon_{vm}^e$  (Eq. 2),  $\varepsilon_{vM}^e$  (Eq. 4),  $\varepsilon_{vML}^p$  (Eq. 7) and  $\varepsilon_{vMSI}^p$  (Eq.8).



(a)  $s = 4.2$  MPa



(b)  $s = 12.6$  MPa

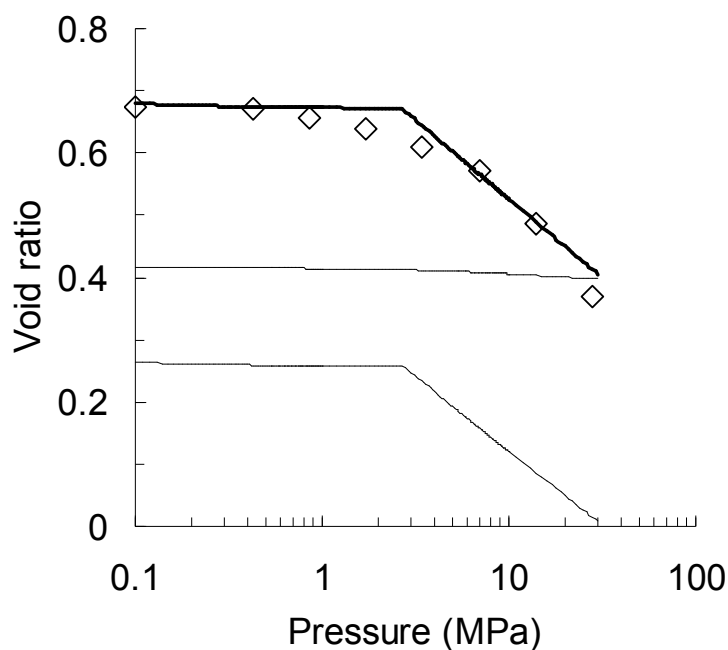
(c)  $s = 38$  MPa

Figure 6. Void ratio changes upon mechanical loading at constant suction

A summary of the model parameters thus determined and the initial conditions is given in Table 1.

Table 1. Parameters used in the simulation

Initial state		Hydro-mechanical behaviour	
$e$	0.635	$\kappa$	0.006
$e_m$	0.391	$\kappa_s$	0.001
$e_M$	0.244	$\lambda(0)$	0.14
$s_0$	65 MPa	$p_c$	0.005
$p_{ini}$	0.1 MPa	$r$	0.82
$p_0^*$	0.92 MPa	$\beta$	0.07
		$\alpha_m$	0.083 MPa <sup>-1</sup>
		$\beta_m$	0.011 MPa <sup>-1</sup>
		$f_D = 0.8 - 1.1 \tanh [20 \times (p/p_0 - 0.25)]$ .	
		$f_I = 0.05 - 0.8 \tanh [20 \times (p/p_0 - 0.25)]$	

## 4 Simulation and interpretation

### Swelling pressure development during suction decrease

The evolution of swelling pressure during suction decrease was simulated by applying the back compaction method (Xie et al. 2007). Following this method, the computation of swelling induced stress can be performed in two stages at a certain suction and stress state (Figure 7): 1) to calculate the micro-porosity change and the macro-volume change potential by allowing swell in the first stage; 2) to press the swelling strain back and calculate the resulting stress after the compression process. From the initial state ( $p_{ini} = 0.1$  MPa,  $e = 0.635$ ,  $s = 65$  MPa), the simulation decreased the suction of the sample to 0.1 MPa in a series of steps at constant volume conditions. In each step, the back compaction process was considered as an inverse process of swelling. Thus, the predicted increase in swelling pressure can be obtained. The deformation under both swelling process and compression process was assumed to be elasto-plastic. The SI and SD yield curves were always activated; the plastic deformation of macro-pores occurred when the yield curve LC was reached.

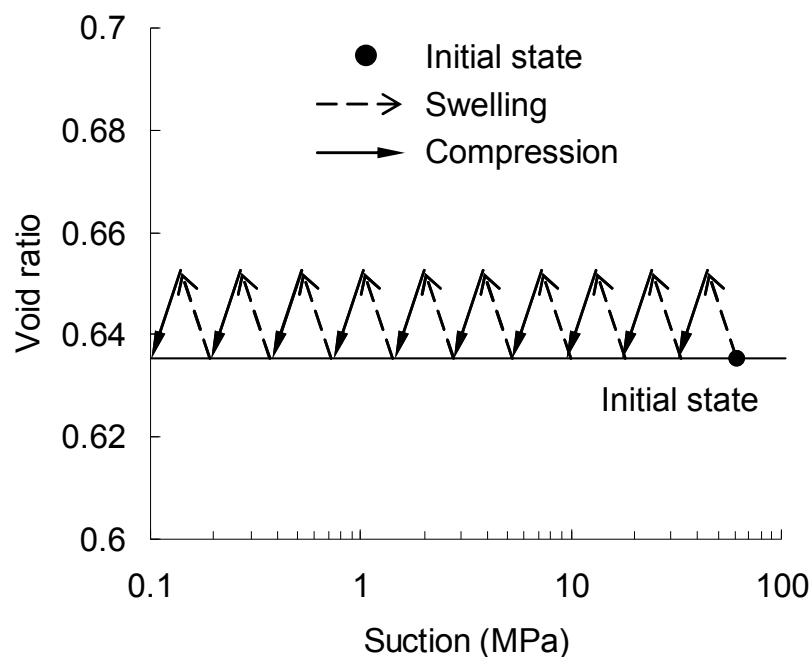


Figure 7. Stress path followed during the swelling pressure simulation

The predicted swelling pressure induced by suction decrease within the soil sample is presented in Figure 8, along with the swelling pressure measured at different suctions (Figure 8). The swelling pressure evolution observed in the laboratory can be well reproduced by considering the occurrence of two concurrent phenomena: initially, when suction is reduced the bentonite aggregates swell and a net pressure increment is developed to maintain a

constant volume condition. During this initial stage, the stress path is in the elastic region and far from the LC yield curve. However, the progressive wetting may bring the stress state to the LC yield curve and the overall macrostructure is prone to undergo collapse. Both phenomena co-exist during the wetting path. As noted by Gens & Alonso (1992) and Alonso et al. (2005), if collapse strains tend to dominate over other contributions to the total volumetric deformation, the stress path will closely follow the LC yield locus. A continuous increasing swelling pressure observed in this study indicates that the macro-pores collapse was fully compensated by the micro-structural swelling; thus no decrease in macro-pores was observed.

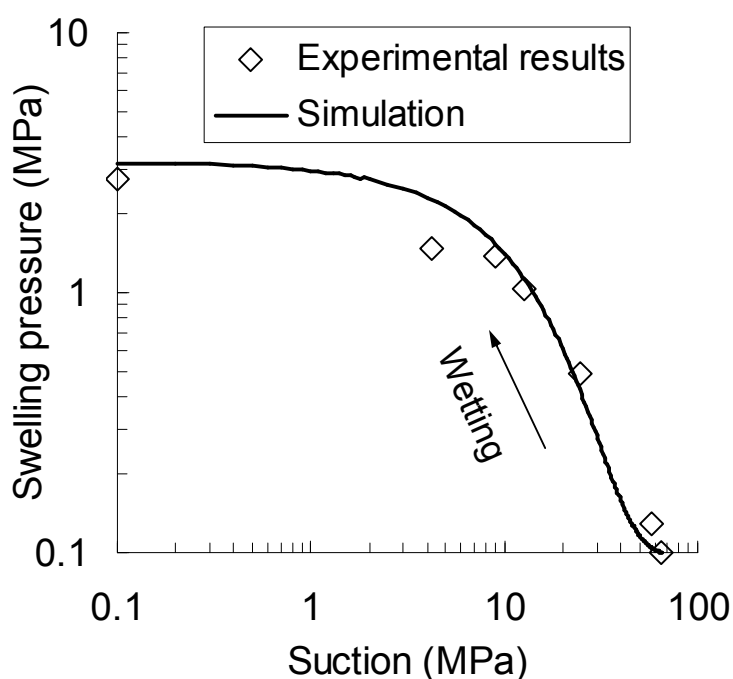


Figure 8. Changes of swelling pressure during suction decrease under constant volume condition

### Microstructure changes during suction decrease

During the swelling pressure simulation under constant volume conditions, the changes of macro- and micro-structural void ratios were calculated at the end of each stage, as shown in Figure 9. The measured values from the MIP results were also presented. The correspondence between the measured and predicted deformations is reasonably good for both micro- and macro-pores, except in the case of suction of 4.2 and 1 MPa where the macro-pores quantity increased again with further suction decrease. The discrepancy was caused by the complexity of microstructure at these suctions: a new pore group (namely 2-D pores in Audiguier et al. 2008) of about 1  $\mu\text{m}$  diameter was formed due to the fissuring of aggregates. The formation

of this new pore population leads to a tri-modal pore size distribution curve (Wang et al. 2012c). Obviously, the two-level soil structure, micro-structural (intra-aggregate) and macro-structural (inter-aggregate), defined in the BExM model can not include this phenomenon.

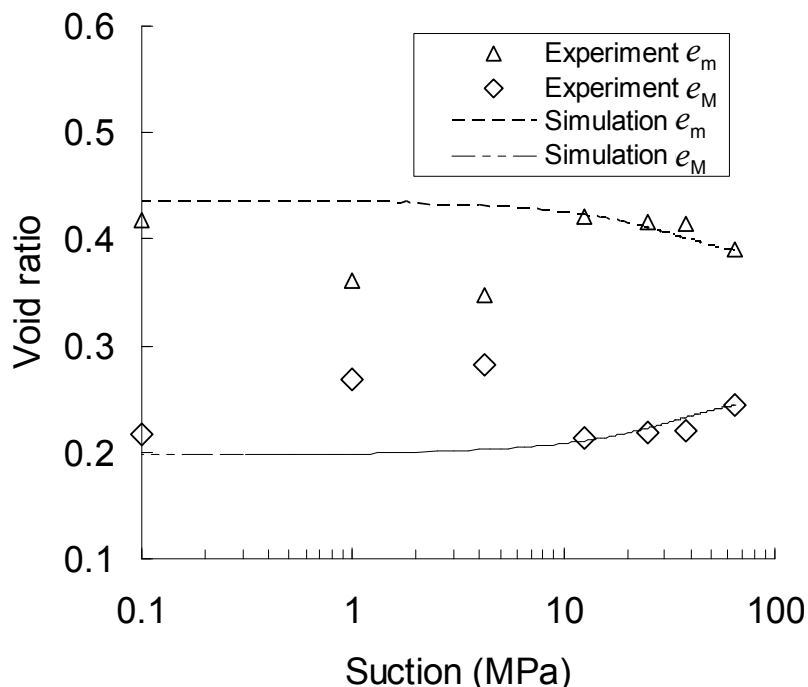


Figure 9. Changes in the  $e_m$  and  $e_M$  during suction decrease under constant volume condition

### Water retention property

As mentioned previously, the BExM model assumes that the micro-pores remain always saturated and the effective stress concept holds. Following this assumption, the amount of water in the micro-pores can be calculated based on the micro-structural void ratio. The changes in micro-structural water content ( $w_{em}$ ) upon wetting were calculated and are presented in Figure 10, together with the experimental water retention curve (WRC, including both micro-structural and macro-structural waters) at constant volume condition (Wang et al. 2012c). The model depicts well the two regions with different water retention mechanisms: intra-aggregate and inter-aggregate region. The simulated micro-structural water content curve and the measured WRC intersect at about 4-5 MPa, indicating that from this point on, the suction–water content relationship was controlled by the inter-aggregate pores. Note that this threshold suction is also close to that observed by Yahia-Aissa et al. (2001) on FoCa 7 clay (3-4 MPa) and Cui et al. (2008) on the mixture (7/3 by dry mass) of Kunigel V1 bentonite/Hostun sand (4-5 MPa).

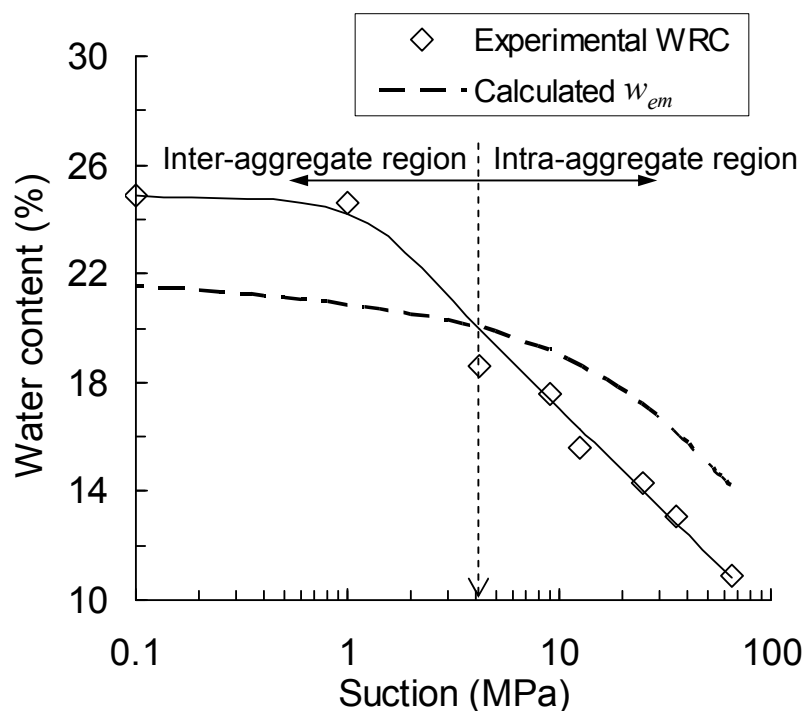


Figure 10. WRC and calculated micro-structural water content

On the other hand, the estimated micro-structural water content ( $w_{em}$ ) was found to be higher than the water content corresponding to the WRC in the intra-aggregate region. This discrepancy is due to the micro-pores that were unsaturated in reality but assumed to be saturated in the BExM model. By considering the two levels of soil structure (Gens & Alonso 1992), the BExM model lumps the intra-particles (inter-layer) space and the inter-particles space together as intra-aggregates pores. Actually, the intra-particles pores can be considered as saturated in the range of suctions of practical interest because it requires an extremely high level of suction (of the order of  $10^5$  kPa) to remove water from the inter-layer space. However, air can enter the intra-aggregate pores ( $< 2 \mu\text{m}$  for the bentonite/sand mixture as shown in Figure 3) at a suction of about 140 kPa, and hence the corresponding voids can become unsaturated (Sharma, 1998).

## 5 Conclusion

The hydro-mechanical behaviour of a compacted MX80 bentonite/sand mixture was investigated within the framework of the Barcelona Expansive Model (BExM). The model parameters were first determined based on the experimental results obtained. The changes of swelling pressure, micro-structural volume change and micro-structural water content were then simulated and compared with the experimental results.

The swelling pressure observed under constant volume was well reproduced by the model. A continuous increasing swelling pressure observed indicates that the macro-pores collapse was fully compensated by the micro-structural swelling.

The macro- and micro-structural void ratio changes upon wetting under constant volume condition were well reproduced in the range of high suctions. However, the model cannot well describe the changes in the range of low suctions (4.2 and 1 MPa). Further examination showed that the pore size distribution curve in the low suction range is tri-modal, different from the assumption of bi-modal distribution in the BExM model.

The model depicts well the two regions of different water retention mechanisms: intra-aggregate and inter-aggregate regions. However, the predicted micro-structural water content was found higher than the water content corresponding to the WRC in the intra-aggregate region. This discrepancy is due to the micro-pores assumed to be always saturated in the BExM model, but unsaturated in reality.

On the whole, the main features of the hydro-mechanical behaviour of bentonite/sand mixture can be described by the BExM model, demonstrating the performance of this model in representing the HM behaviour of bentonite-based materials. However, further considerations should be done when applying the model such as the formation of a third pore population under suction decrease and the de-saturation of intra-aggregate pores at high suctions.

## **Acknowledgements**

The work was conducted in the framework of the SEALEX project of IRSN and the PHC Cai Yuanpei project (24077QE). The support of the National Nature Science Foundation of China (41030748), China Atomic Energy Authority (Project [2011]1051), Program for Changjiang Scholars and Innovative Research Team in University (PCSIRT, IRT1029) and that of the China Scholarship Council (CSC) are also greatly acknowledged.

## **References**

- Alonso, E. E., Gens, A., Josa, A. (1990). A constitutive model for partially saturated soils. *Geotechnique*, 40 (3): 405–430.
- Alonso, E. E., Alcoverro, J., Coste, F., et al. (2005). The FEBEX benchmark test: case definition and comparison of modelling approaches. *International Journal of Rock Mechanics & Mining Science* 42(5-6): 611 – 638.
- Alonso, E. E., Vaunat, J. & Gens, A. (1999). Modelling the mechanical behaviour of expansive clays. *Engng Geol.* 54(1): 173 – 183.
- Alonso, E. E., Romero, E., Hoffmann, C. (2011). Hydromechanical behaviour of compacted granular expansive mixtures: experimental and constitutive study. *Géotechnique*, 61(4): 329 –344.

- Cho, W.J., Lee, J.O., Kwon, S. (2010). Analysis of thermo-hydro-mechanical process in the engineered barrier system of a high-level waste repository. *Nuclear Engineering and Design*. 240:1688-1698.
- Cui Y.J., Yahia-Aissa M. and Delage P. 2002. A model for the volume change behaviour of heavily compacted swelling clays. *Engineering Geology* 64 (2-3), 233-250.
- Cui, Y. J., Tang, A. M., Loiseau, C., Delage, P. (2008). Determining water permeability of compacted bentonite-sand mixture under confined and free-swell conditions. *Physics and Chemistry of the Earth*, 33, S462-S471.
- Delage, P., Howat, M. D., & Cui, Y. J. (1998). The relationship between suction and swelling properties in a heavily compacted unsaturated clay. *Engng Geol.* 50(1): 31 – 48.
- Dixon, D., Chandler, N., Graham, J. & Gray, M. N. (2002). Two large-scale sealing tests conducted at Atomic Energy of Canada's underground research laboratory: the buffercontainer experiment and the isothermal test. *Can. Geotech. J.* 39(3): 503 – 518.
- Gens, A. & Alonso, E. E. (1992). A framework for the behaviour of unsaturated expansive clays. *Can. Geotech. J.* 29(6): 1013 – 1032.
- Kröhn, K. P. (2003). New conceptual models for the resaturation of bentonite. *Applied Clay Science*, 23(1 – 4): 25 – 33.
- Lloret, A., Villar, M. V., Sanchez, M., Gens, A., Pintado, X. & Alonso, E. E. (2003). Mechanical behaviour of heavily compacted bentonite under high suction changes. *Géotechnique* 53(1): 27-40.
- Lloret, A. & Villar, M. V. (2007). Advances on the knowledge of the thermo-hydromechanical behaviour of heavily compacted « FEBEX » bentonite. *Physics and Chemistry of the Earth* 32(8 – 14): 701 – 715.
- Montes-Hernandez, G., Duplay, J., Martinez, L. & Mendoza, C. (2003). Swelling-shrinkage kinetics of MX80 bentonite. *Applied Clay Science*, 22(6): 279 – 293.
- Pusch, R. (1979) Highly compacted sodium bentonite for isolating rock-deposited radioactive waste products. *Nucl. Technol. (United States)*, 45(2):153-157
- Romero, E., Villar, M. V. & Lloret, A. (2005). Thermo-hydro-mechanical behaviour of heavily overconsolidated clays. *Engng Geol.* 81(3): 255 – 268.
- Rutqvist, J., Börgesson, L., Chijimatsu, M., Nguyen, T. S., Jing, L., Noorishad, J. & Tsang, C. F. (2001). Coupled thermo-hydro-mechanical analysis of heater test in fractured rock and bentonite at Kamaishi Mine - comparison of field results to predictions of four finite element codes. *International Journal of Rock Mechanics & Mining Sciences*, 38(1): 129-142.
- Sánchez, M., Villar, M. V., Gens, A., Olivella, S. & do N. Guimaraes, L. (2007). Modelling the effect of temperature on unsaturated swelling clays. *Proc. of the 10th International Symposium on Numerical Models in Geomechanics (Numog X)*, Rhodes, Greece, 57-62.
- Sharma, R.S. (1998). Mechanical behaviour of unsaturated highly expansive clays. University of Oxford. PHD thesis.
- Tang, A. M., Cui, Y. J. (2009). Modelling the thermomechanical volume change behaviour of compacted expansive clays. *Géotechnique*, 59: 185-195
- Villar, M.V., Lloret, A. (2008). Influence of dry density and water content on the swelling of a compacted bentonite. *Applied Clay Science*, 39(1-2):38-49.
- Wang Q., Tang A.M., Cui Y.J., Delage P., Gatmiri B. 2012a. Experimental study on the swelling behaviour of bentonite/claystone mixture. *Engineering Geology* 124, 59-66.
- Wang, Q., Tang, A. M., Cui, Y.J., Delage, P., Barnichon, J.D., & Ye, W.M. 2012b. The effects of technological voids on the hydro-mechanical behaviour of compacted bentonite-sand mixture. *Soils and Foundations*, accepted for publication.
- Wang, Q., Tang, A. M., Cui, Y.J., Delage, P., Barnichon, J.D., & Ye, W.M. 2012c. Hydraulic conductivity and microstructure changes of compacted bentonite/sand mixture during hydration. submitted to *Engineering Geology*.

- Xie, M. L., Wang, W. Q., De-jonge, J., and Kolditz O. (2007). Numerical Modelling of Swelling Pressure in Unsaturated Expansive Elasto-Plastic Porous Media. *Transport in Porous Media*, 66:311–339
- Yahia-Aissa, M., Delage, P., Cui, Y.J., (2001). In: Adachi, Fukue (Ed.), *Suction–water Relationship in Swelling Clays, Clay Science for Engineering, IS-Shizuoka Int Symp on Suction, Swelling, Permeability and Structure of Clays*. In Balkema, pp. 65–68.
- Yong, R.N., Boonsinsuk, P., and Wong, G. (1986). Formulation of backfill material for a nuclear fuel waste disposal vault. *Canadian Geotechnical Journal*, 23(2):216-228.



## CONCLUSION

A study on the hydro-mechanical behaviour of bentonite-based materials, pure MX80 bentonite, mixtures of MX80/crushed claystone and MX80/sand, has been presented. Firstly, the swelling pressure test, water retention test, suction controlled oedometer, infiltration test as well as the microstructure observations were carried out, allowing an overall analysis of the hydro-mechanical response of the compacted bentonite-based materials. Afterwards, a small scale (1/10) mock up test of the SEALEX in situ experiment was performed. The results were used for interpreting the in-situ observations. Finally, the experimental data obtained in the laboratory on a bentonite/sand mixture were interpreted in the framework of the Barcelona Expansive Model (BExM). Based on the analysis of the experimental data and the model simulation, the following conclusions can be drawn.

### Microstructure

The as-compacted samples present a bimodal porosity, defining a population of micro-pores (intra-aggregate pores) and a population of macro-pores (inter-aggregate pores) for both the pure bentonite and bentonite/sand mixture.

During suction decrease under constant volume conditions, the macro-pores were clogged progressively by the exfoliated clay particles; however, when saturation was approached (suction lower than 4.2 MPa) the macro-pores quantity increased again due to the appearance of 2-D pores. The micro-pores changed only when saturation was approached.

With an annular technological void, hydration created a meso-pore family, thus four pore families can be distinguished: nano-pore ( $< 0.006 \mu\text{m}$ ), micro-pore ( $0.006 \mu\text{m} - 0.04 \mu\text{m}$ ), meso-pore ( $0.04 \mu\text{m} - 2 \mu\text{m}$ ) and macro-pore ( $> 2 \mu\text{m}$ ). The changes in soil porosity upon swelling are mainly due to the increase in macro-pores and the meso-pores, and to the decrease in micro-pore void ratio. The microstructure changed over time due to the water re-distribution that occurred among each pore level: both the macro-pores and micro-pores volume decreased along with an increase in the volume of meso-pores. A uniform microstructure can be then expected in long term, and the higher the final dry density the slower the evolution of microstructure changes.

### Water retention properties

Under different conditions (free swell and restrained swell), different water retention

properties were observed depending on the suction value: at high suctions, the relation between the water volume ratio and the suction is unique, independent of the test conditions, indicating that the relatively limited exfoliated clay particles are mainly accommodated by the macro-pore of the soil. On the contrary, in the range of low suctions, the macro-pores available for accommodating exfoliated particles becomes limited in the restrained swell condition, less water is therefore adsorbed in this case.

### **Swelling pressure**

For the bentonite/claystone mixture, there was no obvious effect of water chemistry on the swelling pressure in short term (100 h) due to the high density and the low salinity of synthetic water (having the same). However, after a long period of 700 days, the swelling pressure decreased for all samples, especially for the sample saturated with synthetic water. The chemical effect on the swelling pressure was closely related to changes in microstructure. The sample with higher swelling pressure showed less macro and micro-pores associated with a higher interlayer hydration.

An exponential function was found between the swelling pressure and the suction applied, no effect of hydration procedure on the final swelling pressure was observed in both short and long term (700 days) due to the similar microstructure obtained after water saturation compared to the one-step soaking test.

The swell-consolidation method gives higher swelling pressure mainly because of the coupling between the microstructure deformation and macrostructure deformation. The effect of friction is also to be considered for this phenomenon.

There is a unique relationship between the axial stress (for samples with technological void) or swelling pressure (constant volume condition) and the bentonite void ratio, regardless of the sample nature (homogeneous or not) and presence of sand, suggesting that the technological voids play the same role as the macro-pores of the homogeneous compacted bentonite. It also reveals that the swelling mechanisms of bentonite-sand mixture are the same as that of pure bentonite.

### **Hydraulic conductivity**

Similar relationship between hydraulic conductivity and bentonite void ratio was observed for the bentonite-sand mixture and the pure bentonite without technological void; however, with the technological void, the measured hydraulic conductivity for the same bentonite void ratio

is generally higher, indicating the possible preferential flow pathway formed by the swollen soil that occupied the initial technological void.

With suction decrease under constant volume condition, the unsaturated hydraulic conductivity decreased followed by an increase after certain suction threshold. This change followed the same tendency as the macro-pores quantity. In other words, water transfer was primarily governed by the network of macro-pores. Over time, the hydraulic conductivity is expected to decrease due to the re-organization of microstructure that leads to the closure of 2-D pores.

### **Compressibility**

A slightly S-shaped compression curve was observed at constant suctions. The change in slope of the compression curves at higher stresses corresponds to the transition between two physical mechanisms: from the collapse of dry inter-aggregate pores to the expulsion of inter-aggregate adsorbed water.

The suction decrease significantly reduced the yield stress for both the mixture and pure bentonite. However, at the same bentonite void ratio, bentonite/sand mixture yields at a higher pre-consolidation stress, evidencing the effect of sand on the compression behaviour.

### **Mock up tests**

During the saturation process, the evolution of injected water volume followed a hyperbolic relationship in both field and laboratory small scale tests; a decrease of axial swelling pressure was observed in the small scale test due to the filling of technological void. By contrast, it was not detected in the field test owing to the effect of both the scale and pressure sensors locations.

Comparison of the injected water volume and axial swelling pressure obtained from different scales gave the same up-scaling ratio of 2.5 (in situ experiment /small scale test). Using this up-scaling ratio, the time needed to reach the stabilization of swelling pressure in the in situ experiment was estimated, equal to 754 days.

After removal of the confining pressure, a swelling strain evolution rate (swelling strain/time) of 0.588 mm/day was observed in the case of two-side infiltration. Combined with the up-scaling ratio, this rate allows the prediction of swelling strain evolution in the case of confining structure failure.

A swelling pressure of 0.18 MPa was obtained after filling an additional 20 % void, indicating a satisfactory sealing capacity after filling the technological void.

### **Modeling**

The Barcelona Expansive Model (BExM) model reproduced well the main feature of swelling pressure development, microstructure changes during suction decrease as well as the water retention property.

The simulations also showed some limitations of the approach based on the consideration of two levels of soil structure or double structure: the pore size distribution curve determined by the technique of mercury intrusion porosimetry (MIP) in the range of low suctions (4.2 and 1 MPa) being revealed to be tri-modal, the BExM model cannot capture this aspect to correctly describe the macro-structural and micro-structural void ratio changes. Moreover, because the BExM model lumps clay intra-particle space and inter-particles voids together as micro-pores, it leads to overestimation of the micro-structural water content compared to the experimental value.

## REFERENCES

- Abdullah, W.S., Al-Zou'bi, M.S., Alshibli, K.A., 1997. On the physicochemical aspects of compacted clay compressibility. *Can. Geotech. J.*, Vol 34, 551–559.
- Abdullah, I., Mhaidib, A., 1998. Prediction of swelling potential of an expansive shale. *Proceedings Of The Second International Conference On unsaturated soils.* 27-30 August. Beijing, China: vol. 1.
- Abdullah, I., Mhaidib, A.I., 1999. Swelling behaviour of expansive shales from the middle region of Saudi Arabia. *Geotechnical and Geological Engineering.* 16(4):291–307.
- AFNOR, 1992. AFNOR NF P94-057, Soils: investigation and testing. Granulometric analysis. Hydrometer method. Association Francaise de Normalisation. France.
- AFNOR, 1996. AFNOR NF P94-056, Soils: investigation and testing. Granulometric analysis. Dry sieving method after washing. Association Francaise de Normalisation. France.
- Agus, S., 2005. An Experimental study on hydro-mechanical characteristics of compacted bentonite-sand mixtures. PhD thesis. Weimar.
- Agus, S. and Schanz, T. 2005. Swelling pressures and wetting-drying curves of a highly compacted bentonite-sand mixture, *Unsaturated Soils: Experimental Studies*, 241–256.
- Agus, S.S., and Schanz, T., 2008. A method for predicting swelling pressure of compacted bentonites. *Acta Geotechnica*, 3(2), 125-137.
- Agus, S.S., and Schanz, T., and Fredlund, D.G., 2010. Measurements of suction versus water content for bentonite-sand mixtures. *Can. Geotech. J.*, 47, 583-594.
- Ahmed, S., Lovell, C.W. & Diamond, S. 1974. Pore sizes and strength of compacted clay. *ASCE Journal of the Geotechnical Engineering Division* 100, 407-425.
- Alonso, E. E., Gens, A., Josa, A. 1990. A constitutive model for partially saturated soils. *Geotechnique*, 40 (3): 405–430.
- Alonso, E. E., Vaunat, J. & Gens, A. 1999. Modelling the mechanical behaviour of expansive clays. *Engng Geol.* 54(1): 173 – 183.
- Alonso, E. E., Alcoverro, J., Coste, F., et al. 2005. The FEBEX benchmark test: case definition and comparison of modelling approaches. *International Journal of Rock Mechanics & Mining Science* 42(5-6): 611 – 638.
- Alonso, E. E., Romero, E., Hoffmann, C. 2011. Hydromechanical behaviour of compacted granular expansive mixtures: experimental and constitutive study. *Géotechnique*, 61(4): 329 –344.
- Andra, 2005. Référentiel des matériaux d'un stockage de déchets à haute activité et à vie longue – Tome 4: Les matériaux à base d'argilites excavées et remaniées. Rapport Andra N° CRPASCM040015B.
- Arifin, Y.F., 2008. Thermo-hydro-mechanical behavior of compacted bentonite sand mixtures: An Experimental Study. PhD thesis. Weimar.
- Attom, M.; Abu-Zreig, M. & Obaidat, M. 2001. Changes in clay swelling and shear strength properties with different sample preparation techniques. *ASTM geotechnical testing journal*, ASTM, 24, 157-163.
- Audiguier, M., Geremew, Z., Cojean, R. 2008. Relations enter les microstructures de deux sols argileux de la région parisienne et leur sensibilité au retrait gonflement. SEC2008, Paris, France, 1-3 sept. Editions du LCPC, 235-243.

- Baille, W., Tripathy, S., & Schanz, T. 2010. Swelling pressures and one-dimensional compressibility behaviour of bentonite at large pressures. *Applied Clay Science*, Vol 48, 324-333
- Barnichon, J.D., and Deleruyelle, F., 2009. Sealing Experiments at the Tournemire URL. Towards convergence of technical nuclear safety practices in Europe, EUROSAFE.
- Barnichon, J.D., Dick, P., & Deleruyelle, F. 2010. A sealing performance in situ experiments project (sealex): main objectives and expected outcomes, *Clays in Natural & Engineered Barriers for Radioactive Waste Confinement*, 4th international meeting, march 2010, nantes, France 261-262
- Basma, A.A., Al-Homoud, A.S., Husein, A., 1995. Laboratory assessment of swelling pressure of expansive soils. *Applied Clay Science*, 9(5):355–368.
- Ben Rhaïem, H., Pons, C.H., Tessier, D. 1985. Factors affecting the microstructure of smectites: role of cations and history of applied stresses, In: Schultz et al. (eds) *Proc Int Clay Conf*, Denver, The Clay Mineralogical Soc, 292–297
- Blatz, J.A., Cui, Y. J., Oldecop, L., 2008. Vapour Equilibrium and Osmotic Technique for Suction Control. *Geotech Geol Eng* (2008) 26:661–673.
- Börgesson, L. 1985. Water flow and swelling pressure in non-saturated bentonite-based clay barriers. *Engineering Geology*, 21(3-4):229–237.
- Börgesson, L., Karnland, O., Johannesson L.E., 1996. Modelling of the physical behaviour of clay barriers close to water saturation.pdf: Modelling of the physical behaviour of clay barriers close to water saturation. *Engineering Geology* 41, 127-144.
- Börgesson, L., Chijimatsu, M., Fujita, T., Nguyen, T.S., Rutqvist, J., Jing, L., 2001. Thermo-hydro-mechanical characterisation of a bentonite-based buffer material by laboratory tests and numerical back analyses. *International Journal of Rock Mechanics and Mining Sciences*, 38(1):95–104.
- Börgesson, L., Sandén, T., Fälth, B., Åkesson, M. & Lindgren, E. 2005. Studies of Buffers Behaviour in KBS-3H Concept: Work During 2002-2004, SKB, R-05-50.
- Bradbury, M.H., Baeyens, B., 2003. Porewater chemistry in compacted re-saturated MX-80 bentonite. *Journal of Contaminant Hydrology*, 61, 329– 338
- Castellanos, E., Villar, M.V., Romero, E., Lloret, A., Gens, A., 2008. Chemical impact on the hydro-mechanical behaviour of high-density febex bentonite. *Physics and Chemistry of the Earth, Parts A/B/C*, 33(Supplement 1):S516 – S526.
- Cho, W.J., Lee, J.O., Kang, & C.H. 2000. Influence of temperature elevation on the sealing performance of a potential buffer material for a high-level radioactive waste repository. *Annals of Nuclear Energy*, Vol 27, 1271-1284
- Cho, W.J., Lee, J.O., Kwon, S. 2010. Analysis of thermo-hydro-mechanical process in the engineered barrier system of a high-level waste repository. *Nuclear Engineering and Design*. 240:1688-1698.
- Coleman, J.D. 1962. Stress-Strain relations for partially saturated soils. *Géotechnique* 12 (4), 348-350.
- Cui Y.J., Yahia-Aissa M. and Delage P. 2002. A model for the volume change behaviour of heavily compacted swelling clays. *Engineering Geology* 64 (2-3), 233-250.
- Cui, Y. J., Loiseau, C., Delage, P. 2002. Microstructure changes of a confined swelling soil due to suction controlled hydration Unsaturated soils: proceedings of the Third International Conference on Unsaturated Soils, UNSAT 2002, 10-13 March 2002, Recife, Brazil, 593-598
- Cui, Y.J., Tang, A.M., Loiseau, C., Delage, P., 2008. Determining the unsaturated hydraulic conductivity of a compacted sand-bentonite mixture under constant-volume and free-swell conditions. *Physics and Chemistry of the Earth, Parts A/B/C*, 33(Supplement 1):S462 – S471.
- Cui, Y.J., Tang, A.M., Qian, L.X., Ye, W.M., Chen, B., 2011. Thermal-mechanical behavior of compacted GMZ Bentonite. *Soils and Foundations*, Vol. 51, No. 6, 1065-1074.

- Daniel, D.E., 1982. Measurement of hydraulic conductivity of unsaturated soils with thermocouple psychrometers. *Soil Science Society of America Journal* 20 (6):1125–1129.
- Day, R.W. 1994. Swell-shrink behaviour of expansive compacted clay. *J. Geotechnical Engineering, ASCE* 120, No. 3, 618–623.
- Delage, P. & Lefebvre, G. 1984. Study of the structure of a sensitive Champlain clay and its evolution during consolidation. *Can. Geotech. J.* Vol(21), No. 1, 21–35.
- Delage P. & Graham J. 1995. The mechanical behaviour of unsaturated soils. *Proceedings of the 1st International Conference on Unsaturated soils*, Vol. 3, 1223-1256, Paris, E.E. Alonso and P. Delage eds, Balkema.
- Delage, P., Audiguier, M., Cui, Y.J. & Howat, M.D. 1996. Microstructure of a compacted silt. *Canadian Geotechnical Journal*, 33 (1), 150-158.
- Delage, P., Howat, M.D., & Cui, Y.J. 1998. The relationship between suction and swelling properties in a heavily compacted unsaturated clay. *Engineering Geology*, 50(1-2), 31-48.
- Delage, P. 2006. Some microstructure effects on the behaviour of compacted swelling clays used for engineered barriers. *Chinese Journal of Rock Mechanics and Engineering*, Science Press(Beijing), 16 Donghuangchenggen North St, Beijing, 100717, China., 25, 721-732.
- Delage, P., Marcial, D., Cui, Y.J., Ruiz, X. 2006. Ageing effects in a compacted bentonite: a microstructure approach. *Géotechnique* 56 (5), 291-304.
- Delage, P. 2007, Microstructure features in the behaviour of engineered barriers for nuclear waste disposal, *SPRINGER PROCEEDINGS IN PHYSICS*, 112 (11),11-312
- Delage, P. and Cui, Y.J. 2008a. An evaluation of the osmotic method of controlling suction. *Journal of Geomechanics and Geoengineering* 3 (1), 1-11.
- Delage, P. and Cui, Y.J. 2008b. A novel filtration system for polyethylene glycol solutions used in the osmotic method of controlling suction. *Canadian Geotechnical Journal* 45, 421-424.
- Delage, P., Cui, Y.J., Tang, A.M., 2010. Clays in radioactive waste disposal, *Journal of Rock Mechanics and Geotechnical Engineering*, Vol (2):111–123.
- Dixon, D.A., Gray, M.N. and Thomas, A.W., 1985. A study of the compaction properties of potential clay-sand buffer mixtures for use in nuclear fuel waste disposal. *Engineering Geology*, 21, 247-255.
- Dixon, D.A., Cheung, S.C.H., Gray, M.N., Davidson, B.C., 1987. The hydraulic conductivity of dense clay soils. *Proc. 40th Canadian Geotechnical Conference*, Regina, Saskatchewan - Canada, pp. 389–396.
- Dixon, D.A., Gray, M.N., Hnatiw, D., 1992. Critical gradients and pressures in dense swelling clays. *Canadian Geotechnical Journal* 29 (6), 1113-1119.
- Dixon, D.A., Gray, M.N., Graham, J., 1996. Swelling and hydraulic properties of bentonites from Japan, Canada and USA. In *Proceedings of the second International Congress on Environmental Geotechnics*, Osaka, Japan, 5-8.
- Dixon, D.A., Graham, J., and Gray, M.N., 1999. Hydraulic conductivity of clays in confined tests under low hydraulic gradients. *Canadian Geotechnical Journal*, 36(5):815–825.
- Dixon, D.A., 2000. Porewater salinity and the development of swelling pressure in bentonite-based buffer and backfill materials. *POSIVA Report 2000-04*, Posiva Oy, Helsinki, Finland.
- Dixon, D., Chandler, N., Graham, J. & Gray, M. N. 2002. Two large-scale sealing tests conducted at Atomic Energy of Canada's underground research laboratory: the buffercontainer experiment and the isothermal test. *Can. Geotech. J.* 39(3): 503 – 518.
- Fernández, A.M., Villar, M.V., 2010. Geochemical behaviour of a bentonite barrier in the laboratory after up to 8 years of heating and hydration. *Applied Geochemistry* 25, 809–824

- Fernández, A.M., Baeyens, B., Bradbury, M., Rivas, P., 2004. Analysis of the pore water chemical composition of a Spanish compacted bentonite used in an engineered barrier. *Phys. Chem. Earth* 29, 105–118.
- Fredlund D.G. & Morgenstern N.R. 1977. Stress state variables for unsaturated soils. *ASCE J. Geotech. Eng. Div. GT5*, 103, 447-466.
- Fredlund, D.G., Rahardjo, H., 1993. *Soil mechanics for unsaturated soils*. John Wiley and Sons, New York
- Gatabin, C., Touze, G., Imbert, C., Guillot, W., Billaud, P., 2008. ESDRED Project, Module 1-Selection and THM characterization of the buffer material. In International conference underground disposal unit design&emplacement processes for a deep geological repository, 16-18 June, Prague.
- Gaucher E. C., Blanc P., Bardot F., Braibant G., Buschaert S., Crouzet C., Gautier A., Girard J.-P., Jacquot E., Lassin A., Negrel G., Tournassat C., Vinsot A., and Altmann S. 2006. Modelling the porewater chemistry of the Callovian-Oxfordian formation at a regional scale. *Comptes Rendus Geosciences* 338(12-13), 917-930.
- Gens, A., Alonso, E.E. 1992. A framework for the behaviour of unsaturated expansive clays. *Canadian Geotechnical Journal*, 29(6):1013–1032.
- Gens, A., Alonso, E.E., Suriol, J., Lloret, A., 1995. Effect of structure on the volumetric behaviour of a compacted soil. In: Alonso, Delage (Eds.), *Proc. 1st Int. Conf. on Unsaturated Soils*, Paris, vol. 1. Balkema, Rotterdam, 83-88.
- Gens, A., 1996. Constitutive modelling : Application to compacted soils . *Proc. 1st Int. Conf on Unsaturated Soils UNSAT' 95*, Vol. 3, 1179-1200, Paris.
- Hoteit N, Ozanam-O, Su, K. 2000. Geological radioactive waste disposal project in france- conceptual model of a deep geological formation and underground research laboratory in Meuse Haute-Marne site. In *The 4th North American Rock Mechanics Symposium*, Seattle, July 31-August 3.
- Herbert, H.-J., Kasbohm, J., Moog, H.C. & Henning, K.-H. 2004. Long-term behaviour of the Wyoming bentonite MX-80 in high saline solutions. *Applied Clay Science*, 26, 275-291.
- Herbert, H.-J., Kasbohm, J., Sprenger, H., Fernández, A.M. & Reichelt, C. 2008. Swelling pressures of MX-80 bentonite in solutions of different ionic strength. *Physics and chemistry of the earth*, 33, 327-342.
- Hoteit, N., Ozanam, O., Su, K., 2000. Geological Radioactive Waste Disposal Project in France: Conceptual Model of a Deep Geological Formation and Underground Research Laboratory in Meuse/Haute-Marne Site. *The 4th North American Rock Mechanics Symposium*, Seattle, July 31–August 3, 2000.
- Imbert, C., and Villar, M.V., 2006. Hydro-mechanical response of a bentonite pellets-powder mixture upon infiltration. *Applied Clay Science*, 32(3-4):197–209.
- Jacinto, A. C., Villar, M. V., & Ledesma, A. 2012. Influence of water density on the water-retention curve of expansive clays, *Geotechnique* 62, No. 8, 657–667
- JNC, 2000. H12: Project to establish the scientific and technical basis for HLW disposal in Japan, report TN1410 2000-001, Tokai-Mura.
- Justo, J.L., Delgado, A., Ruiz, J., 1984. The influence of stress-path in the collapse-swelling of soils at the laboratory. In *Fifth International Conference on Expansive Soils 1984*. Australia. Page 67.
- Juvankoski, M., 2010. Description of basic design for buffer (working report 2009-131). Technical report, EURAJOKI, FINLAND.

- Karland, O., 1997. Bentonite swelling pressure in strong NaCl solutions. Correlation between model calculations and experimentally determined data. SKB Technical Report 97-31. Swedish Nuclear Fuel and Waste Management Co., Stockholm, pp. 1–30.
- Karland, O., Muurinen, A., Karlsson, F., 2005. Bentonite swelling pressure in NaCl solutions-Experimentally determined data and model calculations. *Advances in Understanding Engineering Clay Barriers*. Page 241.
- Karland, O., Olsson, S. & Nilsson, U. 2006. Mineralogy and sealing properties of various bentonites and smectite-rich clay materials. SKB TR-06-30. Swedish Nuclear Fuel and Waste Management Co, Stockholm, Sweden.
- Karland, O., Nilsson, U., Weber, H., and Wersin, P., 2008. Sealing ability of Wyoming bentonite pellets foreseen as buffer material-Laboratory results. *Physics and Chemistry of the Earth, Parts A/B/C*, 33, S472-S475.
- Katsumia, T., Ishimorib, H., Onikatac, M., Fukagawab,R., 2008. Long-term barrier performance of modified bentonite materials against sodium and calcium permeant solutions *Geotextiles and Geomembranes* 26,14–30.
- Keller, T., Arvidsson, J., Dawidowski, J.B., Koolen, A.J., 2004. Soil precompression stress. II. A comparison of different compaction tests and stress - displacement behaviour of the soil during wheeling. *Soil Till. Res.* 77, 97-108.
- Kenney, T.C., van Veen, W.A., Swallow, M.A., Sungaila, M.A., 1992. Hydraulic conductivity of compacted bentonite-sand mixtures. *Canadian Geotechnical Journal* 29 (3): 364–374.
- Kochmanová, N., Tanaka, H., 2011. Influence of the Soil Fabric on the Mechanical Behaviour of Unsaturated and Saturated Clay. *Soils and Foundations*, Vol. 51, No. 2, 275-286.
- Komine., H., Ogata, N. 1994. Experimental study on swelling characteristics of compacted bentonite. *Canadian geotechnical journal*, 31(4):478–490.
- Komine., H., Ogata, N. 1998. Thermal influence on compacted bentonite for nuclear waste disposal. In *Proceedings of the 3rd International Congress on Environmental Geotechnics*, volume 1, pages 34–39.
- Komine., H., Ogata, N. 2003. New equations for swelling characteristics of bentonite-based buffer materials. *Canadian Geotechnical Journal*, 40(2):460–475.
- Komine, H., 2004a. Simplified evaluation on hydraulic conductivities of sand-bentonite mixture backfill. *Applied Clay Science* 26 (1–4), 13–19.
- Komine, H., 2004b. Simplified evaluation for swelling characteristics of bentonites, *Engineering geology*, 71(3-4): 265-279.
- Komine., H., Ogata, N. 2004. Predicting swelling characteristics of bentonites. *Journal of Geotechnical and Geoenvironmental engineering*, 130:818.
- Komine, H. and Yasuhara, K. and Murakami, S. 2009. Swelling characteristics of bentonites in artificial seawater. *Canadian Geotechnical Journal*. 46, 177-189
- Komine, H., 2010. Predicting hydraulic conductivity of sand bentonite mixture backfill before and after swelling deformation for underground disposal of radioactive wastes. *Engineering Geology*. 114, 123-134
- Komine, H., Watanabe, Y., 2010. The past, present and future of the geo-environment in Japan. *Soils and Foundations*, Vol. 50 (2010) No. 6 977-982.
- Kröhn, K. P., 2003a. New conceptual models for the resaturation of bentonite. *Applied Clay Science* 23 (1-4), 25-33.

- Kröhn, K. P., 2003b. Results and interpretation of bentonite resaturation experiments with liquid water and water vapour. In: Schanz, T. (Ed.), Proceedings of the International Conference from Experimental Evidence towards Numerical Modeling of Unsaturated Soils, Weimar, Germany, vol. 1. Springer, Berlin, pp. 257–272.
- Laine H., Karttunen P., 2010. Long-Term Stability of Bentonite. A Literature Review. POSIVA Report 2010-53, Posiva Oy, Helsinki, Finland.
- Lebon, P. and Ghoreychi, M. 2000. French underground research laboratory of Meuse, Haute-Marne THM aspects of argillite formation. In Eurock 2000 Symposium, March, pages 27–31.
- Lee, J.O., Cho, W.J. and Chun, K.S., 1999. Swelling Pressures of a Potential Buffer Material for High-Level Waste Repository. Journal of the Korean Nuclear Society, 31: 139-150.
- Lemaire, T., Moyne, C., Stemmelen, D., 2004. Imbibition test in a clay powder (MX-80 bentonite). Applied Clay Science 26: 235-248.
- Li, X.L., Bastiaens, W., Van Marcke, P., Verstricht, J., Chen, G.J., Weetjens, E., Sillen, X. 2010. Design and development of large-scale in-situ PRACLAY heater test and horizontal high-level radioactive waste disposal gallery seal test in Belgian HADES, Journal of Rock Mechanics and Geotechnical Engineering. 2 (2), 103–110
- Li, Z.M., 1995. Compressibility and collapsibility of compacted unsaturated loessial soils. In: Alonso, Delage (Eds.), Proc. 1st Int. Conf. on Unsaturated Soils, Paris, vol. 1. Balkema, Rotterdam, 139-144.
- Lloret, A., Villar, M. V., Sanchez, M., Gens, A., Pintado, X. & Alonso, E. E. (2003). Mechanical behaviour of heavily compacted bentonite under high suction changes. Géotechnique 53(1): 27-40.
- Lloret, A. & Villar, M. V. 2007. Advances on the knowledge of the thermo-hydromechanical behaviour of heavily compacted FEBEX bentonite. Physics and Chemistry of the Earth 32(8 – 14): 701 – 715.
- Loiseau, C., Cui, Y.J. and Delage, P., 2002. The gradient effect on the water flow through a compacted swelling soil, In: Proc. 3rd Int Conf Unsaturated Soils, UNSAT 2002, Recife, Brazil, Balkema 1:395–400.
- Lutz, J.F., Kemper, W.D., 1959. Intrinsic permeability of clay as affected by clay-water interaction. Soil science 88: 83-90.
- Marcial, D. 2003. Comportement hydromécanique et microstructural des matériaux de barrière ouvragée, PHD thesis, École Nationale des Ponts et Chaussées, Paris, France.
- Marcial, D., Delage, P. and Cui, Y.J. 2002. On the high stress compression of bentonites. Canadian Geotechnical Journal 39, 812-820.
- Martin, P.L., Barcala, J.M., and Huertas, F., 2006. Large-scale and long-term coupled thermo-hydro-mechanic experiments with bentonite: the febex mock-up test. Journal of Iberian Geology, 32(2), 259-282.
- Marty, N., Fritz, B., Clément, A., Michau, N., 2010, Modelling the long term alteration of the engineered bentonite barrier in an underground radioactive waste repository, Applied Clay Science 47 (2010) 82–90
- Mata, C., 2003. Hydraulic behaviour of bentonite based mixtures in engineered barriers: The Backfill and Plug Test at the Åspö HRL (Sweden). Ph. D. Thesis. Universitat Politècnica de Catalunya. 257 pp. Barcelona.
- Miller, R.J., Low, P.F., 1963. Threshold Gradient for Water Flow in Clay Systems. Soil Science Society of America Journal. 27 (6):605-609.
- Mitchell, J.K., 1976. Fundamentals of Soil Behavior, John Wiley & Sons, New York.

- Monroy, R. And Zdravkovic, L. And Ridley, A. 2010. Evolution of microstructure in compacted London Clay during wetting and loading, *Geotechnique*, Vol(60),: 105--119
- Montes-H, G., Duplay, J., Martinez, L., and Mendoza, C. 2003. Swelling–shrinkage kinetics of MX80 bentonite. *Applied Clay Science*, 22, 279-293.
- Montes-H, G., Geraud, Y., 2004. Sorption kinetic of water vapour of MX80 bentonite submitted to different physical-chemical and mechanical conditions. *Colloids and Surfaces A: Physicochemical Engineering Aspects* 235, 17–23.
- Montes-H, G., Geraud, Y., Duplay, J. & Reuschlé, 2005. ESEM observations of compacted bentonite submitted to hydration/dehydration conditions. *Colloids and surfaces A: Physicochem. Eng. Aspects*, 262, 14-22.
- Muurinen, A., Lehtikoinen, J., 1999, Porewater chemistry in compacted bentonite, *Engineering Geology* 54, 207–214
- Nagaraj, H.; MOHAMMED Munnas, M.; Sridharan, A., 2009. Critical Evaluation of Determining Swelling Pressure by Swell-Load Method and Constant Volume Method, *ASTM geotechnical testing journal*, ASTM, 32, 305-314.
- Nalezny, C. L. & Li, M. C., 1967. Effects of soil moisture and thixotropic hardening on the swell behaviour of compacted expansive soils. *Highway Res. Rec. Washington, DC: Highway Research Board*. No. 209.
- Nowamooz, H. and Masrouri, F. 2010, Relationships between soil fabric and suction cycles in compacted swelling soils, *Engineering Geology*, Vol (114), 444-455
- Pusch, R. 1979 Highly compacted sodium bentonite for isolating rock-deposited radioactive waste products. *Nucl. Technol. (United States)*, 45(2):153-157
- Pusch, R. 1980. Swelling pressure of highly compacted bentonite. SKBF/KBS technical report: No.80-13.
- Pusch, R., 1982. Mineral-water interactions and their influence on the physical behavior of highly compacted Na bentonite. *Canadian Geotechnical Journal*, 19(3):381–387.
- Pusch, R., 1999. Microstructural evolution of buffers. *Engineering geology*. 54:33-41.
- Pusch, R., 2001a. Experimental study of the effect of high porewater salinity on the physical properties of a natural smectitic clay, SKBF/KBS technical report. No.TR01-07.
- Pusch, R. 2001b. The microstructure of MX-80 clay with respect to its bulk physical properties under different environmental conditions, SKBF/KBS technical report. No.TR01-08.
- Pusch, R., Yong, R., 2003. Water saturation and retention of hydrophilic clay buffer-microstructural aspects. *Applied Clay Science*, 23:61-68.
- Pusch, R., Yong, R.N., 2006, *Microstructure of Smectite Clays and Engineering Performance*, Taylor & Francis, London and New York.
- Romero, E., Della Vecchia, G., and Jommi, C. 2011. An insight into the water retention properties of compacted clayey soils. *Geotechnique* 61, No. 4, 313-328.
- Romero, E., Gens, A. & Lloret, A., 1999. Water permeability, water retention and microstructure of unsaturated compacted Boom clay. *Engineering Geology*. 54, 117-127.
- Romero, E., Gens, A., and Lloret, A., 2001. Temperature effects on the hydraulic behaviour of an unsaturated clay. *Geotechnical and Geological Engineering*, 19(3):311–332.
- Romero, E., Villar, M. V. & Lloret, A. 2005. Thermo-hydro-mechanical behaviour of heavily overconsolidated clays. *Engng Geol.* 81(3): 255 – 268.

- Rutqvist, J., Börgesson, L., Chijimatsu, M., Nguyen, T. S., Jing, L., Noorishad, J. & Tsang, C. F. (2001). Coupled thermo-hydro-mechanical analysis of heater test in fractured rock and bentonite at Kamaishi Mine - comparison of field results to predictions of four finite element codes. *International Journal of Rock Mechanics & Mining Sciences*, 38(1): 129-142.
- Saiyouri, N., Hicher, P.Y., and Tessier, D. 2000. Microstructural approach and transfer water modelling in highly compacted unsaturated swelling clays. *Mechanics of cohesive-frictional materials*, 5, 41-60.
- Saiyouri, N., Tessier, D., and Hicher, P.Y., 2004. Experimental study of swelling in unsaturated compacted clays. *Clay Minerals*, 39(4):469.
- Sánchez, M., Gens, A., Do Nascimento Guimarães, L., Olivella, S., 2005. A double structure generalized plasticity model for expansive materials. *International Journal for Numerical and Analytical Methods in Geomechanics*, 29(8):751-787.
- Sánchez, M., Villar, M. V., Gens, A., Olivella, S. & do N. Guimaraes, L. (2007). Modelling the effect of temperature on unsaturated swelling clays. *Proc. of the 10th International Symposium on Numerical Models in Geomechanics (Numog X)*, Rhodes, Greece, 57-62.
- Sharma, R.S. 1998. Mechanical behaviour of unsaturated highly expansive clays. University of Oxford. PHD thesis.
- Siddiqua, S.; Blatz, J. & Siemens, G. 2011. Evaluation of the impact of pore fluid chemistry on the hydromechanical behaviour of clay-based sealing materials. *Canadian Geotechnical Journal*, NRC Research Press, 48, 199-213.
- Siemens, G., and Blatz, J.A., 2009. Evaluation of the influence of boundary confinement on the behaviour of unsaturated swelling clay soils. *Canadian Geotechnical Journal*, 46(3):339-356.
- Skipper, N.T., Refson, K., McConnell, J.D.C. 1991. Computer simulation of interlayer water in 2:1 clays. *J. Chem. Phys.* 94 (11), 7434-7445.
- Sridharan, A., Altschaeffle, A. G. and Diamond, S. 1971, Pore size distribution studies, *Journal of the Soil Mechanics and Foundations Division, Proceedings of the ASCE*, vol. 97, SM 5, 771-787
- Sridharan, A., Rao, S., Sivapullaiah, P.V., 1986. Swelling pressure of clays. *ASTM geotechnical testing journal*, 9(1):24-33.
- Stroes-Gascoyne, S. 2010. Microbial occurrence in bentonite-based buffer, backfill and sealing materials from large-scale experiments at AECL's underground research laboratory. *Applied Clay Science*, 47(1-2), 36-42.
- Studds, P.G., Stewart, D.I., and Cousens, T.W. 1998. The effects of salt solutions on the properties of bentonite-sand mixtures. *Clay Minerals*, 33: 651-660.
- Subba Rao, K. S. & Tripathy, S. 2003. Effect of aging on swelling and swell-shrink behaviour of a compacted expansive soil. *ASTM Geotech. Test. J.* 26, No. 1, 36-46.
- Sugita, Y., Chijimatsu, M., and Suzuki, H., 2005. Fundamental properties of bentonite pellet for Prototype Repository Project. *Advances in Understanding Engineering Clay Barriers*, page 293.
- Suzuki, S.; Prayongphan, S.; Ichikawa, Y. & Chae, B. 2005. In situ observations of the swelling of bentonite aggregates in NaCl solution, *Applied Clay Science*, Elsevier, 29: 89-98.
- Tang, A.M., Cui, Y.J., 2005. Controlling suction by the vapour equilibrium technique at different temperatures and its application in determining the water retention properties of MX80 clay. *Canadian Geotechnical Journal*, 42 (1): 287-296.
- Tang, A.M., Cui, Y.J., Barnel, N., 2007. A new isotropic cell for studying the thermo-mechanical behavior of unsaturated expansive soil. *Geotechnical Testing Journal*, 30 (5): 341 - 348.
- Tang, A.M., Cui, Y.J., Barnel, N., 2008. Thermo-mechanical behaviour of a compacted swelling clay. *Géotechnique*, 58 (1): 45-54.

- Tang, A.M., Cui, Y.J., Le, T.T., 2008. A study on the thermal conductivity of compacted bentonites. *Applied Clay Science*, 41 (3-4): 181 – 189.
- Tang, A.M., Munoz, J.J., Cui, Y.J., Delage, P., Li, X.L. 2008. Experimental Evaluation of the Hydraulic Resistance of Compacted Bentonite/Boom Clay Interface, In: *Proceedings of the International Technical Conference on the Practical Aspects of Deep Geological Disposal of Radioactive Waste*, Prague, Czech Republic, June 2008, 16-18
- Tang, A. M., Cui, Y. J. 2009. Modelling the thermomechanical volume change behaviour of compacted expansive clays. *Géotechnique*, 59: 185-195
- Tang, A.M., Cui, Y.J., Eslami, J. Defossez, P., 2009. Analysing the form of the confined uniaxial compression curve of various soils . *Geoderma* vol (148)3-4, 282-290.
- Tang, A.M and Cui, Y.J., 2010, Effects of mineralogy on thermo-hydro-mechanical parameters of MX80 bentonite, *Journal of Rock Mechanics and Geotechnical Engineering*. 2 (1), 91-96.
- Tang, C.S., Tang, A.M., Cui, Y.J., Delage, P., Barnichon, J.D., Shi, B., 2011a. A study of the hydro-mechanical behaviour of compacted crushed argillite. *Engineering Geology*. 118 (3-4):93-103.
- Tang, C.S., Tang, A.M., Cui, Y.J., Delage, P., Schroeder, C., De Laure, E., 2011b. Investigating the swelling pressure of compacted crushed Callovo-Oxfordian argillite. *Physics and Chemistry of the Earth (special issue)*, Volume 36, Issues 17–18, 1857–1866
- Tarantino, S. and De Col, E., 2008. Compaction behaviour of clay. *Géotechnique*, vol. 58 (3), 199-213.
- Thom. R., Sivakumar, R., Sivakumar, V., Murray, E.J., Mackinnon, P. 2007. Pore size distribution of unsaturated compacted kaolin: the initial states and final states following saturation. *Geotechnique* 57(5), 469–474
- Van Genuchten, M.T., 1980. A closed-form equation for predicting the hydraulic conductivity of unsaturated soils. *Soil Science Society of America Journal*, 44: 892-898.
- Villar, M.V., 1999. Investigation of the behaviour of bentonite by means of suction-controlled oedometer tests. *Engineering Geology*, 54(1-2):67–73.
- Villar, M.V., 2002. Thermo-hydro-mechanical characterisation of a bentonite from Cabo de Gata. A study applied to the use of bentonite as sealing material in high level radioactive waste repositories. *Publicación Técnica ENRESA 01/2002*, Madrid, 258 pp.
- Villar, M.V. & Lloret. A. 2004. Influence of temperature on the hydro-mechanical behaviour of a compacted bentonite. *Applied Clay Science*, 26(1-4), 337-350.
- Villar, M.V., 2005, MX-80 Bentonite. Thermo-Hydro-Mechanical Characterisation Performed at CIEMAT in the Context of the Prototype Project. CIEMAT Technical Report: CIEMAT/DIAE/54540/2/04.
- Villar, M.V., Lloret, A., 2008. Influence of dry density and water content on the swelling of a compacted bentonite. *Applied Clay Science*, 39(1-2):38–49.
- Wang, Q., Tang, A. M., Cui, Y.J., Delage, P., & Gatmiri, B. 2012a. Experimental study on the swelling behaviour of bentonite/claystone mixture, *Engineering Geology*, Vol. 124, 59–66.
- Wang, Q., Tang, A. M., Cui, Y.J., Delage, P., Barnichon, J.D., & Ye, W.M. 2012b. The effects of technological voids on the hydro-mechanical behaviour of compacted bentonite-sand mixture. *Soils and Foundations*, accepted for publication.
- Xie, M. L., Wang, W. Q., De-jonge, J., and Kolditz O. (2007). Numerical Modelling of Swelling Pressure in Unsaturated Expansive Elasto-Plastic Porous Media. *Transport in Porous Media*, 66:311–339

- Yahia-Aissa, M., Delage, P., & Cui, Y.J. 2001. Suction-water relationship in swelling clays. Clay science for engineering, IS-Shizuoka International Symposium on Suction, Swelling, Permeability and Structure of Clays, 65-68, Adachi & Fukue eds, Balkema.
- Yahia-Aissa, M., Delage, P., Cui, Y.J., (2001). In: Adachi, Fukue (Ed.), Suction–water Relationship in Swelling Clays, Clay Science for Engineering, IS-Shizuoka Int Symp on Suction, Swelling, Permeability and Structure of Clays. In Balkema, pp. 65–68.
- Yang, J., Samper, C., and Montenegro, L., 2008. A coupled non-isothermal reactive transport model for long-term geochemical evolution of a HLW repository in clay. *Environmental Geology*, 53(8):1627–1638.
- Ye, W.M., Cui, Y.J., Qian, L.X., Chen. B., 2009. An experimental study of the water transfer through confined compacted GMZ bentonite. *Engineering Geology*, 108(3-4):169–176.
- Yong, R.N., Warkentin, B.P., 1975. Soil properties and behaviour. Elsevier, Amsterdam.
- Yong, R.N., Boonsinsuk, P., and Wong, G., 1986. Formulation of backfill material for a nuclear fuel waste disposal vault. *Canadian Geotechnical Journal*, 23(2), 216-228.
- Yukselen-Aksoy, Y., Kaya, A., Ören, A.H., 2008, Seawater effect on consistency limits and compressibility characteristics of clays, *Engineering Geology* 102 (2008) 54–61
- Zhang, C., and Rothfuchs, T., 2004. Experimental study of the hydro-mechanical behaviour of the Callovo-Oxfordian argillite. *Applied Clay Science*, 26(1-4):325–336.
- Zou, Y., 1996. A non-linear permeability relation depending on the activation energy of pore liquid. *Géotechnique* 46 (4), 769-774.